ABSTRACT

Title of Dissertation:	THE IMPORTANCE OF PHYSICAL MIXING AND SEDIMENT CHEMISTRY IN MERCURY AND METHYLMERCURY BIOGEOCHEMICAL CYCLING AND BIOACCUMULATION WITHIN SHALLOW ESTUARIES
	Eun-Hee Kim, Doctor of Philosophy, 2004
Dissertation Directed By:	Professor Robert P. Mason, Marine Estuarine Environmental Science

The objective of this study was to examine, using mesocosm experiments, the long-term effects of sediment resuspension on the fate, transport, and bioaccumulation of Hg and MeHg in shallow ecosystems. A bioenergetic-based model including sediment resuspension was developed to assess MeHg bioaccumulation into benthic and pelagic organisms under the experimental conditions. In addition, this study examined the spatial distribution of Hg and MeHg in the sediments from the Chesapeake Bay and used the model developed to examine the important factors in Hg and MeHg distribution and bioaccumulation in the Bay.

Using STORM (high bottom Shear realistic water column Turbulence Resuspension Mesocosm) mesocosms, two 4-week experiments were conducted in July and October of 2001 (experiments 1 and 2) with Baltimore Harbor sediments. Tidal resuspension (4 h-on and 2 h-off cycles) was simulated with three replicates of the resuspension (R) and no-resuspension (NR) tanks. In experiment 1, there was no benthic macrofauna. In experiment 2, hard clams, *Mercenaria mercenaria*, were

added to the sediment in the mesocosm tanks. Water, sediment, and biota (zooplankton and clams) samples were collected and analyzed for Hg and MeHg. Using Hg stable isotopes, Hg methylation and MeHg demethylation rates were determined.

The STORM experiments showed that during sediment resuspension there was a significantly higher suspended particulate total Hg (THg) (on a mass basis), while particulate MeHg was significantly lower, as sediment particles with relatively poor MeHg were dominant in the water column. The results suggested that equilibrium partitioning between the dissolved and particulate phases for THg and MeHg was not occurring. It appeared that resuspension enhanced Hg methylation in the top sediment layer, especially in summer. Concentrations of THg and MeHg in biota showed that resuspension had a complex effect of system productivity and bioaccumulation. It appeared that organic matter content played an important role in the distribution of THg and MeHg in sediments and bioaccumulation into benthic and pelagic organisms. The modeling studies demonstrated that sediment resuspension played a role in transporting the enhanced MeHg to the water column and ultimately in increasing the MeHg burden into biota.

THE IMPORTANCE OF PHYSICAL MIXING AND SEDIMENT CHEMISTRY IN MERCURY AND METHYLMERCURY BIOGEOCHEMICAL CYCLING AND BIOACCUMULATION WITHIN SHALLOW ESTUARIES

by

Eun-Hee Kim

Dissertation submitted to the Faculty of the Graduate School of the
University of Maryland, College Park, in partial fulfillment
of the requirements for the degree of
Doctor of Philosophy
2004

Advisory Committee:
Professor Robert P. Mason, Chair
Professor Joel E. Baker
Research Associate Professor Jeffrey C. Cornwell
Associate Professor Judd Nelson
Assistant Professor Christopher L. Rowe
Professor Lawrence P. Sanford

Dedication

I’d like to dedicate this work to my parents for their endless and unconditional love throughout years. I would not have come this far without them.

Acknowledgements

I would like to thank my advisor, Dr. Robert Mason, for taking me as his student, opening my eyes to the mercury world, and guiding me throughout my study. I am truly grateful for his knowledge, patience, support, and encouragement. I would also like to thank my committee members, Drs. Joel Baker, Jeffrey Cornwell, Christopher Rowe, and Larry Sanford for their advice and encouragement. I would like to acknowledge Dr. Judd Nelson who kindly agreed to serve as a Dean's Representative at short notice.

I would like to thank Dr. Elka Porter and Heather Soulen for their enormous efforts on the STORM experiments. Certainly, I would have not been able to do what I accomplish today without them. Special thanks to Melissa Bonner, Sandra Fernandes, Carrie Miller, and Lindsay Whalin for their help during the experiments. I would like to extend my gratitude to Dr. Andrew Heyes and Debby Heyes for teaching me a lot of lab techniques and mercury isotope analysis, and to Christine Bergeron for providing mercury data for the modeling study. Special thanks to my colleagues and friends, both in the past and present, in the Mason lab for their help, advice, and support. I would like to thank Joy Leaner and Auja Sveinsdottir for their friendship. It has been wonderful to be part of the Mason lab and only good memories will remain in my heart forever.

I would like to thank my family and longtime friends in Korea for their unending love, support, and encouragement throughout my study. They have made me laugh, when it was needed, reminded me of our happy memories, and kept me realizing how

grateful I am to have them all in my life. I am also thankful that I have met so many good people and friends throughout my time in USA.

I would like to thank Cherrystone Aqua Farms for providing clams, the crew of *Aquaris* for getting sediments from Baltimore Harbor, and the Analytical Service at CBL for analyzing samples. This research was supported by the Hudson River Foundation (HRF) (grant No. 009-01A) and USEPA STAR program (grant No. R 824850-01-0) as part of the Multiscale Experimental Ecosystem Research Center (MEERC) at the University of Maryland Center for Environmental Science (UMCES).

Table of Contents

List of Tables

List of Figures

Chapter 1: Introduction

1.1. Introduction

Over the last century the mercury (Hg) concentration in estuarine and coastal environments has been increased by human activities with inputs from sources such as urban runoff, industrial effluents, and atmospheric deposition (Mason et al., 1994; Gagnon et al, 1997). The contamination of Hg in estuaries is a concern as most estuarine and coastal environments are in close proximity to urban centers. In addition, they are productive ecosystems and provide an important food source for humans as well as being nursery areas for young fish (Benoit et al., 1998; Mason et al, 1999). Within oxic waters, Hg binds with inorganic ligands (e.g. Cl^-, OH^-) or dissolved organic carbon (DOC), or sorbs to particulate matter. Hg can also be reduced microbially or abiotically to elemental Hg and it is volatilized to the atmosphere as most waters are supersaturated with respect to the solubility of atmospheric elemental Hg (Mason et al., 1994). Within anoxic environments, Hg forms strong aqueous complexes with sulfide and precipitates as HgS or is incorporated with sulfide phases such as acid volatile sulfide (AVS) (Driscoll et al., 1994; Paquette and Helz, 1995; Jay et al., 2000). Hg can be converted to methyl mercury (MeHg) in anaerobic environments by sulfate-reducing bacteria, the important mediators of Hg methylation (Gilmour and Henry, 1992). MeHg, a major

organic form of Hg, bioaccumulates through aquatic food chains more efficiently than inorganic Hg.

The important processes in terms of Hg and MeHg biogeochemical cycling are summarized in Fig.1.1. Sediments are the main repository of Hg in estuaries (Benoit et al., 1998; Wang et al, 1998) and can be a significant source to the overlying water column via various processes including diffusion, resuspension, and bioturbation (Gagnon et al, 1997; Bloom et al., 1999; Mason and Lawrence, 1999; Sunderland et al., 2004; Heyes et al., 2004). In addition, Hg in sediments constitutes an enriched pool potentially available to organisms. Lower trophic levels play an important role in Hg bioaccumulation into fish as the greatest bioconcentration occurs between the water and phytoplankton (Lindqvist et al, 1991; Mason et al., 1996). Elevated MeHg in fish is reported in aquatic environments (Clarkson, 1990; Driscoll et al., 1995; Park et al., 1997). This is of the greatest concern to human health because fish consumption is the major exposure route of MeHg to humans (Clarkson, 1990). The bioavailability of Hg and MeHg to benthic organisms from sediment has been actively investigated, especially as they often dominate the lower trophic level of the aquatic food chain in shallow systems and have the potential to transfer the bioaccumulated Hg and MeHg from sediments to upper levels of the food chain (Gagnon and Fisher, 1997; Wang et al., 1998; Mason and Lawrence, 1999). Benthic animals can be potentially exposed to Hg and MeHg from the pore water/ overlying water and the sediments (solid phase). In addition, the bioavailability of Hg to benthic invertebrates from the sediment can be affected by sediment geochemical factors such as organic content, metal oxide, and sulfide mineral content. Inverse relationships

between Hg bioaccumulation in benthic organisms and organic content in the sediment have been observed (Lawrence et al., 1999; Mason and Lawrence, 1999).

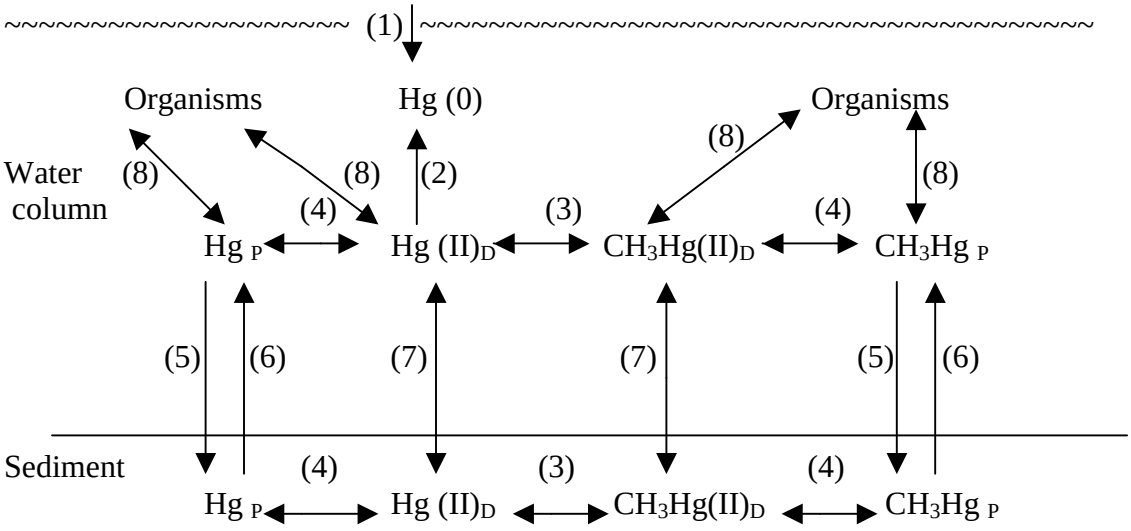

Figure 1.1. Mercury biogeochemical cycling: (1) air-water exchange; (2) reduction; (3) methylation/demethylation; (4) adsorption/desorption; (5) particle settling; (6) resuspension; (7) diffusion; (8) bioaccumulation. Hg(0) : elemental Hg; Hg_P: particulate inorganic Hg; $Hg(II)_D$: dissolved inorganic Hg; CH_3Hg_P: particulate MeHg; $CH_3Hg(II)_D$: dissolved MeHg.

The mobility and bioavailability of Hg and MeHg depend upon the nature and concentration of the binding phases in the sediment, which apparently are controlled by sediment redox status. Hg associates primarily with particulate organic matter and iron/manganese oxides through adsorption and coprecipitation reactions in oxidized sediments while in anoxic sediments, Hg is adsorbed onto and coprecipitated with sulfide minerals (Gobeil and Cossa, 1993; Gagnon et al, 1997; Wang et al, 1998). When metal oxides are reduced Hg can be released into porewater (and eventually to

overlying water via diffusion) or can be removed by adsorption and coprecipitation with sulfide minerals under anoxic conditions. It can also be released as a result of the microbial degradation of organic matter and by chemical dissolution due to redox changes during diagenesis. Very few studies have been published that have incorporated the relative importance of these geochemical factors, in controlling the behavior of Hg and MeHg, in conjunction with physical disturbance of these environments through processes such as sediment resuspension, which will change sediment redox state.

Resuspension is an important process in the cycling of particles and associated nutrients and contaminants at the sediment-water interface (Bloesch, 1995). In estuarine and coastal environments, bottom-sediment resuspension can be caused by natural events (e.g. tidal currents, storm events, and wave-current interaction) and anthropogenic activities (e.g. dredging and trawling) (Schoellhamer, 1996; Sloth et al., 1996). Sediment resuspension takes place when the bottom shear stress is sufficient to disrupt the cohesion of the bottom materials (Evans, 1994). Resuspension is a function of the properties of bottom sediments such as grain size, type of sediments, organic content, and water content. Once particles are resuspended, they tend to resettle by gravity when the shear stress diminishes and this process of resuspension may occur repeatedly (Bloesch, 1995).

Chang (1999) developed a sediment resuspension model that coupled physical processes, including particle transport induced by tidal resuspension, with organic matter degradation above and below the sediment-water interface. This water quality model consisted of a water column, a floc layer of time varying thickness, and a

surface sediment layer characterized by a high degree of chemical and biological activity. The Chang model simulations suggested that resuspension at the sediment-water interface increased the dissolved organic contaminant concentrations, organic matter degradation rates, desorption rates and nitrification in the water column. The model results also indicated that resuspension decreased sediment diffusive fluxes but increased advective fluxes under conditions of continuous tidal forcing, and increased both diffusive and advcetive fluxes if resuspension was induced by storm events only. In addition, resuspension also decreased accumulation (burial flux) and enhanced recycling rates.

Since sediment resuspension in shallow ecosystems controls the movement and redistribution of particles, it could play a major role in the mobility and bioavailability of Hg and MeHg in shallow systems. There is, however, a paucity of information available on the degree to which sediment resuspension influences the fate and bioavailability of Hg and MeHg across the sediment-water interface.

1.2. Background

1.2.1. Sources, fate and biogeochemical cycling of mercury and methyl mercury in estuarine systems

1.2.1.1. Sources of mercury inputs

A variety of anthropogenic activities (e.g. mining, smelting, burning of fossil fuel, waste incineration, and the production of steel, cement, and phosphate) contribute to the increase of Hg levels in the environment. The principal industrial users of Hg are the chlor-alkali industry, the pulp industry, and electrical equipment manufacturers (Lu, 1996). Atmospheric deposition and riverine inputs are typically the primary sources of Hg to aquatic systems with the relative importance of each being a function of: 1) the watershed area to surface area of the waterbody and 2) the magnitude of point source inputs (e.g. urban runoff, industrial effluent inputs) (Wang and Driscoll, 1996; Gagnon et al, 1997; Bloom et al., 1999; Covelli et al., 1999; Mason et al., 1999).

Table 1.1 shows the range in total Hg (THg) concentrations in the water column typically measured in different aquatic systems. The Lower Fox River, Onondaga Lake, and Clay Lake have all received municipal effluent and industrial waste for decades (Hurley et al., 1998; Wang and Driscoll, 1995; Parks et al., 1989). Not surprisingly, the Lower Fox River is listed as an Area of Concern by the USEPA. Concentrations of THg in the bottom sediment as high as 37 nmol g^{-1} have been found in such environments and those of THg in water samples ranged from near-background levels (10 pM or less) to 910 pM with a median of 120 pM. Both Onondaga Lake and Clay Lake received, respectively, approximately 76 tons and 10

tons of Hg discharge from adjacent chlor-alkali plants until 1970. The Patuxent River, a subestuary of the Chesapeake Bay, lies within the suburbs of Washington and Baltimore and 38 % of the drainage basin area is developed, while the Adirondacks Lakes and pristine lakes of Glacier National Park represent lakes relatively remote from direct anthropogenic sources of Hg (Table 1.1). Both receive the majority of their Hg from atmospheric deposition.

Table 1.1. Water column THg concentrations (pM) measured in different aquatic systems.

Aquatic systems	THg	References
The Lower Fox River, Wisconsin	9.0 – 910	Hurley et al. (1998)
Onondaga Lake, New York	13 – 180	Wang and Driscoll (1995)
Clay Lake, Ontario	25 – 400	Parks et al. (1989)
The Patuxent River Estuary, Maryland	2.5 – 30	Benoit et al. (1998)
Baltimore Harbor and the Chesapeake Bay, Maryland	2.5 – 39	Mason et al. (1999)
Adirondacks Lakes, New York	7.0 – 33	Driscoll et al. (1994)
Remote lakes of Glacier National Park, Montana	1.8 – 14	Watras et al. (1995)
San Francisco Bay, California	0.73 – 440	Conaway et al. (2003)
Hudson River Estuary, New York	0.18 - 580	Heyes et al. (2004)

1.2.1.2. Total mercury in the water column

Hg is mostly associated with suspended particulate matter (SPM) in water. The relative affinity of Hg for dissolved and particulate phases is often parameterized by the distribution coefficient (K_d), where Kd = particulate concentration (ng kg^{-1})/ dissolved concentration (ng L^{-1}). A higher K_d value indicates a higher affinity for the particulate phase. Hg has one of the highest K_d values of the heavy metals (Lawson et al., 2001). For a log K_d of 5, more than 75 % of the Hg will be in the particulate phase at 30 mg L^{-1} SPM; for a log K_d of 5.5, > 90% will be particulate at 30 mg L^{-1} SPM. Benoit et al. (1998) observed that in the Patuxent River, the log K_d ranged from 4.8 to 5.7. These values are within a similar range with those found for other coastal water (Stordal et al., 1996).

Coquery et al. (1997) found that the particulate fractions were more than 95 % of the THg in the estuarine mixing zones between freshwater and seawater in the highly turbid Loire and the Seine estuaries, France. Their calculated K_d did not show any relationship with salinity, suggesting that dissolved Hg mainly was associated with organic matter, most likely through thiol complexation (i.e. chlorocomplexes did not seem to play a major role in the Hg distribution). Mason et al.(1999) found that a substantial portion (35 –75 %) of THg was in particulate phase and that 70 – 80 % of the total dissolved Hg was bound to dissolved organic matter in the Chesapeake Bay where SPM ranges from 5 – 30 mg L^{-1} and DOC ranges from 160 – 500 μM. A small fraction of the total dissolved Hg was dissolved gaseous Hg and MeHg, with about 10 % or less of the THg being inorganically bound dissolved ionic Hg. The concentration of THg was higher in the bottom water when oxygen was depleted,

suggesting the release of Hg from the sediment during anoxia via mechanisms discussed above.

1.2.1.3. Methyl mercury in the water column

It has been observed that MeHg concentration is low in freshwater and estuarine systems compared to those of THg (Benoit et al., 1998; Hurley et al., 1998; Monson and Brezonik, 1998; Mason et al., 1999). Benoit et al. (1998) found that MeHg accounted for < 5 % of the THg (unfiltered) and < 2 % of the dissolved Hg (filterable) in the Patuxent River and that the log K_d for MeHg was lower compared to that for Hg, ranging from 3.8 to 4. Mason et al. (1999) found that concentrations of MeHg ranged from the detection limit (0.03) to 1.0 pM (0.28 ± 0.03 pM) in the water column of the Chesapeake Bay, while significantly higher concentrations of MeHg were found in the low oxygen bottom water of Baltimore Harbor. Additionally, a flux experiment with Baltimore Harbor sediments has found that release of MeHg from sediments occurred under anoxic conditions likely due to particulate dissolution (Mason, et al., submitted). Similar patterns of MeHg in the water column under anoxic conditions have been reported in other lakes and estuarine systems (Mason et al., 1993; Regnell et al., 1997; Benoit et al., 1998; Hurley et al., 1998). This suggests that MeHg is either released from the sediment under anoxic conditions or that MeHg production occurs in the water column. With sediment flux chamber deployments in Lavaca Bay, Texas, Gill et al. (1999) found during a diurnal study that MeHg was released into the water column from the sediment as water column dissolved oxygen

decreased at night, suggesting a change in the sediment redox status in the absence of benthic photosynthesis.

1.2.1.4. Total mercury in sediment

As mentioned earlier, sediment is an important sink for Hg. Hg contamination in the sediment, however, is of concern because there are many potential pathways for the Hg to be transported to aquatic food chains, and sediment can also be a significant source of Hg into the overlying water. In estuarine environments, THg concentrations vary from parts per billion (ng g^{-1}) in clean sediments to parts per million (μg g^{-1}) in contaminated zones with MeHg typically accounting for less than 0.5 % of the THg concentrations (Gobeil and Cossa, 1993; Gagnon et al., 1996; Benoit et al., 1998; Conaway et al., 2003; Chapter 5). Table1.2 shows the sediment concentrati on of THg in various regions of the Chesapeake Bay and other east coastal urbanized estuaries. On average, the sediment concentrations of THg in the Baltimore Harbor region fall within the same order as other east coastal estuaries, which contain large urban environments and harbors. While some of these other regions show extremely elevated sediment concentration of Hg, this is not the case for Baltimore Harbor. In terms of the perceived environmental impact, Boston Harbor ranks highest followed by the Hudson River and Baltimore Harbor as determined by the U.S. EPA tier system ranking (Mason and Lawrence, 1999). In addition, there was a decline in the concentration of Hg from north to south of the Chesapeake Bay (Chapter 5).

Table 1.2. Chesapeake Bay regions and a number of coastal sediments concentrations for THg.

Sites	THg (nmol g^{-1}) Mean	References
Mainstem of the Chesapeake Bay	0.4 ± 0.5	This study (Chapter 5)
Hart-Miller Island, MD	0.8 ± 0.4	This study (Chapter 5)
Baltimore Harbor/Gunpower-Patapsco, MD	1.7	Mason and Lawrence, 1999
Boston Harbor/Charles River, MA	3.0	Mason and Lawrence, 1999
Hudson River, NY-NJ	5.0	Heyes et al., 2004
San Francisco Bay, CA	1.0	Conaway et al., 2003
Long Island Sound, NY	0.2 – 1.7	Hammerschmidt and Fitzgerald, 2004

Gobeil and Cossa (1993) found that the pore water concentration for Hg was low near the sediment surface but increased to a maximum at about 5 cm depth with a decreasing concentration in deeper sediments. They also observed the coincidental increase of iron and Hg, suggesting that the Hg released into the pore water could be related to the solubility changes of iron oxide/hydroxides as a result of low oxygen conditions. These oxides are insoluble in oxic environments but are solubilized in suboxic and anoxic conditions. Gobeil and Cossa (1993) also suggested that the decrease in dissolved Hg below 5 cm depth in the sediment core accounted for the coprecipitation of Hg with iron sulfides. Similar results were also found in the Gulf of Trieste, Northern Adriatic Sea (Covelli et al., 1999) and in Lavaca Bay, Texas (Bloom et al., 1999). Overall, depending on the redox conditions, Hg is scavenged by iron oxides either directly or indirectly via the adsorption of organic carbon to oxides or released to the pore water as iron oxides are solubilized under suboxic conditions. Under anoxic conditions, insoluble iron sulfide species form removing iron from solution. Thus, there is a resulting peak in pore water iron in the oxic-anoxic

transition zone. Depending on sediment conditions, there may be an associated peak in Hg or MeHg in this region. Thus, the formation of insoluble metal sulfides inhibits the metal release from the sediment. Bloom et al. (1999) found that in the pore water (Lavaca Bay, Texas) below 4 cm, the concentration of inorganic Hg increased with the concentrations of dissolved sulfide and DOC in the pore water, suggesting that the mobility of inorganic Hg was controlled by the formation of soluble polysulfides or soluble organic complexes.

1.2.1.5. Methyl mercury in sediment

Despite the low percent of MeHg in estuarine sediments, MeHg is the form of Hg that is most toxic and bioaccumulates most efficiently due to its capability of passing the biological membrane, its high chemical stability and slow excretion from most organisms (Regnell and Ewald, 1997). Recent studies have shown that *in situ* MeHg production is a significant source to estuarine environments (Mason et al, 1999; Sunderland et al., 2004; Hammerschmidt and Fitzgerald, 2004; Balcom et al., 2004). Benoit et al. (1998) reported that THg, sulfide, and organic matter were the factors most related to the percent of MeHg in the Patuxent River sediments. They found that there was a weak positive relationship between the concentrations of THg and MeHg ($r^2 = 0.61$, $p = 0.05$). Both THg and MeHg concentrations were correlated with organic matter. This is consistent with the observation of a positive relationship ($r^2 = 0.61$, $p < 0.05$, $n = 36$ for MeHg; $r^2 = 0.60$, $p < 0.05$, $n = 36$, for THg) between organic content and the concentration of MeHg and THg in the mainstem of the Chesapeake Bay (Chapter 5).

Bloom et al. (1999) and others have found that MeHg is less strongly bound to the solid phase (a mean log K_d of 2.7 ± 0.8) compared to inorganic Hg (a mean log K_d of 4.9 ± 0.4). They also observed that the K_d values for MeHg were low at the depths where the dissolved iron concentration was maximum. Covelli et al. (1999) also found that the concentration of MeHg in the pore water increased with the dissolved iron concentration below the subsurface but decreased toward surficial oxic layers. These results support the proposal that the oxic surficial sediment layer may act as a barrier to diffusion of dissolved MeHg to the overlying water (Gagnon et al., 1996). As mentioned earlier, Gill et al. (1999) observed a strong diurnal flux of MeHg from Lavaca Bay, Texas sediment into the overlying water during dark periods, suggesting that the sediment-water exchange of MeHg was strongly mediated by sediment redox status, as determined by the microbial activity in sediments. Responding to the photosynthetic and respiratory activity of benthic organisms, the redox boundary migrates diurnally. As a result, it is postulated that MeHg, adsorbed onto iron oxides (either directly or through association with adsorbed organic matter) under oxic conditions, can be released into solution as iron oxides are reduced under anoxic periods. However, diffusion is not the only mechanism for transferring Hg and MeHg from sediments to the water column. While diffusive fluxes may be small under oxic conditions because MeHg is bound to oxide phases, Gagnon et al. (1996) suggest that benthic organisms such as worms and amphipods that assimilate MeHg in the anoxic sediment can be important vectors of MeHg to benthic predators. Additionally, processes such as bioturbation and physical mixing can enhance the transfer of Hg and MeHg from the sediment to the water column.

1.2.2. The role of sediment geochemistry and resuspension in the mobility and bioavailability of mercury and methyl mercury

As discussed earlier, in the oxic environment, there is a competition between the oxide phases and the organic phases for the binding of Hg and MeHg. However, complexation to organic matter via thiol ligands becomes dominant as the relative concentration of thiol ligands increases with the dissolution of oxide phases in reduced environments or because of competition between phases in high organic carbon or low iron environments. At higher sulfide concentrations, as Benoit et al. (1999a) suggested, complexation of inorganic Hg to sulfide in anoxic pore water was more important than complexation to dissolved organic carbon. The model of Benoit et al. (1999a) included the binding of Hg to reduced sulfide solid phases, although it was not identified whether these phases were inorganic (e.g. FeS, FeS_2) or organic compounds containing thiol groups. Typically, however, in surface sediments there are both the reduced (e.g. FeS/AVS) and oxidized solid iron phases coexisting and thus the association of Hg and MeHg is complicated and depends on the relative concentrations of iron, AVS, and organic carbon (Mason and Lawrence, 1999).

Lawrence and Mason (2000) developed a simple bioaccumulation model to examine the relative importance of various uptake routes for amphipods (e.g. water, pore water, in-place sediment, and food). The model was constructed using the results from laboratory experiments (e.g. sediment exposure assays with amphipods and water only exposure experiments). Bioaccumulation factors were determined to be a function of the organic carbon of the medium. The model developed was applied to data obtained from Lavaca Bay, Texas. The model results suggest that the sediment

and fresh algal matter were the most important sources to the amphipods and that uptake from either overlying water or porewater was small. At high organic matter, the sediment bioaccumulation factor (BSAF) was small, indicating that MeHg was tightly bound to organic matter and relatively less bioavailable. Given the importance of the solid phase as a source of Hg and MeHg to benthic organisms, processes that alter particle distribution and fate, such as resuspension, may have an important impact on bioaccumulation.

1.2.3. The effect of resuspension on mercury methylation

The effect of resuspension on Hg methylation is difficult to quantify because it will depend on a variety of variables. The methylation of Hg depends upon environmental factors that control the overall metabolic activity of the methylating organisms and the bioavailability of Hg in the matrix where methylation occurs. As the supply of organic carbon enhances the Hg methylation rate (Choi and Bartha, 1994), the distribution of methylation activity is dependent upon the distribution of biodegradable organic matter. Thus, maximal methylation rates are often observed in biologically active surface sediments (Callister and Winfrey, 1986; Korthals and Winfrey, 1987).

Sulfate can stimulate both sulfate reduction and Hg methylation by sulfate reducing bacteria at relatively low sulfate concentrations (Gilmour and Henry, 1991). However, high concentrations of sulfate, such as found in estuarine and marine environments, enhance pore water dissolved sulfide and thereby inhibit Hg methylation (Compeau and Bartha, 1983; 1987; Gilmour et al., 1998; Benoit et al.,

1998). Benoit et al. (1999a) developed a chemical equilibrium model to test the hypothesis that the bioavailability of Hg to sulfate reducing bacteria was a function of the concentration of neutral Hg sulfide complexes that can readily diffuse across the bacterial membrane. The model results suggest that as sulfide increases, the dominant Hg speciation changes from neutral dissolved Hg complexes (e.g. HgS (aq)) to charged sulfide complexes and thus, bioavailability to bacteria decreases. Octanol-water partition experiments (Benoit et al., 1999b) and culture experiments (Benoit et al., 2001) have confirmed this hypothesis.

Thus, resuspension may enhance methylation by decreasing sulfide levels, but it may also limit methylation if sediments become too oxic by limiting the activity of sulfate reducing bacteria. Further, resuspension can change the availability of organic carbon to sulfate reducing bacteria and thus further influence bacterial activity. In addition, demethylation occurs primarily under oxygenated conditions (Matilainen and Verta, 1995). Higher demethylation rates were observed in oxygenated sediments than in anoxic sediments (Compeau and Bartha, 1984). Marvin-Dipasquale and Oremland (1998) found during their incubation experiments with sediments from the Florida Everglades that oxidative demethylation in all samples was an important degradation mechanism. Thus, resuspension may enhance the demethylation of MeHg by introducing oxygenated conditions to anoxic environments.

1.2.4. The novelty of the proposed research

There have been a number of laboratory studies demonstrating that resuspension of sediments results in the release of organic contaminants, such as PAHs and PCBs (Latimer et al., 1999), as well as trace metals, such as Mn, Fe, Zn, Cu, and Cd, into overlying water (Calvo et al., 1991; Petersen et al., 1997; Laima et al., 1998). In contrast, Brassard et al. (1997) concluded from their small reactor experiment that surficial sediments were not significant sources of trace metals into water column when resuspended. They postulated, however, that this might not be applicable to anoxic sediments from deeper layer because of the potential for oxidative release of metals. Bloom and Lasorsa (1999) found from their laboratory mixing experiment that approximately 5 % of the sediment bound MeHg and less than 1 % of THg were released upon shaking with seawater.

Overall, the previous laboratory experiments have been limited as they failed to mimic nature (i.e. both realistic bottom shear stress and water turbulence). In nature, resuspension typically removes only mm of surface sediments and therefore the experiments in the laboratory likely overestimate the potential for anoxic sediments being resuspended into the water column. Most laboratory experiments were run for no more than 24 hours. This likely results in an incorrect assessment of partitioning between particle and dissolved fractions because the sorption processes can be quite slow (Chang, 1999). Thus, it is not possible to extrapolate from the small scale of these laboratory studies to natural conditions. In a laboratory experiment for partitioning of radioactive trace metals between seawater and particulate matter, Nyffeler et al. (1984) found that for group 1 elements (e.g. Na, Zn, Se, Sr, Cd, Sn, Sb,

Cs, Ba, Hg, Th and Pa) constant distribution coefficients were reached after 2-3 days of equilibrium. They also found that group II elements (e.g. Be, Mn, Co, and Fe) showed an increasing distribution coefficient over the whole observation time (108 days). Thus, the previous laboratory resuspension experiments may not represent what occurs in terms of partitioning under long-term steady state conditions. In addition, none of the previous studies have assessed the impact of resuspension on Hg fate and transport and how it would affect bioaccumulation of Hg and MeHg to organisms inhabiting the sediment-water interface.

Interest in bioaccumulation of Hg and MeHg by benthic organisms stems from public health concerns because these organisms serve as essential links for higher levels of the food chain, such as fish and larger invertebrates. As mentioned earlier, fish consumption is the major exposure route to humans (Clarkson, 1990). Benthic invertebrates can be exposed to Hg and MeHg from both dissolved phase (e.g. overlying water and pore water) and sediments (Fisher et al., 1996; Gagnon and Fisher, 1997; Lawrence and Mason, 2001). Kinetic models have been developed to effectively and quantitatively separate uptake pathways of contaminants by aquatic organisms (Thomann et al., 1995; Morrison et al., 1997; Wang et al., 1998; Fisher et al., 2000; Roditi et al., 2000). The previous models, however, did not include physically induced processes such as resuspension that can be a significant factor in the bioaccumulation of Hg and MeHg into benthic animals. As mentioned earlier, resuspension could increase the bioavailability of Hg and MeHg to these organisms via release from the sediments, and could also alter methylation within the sediments.

This dissertation research is different from the previous studies in that 1) a new experimental design, that has been successfully developed to produce both realistic bottom shear stress and water column turbulence (Porter et al., 2000), was used in the bioaccumulation studies; and 2) long-term (4 weeks) resuspension experiments were conducted to examine how resuspension would affect the mobility and bioavailability of Hg and MeHg. To integrate the resuspension experiments and the other studies, a bioaccumulation model was developed that included sediment resuspension and the dynamics of adsorption/desorption between dissolved and particulate phases, and other processes.

1.3. Hypotheses

The research was driven by the following hypotheses:

1) Resuspension through a series of direct and indirect interactions decreases MeHg sediment concentration but increases MeHg flux at the sediment-water interface; and
2) Resuspension will lead to an enhancement of MeHg accumulation into higher trophic level organisms.

More specifically, it is postulated that long-term resuspension may increase the dissolved Hg and MeHg in the water column due to oxidation of sulfide phases and other processes enhancing desorption. This enhanced concentration can lead to an increased uptake of Hg and MeHg into algae, the preferred food of the filter feeding benthic organisms. In addition, resuspension likely decreases the productivity but

increases the consumption of microphytobenthos by filter feeders. Additionally, by recycling and resupplying organic mater to the surface sediment, resuspension may also increase bioaccumulation into surface deposit feeders. While short term resuspension may increase the methylation due to partial oxidation of sediments thereby decreasing pore water sulfide gradients, upon longer term resuspension, the methylation may decrease in the surface layers due to the removal of organic material, the inhibition of benthic algal formation, and the decrease in sulfate reducing bacterial activity. Also, sediment oxygenation likely increases demethylation. It is hypothesized that the increase in the flux of Hg and MeHg from sediments and the increased bioavailability of sediment Hg and MeHg that can result from resuspension may negate any impact of resuspension on methylation activity. Finally, given the strength of binding of Hg and MeHg to various sedimentary phases, it is postulated that resuspension, by oxygenating surface sediment, likely results in an increase in the bioavailability of solid phase sediment Hg and MeHg to benthic organisms. Overall, the complexity of such interactions is difficult to ascertain from simple experiments and thus, the mesocosm studies, in conjunction with modeling, provided a unique mechanism to investigate these complex direct and indirect effects.

1.4. Objectives

To test these hypotheses, the objectives of this dissertation research were to:

1) investigate using mesocosms the long-term effects of resuspension on the fate and bioaccumulation of Hg and MeHg in shallow systems;
2) develop a bioenergetic-based model including the effects of resuspension to assess MeHg bioaccumulation in shallow systems;
3) calibrate the bioaccumulation model by comparing the model results to data from the mesocosm study, and then apply the model to field situations to estimate the potential impact of resuspension of MeHg bioaccumulation into benthic and pelagic organisms in representative shallow water environments; and
4) examine the spatial distribution of Hg and MeHg in the sediments from the Chesapeake Bay and the important controlling factors in determining Hg and MeHg concentrations and their bioaccumulation.

This thesis is composed of 4 chapters examining the objectives above. Chapter 2 and 3 present two mesocosm experiments conducted in July and October of 2001. There were two treatments (resuspension vs. no-resuspension) and three replicates without clams (experiment 1) and with clams (experiment 2). Chapter 4 describes the model development, calibration, and model results in comparison with the data in experiment 2. Chapter 5 includes model applications examining the impact of running the model for a longer period, with different sediment organic contents, and with THg

and MeHg concentrations as found in the sediments of the Chesapeake Bay. Finally, Chapter 6 summarizes the overall results and conclusions of this study.

In Chapter 2, water column data are presented from both experiment 1 and 2. The data include THg and MeHg concentrations in both particulate and dissolved phases as well as total suspended solids (TSS), particulate matter (POM), DOC, and phytoplankton biomass. The relationships between THg/MeHg concentrations and other variables (e.g. TSS, POM, DOC) are presented and discussed. In addition, the effects of sediment resuspension on Hg partitioning in the water column are discussed.

Chapter 3 examines the effects of resuspension on the fate and bioaccumulation of THg and MeHg in experiments 1 and 2. The results are mostly focused on THg and MeHg dynamics in sediments as well as bioaccumulation into benthic and pelagic organisms. The effects of resuspension on Hg methylation and demethylation are also discussed. The relationships between THg and MeHg concentrations, as well as AVS and organic matter in sediments are discussed. Important factors in controlling Hg and MeHg bioaccumulation are also examined.

Chapter 4 models MeHg bioaccumulation into benthic and pelagic organisms. The model development and calibration are described and the model results are calibrated with the data in experiment 2. Different model scenarios are described and the model results are presented. The model applications include the effects of clams on phytoplankton and zooplankton biomass and MeHg accumulation into biota. Important parameters in controlling biomass and subsequent MeHg concentration in biota are examined and discussed using sensitivity analysis of the model parameters.

Chapter 5 investigates the spatial distribution and bioaccumulation of THg and MeHg in the Chesapeake Bay region including the mainstem of the Bay, Baltimore Harbor, and its vicinities (e.g. the Hart-Miller Island [HMI]; Dredge Material Contaminant Facility). This chapter discusses the controlling factors in the distribution of THg and MeHg in sediments and the controlling factors in the transport and bioaccumulation of THg and MeHg. The chapter focuses on the role of organic content in sediments in determining THg and MeHg concentrations in sediments and bioaccumulation into benthic and pelagic organisms. Additionally, representative Chesapeake Bay conditions are used in the model, and the model is simulated over a longer period, to examine the effect of organic content and Hg methylation on MeHg bioaccumulation and burden in biota.

Finally, Chapter 6 summarizes the overall conclusions of the mesocosm experiments, field studies and modeling studies. Model limitations and further applications are included in this chapter. Implications and suggestions for future study are also discussed.

Chapter 2: The effect of resuspension on the fate of total mercury and methylmercury in a shallow estuarine ecosystem: A mesocosm study

2.1. Introduction

Estuaries provide an essential link in the global biogeochemical cycling of mercury between the terrestrial and the marine environment. Similar to other metals, only a small fraction of the mercury transported in rivers is exported to the ocean due to the high retention of mercury in estuarine environments (Cossa et al., 1996; Benoit et al., 1998; Mason et al., 1999), mainly as a result of sediment burial. Sediment resuspension is an important process for re-introducing metals into the water column and in the cycling of particles and associated nutrients and contaminants at the sediment-water interface (Bloesch, 1995). In estuarine and coastal environments, bottom-sediment resuspension can be caused by natural events (e.g. tidal currents, wind waves, storm events, and wave-current interaction) (Sanford et al., 1991; Arfi et al., 1993) and anthropogenic activities (e.g. dredging and trawling) (Schoellhamer, 1996; Lewis et. al., 2001). Sediment resuspension takes place when the bottom shear stress is sufficient to disrupt the cohesion of the bottom materials (Evans, 1994).

Resuspension is a function of the properties of bottom sediments such as grain size, type of sediments, organic content, and water content. Once particles are resuspended, they tend to resettle by gravity when the shear stress diminishes and this process of resuspension may occur repeatedly (Bloesch, 1995).

Since resuspension of sediments in shallow aquatic ecosystems controls the movement and redistribution of particles, it can play a major role in the mobility and bioavailability of trace metals in these systems. For example, Simpson et al. (1998) observed in a laboratory experiment that during an 8-h resuspension, acid volatile sulfide (AVS) decreased to values lower than the concentrations of simultaneously extracted metals (SEM), suggesting that a significant fraction of metal sulfide phases were oxidized. As trace metals are likely associated with FeS phases either through coprecipitation or adsorption, these metals may be released as the FeS phases are oxidized and released, in concert with the oxidized sulfur species, to the overlying water. Thus, resuspension can act as a potential source of toxic metals to the water column, increasing the potential metal bioavailability. The released metal may, however, be quickly scavenged by or coprecipitated with iron and manganese oxides or complexed to organic matter. While studies have focused on other metals, to date there is a paucity of information available on the fate of mercury and methyl mercury during resuspension, or on their potential release from reduced sulfide phases upon resuspension.

A number of laboratory studies have demonstrated that resuspension of sediments results in the release of organic contaminants, such as PAHs and PCBs (Latimer et al., 1999), as well as trace metals, such as Mn, Fe, Zn, Cu, and Cd, into

overlying water (Calvo et al., 1991; Petersen et al., 1997; Laima et al., 1998). In contrast, however, Brassard et al. (1997) concluded from their small reactor experiment that surficial sediments were not significant sources of trace metals into the water column when resuspended. They postulated, however, that this might not be applicable to anoxic sediments from deeper layers because of the potential for oxidative release of metals. However, the degree to which this may occur in the environment is limited.

Overall, the previous laboratory experiments have been limited as they failed to mimic nature (i.e. both realistic bottom shear stress and water turbulence) (Porter et al., 2003), have been of short duration and have used high suspended sediment: water ratios greater than found in nature. Thus, it is not possible to extrapolate from the small scale of these laboratory studies to natural conditions. The objective of this study was, therefore, to investigate the effect of sediment resuspension on the fate and bioavailability of total mercury (THg) and methylmercury (MeHg) using the new STORM (high bottomS hear realistic water column Turbulence Resuspension Mesocosm) facility designed and developed by Elka Porter (Porter, 1999; Porter et al., 2004b). The experimental system can mimic both realistic bottom shear stress and water column turbulence. We conducted two experiments, one in July (experiment 1) and the other in October of 2001 (experiment 2). In experiment 1, no benthic macrofauna were introduced to the mesocosms while in experiment 2, hard clams, *Mercenaria mercenaria,* were added to the sediment in the mesocosms. Experiment 2 was aimed at investigating the effect of resuspension on the bioavailability of Hg and its bioaccumulation into clams, as well as the methylation and demethylation of Hg in

the sediment. In this chapter, however, the fate of Hg in the water column will be specifically discussed. A companion chapter will discuss the sedimentary dynamics of THg and MeMg and their bioaccumulation in zooplankton and clams (Chapter 3, Kim et al., submitted).

2.2. Material and methods

2.2.1. Mesocosm set-up

Muddy surface sediment was collected from Baltimore Harbor in the spring of 2001 and transferred to a fiberglass holding tank and prepared for each experiment following techniques developed in Porter (1999). The sediment was covered with a black plastic sheet for defaunation (4 days) and it was kept in the holding tank until the experiment. After the top 10 cm layer of sediment was scooped off to remove any remaining live macrofauna, the sediment was transferred to six STORM tanks ($1m^2$ sediment surface area). The sediment was mixed thoroughly and flattened. Ambient water from the mouth of the Patuxent River, a subestuary of the Chesapeake Bay, Maryland, USA, was filtered through filtration units (pore size 0.5 μm absolute) and carefully added into the tanks to a depth of 20 cm above the sediment surface without any disturbance of the sediment layer. The mesocosms then underwent an equilibration period (about 2 weeks) with the water column oxygenated by bubbling. During this period, 50 % of water was exchanged daily with filtered ambient water. The final sediment depth was about 10 cm after the equilibration period. After this period, unfiltered ambient water from the Patuxent River was added to the tanks (total

volume of 1000 L) without any sediment disturbance. There were 3 replicates of resuspension (R) and no resuspension (NR) mesocosms set up for the experiments. Tidal resuspension (4 h on and 2 h off-cycles) was simulated using the STORM tank mixing design. In both R and NR tanks, water turbulence intensity was similar and water mixing was set to have 4 h on- and 2 h off cycles in both tanks. Thus, there were both sediment resuspension and water turbulence in the R tanks while there was water turbulence only in the NR tanks. Water was exchanged daily at a rate of 10 % of the total volume with filtered Patuxent River water to mimic the flushing time scale of the Chesapeake Bay. In addition, water exchange was always performed near the end of the off-phase in order to minimize particle loss in the R tanks.

The sediment in the mesocosms was transferred to the holding tank after experiment 1 and stored until the next experiment. Experiment 2 was basically set up in a similar manner as experiment 1. However, a scaled population of about 50 ca 40 mm long clams, *M. mercenaria*, was placed into the sediment individually by hand after the sediment equilibration period. Hard clams were allowed to bury themselves into the sediments overnight. Those clams that had not buried themselves by the next morning were collected and discarded and replaced with new clams. New clams that again had not buried themselves by the next morning were removed and not replaced. Since negative effects (e.g. inhibition of feeding rate, burrowing, growth, and survival of juveniles and adults) on clams result from salinities below 15 ppt (Grizzle et al., 2001 and references therein), salinity was maintained approximately 19 ppt throughout experiment 2, compared to a salinity of around 14 ppt for experiment 1.

2.2.2. Sample collection

Water samples were collected every 2-3 days during the on-cycle (sediment resuspension in the R tanks) by siphoning water from 50 cm below the surface by gravity flow into a sample bottle. Additionally, on three occasions samples were collected after the cessation of resuspension in all tanks. Water samples were taken separately for Hg and other variables such as TSS, dissolved organic carbon (DOC) and Chlorophyll *a* (Chl *a*). All sample bottles for Hg were Teflon and were acid-cleaned according to our established protocols before use (e.g. Mason et al., 1999). Water samples were filtered onto 0.4 μm polycarbonate filters for particulate THg and MeHg. The filters were then stored double bagged and frozen until subsequent digestion and analysis. The filtrate was collected for dissolved THg and MeHg in acid-cleaned Teflon bottles and kept frozen. For TSS and particulate organic matter (POM), samples were filtered through pre-weighed 0.7 μm Whatman GF/F glass fiber filters. POM was calculated from loss on ignition at 450 °C for 4 h after the samples had been dried. The samples for Chl *a* and DOC were filtered in the same way as mentioned above and were sent to the Analytical Service at CBL for analyses.

2.2.3. Sample analyses

2.2.3.1. Total mercury

The filtrates were thawed and oxidized with bromine monochloride (BrCl) for 1/2 - 1 h while the particulate filter samples were digested in a solution of 7:3 sulfuric acid: nitric acid in Teflon vials in an oven at 60 °C overnight prior to BrCl oxidation. For all samples, excess oxidant was neutralized with 10 % hydroxylamine hydrochloride prior to analysis (Bloom and Crecelius, 1983). The samples were then reduced by tin chloride, sparged, and the elemental Hg trapped on gold traps. Quantification was done by dual-stage gold amalgamation/Cold Vapor Atomic Florescence detection (CVAFS) (Bloom and Fitzgerald, 1988) in accordance with protocols outlined in EPA method 1631 (EPA, 1995). A calibration curve with an r^2 of at least 0.99 was achieved daily. Detection limits for THg were based on three standard deviations of blank measurements (digestion blanks for filters and $SnCl_2$ bubbler blanks for filtered water). The detection limits for THg were 0.2 pmol g^{-1} for filters and 0.4 pmol l^{-1} for filtered water. Analysis of duplicate samples yielded an average relative percent difference (R D) of less than 20 %. A recovery of estuarine sediment standard reference material (IAEA-405) was greater than 85 %.

2.2.3.2. Methylmercury

Details of the analytical protocols are given elsewhere (Mason et al., 1999; Mason and Lawrence, 1999). Briefly, samples were distilled with a 50 % sulfuric acid/ 20 % potassium chloride solution (Horvat et al., 1993). A sodium tetraethylborate solution was added to the distillate to convert the nonvolatile MeHg to gaseous

methylethylmercury (Bloom, 1989). The volatile adduct was then purged from solution and recollected on a graphitic carbon column at room temperature. The methylethylmercury was thermally desorbed from the column, and analyzed by isothermal gas chromatography with CVAFS. This method was used for the analysis of MeHg in both filters and water. A calibration curve with an r^2 of at least 0.99 was achieved daily. Detection limits for MeHg were based on three standard deviations of distillation blanks. The detections for MeHg were 0.005 pmol g^{-1} for filters and 0.09 pmol l^{-1} for filtered water. Spike recoveries for MeHg were 92 ± 18 % for filters and 86 ± 18 % for filtered water.

2.2.4. Statistics

The data of all the sampling days in each system were averaged for statistical analysis. The data analysis was performed using ANOVA to test if there was a significant difference between two treatments (R vs. NR). Data were checked for normality and equal variances and log-transformed if necessary. A nonparametric test (Wilcoxon Test) was performed when the assumption of equal variances was not met. Correlation coefficient (r) was obtained using Pearson product-moment correlation to see if there was a linear relation between variables. All the statistical results were reported as significant at a level of $p < 0.05$. We used JMP®, version 4 by SAS institute Inc., Cary, NC, USA for all the statistical analyses.

2.3. Results and discussion

2.3.1. Experiment 1 (without clams)

2.3.1.1. Water column characteristics

As seen in Fig. 2.1a, TSS in the R tanks was significantly higher during resuspension, averaging 150 ± 27 mg l^{-1} than that in the NR tanks (10 ± 0.2 mg l^{-1}) throughout the experiment period (28 days). As mentioned earlier, experiment 1 started with unfiltered ambient water from the Patuxent River. Thus, TSS in the NR tanks represented particles from the Patuxent River and *in situ* production during the course of the experiment. Over time, TSS in the R tanks showed a slight decrease for the initial two weeks but tended to increase toward the end of the experiment. It should be noted, however, that the R system was accidentally shut off on the 20^{th} day and all the R tanks were not disturbed overnight. The arrow in Figure 2.1a shows when the system was down. As mentioned above, there were three additional samplings during the off-cycle in accordance with the on-cycle sampling to assess changes in parameters during the non-resuspension phase (day 12, 18, and 25). Average TSS and other variables during the non-resuspension phase were only compared to the resuspension phase on those corresponding days. Although these data are not shown in the figures, average values (n = 3) are discussed in the text only when there is a significant difference between the two cycles for all the variables. In that case, average values only for the off-cycle (non-resuspension) were given, as those for the on-cycle (n = 3) were similar to average values for the entire sampling period (n = 11). Average concentration of TSS in the R tanks decreased significantly during the off-cycle (20 ± 1 mg l^{-1}, n = 3), compared to the on-cycle.

Similarly, POM was significantly higher in the R tanks than the NR tanks, averaging 22 ± 3 and 5.4 ± 0.1 mg l^{-1}, respectively (Fig. 2.1b). Average POM decreased significantly in the R tanks during the off-cycle (5.2 ± 0.2 mg l^{-1}, n = 3), compared to the on-cycle. The result confirms that POM was introduced to the water column as TSS increased during resuspension events. There was a significant positive correlation between TSS and POM in the R tanks (r = 0.99, n = 33) as well as in the NR tanks (r = 0.90, n = 33). However, average % POM was significantly higher in the NR tanks (53 ± 1 %) than the R tanks (18 ± 0.9 %) (Fig. 2.1b). While POM in the R tanks decreased during the off-cycle, there was a significant increase in % POM (26 ± 2 %, n = 3) in the R tanks, compared to the on-cycle. This was because the large amount of sediment particles, which were transferred to the water column during resuspension events, settled rapidly during the off-cycle. In addition, the higher % POM in the NR tanks was partially due to a relatively higher fraction of phytoplankton and zooplankton, compared to the R tanks (Appendix I). Average ratios of phytoplankton and POM were 0.2 ± 0.1 in the R tanks and 0.3 ± 0.2 in the NR tanks, respectively (Fig. A in Appendix I). In addition, average ratios between zooplankton and POM were 0.02 ± 0.01 (R) and 0.2 ± 0.1 (NR), respectively (Fig. B in Appendix I).

In both systems, two distinct phytoplankton “blooms” occurred during the experiment with an earlier bloom in the NR tanks, compared to the R tanks (Fig. 2.1c). Chl *a* in the R tanks was significantly higher on average than the NR tanks, averaging 24 ± 2 and 13 ± 0.9 μg l^{-1}, respectively. These results appear counter-intuitive to expectation (i.e. increased turbidity would result in a reduction of primary

productivity). In corroboration, Wainright (1987) also found that planktonic microbial growth was stimulated by resuspended sediments. In addition, other studies have demonstrated that sediment microbial production (e.g. benthic bacteria and microalgae) and settled phytoplankton are transferred to the water column during resuspension (Wainright, 1990). However, it appears that this is not the case for our experiment as Chl *a* during the on-cycle was not significantly different from that of the off-cycle, suggesting that benthic phytoplankton were not transferred to the water column to any significant degree as resuspension occurred. Sloth et al. (1996) similarly found in their mesocosm experiment that less than 2 % of the benthic algal chlorophyll was transferred to the water column during the resuspension period (2 h). While there were significant correlations between Chl *a* and TSS ($r = 0.56$, $n = 33$) as well as POM ($r = 0.62$, $n = 33$) in the NR tanks, there was no correlation found in the R tanks. This also supports the contention that benthic phytoplankton was not transported to the water column in any substantial way as resuspension occurred.

DOC in the NR tanks was significantly higher than in the R tanks, averaging 280 ± 3 µM (NR) and 240 ± 8 µM (R) during the on-cycle (Fig. 2.1d). There are no data available during the off-cycle. The range in DOC falls well within the range found in the Chesapeake Bay (160 – 500 µM) where TSS varies from 5 – 30 mg l^{-1} (Mason et al., 1999). As mentioned earlier, the higher biomass of zooplankton may explain the higher DOC in the NR tanks because DOC can be produced by zooplankton excretion. In fact, Park et al. (1997) found a significant correlation between labile DOC production rates and zooplankton densities in their outdoor continuous flow-through pond experiment.

Table 2.1 presents the water chemical characteristics measured daily (during the on-cycle) over the experiment period. The salinity and temperature were similar in both systems. DO and pH in the NR tanks were higher than those in the R tanks.

Table 2.1. Average and standard deviation for ancillary parameters in the water column of the R and NR tanks during the course of experiment 1 and 2.

	Parameters	R	NR
Experiment 1	DO (mg l^{-1})	5.7 ± 1.2	8.5 ± 1.5
	Salinity (ppt)	14 ± 0.3	14 ± 0.3
	Temperature (ºC)	25 ± 1.2	25 ± 1.3
	pH	7.7 ± 0.2	8.1 ± 0.3
Experiment 2	DO (mg l^{-1})	6.7 ± 0.8	8.2 ± 1.3
	Salinity (ppt)	19 ± 0.2	19 ± 0.2
	Temperature (ºC)	20 ± 1.9	20 ± 2.0
	pH	7.5 ± 0.3	7.8 ± 0.2

Figure 2.1. Average concentrations of the following variables in the R and NR tanks (experiment 1). (a) TSS concentration. (b) POM and % POM. (c) Chl *a* concentration. (d) DOC concentration.

Error bars show standard deviations of 3 replicates in each system.

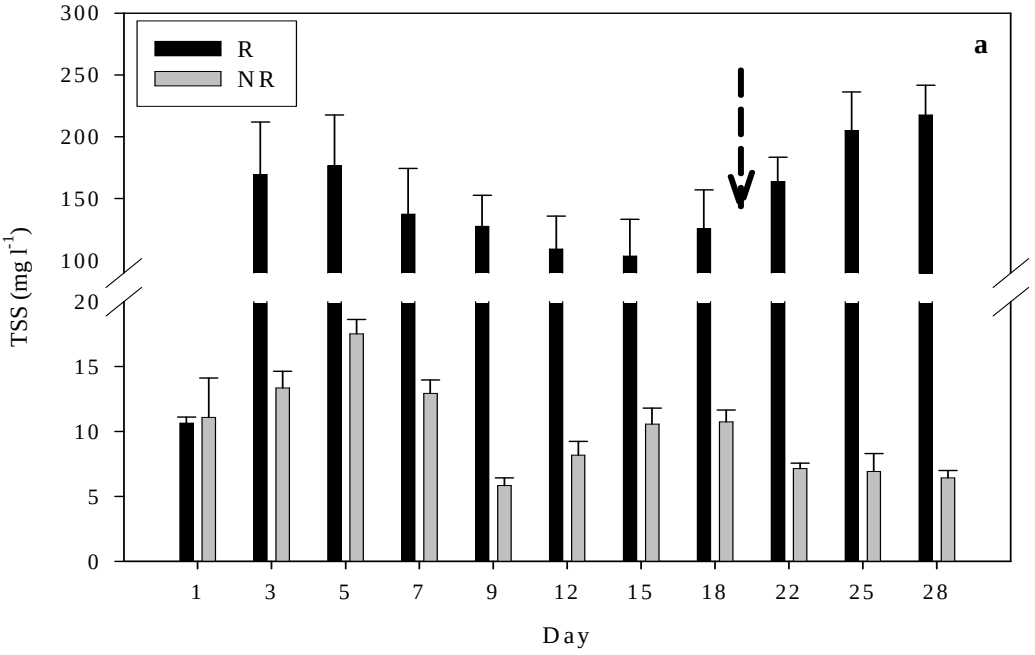
a
R
NR
TSS (mg l-1)
300
250
200
150
100
20
15
10
5
0
1
3
5
7
9
12
15
18
22
25
28
Day

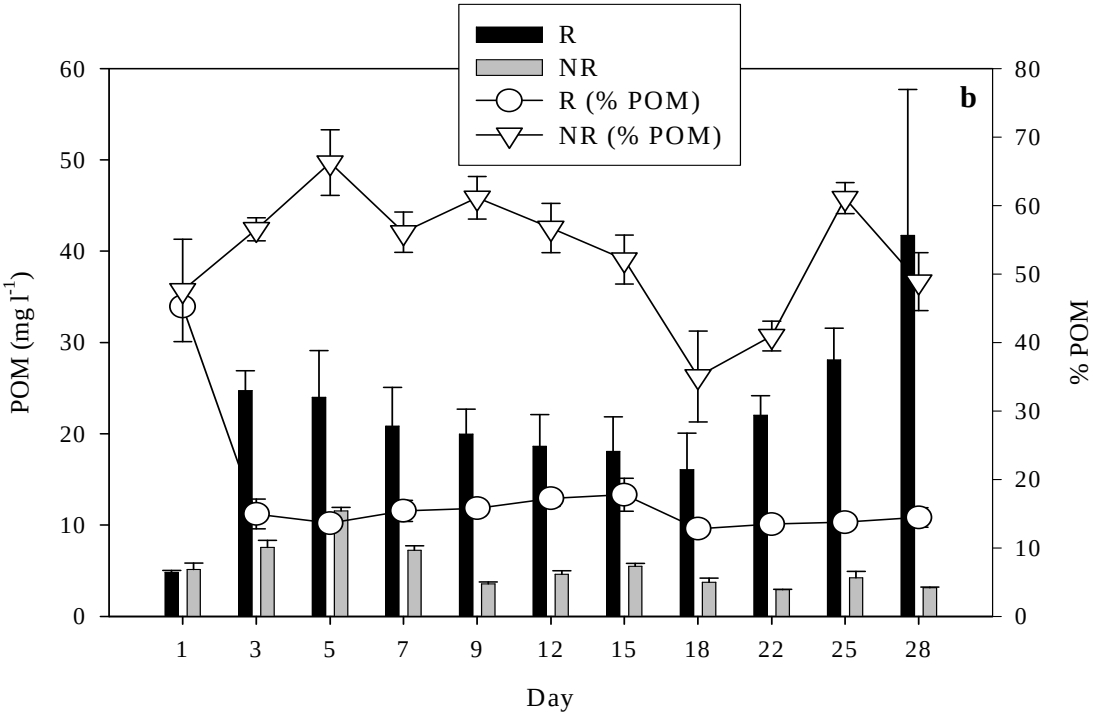
b
R
NR
R (% POM)
NR (% POM)
POM (mg l-1)
% POM
60
50
40
30
20
10
0
80
70
60
50
40
30
20
10
0
1
3
5
7
9
12
15
18
22
25
28
Day

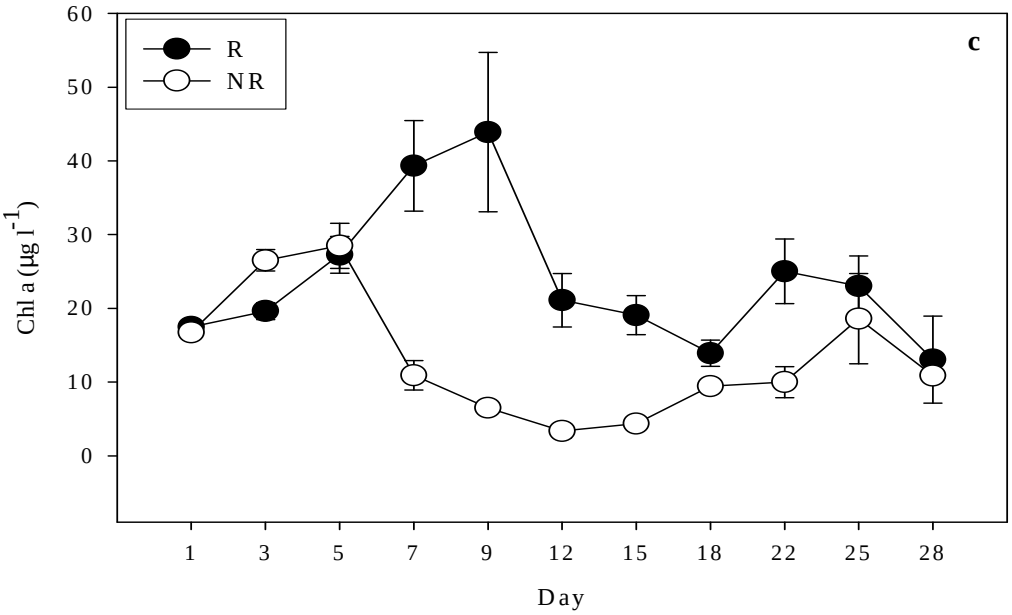
c
R
NR
Chl a (µg l-1)
60
50
40
30
20
10
0
1
3
5
7
9
12
15
18
22
25
28
Day

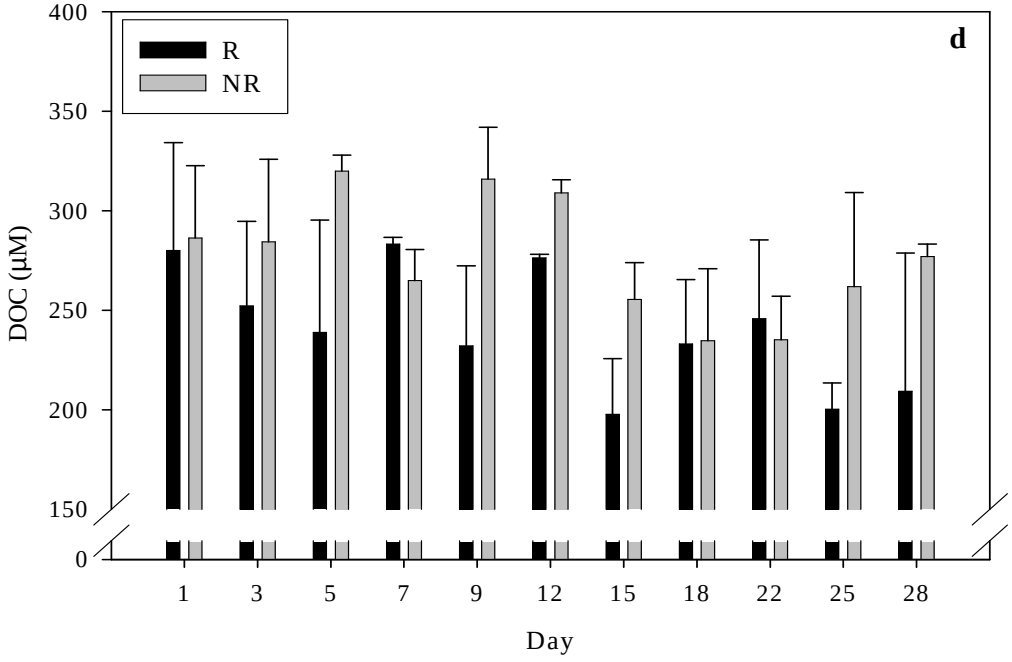
d
R
NR
DOC (µM)
400
350
300
250
200
150
0
1
3
5
7
9
12
15
18
22
25
28
Day

2.3.1.2. Mercury distribution

The average concentration of particulate THg (on a mass basis) was significantly higher in the R tanks than the NR tanks, being 2.3 ± 0.1 (R) and 1.1 ± 0.05 nmol g^{-1} (NR) (Fig. 2.2a). This suggests that resuspended sediments contributed to higher particulate THg in the R tanks. Unfortunately, there are no data available for the first 9 days due to loss of the samples. Even during the off-cycle (non-resuspension), a similar pattern was observed (e.g. significantly higher particulate THg in the R tanks). The average concentration of particulate THg was not significantly different in the R tanks during the off-cycle, compared to the on-cycle.

Although sediment data are not discussed here, sediment cores were taken from all the R and NR tanks for Hg analyses (Chapter 3, Kim et al., submitted). The average concentrations of THg in the top sediment (0-0.5 cm) were 2.6 ± 0.3 (R) and 2.3 ± 0.8 nmol g^{-1} (dry weight) (NR) at the end of the experiment. In the R tanks, THg in surface sediment was comparable with particulate THg in the water column but this was not the case in the NR tanks. Given that the unfiltered ambient water added at the beginning of the experiment was from the Patuxent River and that this was the major source of particles for the NR tanks, besides *in situ* production, it was possible that THg in the water column would be similar to that in the Patuxent River. Our THg data (particulate + dissolved THg on a pM basis) in the water column fell within the range of THg in unfiltered Patuxent River water reported by Benoit et al. (1998). In addition, phytoplankton growth would change the average concentration of THg on particles. Overall, particulate THg in the water column in the R tanks also represented its origin (i.e. from the sediment during resuspension).

Dissolved THg, unlike particulate THg, was remarkably similar between the two systems, averaging 5.5 ± 1.0 pM and varied during the experiment period (Fig. 2.2b). As mentioned earlier, there was a water exchange every day at a rate of 10 % with ambient filtered water. Input water was also collected for Hg analysis three times throughout the experiment period (day 18, 22 and 28). The average concentration of input water was 3.0 ± 0.5 pM (n = 3). The disparity of dissolved THg concentrations between the input water and the mesocosms could be due to daily fluctuations of THg concentration in the input water or could reflect Hg input from the suspended particle phase or from the sediment. There was no significant difference in dissolved THg between the resuspension and non-resuspension phases in the R tanks, suggesting that particle desorption processes were not occurring substantially during resuspension. Overall, the dissolved THg did not seem to change in concert with changes in the particulate THg. This suggests that particles and water did not reach equilibrium very quickly (i.e. not on the timescale of the on- and off- cycles), or that Hg bound to particles was not available for exchange.

Mason et al. (1999) estimated that 70 – 80 % of the dissolved THg was bound to DOC in the Chesapeake Bay. There was, however, no correlation found between DOC and the dissolved THg in this experiment. DOC in our experiment ranged from 130 to 320 (R) and 210 to 330 μM (NR). It is possible that the lack of correlation results from the small range of DOC found in the mesocosms. Similarly, Lacerda and Gonçalves (2001) did not find a significant correlation between DOC and dissolved THg in waters of the coastal lagoons of Rio de Janeiro, Brazil probably due to the small range of DOC (520 - 730 μM) and the limited dataset. In contrast, Conaway et

al. (2003) found that dissolved THg was significantly correlated with DOC in the San Francisco Bay estuary, USA, where DOC ranged widely (e.g. from 80 to 890 μM).

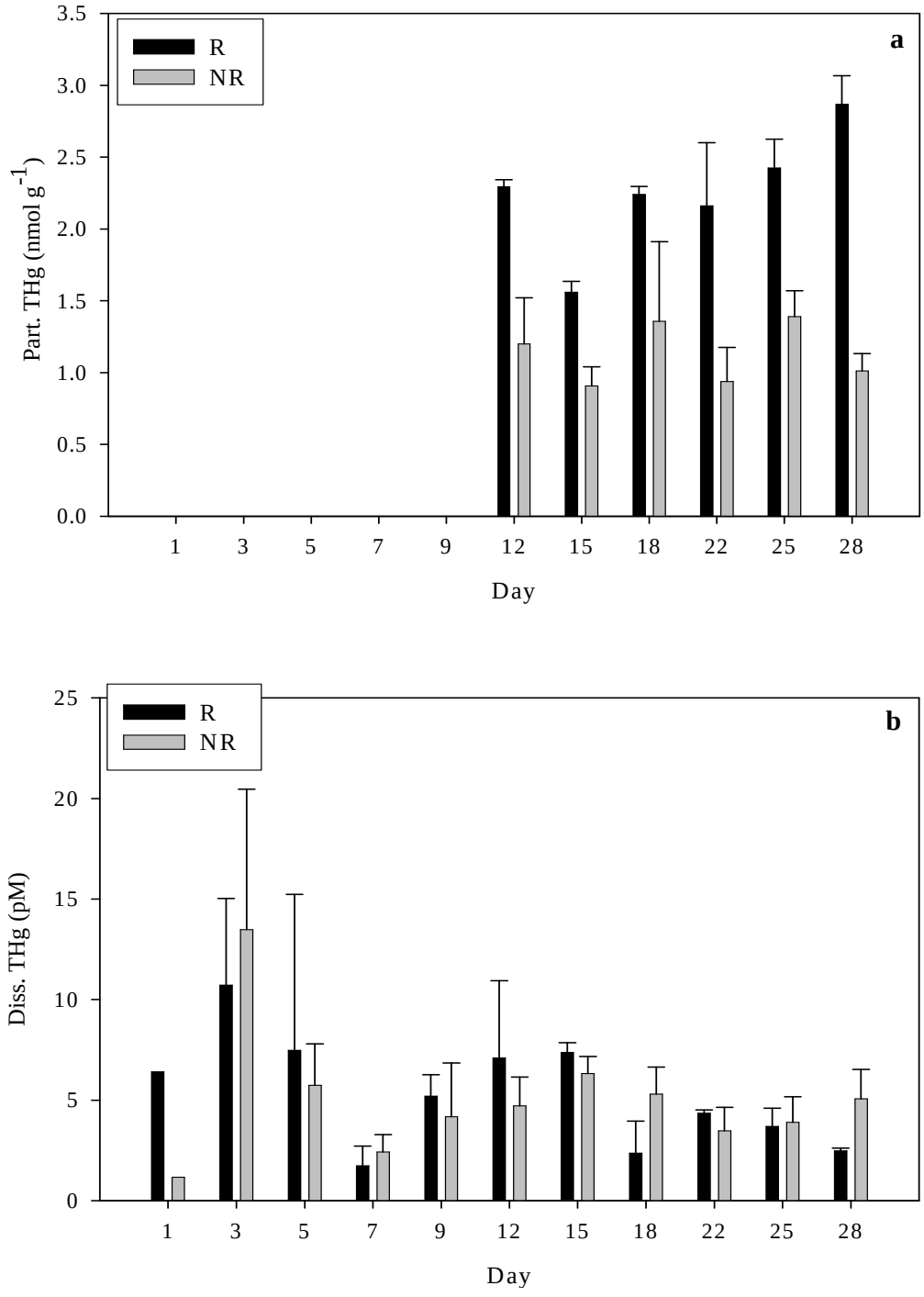

Figure 2.2. Average concentrations of THg in particulate and dissolved phases in the R and NR tanks (experiment 1). (a) Particulate THg concentration. (b) Dissolved THg concentration.

Error bars show standard deviations of 3 replicates in each system.

Particulate and % MeHg are presented in Fig. 2.3a, showing an opposite trend to particulate THg. The concentration of particulate MeHg was significantly higher in the NR tanks than in the R tanks, averaging 34 ± 5.0 and 11 ± 2.0 pmol g^{-1}, respectively. Although % MeHg was available only from the 12th day onwards due to the sample loss for particulate THg, it was also higher in the NR tanks than the R tanks. This difference likely resulted from the introduction of sediment particles that contained lower MeHg concentration (< 1 % of THg) to the water column during resuspension. While sediment particles were dominant in the R tanks, higher fractions of the POM were phytoplankton and zooplankton in the NR tanks, as mentioned earlier. During the off-cycle, particulate MeHg in the R tanks increased significantly (26 ± 6.5 pmol g^{-1}, n = 3), compared to the on-cycle, as sediment particles, primarily less MeHg-rich particles, settled quickly. Particulate MeHg per gram increased due to its higher concentrations in the higher POM non-settling particles, a large fraction of which was likely plankton. As mentioned earlier, % POM actually increased in the R tanks during the off-phase. In addition, particulate MeHg (on a pM basis) was significantly correlated with Chl *a* (r = 0.35, n = 33) and POM (r = 0.78, n = 33) in the R tanks and similarly with Chl *a* (r = 0.39, n = 33) as well as POM (r = 0.34, n = 33) in the NR tanks. As mentioned earlier, NR tanks had higher % POM and zooplankton biomass. Sediment MeHg (5.0 ± 1.0 pmol g^{-1}) in the R tank was comparable to particulate MeHg in the water column during the on-phase while sediment MeHg (5.0 ± 2.5 pmol g^{-1}) was lower than particulate MeHg in the NR tanks. As mentioned earlier, these sediment MeHg data were from the averages respectively of all the R and NR tanks at the end of experiment.

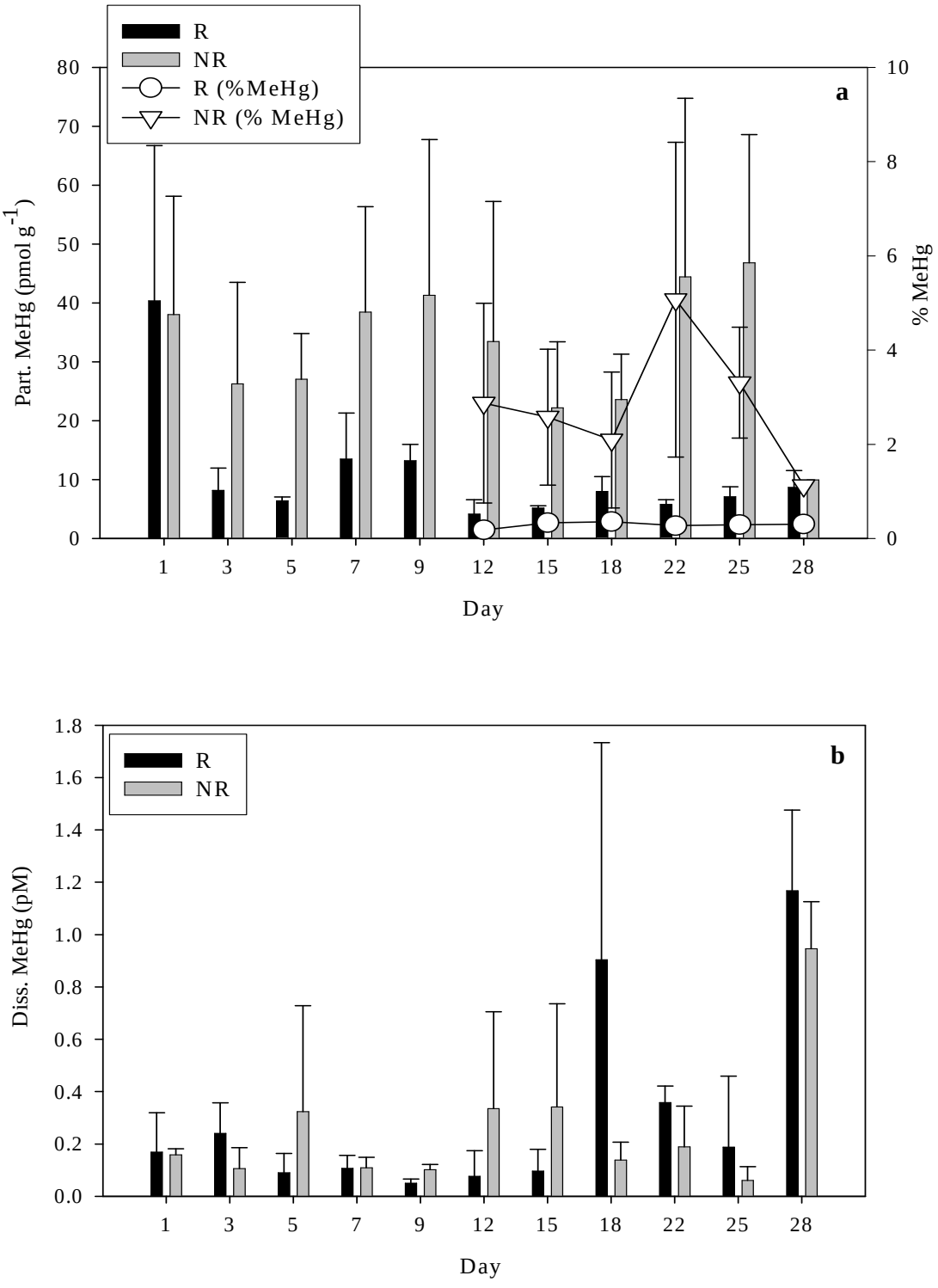

Figure 2.3. Average concentrations of MeHg in particulate and dissolved phases in the R and NR tanks (experiment 1). (a) Particulate MeHg concentration. (b) Dissolved MeHg concentration.

Error bars show standard deviations of 3 replicates in each system.

Dissolved MeHg in both systems varied throughout the experiment, as observed for dissolved THg. The average concentrations of dissolved MeHg were 0.3 ± 0.2 (R) and 0.3 ± 0.1 pM (NR) (Fig. 2.3b). Again, dissolved MeHg did not appear to change in concert with particulate MeHg in both systems. As mentioned before, dissolved concentration seemed to be influenced by the incoming water as much as by partitioning between particles and dissolved fractions. The average MeHg concentration in the inflow water was 0.5 ± 0.5 pM (n = 3). No significant correlation was found between the dissolved MeHg and DOC in both systems, as observed for dissolved THg and DOC.

2.3.1.3. Distribution coefficients

The relative affinity of Hg for dissolved and particulate phases is often parameterized by the distribution coefficient: K_d = S/D (l kg^{-1}); where S = concentration of Hg sorbed to particles (ng kg^{-1}), calculated as [particulate Hg (ng l^{-1})]/TSS (kg l^{-1}); and D = dissolved concentration (ng l^{-1}). A higher K_d value indicates a higher affinity for the particulate phase. Table 2.2 shows the average water column distribution coefficient (log K_d) and standard deviation for THg and MeHg in this experiment. The K_d values for both THg and MeHg were in a similar range to those found for other aquatic systems (Babiarz et al., 1998, Coquery et al. 1997, Mason and Sullivan, 1997, Muhaya et al., 1988, Stordal et al., 1996). In experiment 1, lower K_d values were found for MeHg than for THg. Others have found this pattern, for example, Benoit et al. (1998) found in the Patuxent River that the log K_d for MeHg (3.8 – 4.0) was lower compared to that for THg (4.8 - 5.7).

The K_d for THg in the R tanks was significantly higher than in the NR tanks during both cycles because of higher particulate THg (on nmol g^{-1} basis) in the R tanks. There was, however, no significant difference in K_d for THg in the R tanks between the two cycles. This was because particulate THg in the R tank remained relatively constant between the two cycles. The K_d for MeHg in the NR tanks was significantly higher only during the on-cycle compared to the R tanks. Coquery et al. (1997) observed a lower K_d value with increasing TSS, which has been noted by others (Honeyman and Santschi, 1989) and which is explained by the increase of the proportion of colloidal material in the filter passing (so-called dissolved) fraction with increasing TSS. Lawson et al. (2001) showed that the K_d values for both THg and MeHg decreased with particulate organic content, confirming the notion that Hg binding to suspended particulate involves complexation to organic material. Others have found similar results (Bloom et al., 1999; Mason and Sullivan, 1998). Here, while the presence of colloidal material may explain the results, it is more likely that the effect is due to the higher relative MeHg concentration of the smaller particulate, living and dead, which does not settle during the off-cycle compared to the quickly settling larger particles. This notion is given credence by the fact that the K_d for MeHg in the R tanks during the off-cycle is very similar to that of the NR tanks.

2.3.2. Experiment 2 (with clams)

2.3.2.1. Water column characteristics

The concentration of TSS was significantly higher in the RC tanks than the NRC tanks, averaging 63 ± 22 (RC) and 4.5 ± 0.6 (NRC) mg l^{-1} (Fig. 2.4a). As mentioned in experiment 1, there were three sampling times of the resuspension off-cycle (day 4, 10, and 17). In the RC tanks, average TSS significantly decreased during the off-cycle (9.5 ± 2.2 mg l^{-1}, n = 3) compared to the on-cycle, which was a similar pattern with that in experiment 1. However, TSS concentrations were about half those of experiment 1. Less TSS in the NRC tanks was due to a combination of clam feeding on phytoplankton and lower temperature compared to that in experiment 1. Less TSS in the RC tanks likely resulted from a change in sediment properties as the sediment from experiment 1 was reused for experiment 2. In addition, TSS tended to decrease toward the end of experiment, suggesting that clams in the RC tanks were active in removing particulate from the water column, or that initially clams destabilized sediments and increased resuspension in the initial part of the experiment.

POM was significantly higher in the RC tanks than the NRC tanks, averaging 10 ± 4.2 (R) and 2.0 ± 0.2 mg l^{-1} (NR) (Fig. 2.4b). The average POM in the RC tanks decreased significantly to 2.5 ± 0.4 mg l^{-1} (n = 3) during the off-cycle compared to the on-phase. POM was positively correlated with TSS in both RC tanks (r = 0.77, n = 24) and NRC tanks (r = 0.96, n = 24), as observed in experiment 1. Overall, POM in experiment 2 showed a similar pattern with that in experiment 1. The average POM in experiment 2, however, was also less than that in experiment 1 due to a decrease in

TSS in the water column. In addition, although it is not possible to directly compare zooplankton biomass between the two experiments due to differences in water temperature, salinity, and clam presence, this biomass decreased roughly by 80 % in the RC tanks and 87 % in the NRC tanks in experiment 2, compared to experiment 1. One explanation for a zooplankton decrease could be due to reduced food availability. As discussed later, less standing stock of phytoplankton was observed in experiment 2, compared to experiment 1, potentially as a result of not only lower water temperature (Table 2.1) but also clam feeding. Percent POM was significantly higher in the NRC tanks, averaging 46 ± 2.3 (NR) and 16 ± 0.7 % (R) (Fig. 2.4b). In the RC tanks, % POM significantly increased to 29 ± 6.6 % (n = 3) during the off-cycle compared to the on-cycle, as seen in experiment 1. Overall, % POM was similar in both sets of the tanks during the two experiments.

There was a small phytoplankton bloom observed in the RC tanks later in this experiment while there was an overall decreasing trend in Chl *a* in the NRC tanks (Fig. 2.4c). As seen in experiment 1, Chl *a* was significantly higher in the RC tanks than NRC tanks, averaging 6.7 ± 0.3 and 3.6 ± 0.1 $\mu g\ l^{-1}$, respectively. Compared to experiment 1, Chl *a* concentration in both systems decreased by 72 % as water temperature was lower in experiment 2. Chl *a* in the RC tanks was significantly higher during the on-cycle compared to the off-phase (5.3 ± 0.9 $\mu g\ l^{-1}$, n = 3). In experiment 1, however, there was no significant difference in Chl *a* between the two cycles in the RC tanks. This was probably due to larger variability in Chl *a* in experiment 1. In addition, Chl *a* was not correlated with either TSS or POM in the RC tanks, whereas there was a positive correlation between Chl *a* and TSS (r = 0.48, n =

24) and POM (r = 0.46, n = 24) in the NRC tanks, as observed in experiment 1. The lower Chl *a* standing stock in this experiment results from a combination of lower water temperature as well as the existence of clams in both systems. As in experiment 1, DOC data were available only during the on-cycle (Fig. 2.4d). Although the average DOC in the NRC tanks (330 ± 10 μM) was higher than that in the RC tanks (300 ± 54 μM), the difference was not significant.

Water column characteristics for experiment 2 are presented in Table 2.1. These measurements were made during the on-cycle. More diurnal fluctuation in temperature was observed in experiment 2. A heating system was occasionally used when the water temperature was unusually low in order to prevent large temperature differences potentially harmful to the ecological community in the mesocosms. As seen in experiment 1, DO and pH were slightly higher in the NRC tanks than the RC tanks. Sloth et al. (1996) found that oxygen concentration decreased by 5 % during a 2 h-resuspension event in their mesocosm experiment and that the decrease in oxygen content corresponded to an oxygen consumption rate of 500 mmol m^{-2} d^{-1}, or 10 times the normal oxygen consumption rate of the sediment. They suggested that the increase in oxygen consumption was probably due to liberation of pools of reduced inorganic and organic products from anaerobic processes in the sediment. Similar procedures are likely consuming DO in the RC tanks in our experiment.

Figure 2.4. Average concentrations of the following variables in the R and NR tanks (experiment 2). (a) TSS concentration. (b) POM and % POM. (c) Chl a concentration. (d) DOC concentration.
Error bars show standard deviations of 3 replicates in each system.

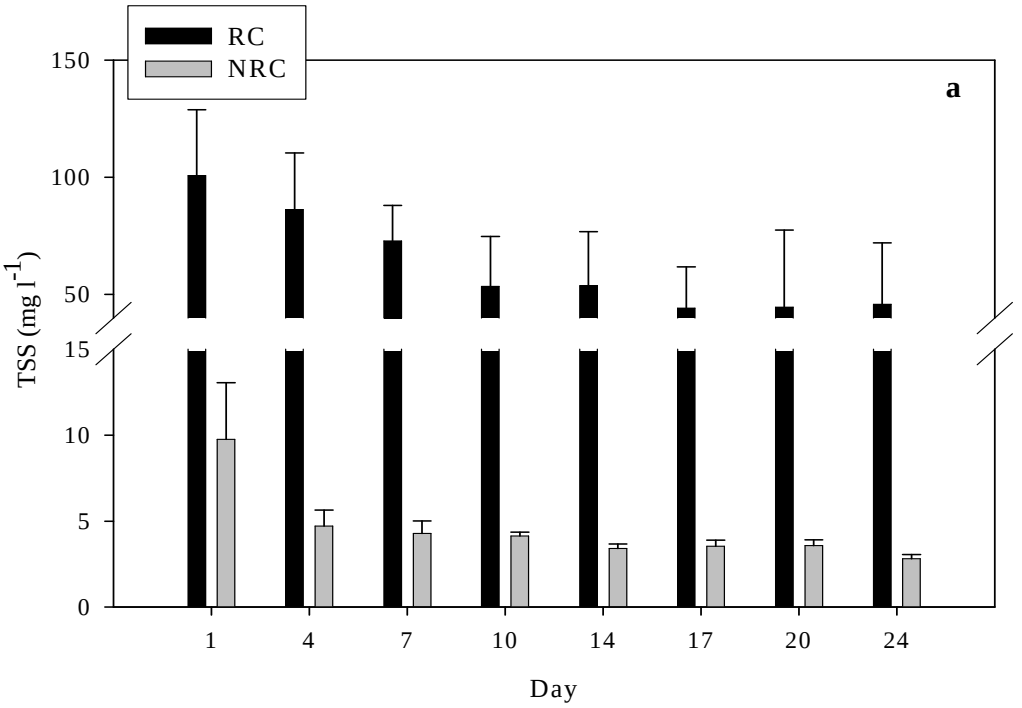
RC
NRC
a
150
100
50
15
10
5
0
TSS (mg l-1)
1
4
7
10
14
17
20
24
Day

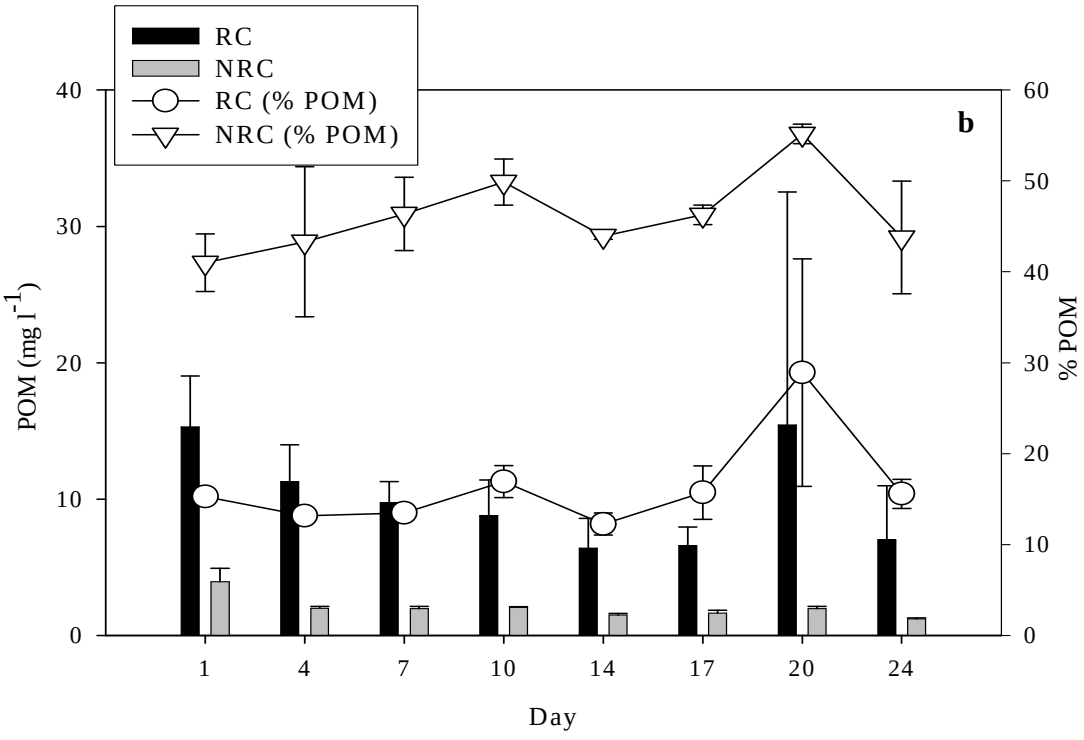
RC
NRC
RC (% POM)
NRC (% POM)
b
40
30
20
10
0
60
50
40
30
20
10
0
POM (mg l-1)
% POM
1
4
7
10
14
17
20
24
Day

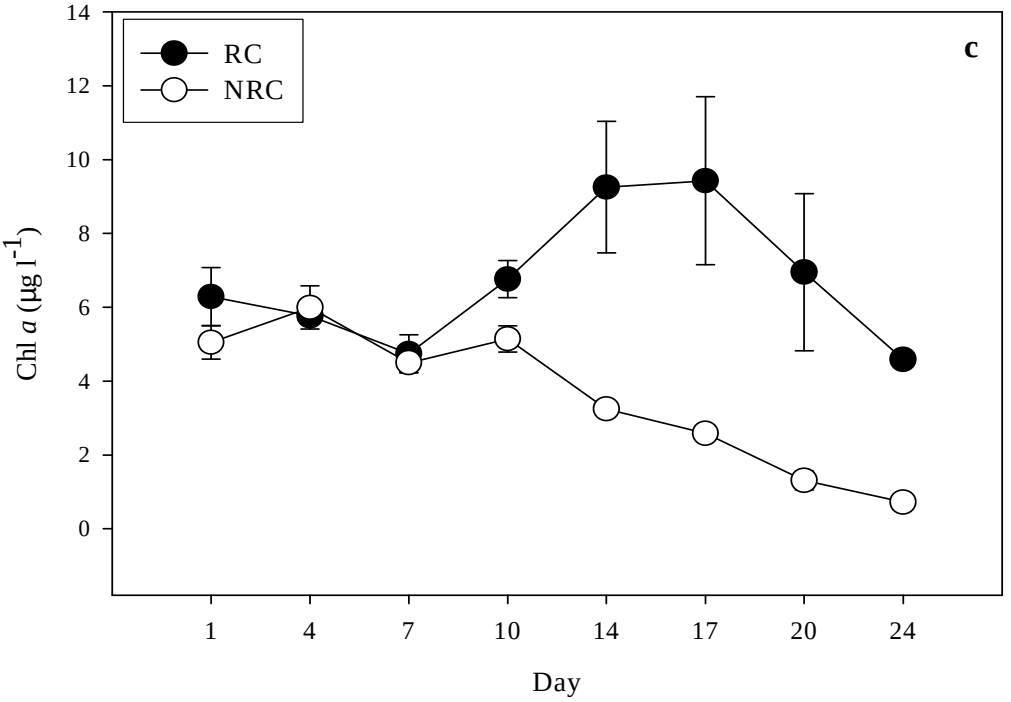
RC
NRC
c
Chl a (µg l-1)
14
12
10
8
6
4
2
0
1
4
7
10
14
17
20
24
Day

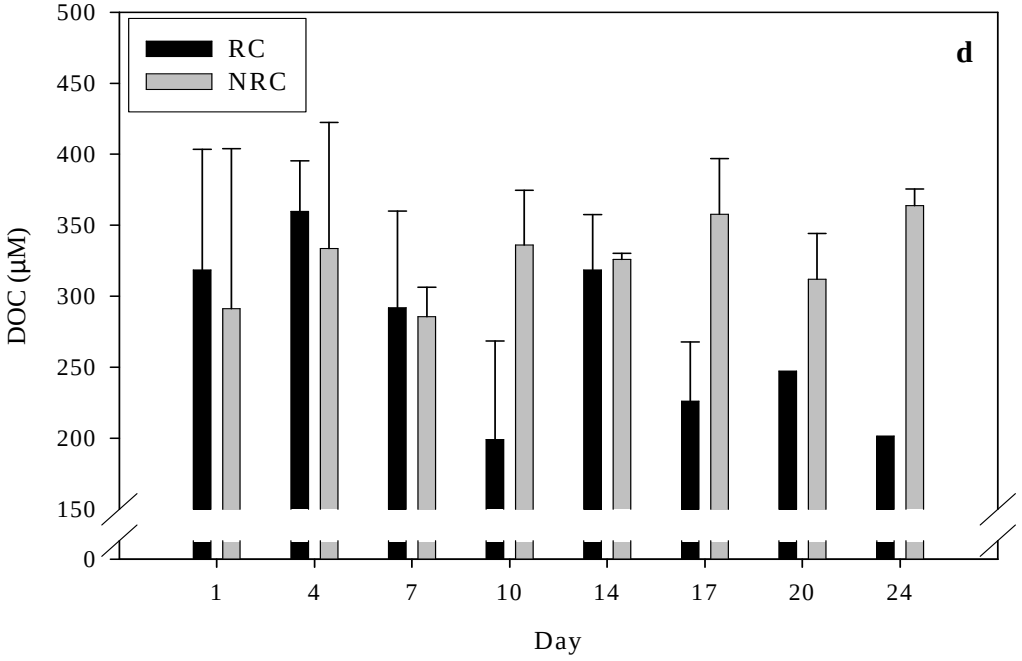
RC
NRC
d
DOC (µM)
500
450
400
350
300
250
200
150
0
1
4
7
10
14
17
20
24
Day

2.3.2.2. Mercury distribution

Particulate THg was significantly higher in the RC tanks than the NRC tanks, as seen in experiment 1, averaging 2.3 ± 0.2 (RC) and 1.4 ± 0.05 nmol g^{-1} (NRC) (Fig. 2.5a). Particulate THg (on nmol l^{-1} basis) was significantly correlated with TSS (r = 0.97, n = 24) and POM (r = 0.77, n = 24) in the RC tanks, as seen in experiment 1. In addition, there was a significant correlation between particulate THg and TSS (r = 0.39, n = 24), as well as POM (r = 0.40, n = 24), in the NRC tanks. The lack of correlation between particulate THg and TSS or POM found in experiment 1 was unexpected because Hg is one of the most strongly particle-associated metals. This was probably because of the smaller data set in experiment 1 due to sample loss. In experiment 2, sediment cores were also taken from all the tanks in the end of the experiment for Hg analysis (Chapter 3, Kim et al., submitted). The average concentrations of surface sediment THg in the cores were 1.8 ± 0.5 (RC) and 1.3 ± 0.4 nmol g^{-1} (NRC), showing a slightly lower range than that in experiment 1. This was likely due to inherent sediment heterogeneity, as discussed in Chapter 3 (Kim et al., submitted).

Dissolved THg was significantly higher in the RC tanks than the NRC tanks (Fig. 2.5b). The average concentrations of dissolved THg were 8.0 ± 0.5 (RC) and 6.0 ± 0.3 pM (NRC). A similar range of dissolved THg was found during the off-phase. Dissolved THg tended to increase toward the end of the experiment. However, the change in dissolved THg did not correspond to the change in particulate THg, as seen in experiment 1. Dissolved THg in the input water was measured also for the same sampling days, except the 4^{th} day. A similar range of THg in the input water was

found (average of 7.0 ± 5.5 pM). Given that water exchange was always done after sampling, dissolved THg in the mesocosms did not directly represent the concentration of THg in the input water on the corresponding day. Nonetheless, it appears that dissolved THg in the tanks may have been driven as much by the change in the incoming water than by the release of THg from particles upon resuspension.

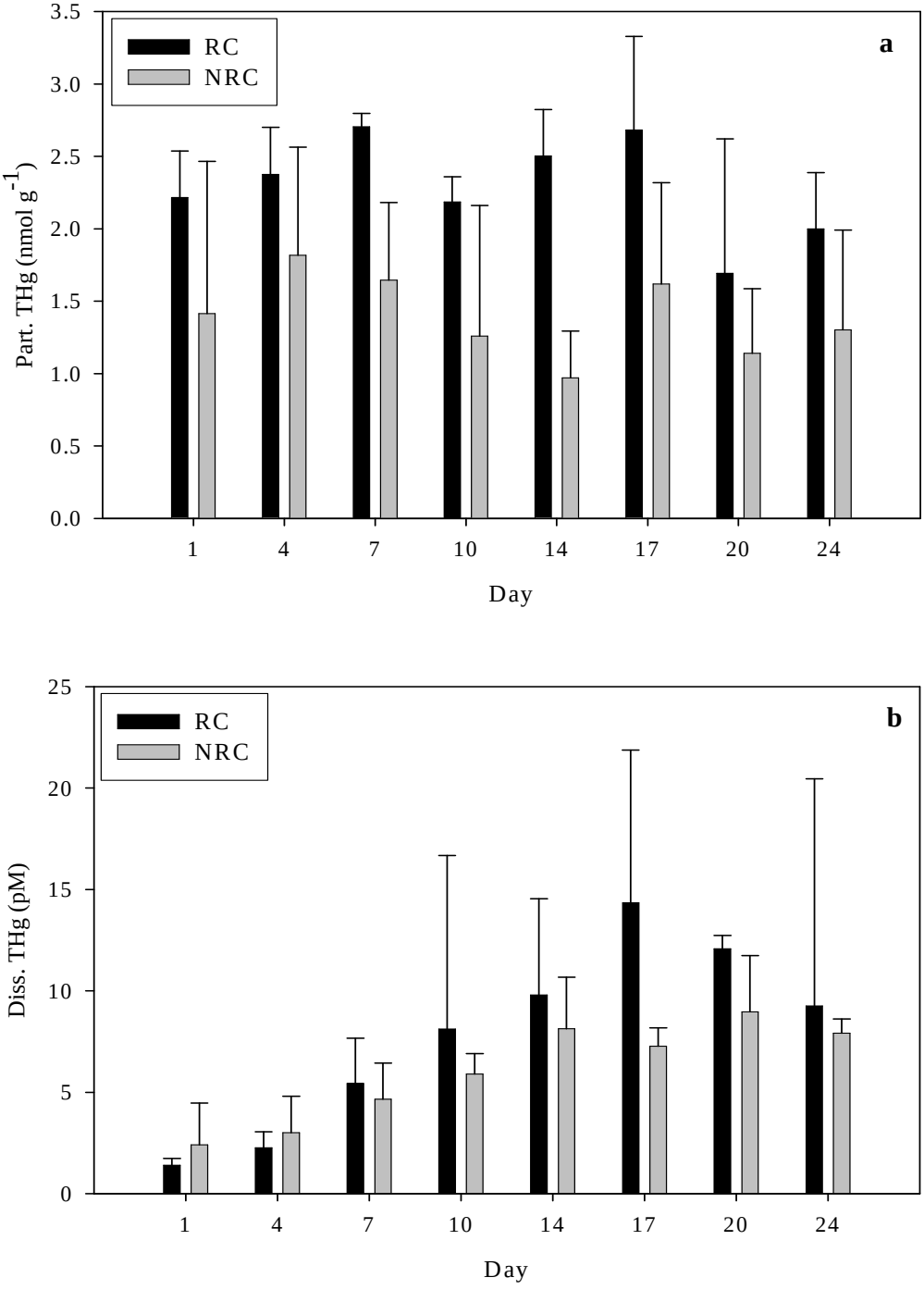

Figure 2.5. Average concentrations of THg in particulate and dissolved phases in the R and NR tanks (experiment 2). (a) Particulate THg concentration. (b) Dissolved THg concentration.
Error bars show standard deviations of 3 replicates in each system.

Particulate MeHg was significantly higher in the NRC tanks than the RC tanks, averaging 26 ± 5.0 (NR) and 6.0 ± 1.0 pmol g^{-1} (R), as seen in experiment 1 (Fig. 2.6a). The percent MeHg was also higher in the NRC tanks than the RC tanks throughout the experiment. During the off-cycle, the average concentration of particulate MeHg increased to 15 ± 7.0 pmol g^{-1} (n = 3) in the RC tanks. It appears that suspended particulate MeHg was somewhat diluted by material of lower MeHg during the on-phase and higher particulate MeHg was found during the off-phase, as TSS decreased (concentration effect). The average concentrations of MeHg in surface sediments were similar between the two systems, being 5.0 ± 0.5 (R) and 5.0 ± 0.4 pmol g^{-1} (NRC) from all the tanks. The results showed that sediment MeHg was comparable to particulate MeHg in the R tanks (during the on-cycle) but lower than that in the NR tanks.

There was a significant correlation between particulate MeHg (on a pM basis) and TSS (r = 0.76, n = 24) as well as POM (r = 0.57, n = 24) in the RC tanks. Particulate MeHg was also significantly correlated with particulate THg (r = 0.77, n = 24) but not with Chl *a* in the RC tanks. The lack of correlation between particulate MeHg and Chl *a* may be due to the smaller range of Chl *a* concentration compared to experiment 1. It is interesting that particulate MeHg was negatively but significantly correlated with POM (r = - 0.41, n = 24) as well as Chl *a* (r = - 0.37, n = 24) in the NRC tanks while there were positive correlations found in experiment 1.

The average concentration of dissolved MeHg was 0.2 ± 0.05 (NRC) and 0.2 ± 0.05 pM (RC) (Fig. 2.6b). As seen in experiment 1, dissolved MeHg was remarkably similar in both systems. The average concentration of dissolved MeHg in the input

water was 0.2 ± 0.1 pM, which was in a similar range of MeHg found in the mesocosms. Overall, it is unlikely that resuspension increased dissolved MeHg in the water column, suggesting that release due to oxidation of sulfide phases, or other processes enhancing desorption, were not significant.

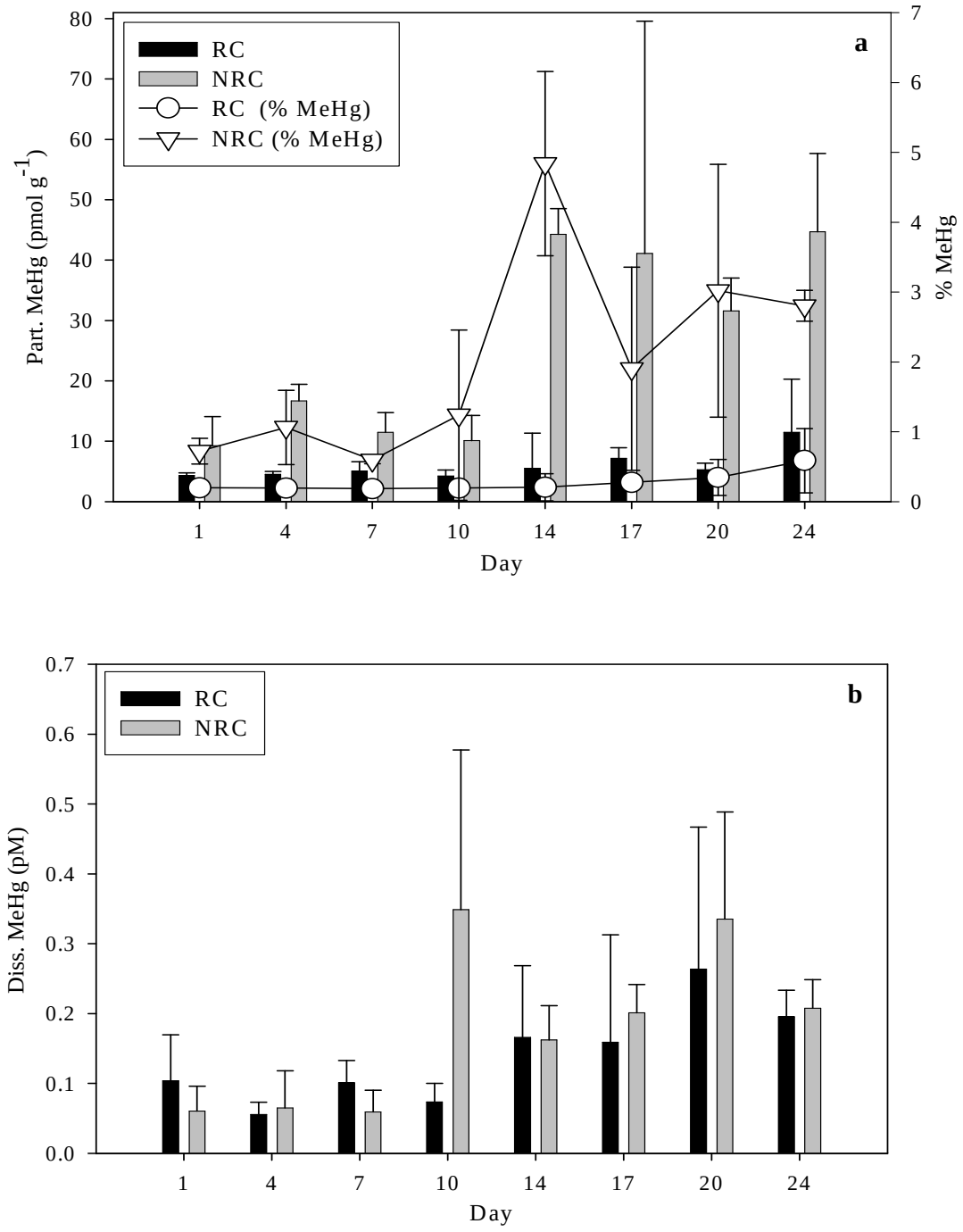

Figure 2.6. Average concentrations of MeHg in particulate and dissolved phases in the R and NR tanks (experiment 2). (a) Particulate MeHg concentration. (b) Dissolved MeHg concentration.
Error bars show standard deviations of 3 replicates in each system.

2.3.2.3. Distribution coefficients

As seen in experiment 1, the average K_d for THg was significantly higher in the RC tanks than the NRC tanks during both cycles (Table 2.2). The average K_d for MeHg was significantly higher in the NRC tanks during the on-cycle only, as seen in experiment 1. These observations suggest that there are two types of particles in the RC tanks: one that is relatively inorganic, consisting mostly of sediment particles, which does not release Hg rapidly (non-reactive) and the other that is reactive and takes up Hg actively, or contains Hg which is readily exchangeable. Also, it appears that the non-reactive particles had a higher THg than the reactive ones. However, these concentrations in the RC tanks were similar to that of the surface sediment. The much higher Hg in the non-reactive particles results in the trends observed for the two experiments. The opposite was observed for MeHg in that the K_d was higher in the NRC tanks than the RC tanks during the on-phase, suggesting that suspended particles were actively accumulating MeHg compared to the sediment. In addition, the K_d for MeHg in the RC tanks was higher during the off-phase in both experiment 1 and 2 when TSS concentration was lower as most of resuspended sediment particles settled quickly.

Table 2.2. Average and standard deviation for log K_d in the R and NR tanks during the course of experiments 1 and 2.

	log K_d	R	NR
Experiment 1	THg (on)[a]	5.7 ± 0.05	5.4 ± 0.06
	THg (off)[b]	5.8 ± 0.07	5.5 ± 0.1
	MeHg (on)	4.8 ± 0.2	5.3 ± 0.1
	MeHg (off)	5.1 ± 0.6	5.2 ± 0.06
Experiment 2	THg (on)	5.6 ± 0.09	5.4 ± 0.05
	THg (off)	5.4 ± 0.09	5.2 ± 0.1
	MeHg (on)	4.7 ± 0.2	5.2 ± 0.3
	MeHg (off)	4.9 ± 1.1	5.2 ± 0.5

a: on-cycles when both resuspension and water mixing system was on in the R tanks while in the NR tanks only water mixing was on.
b: off-cycles when both resuspension and water mixing was ceased in the R tanks. Off-cycles in the NR tanks means there was no water mixing. See the text for details.

Scaling calculations for Hg uptake in phytoplankton confirm that uptake by phytoplankton would not lead to enhanced particulate Hg concentration in the water column, given the relatively high sediment Hg concentration. Based on the Chl *a* concentration in the R tanks during the off-phase, and some reasonable assumptions about phytoplankton size and growth rate, the data in Mason et al. (1996) can be used to estimate the steady state phytoplankton Hg burden under the experiment conditions. MeHg uptake rate for phytoplankton was obtained from Mason et al. (1996), which was similar to uptake rate used in the bioaccumulation model (Chapter 4). A range in Hg concentration of 0.3 – 0.5 nmol g^{-1} is estimated, much lower than the sediment load (i.e. uptake of Hg from the dissolved phase into plankton is unlikely to significantly alter the Hg burden in the suspended particles and thus no difference is expected between the on-phase (sediment particles dominant) and the off-phase (phytoplankton more dominant).

Similar calculations for MeHg give a range in values of 5 – 30 pmol g^{-1}, comparable to the measured values in the NR tanks and in the R tanks during the off-phase. Thus, active uptake by phytoplankton could be influencing the overall MeHg particulate load given that the steady state phytoplankton MeHg concentration is higher than that of the surface sediments. Thus, our scaling arguments confirm the observations and measurements. While this uptake into biota is important in defining the MeHg concentration on a pmol g^{-1} TSS basis, it is not an important sink for dissolved MeHg given the large size of the tank (1000 L) and the estimated rate of uptake.

Additionally, a similar pattern in dissolved THg and MeHg in both R and NR tanks show that dissolved and particulate fractionation cannot be explained purely by equilibrium partitioning. As suggested above, THg is more particle associated and strongly bound to the non-living (or sediment) fraction that cycles between the water column and the sediment, with very little release during resuspension. Heyes et al. (2004) found from a Hudson River study that particulate THg in the water column was mostly bound to reactive phases, such as iron oxides and amorphous iron sulfide, and organic phases and that Hg partitioning on resuspended particles did not change over a tidal diurnal cycle resuspension event. In contrast to inorganic Hg, MeHg partitioning appears to be controlled more by the biotic fraction that actively accumulates MeHg.

2.3.2.4. Mass Balance Calculations

A simple mass balance in the water column provides useful insights into MeHg fate and production. Given measured concentrations in input waters, and in the tanks during the off-phase, the following is estimated: experiment 1 input of MeHg ~ 50 pmol d^{-1} from the input water with output of ~ 55 pmol d^{-1} for the NR tanks and ~ 80 pmol d^{-1} for the R tanks, which have higher TSS. Thus, it appears that MeHg is produced within the R mesocosms and that the methylation rate is overall higher in the R system. Our results for Hg methylation in the sediment, which are contained in Chapter 3 (Kim et al., submitted), confirm this notion of higher methylation in the R tanks. However, the overall net rate derived from mass balance is low compared to what others have measured for estuarine sediments using Hg core spike incubations (Benoit et al. 1998) and compared to our rates from core incubations of these sediments. As suggested by others, these results suggest that while core spike incubation experiments give a relative measure of the methylation rate between treatments, they do not provide an accurate estimate of *in situ* methylation. These mesocosm studies therefore provide useful information about net MeHg production in estuarine systems that are not easily obtained by other approaches.

The results of the mesocosm experiments suggest that resuspension can enhance MeHg production. While this may appear counter-intuitive, the likely explanation is that the oxygenation of the sediment that results from resuspension reduces sediment AVS and pore water sulfides in estuarine sediments and thus improves the methylation environment by enhancing Hg bioavailability to bacteria, by mechanisms proposed by Benoit et al. (1999). Furthermore, in an estuarine system, or any aquatic

system with high TSS, the fate of Hg will be linked closely to that of the particulate phase. Thus, from a mass balance perspective, understanding the sediment transport is crucial in ascertaining whether the system will be a net source or sink for Hg. For MeHg, this is less true, even given the high K_d for MeHg in many environments as internal sources of MeHg (i.e. Hg methylation) are likely a complicating factor in the overall MeHg mass balance.

2.4. Summary

Our experiments showed that significant amounts of particulate THg in the R tanks were introduced to the water column by resuspension. However, particulate MeHg was found to be significantly lower than that in the NR tanks. Dissolved concentrations of THg and MeHg showed a similar pattern between the two systems and appeared little impacted by sediment load. The dynamics between the dissolved and particulate phases in these experiments suggests that the notion of equilibrium partitioning for Hg is not valid. There appears to be two types of particles, those that readily accumulate and/or potentially release Hg and MeHg, and those that do not. Our mass balance calculation suggests that resuspension likely enhances MeHg production in these sediments.

Chapter 3: The importance of resuspension on sediment mercury dynamics, and methylmercury production and fate: a mesocosm study

Submitted to Marine Chemistry

3.1. Introduction

Sediments are the main repository of mercury (Hg) in estuaries (Benoit et al., 1998; Wang et al, 1998) and can be a significant source to the overlying water column via various processes including diffusion, resuspension, and bioturbation (Gagnon et al, 1997; Bloom et al., 1999; Mason and Lawrence, 1999). The mobility and bioavailability of Hg and methylmercury (MeHg) depends upon the nature and concentration of the binding phases in the sediment, which apparently are controlled by sediment redox status. Hg associates primarily with particulate organic matter or iron/manganese oxides through adsorption and coprecipitation reactions in oxidized sediments (Gagnon, Pelletier et al. 1997). Miller and Mason (submitted) found from laboratory experiments and surface complexation modeling that organic matter, not iron oxides, was the dominant complexer of Hg. In anoxic sediments, Hg is adsorbed onto and coprecipitated with sulfide minerals (Gobeil and Cossa, 1993; Gagnon et al, 1997; Wang et al, 1998). When metal oxides are reduced, Hg can be released into pore water (and eventually to overlying water via diffusion) or be removed by

adsorption and coprecipitation with sulfide minerals under anoxic conditions. Hg can also be released as a result of the microbial degradation of organic matter and by chemical dissolution of sulfides due to redox changes during diagenesis.

Under anoxic conditions, dissolved sulfide may precipitate with Fe^{2+} ions, which are released by reduction of iron (hydr)oxides. Iron sulfide can then adsorb and coprecipitate divalent metals. Many toxic metals can form highly insoluble sulfide minerals and adsorb/coprecipitate with pyrite and acid volatile sulfide (AVS). Consequently, it may be less bioavailable to aquatic organisms (Allen, 1995). However, Copper and Morse (1996) concluded that sulfide-associated trace metals could be a more bioavailable phase following a major oxidation event such as that caused by dredging, resuspension, and seasonal migration of the redoxcline. During the oxidation event, these metal sulfides may oxidize and thereby release the associated metals and the oxidized sulfur species to the overlying water. Thus, this process can act as a potential source of toxic metals to the water column, possible increasing bioavailability. The released metal may be, however, quickly scavenged or coprecipitated with iron and manganese hydroxides or be complexed by organic matter (Simpson et al., 1998). However, Heyes et al. (2004) found from the Hudson River study that Hg release from particles did not readily occur upon sediment resuspension.

As mentioned above, sediment resuspension can induce a change in sediment redox status, which can be an important factor in controlling the methylation of Hg in sediments. Hg methylation depends upon environmental factors that control the overall metabolic activity of the methylating organisms (e.g. sulfate reducing

bacteria) and the bioavailability of Hg in the matrix where methylation occurs. As the supply of organic carbon enhances Hg methylation rate (Choi and Bartha, 1994), the distribution of methylation activity depends upon the distribution of biodegradable organic matter. Thus, maximal methylation rates are often observed in biologically active surface sediments near the sediment-water interface (Callister and Winfrey, 1986; Korthals and Winfrey, 1987). While sulfate can stimulate both sulfate reduction and Hg methylation by sulfate reducing bacteria at relatively low sulfate concentrations (Gilmour and Henry, 1991), the high concentrations of sulfate typically found in estuarine and marine environments enhance pore water dissolved sulfide, which can inhibit methylation (Compeau and Bartha, 1983; 1987; Gilmour et al., 1998; Benoit et al., 1998). Thus, resuspension may enhance methylation by decreasing sulfide levels, but it may also limit methylation if sediments become too oxic by limiting the activity of sulfate reducing bacteria. In addition, demethylation occurs primarily under oxygenated conditions (Matilainen and Verta, 1995; Marvin-Dipasquale and Oremland, 1998). Higher demethylation rates were observed in oxygenated sediments than in anoxic sediments (Compeau and Bartha, 1984). Thus, it is likely that resuspension enhances the demethylation by introducing oxygenated conditions to anoxic environments. There is, however, very little information available on to what degree resuspension affects the methylation/demethylation of Hg.

Elevated MeHg in fish has been found in many aquatic environments (Clarkson, 1990; Driscoll et al., 1995; Park et al., 1997) and this is of the greatest concern to human health because fish consumption is the main MeHg exposure route to humans

(Clarkson, 1990). Lower trophic levels play an important role in Hg and MeHg bioaccumulation into fish as the greatest bioconcentration occurs between water and phytoplankton (Lindqvist et al, 1991; Mason et al., 1996). However, Hg and MeHg in sediments also constitute an enriched pool potentially available to organisms. The bioavailability of Hg and MeHg to benthic organisms from sediments has been actively investigated as these organisms often dominate the lower trophic level of aquatic food chains in shallow systems, and have the potential to transfer the bioaccumulated Hg to upper levels of the food chain (Gagnon and Fisher, 1997; Wang et al., 1998; Mason and Lawrence, 1999). Filter-feeding bivalves (e.g. mussels, oysters) in the second trophic level are capable of accumulating toxic metals and organic contaminants from the large volume of water they filter. Thus, these organisms have been used as effective biomonitors for a variety of coastal toxicants (Claisse et al., 2001; Kawaguchi et al., 1999; Roper et al., 1996).

Although sedimentary dynamics and bioavailability of Hg have been actively studied, there are few studies that have investigated how resuspension affects the fate and bioavailability of Hg in the sediment and possible release of Hg to the water column. Therefore, the objective of this study was to investigate the effects of tidal sediment resuspension over a 4-week period on the fate of total mercury (THg) and MeHg and their bioaccumulation. We used the new STORM (high bottom Shear realistic water column Turbulence Resuspension Mesocosms) facility designed and developed by E.T. Porter (Porter 1999, Porter et al., in press a). The STORM system can simulate both realistic bottom shear stress and water column turbulence levels in a single system, mimicking benthic-pelagic coupling processes realistically, including

tidal or episodic sediment resuspension, over long time periods. Two 4-week experiments were conducted in 2001; one in July without clams (experiment 1) and the other in October with clams (experiment 2). In experiment 2, hard clams, *Mercenaria mercenaria*, were introduced into the sediment for the bioaccumulation study. Hard clams were chosen because they are suspension feeders, common in the eastern coastal and estuarine regions of USA (Stanley 1985) and there is little information on Hg (especially MeHg) bioaccumulation into hard clams. This chapter discusses the effects of sediment resuspension on the sedimentary dynamics of THg and MeHg and their bioaccumulation. A companion chapter (Chapter 2, Kim et al., 2004) discusses the impact of sediment resuspension on water column THg and MeHg dynamics.

3.2. Material and Methods

3.2.1. Mesocosm and experimental set-up

Muddy sediment from Baltimore Harbor was collected in the spring of 2001 and transferred to a fiberglass holding tank at CBL and prepared for each experiment following techniques developed in Porter (1999) and Porter et al. (2004b). The details of the experimental set-up are described in Chapter 2 (Kim et al., 2004). Briefly, the sediment was transferred into 6 STORM tanks after defaunation (4 days). The sediment was thoroughly mixed and flattened. Filtered ambient water from the mouth of the Patuxent River (a tributary of the Chesapeake Bay, Maryland, USA) was added into the tanks without any disturbance of the sediment layer to a depth of 20 cm above the sediment surface. After a 2-week sediment equilibration period, to re-

establish realistic pore water gradients (Porter 1999), unfiltered ambient water was added to the tanks. There were 3 resuspension (R) tanks (T1, T2, and T3) and 3 non-resuspension (NR) tanks (T4, T5, and T6) for each experiment. In both systems, water column turbulence intensities were similar. However, high instantaneous bottom shear induced sediment resuspension in the R systems whereas bottom shear velocity was low in the NR systems (Crawford and Sanford, 2001; Porter et al., 2004a). Tidal resuspension (4 h-on and 2 h-off cycles) over the 4-week period was simulated using the STORM tank mixing design.

As mentioned above, in experiment 2, a scaled population of about 50 - 40 mm long hard clams were placed into the sediment individually by hand after the sediment equilibration period. Five clams were also placed in a plastic basket hanging at 50 cm below the water surface near the wall of each tank (so-called “suspended clams”). Since the clams buried themselves in the sediment and it was not possible to observe them (especially in the R tanks due to turbidity), these suspended clams in the water column helped confirm whether or not the clams were feeding. Given that some negative effects (i.e. inhibition of feeding rate, burrowing, growth and survival of juveniles and adults) result when the clams are exposed to salinities below 15 ppt (Grizzle et al., 2001 and references therein), salinity adjustment was necessary in experiment 2. The average salinity for all the tanks was approximately 19 ppt throughout the experiment period. The salinity of the input water (Patuxent River water) was around 13 ppt.

3.2.2. Sample collection

Sediment cores for THg, MeHg, and AVS were taken at the start of the experiment (initial sediment cores were incubated in a separate benthic chamber setup as discussed below), around the mid point of experiment 1, and at the end of the experiment, during the "on-cycle" (resuspension actively occurring). There was no mid point sampling for experiment 2. The sediment cores were generally about 9 cm deep, taken in 3.5 cm ID and 25 cm long acrylic tubes and sliced immediately at the following intervals: 0-0.5, 0.5-1, 1-2, 2-3, 3-5, and 5-7 cm. The sliced sediment was then quickly stored frozen until analysis. The initial cores were taken from approximately 13.5 cm ID and 35 cm long benthic chambers. These chambers were set up separately in a flow through water bath in the dark for initial Hg and AVS measurements so that the sediment surface in the tanks was not disturbed before the experiments began. The separate cores underwent a 2-week equilibration period indoors in the same manner as the STORM tanks (Chapter 2, Kim et al., 2004), representing a similar initial condition as in the tanks. Percent organic content in each interval of sediment samples was determined as loss on ignition to 550 °C overnight.

Clams were shipped on ice from Cherrystone Aqua Farms, Cheriton, Virginia. They were kept in a holding tank with a constant water circulation until experiment 2 began. Clams were acclimated, a salinity change from the 21 ppt at which they were cultured, to 18-19 ppt, our experimental condition (i.e. decreasing salinity by 1 ppt per day). For water quality assurance, levels of ammonia, nitrate, nitrite, salinity, and pH were measured on a daily basis. Algae paste (Aquaculture Supply USA) was fed to clams once a day until the experiment. Ten to 15 clams from the holding tank were

sacrificed for initial Hg measurements. Clams were retrieved from all 6 tanks at the end of the experiment. In general, for Hg analysis, tissue samples from 10-15 clams in each tank were ground homogeneously and kept frozen in acid-cleaned containers until analysis.

Zooplankton samples for Hg analysis were collected during experiment 2 roughly once a week using pre-acid cleaned polypropylene nets of 210 μm. A sampling hose attached to a PVC rod was continuously moving in the water column while water was being withdrawn to sample zooplankton as homogeneously as possible. For sampling, an electric pump was used that was specially designed to sample "gently" without destroying zooplankton and to sample fast enough so that they did not escape. Then, zooplankton was transferred from the nets to Teflon vials and filtered onto polycarbonate filters. The filters were then stored in an acid-cleaned petri dish, double bagged and frozen until Hg analysis. Polycarbonate filters and filtration units were acid-cleaned prior to use.

3.2.3. Stable isotope spike addition incubation

Acrylic tubes with 1cm interval holes were used for stable isotope spike addition methylation/demethylation incubation experiments from only one tank of each system (i.e. T1 for R and T4 for NR tanks in experiment 1; T2 for R and T5 for NR tanks in experiment 2). This sampling was made in accordance with other sediment core sampling for Hg and AVS analysis for the initial, mid (experiment 1 only), and final conditions. Four sediment cores were obtained from each tank and transferred to the

lab immediately. Hg stable isotope (^{199}Hg) was obtained from the Oak Ridge National Laboratory (purity of > 90 %). The ^{199}Hg was prepared with the overlying water from the mesocosm tanks, aiming at a 20 % increase of background concentration found in Baltimore Harbor sediments (Mason and Lawrence, 1999; Mason et al., submitted for publication). The ^{199}Hg was then injected into two cores at 1 cm intervals (except for the top 1 cm of sediment cores; 0.5 cm intervals) to determine the methylation rate. MeHg stable isotope (Me^{199}Hg) was synthesized from the ^{199}Hg using methylcobalamin reaction followed by methylene chloride extraction. The Me^{199}Hg was diluted in the overlying water from the mesocosm tanks. The target concentration was double the MeHg concentration found in Baltimore Harbor (Mason and Lawrence, 1999). Then, the Me^{199}Hg was injected into the other two cores at 1 cm intervals (except for the top 1 cm of sediment cores; 0.5 cm intervals) to obtain the demethylation rate. After a 2h-incubation at room temperature, the cores were sliced as described above and immediately frozen until analysis. All Hg isotope amended samples were analyzed using an Inductively Coupled Plasma-Mass Spectrometer (ICP-MS).

3.2.4. Sample analyses

3.2.4.1. Total mercury

Both sediment and biota samples were thawed and digested in a solution of 7:3 sulfuric acid: nitric acid in Teflon vials in an oven at 60 °C overnight prior to BrCl oxidation (1/2-1 h). Then, excess oxidant was neutralized with 10 % hydroxylamine hydrochloride prior to analysis (Bloom and Crecelius, 1983). The samples were then reduced by tin chloride, sparged, and the elemental Hg trapped on gold traps. Quantification was done by dual-stage gold amalgamation/Cold Vapor Atomic Florescence detection (CVAFS) (Bloom and Fitzgerald, 1988) in accordance with protocols outlined in EPA method 1631 (EPA, 1995). Standard calibration curves with r^2 of > 0.99 for THg were achieved daily. THg concentration was determined by both ICP and CVAFS. Analysis of standard reference material, estuarine sediments IAEA-405 (3.9 – 4.3 nmol g^{-1}), typically gave a 90 % recovery for CVAFS, and a 83 % for ICP-MS. Analysis of duplicate samples typically yielded a relative percent difference (RPD) of less than 20 % for both CVAFS and ICP-MS. Detection limits were based on 3 standard deviations of digestion blank measurements. For CVAFS, detection limits for THg were 1.1 pmol g^{-1} for sediments, and 0.1 pmol g^{-1} for biota. For ICP-MS, the detection limit for THg was 0.5 pmol g^{-1} for sediments amended with the Hg isotopes.

3.2.4.2. Methyl mercury

Details of the analytical protocols are given elsewhere (Mason et al., 1999; Mason and Lawrence, 1999). Sediment and biota samples were distilled with a 50 % sulfuric acid/ 20 % potassium chloride solution (Horvat et al., 1993). A sodium tetraethylborate solution was added to the distillate to convert the nonvolatile MeHg to gaseous methylethylmercury (Bloom, 1989). The volatile adduct was then purged from solution and recollected on a graphitic carbon column at room temperature. The methylethylmercury was thermally desorbed from the column, and analyzed by isothermal gas chromatography with CVAFS. Samples for $Me^{199}Hg$ were distilled in the same manner, as described above, and analyzed using ICP-MS after gas chromatographic separation. A calibration curve with an r^2 of > 0.99 was achieved on a daily basis. Analysis of duplicate samples typically gave a RPD of less than 20 %. Detection limits were based on 3 standard deviations of distillation blank measurements. For CVAFS, detection limits for MeHg were 0.02 pmol g^{-1} for sediments and 0.005 pmol g^{-1} for biota. For ICP-MS, detection limit for $Me^{199}Hg$ was 0.009 pmol g^{-1} for sediment samples. For both ICP-MS and CVAFS, analysis of IAEA-405 (25 - 30 pmol g^{-1}) generally gave a 90 % recovery. Spike recoveries yielded 87 % for CVAFS, and 94 % for ICP-MS.

3.2.4.3. Trace metals

A subsample of sediment was placed in acid-cleaned flasks for digestion (EPA, 1996; Keith, 1991). Optima HNO_3 was added and the flasks were covered with watch glasses. The samples were then heated to 95°C and allowed to reflux for 15 min without boiling. Once the samples were cooled, HNO_3 was added, followed by refluxing for 30 min. This procedure was repeated in order to ensure complete oxidation. After the watch glasses were removed, the samples were allowed to evaporate to approximately 5 mL without boiling. When the samples were cooled, aliquots of 30 % H_2O_2 were added until the effervescence was minimal. Then, concentrated HCl and deionized water were added and the samples refluxed for 15 min. Finally, the samples were allowed to cool and diluted to 50 mL with deionized water. The digestates were analyzed for trace metals by ICP-MS using a quadrapole Hewlett-Packard 4500. A calibration curve with an r^2 of at least 0.99 was obtained daily. Analysis of duplicate samples generally gave a RPD of less than 10 %. Detection limits for metals, based on 3 standard deviations of digestion blanks, were generally lower than 0.1 nmol g^{-1}. Analysis of standard reference material, estuarine sediment NIST 1646a, typically yielded a recovery of 84 %. Spike recovery averaged 83 %.

3.2.4.4. Acid Volatile Sulfide (AVS)

A subsample of sediment was weighed and added into a tared 3 neck flask. The flasks were attached immediately to a gas manifold with nitrogen gas purging in order to minimize exposure to oxygen. Van Griethuysen et al. (2002) found that losses of AVS due to air–sample contact (less than 15 min) did not occur. While gassing, deoxygenated HCl was added into each flask. The samples then were distilled for 1.5 to 2 h at room temperature under nitrogen gas flow. Sulfide volatilized during distillation was collected in traps filled with SAOB (sulfide antioxidant buffer) solution (EPA, 1996). Total sulfide in the traps was measured using an ion specific sulfide electrode (Baumann, 1974; Allen et al., 1991; EPA, 1996). A calibration curve with an r^2 of at least 0.99 was achieved daily. Analysis of duplicate samples yielded a RPD of less than 20 %. Spike recovery averaged 95 %. The detection limit was 0.4 µM.

3.2.5. Statistics

In order to examine correlation between two variables, Pearson's product-moment correlation coefficient (r) and associated significant probability (P) were obtained for the data. All the statistical results were reported as significant at a level of $p < 0.05$. We used JMP®, version 4 by SAS institute Inc., Cary, NC, USA for all the statistical analyses. Repeated measures ANOVA was tested using SAS PROC MIXED to see if there was a significant effect on Hg concentration in biota between treatments (R vs. NR) as well as between each time point within the treatments.

3.3. Results and discussion

3.3.1. Experiment 1 (without clams)

3.3.1.1. Overall sediment trends

Table 3.1 shows average and standard deviation of AVS concentration and % organic content for all the tanks. There was only one core taken for the initial condition and no standard deviation is shown. AVS concentration in the initial core tended to increase with depth, while % organic content remained relatively constant. In the R tanks, AVS in the top 0.5 cm decreased to an average of 12 μmole g^{-1} in the mid point cores, compared to the initial AVS, and then increased to an average of 31 μmole g^{-1} in the final cores at the end of the experiment. A similar pattern was observed in deeper sediments. In the NR tank, however, AVS in the top 0.5 cm decreased over the entire experiment from the initial concentration of 36 μmole g^{-1} to 8.0 μmole g^{-1} (final). In all the cores, AVS concentration fell within the lower range of AVS values found in surface sediments (top 2 cm) of Baltimore Harbor (e.g. AVS concentration was mostly < 100 μmole g^{-1} but was as high as 800 μmole g^{-1}) (Mason and Lawrence, 1999). Overall, increasing AVS with depth can be explained by sulfate reduction, which is a major pathway for the oxidation of organic matter in anoxic estuarine sediments (Van Den Berg et al., 1998, Lin et al., 2002).

Percent organic content in the R tanks remained constant with depth and also showed little change over time (Table 3.1). In the NR tanks, % organic content showed a distinct increase in the top 1 cm sediment at the end, compared to the mid point cores. Although this may not be quantitatively substantial, one explanation for the change can be that settling particles (once deposited in sediments and not

resuspended) in the NR tanks likely contributed to an increase of % organic content in the top sediment layer. In fact, % organic content in the water column was significantly higher in the NR tanks, averaging 53 %, while being only 18 % in the R tanks during resuspension (Chapter 2, Kim et al., 2004). Another explanation is that there was an increase in microphytobenthos over time (Porter et al., unpublished data) in the NR systems as there was no resuspension and light penetrated to the sediment surface. On the other hand, in the R tanks, a large amount of sediment was resuspended to the water column. However, this material settled rapidly during the off-cycle. Thus, % organic matter significantly increased (26 % of TSS) in the water column as sediment settled quickly upon cessation of resuspension, and was similar to that of the NR tanks (Chapter 2, Kim et al., 2004).

The average concentrations and standard deviations of THg are presented in Table 3.1. THg in the initial cores showed a peak at a depth of 1-2 cm, averaging 2.9 nmol g^{-1}. The R tank in the mid point cores showed a somewhat lower range of THg, compared to both initial and final cores. THg concentration in the final cores was highest in the top 0.5 cm, averaging 2.6 ± 0.3 nmol g^{-1}. In the NR tank, THg was highest in the top 0.5 cm for both mid point and final cores, averaging 2.3 ± 0.06 nmol g^{-1} and 2.3 ± 0.8 nmol g^{-1}, respectively. THg concentrations in the final cores of both R and NR tanks appeared to be higher than the mid point cores. However, this is likely due to inherent sediment heterogeneity as large standard deviations were often found between the three replicate tanks. Relative standard deviations (RSD) between the replicate tanks (20 - 40 %) were overall comparable to RPDs between the duplicate cores within the tank. In comparison with analytical errors, as mentioned

earlier, analysis of duplicate samples typically yielded a RPD of less than 15 %. Mason et al. (1998) similarly found in the field relatively large variability between cores collected further apart owing to sediment inhomogeneity. The range of THg in the surficial sediment agreed well with concentrations in Baltimore Harbor found by Mason and Lawrence (1999) (average of 2.3 nmol g^{-1}).

There was a significant positive correlation between THg concentration and % organic content ($r = 0.5$, $n = 36$). Similarly, Mason and Lawrence (1999) concluded that organic complexation/adsorption was an important factor controlling Hg distribution in the surface sediment of Baltimore Harbor as the two parameters were strongly correlated. Mason and Lawrence (1999) found no significant correlation between THg and AVS in the surface sediment from Baltimore Harbor. They estimated the maximum degree of pyritization (% DOP), as defined by Huerta-Diaz and Morse (1990), for the Baltimore Harbor sediments. Percent DOP yielded 6.8 ± 5.7 %, which was in a relatively low range but fell within the range of other values for surface sediments (Huerta-Diaz and Morse, 1990). Thus, based on the relationships with Fe and S, it is estimated that 10 % or less of the Fe is associated with S phases in the surface sediment (i.e. Fe is likely bound in other forms, for example, Fe-oxyhydroxides). If Hg was associated with Fe-S or Fe-oxide phases, then there should have been a relationship between Hg and Fe. The data of Mason and Lawrence (1999), however, did not show any relationship between Hg and Fe. Therefore, it appeared that Hg binding in the Baltimore Harbor sediments was not controlled to a large degree by sulfide or Fe chemistry. This was likely because of the high organic content and the low % DOP of these surficial sediments. In our

experiment, this may also be an explanation for the lack of relationship between THg and AVS in the top sediment layers in this experiment. However, in deeper layers where sediments are anoxic, AVS and organic matter both likely become important binding phases.

Table 3.1 also shows the average concentration and standard deviations of MeHg. The initial concentration of MeHg showed a peak below the top 1 cm of sediment. MeHg concentration in the R tanks was highest near the surface but changed little over the course of the experiment. A similar pattern was found in the NR tanks. In addition, the fraction of the Hg as MeHg was generally low (< 0.5 % of THg concentration), as found by others in estuarine sediments (Gobeil and Cossa, 1994; Gagnon et al., 1996, Benoit et al., 1998). MeHg concentration was significantly and positively correlated with % organic content ($r = 0.3$, $n = 36$) but negatively with AVS ($r = - 0.4$, $n = 36$). Benoit et al. (1998) found that % organic content was correlated with both THg and MeHg concentrations in sediments from the Patuxent River, suggesting their affinity for, or association with, depositing organic matter, and a potential interaction between MeHg production and sediment organic content.

Table 3.1. Average concentrations of THg, MeHg, AVS, and % organic content with standard deviations from all the tanks in experiment 1.

	Depth (cm)	THg (nmol g^{-1})	MeHg (pmol g^{-1})	AVS[b] (μmole g^{-1})	% organic matter[c]
Initial A[a]	0-0.5	2.0	6.2	36	12
	0.5-1	2.0	6.4	132	12
	1-2	2.9	5.1	114	13
	2-3	2.3	5.2	81	13
	3-5	2.1	4.5	122	13
Initial B[a]	0-0.5	1.5	3.2		
	0.5-1	2.8	2.8		
	1-2	2.8	6.7		
	2-3	2.8	7.6		
	3-5	2.2	5.4		
Mid-R[d]	0-0.5	1.4 ± 0.6	5.4 ± 1.2	12 ± 2.6	12 ± 0.6
	0.5-1	0.9 ± 0.3	5.1 ± 0.7	34 ± 4.1	12 ± 1.0
	1-2	1.3 ± 0.3	3.0 ± 0.4	42 ± 21	12 ± 0.1
	2-3	1.2 ± 0.7	2.4 ± 1.6	69 ± 20	12 ± 0.4
	3-5	1.3 ± 0.2	3.7 ± 0.2	94 ± 10	12 ± 0.1
	5-7	1.4 ± 0.2	3.1	94	12 ± 0.8
Final-R	0-0.5	2.6 ± 0.3	4.8 ± 1.0	31 ± 5.5	13 ± 0.5
	0.5-1	2.0 ± 0.8	3.9 ± 1.3	57 ± 8.2	13 ± 0.9
	1-2	1.6 ± 0.5	3.6 ± 1.3	66 ± 17	13 ± 0.4
	2-3	2.2 ± 0.8	2.3 ± 0.4	85 ± 12	13 ± 0.6
	3-5	2.4 ± 0.9	2.1 ± 0.7	85 ± 14	12 ± 0.04
	5-7	2.2 ± 1.0	2.8 ± 0.8	103 ± 17	12 ± 0.1
Mid-NR[d]	0-0.5	2.3 ± 0.06	5.5 ± 1.1	18 ± 6.0	13 ± 0.3
	0.5-1	1.9 ± 0.4	3.1 ± 2.4	49 ± 5.9	12 ± 0.5
	1-2	1.3 ± 0.1	2.7 ± 0.2	58 ± 12	12 ± 0.1
	2-3	1.4 ± 0.4	3.9 ± 0.4	60 ± 4.2	12 ± 0.2
	3-5	1.2 ± 0.06	3.9 ± 0.09	75 ± 30	12 ± 0.2
	5-7	1.5 ± 0.3	3.9 ± 1.1	69 ± 10	12 ± 0.5
Final-NR	0-0.5	2.3 ± 0.8	5.0 ± 2.6	8.0 ± 7.2	15 ± 0.3
	0.5-1	1.9 ± 0.3	5.2 ± 4.4	31 ± 12	14 ± 0.7
	1-2	1.7 ± 0.2	3.9 ± 1.5	53 ± 7.1	13 ± 0.3
	2-3	1.8 ± 0.08	4.5 ± 2.5	71 ± 5.0	13 ± 0.2
	3-5	1.8 ± 0.2	3.9 ± 2.0	72 ± 8.7	13 ± 0.1
	5-7	1.7 ± 0.2	3.0 ± 0.8	82 ± 11	12 ± 0.4

a: initial duplicate cores run by ICP for THg and MeHg.
b and c: only one core was used for the initial condition.
d: the rest of samples are presented in averages of all three replicate tanks run by both ICP and CVAFS (see the text for details).

3.3.1.2. Mercury methylation

The % methylation from spiked core incubation experiments using ^{199}Hg in the initial cores ranged from 0.07 to 0.3 %, showing a tendency to slightly increase with depth (Fig. 3.1a). The R tank in the mid point cores showed a large variability in % methylation, with peaks at depths of 0-0.5 cm and 2-3 cm sediment. Percent methylation was highest in the top 0.5 cm of sediment (Fig. 3.1b). The average % methylation in the mid point cores was 0.6 ± 0.5 % in the 0-0.5 cm depth range and 0.4 ± 0.06 % in the 0.5-1 cm range, and 0.5 ± 0.1 % in the 0-0.5 cm and 0.2 ± 0.1 % in the 0.5-1 cm range in the final cores. In the NR tank, % methylation appeared to increase in the top 1 cm of the sediment over time and averaged 0.1 ± 0.03 % in the 0-0.5 cm and 0.3 ± 0.1 % in the 0.5-1 cm depth sediment in the mid point cores, and 0.3 ± 0.1 % in the 0-0.5 cm and 0.6 ± 0.3 % in the 0.5-1 cm range in the final cores (Fig. 3.1c). However, overall % methylation was higher in the R tanks than in the NR tanks in the upper sediment layers.

Figure 3.1. Percent methylation in sediment cores (experiment 1): (a) initial cores; (b) R tank (T1); (c) NR tank (T4).
Duplicate core IDs are presented in parenthesis for each time point (see text for details).

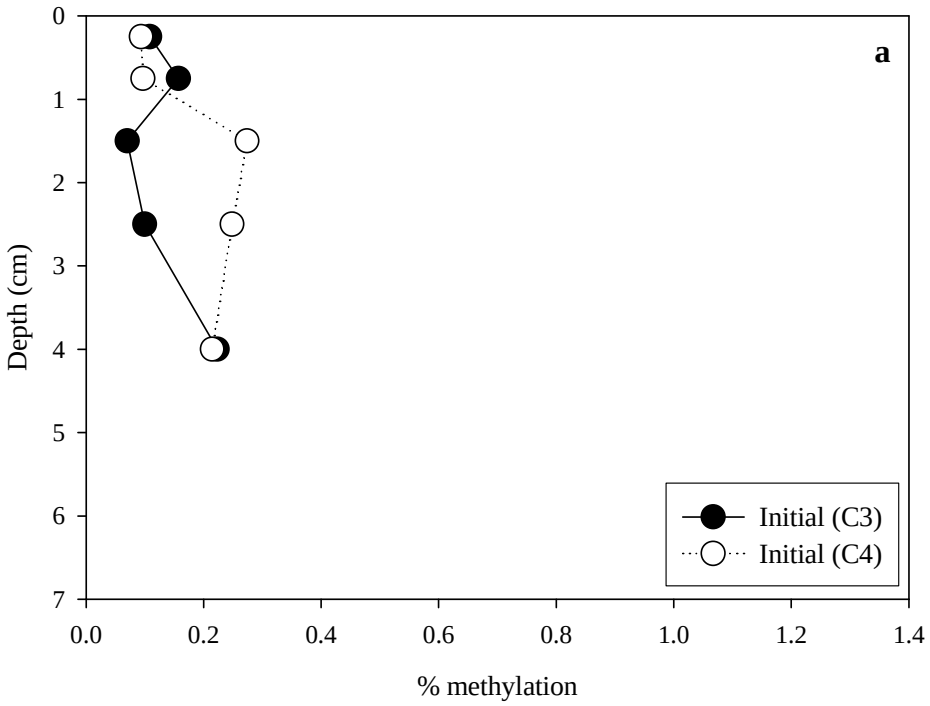
a
Depth (cm)
% methylation
Initial (C3)
Initial (C4)

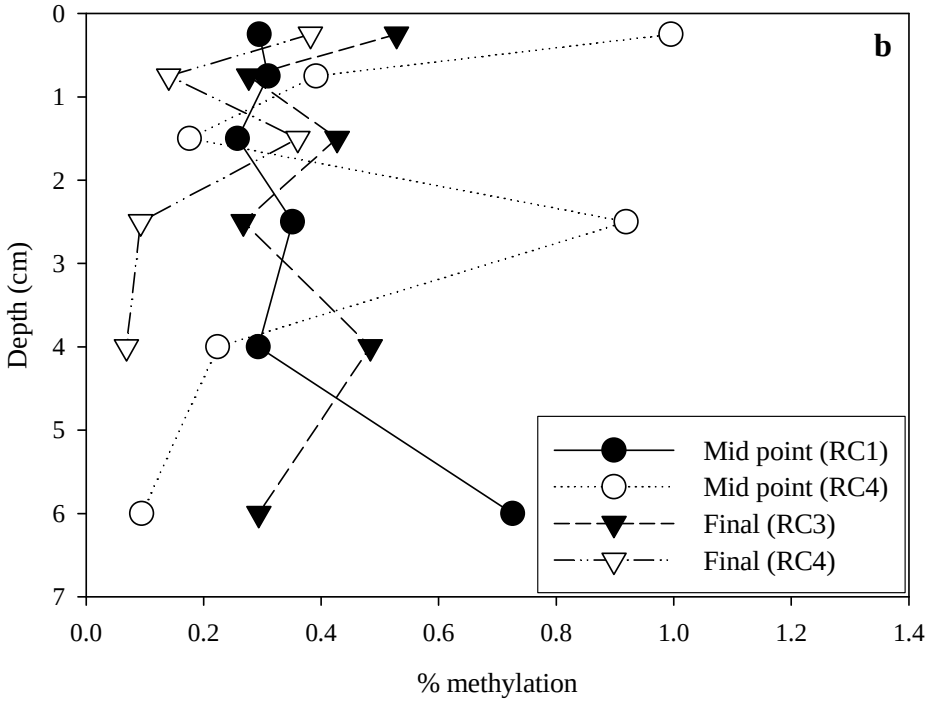
b
Depth (cm)
% methylation
Mid point (RC1)
Mid point (RC4)
Final (RC3)
Final (RC4)

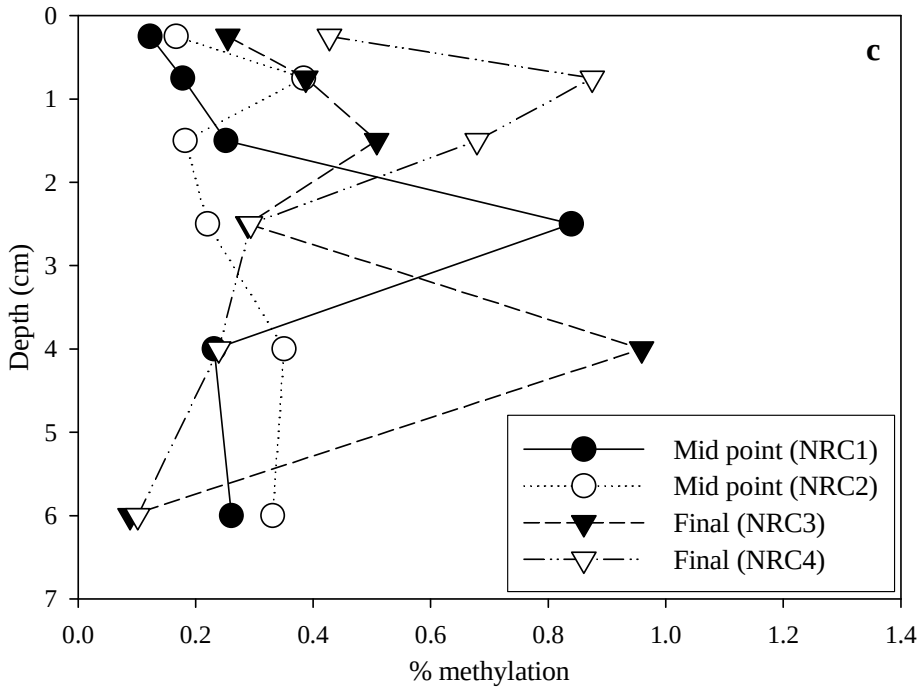
c
Depth (cm)
0
1
2
3
4
5
6
7
0.0
0.2
0.4
0.6
0.8
1.0
1.2
1.4
% methylation
Mid point (NRC1)
Mid point (NRC2)
Final (NRC3)
Final (NRC4)

The amount of $Me^{199}Hg$ produced in the 2 h-incubation was significantly and positively correlated with MeHg concentration in the sediment ($r = 0.8$, $n = 58$) (Fig. 3.2a). In the R tank, the amount of $Me^{199}Hg$ produced in the mid point cores appeared to be in a slightly higher range, compared to the final cores, with the initial concentration being in between. On the other hand, the NR tank had an opposite trend in that the amount of $Me^{199}Hg$ produced in the final cores was higher than the mid point cores. As seen in Fig. 3.2b, there was also a significant positive but weak correlation found between % methylation and *in situ* MeHg concentration ($r = 0.4$, $n = 58$). The relationship showed more variability than the correlation between $Me^{199}Hg$ produced and *in situ* MeHg concentration. Heyes et al. (in preparation) found a similar result in their Hg isotope addition incubation experiment with sediments from Mackall Cove, a small inlet off the Patuxent River, Maryland. Similarly, such relationships were found for sediments from the Hudson River turbidity maximum zone (Heyes et al., 2004) and for the Bay of Fundy (Sunderland et al., 2004).

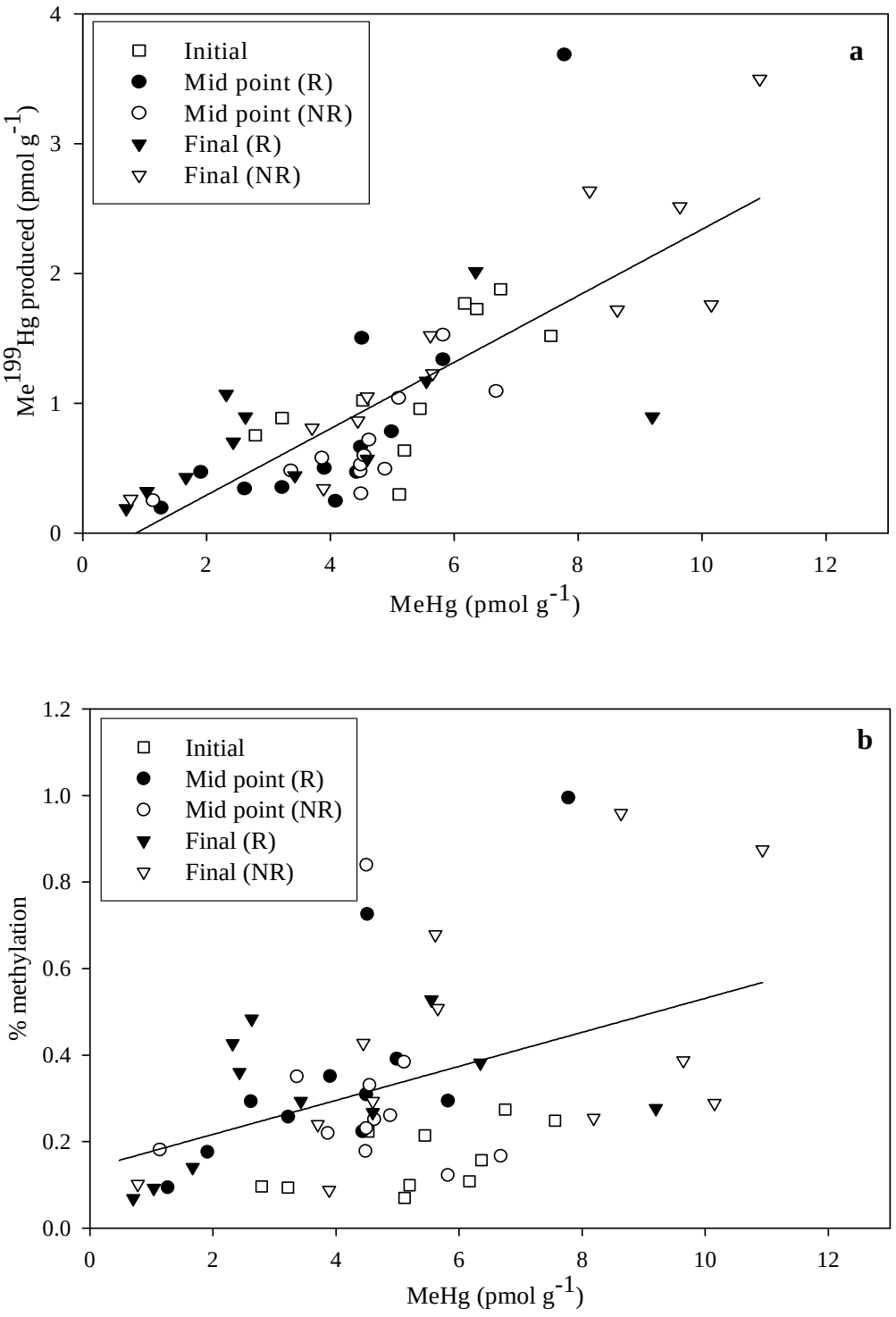

Figure 3.2. The correlations between (a) $Me^{199}Hg$ produced in 2 h and sediment MeHg; (b) % methylation and sediment MeHg (experiment 1).

Based on our results, Hg methylation rate constants were calculated using the following equation given by Hintelmann et al. (2000), which treats both methylation and demethylation as pseudo first order reactions. The net rate of $Me^{199}Hg$ production is:

$$d[Me^{199}Hg])/dt = k_1 [^{199}Hg(II)] - k_2 [Me^{199}Hg] \quad (1)$$

where k_1 = methylation rate constant (d^{-1})
k_2 = demethylation rate constant (d^{-1})
$[^{199}Hg]$ = concentration of added ^{199}Hg (nmol g^{-1})
$[Me^{199}Hg]$ = concentration of $Me^{199}Hg$ (nmol g^{-1}) produced.

For a short-term assay, the second term in equation 1 can be ignored because $[Me^{199}Hg]$ is low enough at the early stage in the stable isotope incubation experiment. Thus, equation 1 leads to:

$$d[Me^{199}Hg])/dt = k_1 [^{199}Hg] \quad (2)$$

By integrating equation 2, the methylation rate constant is obtained as below:

$$k_1 = [Me^{199}Hg)]/ ([\ ^{199}Hg] \cdot t) \quad (3)$$

In the mid point cores, the R tank had a higher rate constant for Hg methylation (0.08 ± 0.06 d^{-1}) than the NR tank (0.02 ± 0.004 d^{-1}) in the top 0.5 cm of sediments. However, the rate constant in the R tank slightly decreased to 0.05 ± 0.01 d^{-1} in the final cores, whereas, in the NR tank, the rate constant increased to 0.04 ± 0.01 d^{-1}. A similar trend was found in the 0.5-1 cm of sediment. Overall, resuspension appeared

to increase Hg methylation in the sediment, especially in the top layer (0-1 cm), with the impact being to some degree more pronounced earlier in the experiment. The R tank showed a decrease in Hg methylation at the end of experiment. It should be noted that the R system was accidentally shut off on the 20th day and all the R tanks were not disturbed overnight. This event may have influenced the sediment redox state and may have resulted in an AVS increase and a Hg methylation decrease in the final core samples.

3.3.1.3. Methylmercury demethylation

The initial cores showed more than 60 % demethylation in the 2-h incubation throughout the core depth, with less demethylation occurring in the top sediment (Fig. 3.3a). In the R tank, demethylation in the mid point cores appeared to be similar to that of the initial cores, while the final cores showed a relatively constant % demethylation except for the top 0.5 cm of the sediment (Fig. 3.3b). In the NR tank, demethylation in the mid point core showed large variability between the duplicate cores (Fig. 3.3c). Percent demethylation in the final cores of the NR tank was fairly constant with depth. In general, the demethylation rate appeared to be higher than the methylation rate in these sediments.

Figure 3.3. Percent demethylation in sediment cores (experiment 1): (a) initial cores; (b) R tank (T1); (c) NR tank (T4).

Duplicate core IDs are presented in parenthesis for each time point (see text for details).

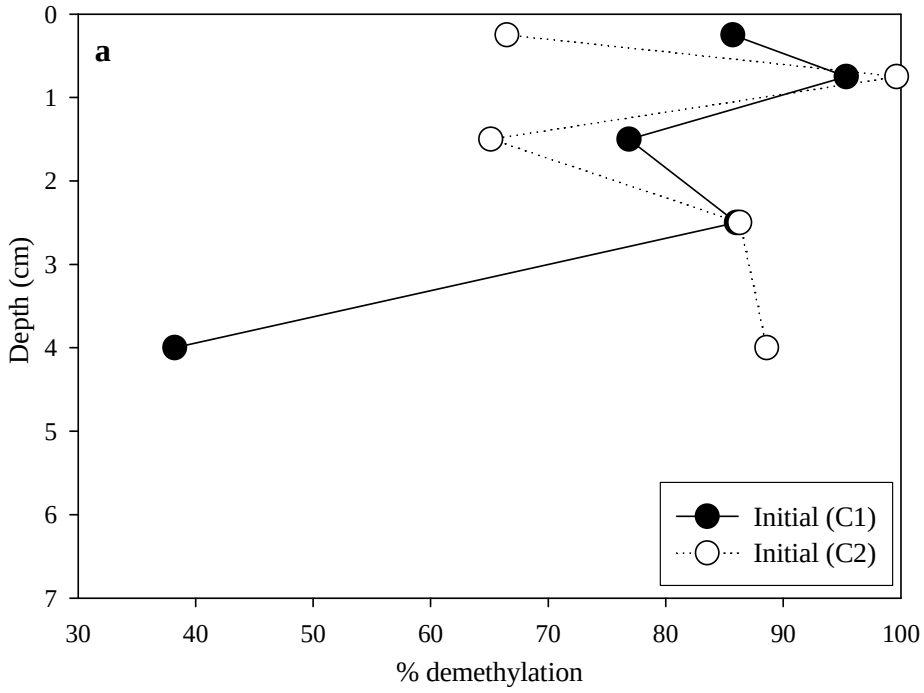
a
Depth (cm)
% demethylation
Initial (C1)
Initial (C2)

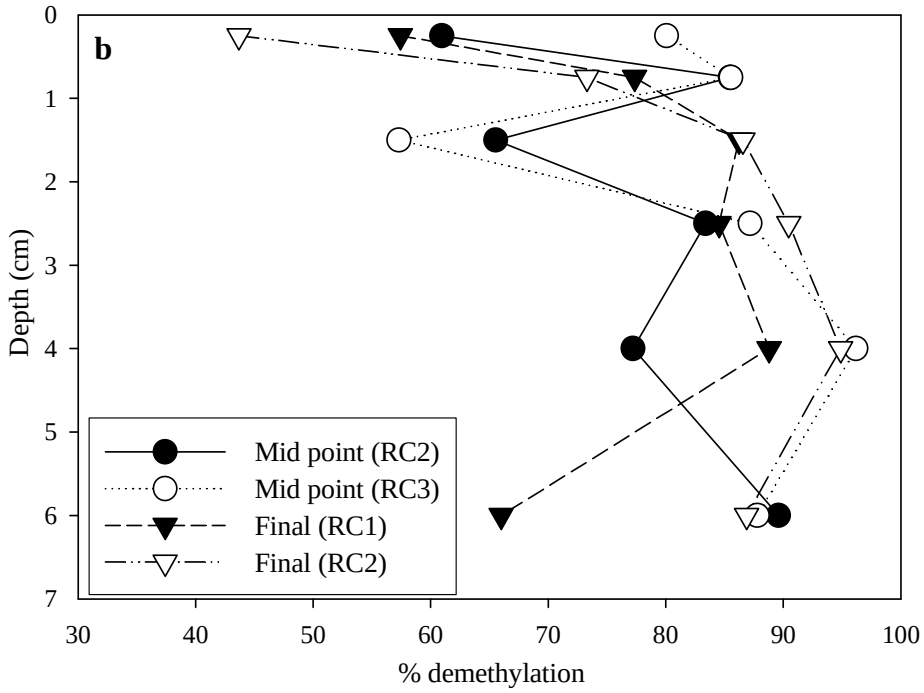
b
Depth (cm)
% demethylation
Mid point (RC2)
Mid point (RC3)
Final (RC1)
Final (RC2)

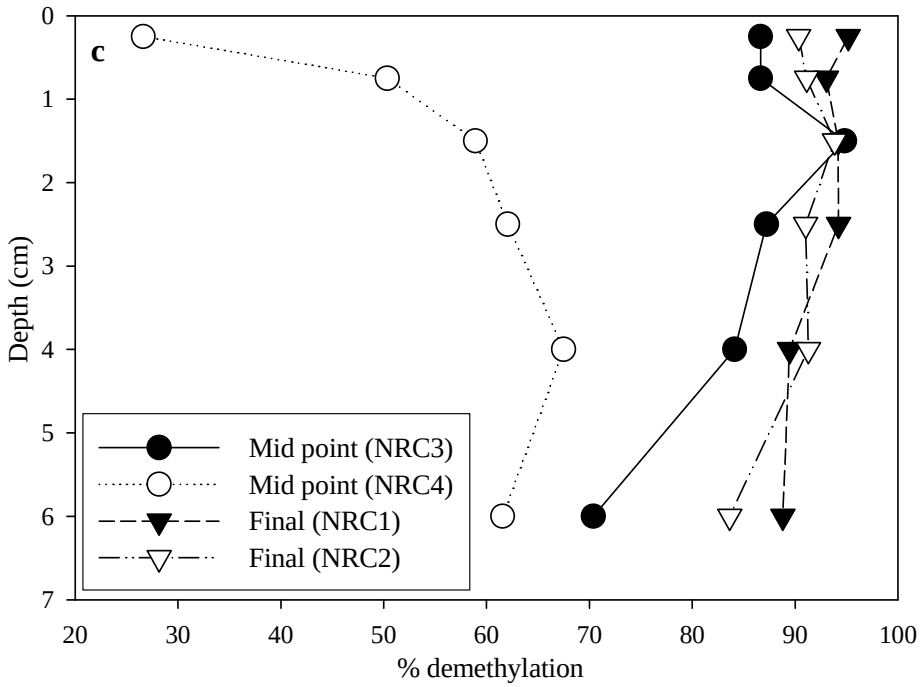
c
Depth (cm)
% demethylation
Mid point (NRC3)
Mid point (NRC4)
Final (NRC1)
Final (NRC2)
0
1
2
3
4
5
6
7
20
30
40
50
60
70
80
90
100

The demethylation rate constants were also calculated using equation 4 derived from equation 1 (Hintelmann et al., 2000). At the beginning of the incubation experiment, as there is no excess [^{199}Hg], then equation 1 reduces to

$$d[Me^{199}Hg])/dt = - k_2 [Me^{199}Hg] \quad (4)$$

By integration,

$$k_2 = (1/t)\cdot\ln([Me^{199}Hg]_0/[\ Me^{199}Hg]) \quad (5)$$

where $[Me^{199}Hg]_0$ is the initial concentration of $Me^{199}Hg$ in the sediment.

The demethylation rate constants in the mid point cores were 15.3 ± 5.7 d^{-1} for the R tank and 13.9 ± 14.5 d^{-1} for the NR tank in the top 0.5 cm of sediments. The rate constants for the R tank in the final cores decreased to 8.6 ± 2.4 d^{-1} in the top 0.5 cm of sediments, whereas the NR tanks showed a demethylation increase, with an average of 32.2 ± 5.9 d^{-1} in the top 0.5 cm of sediments.

At a steady state, if equal fractions of added spike isotopes are bioavailable, then equation 1 leads to [MeHg]/[Hg] = k_1 / k_2. As seen in Table 3.2, the ratio of the two rate constants (k_1 / k_2) for the R tank yielded around 0.005 and the ratio for the NR tank was approximately 0.001 in the top 0.5 cm of the sediment. The ratios of *in situ* THg and MeHg concentrations yielded ratios of the same order of magnitude as the calculated values for both R and NR tanks (Table 3.2). Thus, although demethylation rate constants were orders of magnitude higher than methylation rate constants, our

results from isotope spike incubation experiments appear to be reasonably consistent with ambient Hg pools in sediments. These results suggest that MeHg must be similarly available in sediments for demethylation, compared to inorganic Hg for methylation. The differences between the results for the R and NR tanks suggest a higher rate of net methylation in the R tank compared to the NR tank. Moreover, the half-life of MeHg ($t_{½} = \ln 2 \times 1/k_2$) was generally less than 2 h, suggesting that MeHg turnover occurred very rapidly in the sediment. Thus, methylation process seems to play an important role in determining MeHg concentration in sediments as in the absence of continuous methylation, MeHg would be rapidly depleted. Our preliminary mass balance, discussed in Chapter 2 (Kim et al., 2004), suggested that net MeHg production within the mesocosm tanks was higher in the R tanks than in the NR tanks. While the mass balance suggested an overall net formation of MeHg in the R tanks, the results for the NR tanks were equivocal given the errors associated with the mass balance estimates. The discussion above is consistent with the mass balance in terms of the higher net methylation rate in the R tanks compared to the NR tanks.

Table 3.2. Comparison of methylation and demethylation rates in the top sediment (0-0.5 cm).

		k_1 ($\times 10^{-2}$) (d^{-1})	k_2 (d^{-1})	k_1/k_2 ($\times 10^{-3}$)	**$[MeHg]_{tot}/[Hg]_{tot}$ ($\times 10^{-3}$)**
Experiment 1	Initial	1.2	18.2	0.66	**2.5**
	Mid-R	7.7	15.3	5.0	**4.0**
	Final-R	5.4	8.6	6.3	**1.9**
	Mid-NR	1.7	13.9	1.2	**2.2**
	Final-NR	2.5	28.1	0.89	**2.2**
Experiment 2	**Initial**	**1.9**	**13.5**	**1.4**	**3.9**
	Final-R	**2.0**	**17.2**	**1.2**	**2.5**
	Final-NR	**2.7**	**16.2**	**1.7**	**3.3**

3.3.2. Experiment 2 with clams

3.3.2.1. Overall sediment profiles

AVS and % organic content for this experiment are presented in Table 3.3. AVS in the initial cores showed a tendency to increase with depth, which was similar to the initial AVS concentration in experiment 1. Both RC and NRC tanks showed a similar pattern with AVS concentration at the end of the experiment. Unlike experiment 1, AVS in the top 0.5 cm of sediment was comparable between the two systems. Percent organic content in the initial cores was fairly constant with depth, which was very similar to experiment 1. The RC tanks showed a slight increase in % organic content in the top 0.5 cm of sediment. In the NRC tanks, % organic content increased by 15 % in the top sediment. This is consistent with the result in experiment 1 that, in the NRC tanks, organic content tended to increase in the top sediment over time.

As discussed in Chapter 2 (Kim et al., 2004), POM in the water column decreased by 80 % (RC) and 87 % (NRC), on average, compared to POM concentration in experiment 1, due to a combination of lower water temperature and the presence of clams in experiment 2. However, % POM in both systems remained similar to experiment 1 (higher % POM in the NRC tanks). Thus, even with the presence of clams and the lower phytoplankton stock, settling particles that contained higher % POM likely contributed to the accumulation of higher % organic content in surface sediments over time in the NRC tanks. As mentioned earlier, the presence of microphytobenthos mediated by enhanced light reaching the bottom could also contribute to the higher surface % organic content. Moreover, biodeposits by clams that do not ever get resuspended in the NR tanks might have accumulated in the surface sediment as well.

THg concentration in the initial cores showed peaks in depths of 0.5-1 and 3-5 cm sediment (Table 3.3). Both RC and NRC tanks showed a similar range and vertical distribution of THg. There was no significant correlation between THg and % organic content, which was in contrast to the result in experiment 1. The lack of relationship is likely due to the smaller set of data, as we did not have the mid point measurement for this experiment. THg was not significantly correlated with AVS, as observed in experiment 1. Indeed, a relationship between AVS and THg in field samples has not been shown in any published data.

MeHg concentration in the initial cores showed a relatively constant profile with depth and a similar pattern was observed in both RC and NRC tanks (Table 3.3). There was no significant correlation found between MeHg concentration and %

organic content, as well as AVS. MeHg concentration was not significantly correlated with THg. Mason and Lawrence (1999) found that MeHg concentration was not significantly correlated with organic matter or AVS for Baltimore Harbor sediments. As mentioned above, Baltimore Harbor samples were from the surface sediments only (top 2 cm). In contrast, Hintelmann and Wilken (1995) found a significant positive correlation between MeHg and AVS in an Elbe River (Germany) sediment profile. While the AVS profile was comparable to the results in our experiment, MeHg concentration (e.g., highest value of 180 pmol g^{-1}) was an order of magnitude higher than our results.

Table 3.3. Average concentrations of THg, MeHg, AVS, and % organic content with standard deviations from all the tanks in experiment 2.

	Depth (cm)	THg (nmol g^{-1})	MeHg (pmol g^{-1})	AVS[b] (μmole g^{-1})	% organic matter[c]
Initial A[a]	0-0.5	1.1	6.6	39	12
	0.5-1	1.4	5.4	86	12
	1-2	1.5	5.9	75	13
	2-3	1.4	2.6	72	13
	3-5	1.7	4.9	94	13
	5-7	1.4	2.3	94	12
Initial B	0-0.5	1.2	3.4		
	0.5-1	1.8	4.0		
	1-2	1.5	3.1		
	2-3	1.2	2.9		
	3-5	1.7	3.3		
	5-7	1.6	3.6		
Final-RC[d]	0-0.5	1.8 ± 0.5	4.4 ± 0.7	28 ± 9.4	13 ± 0.3
	0.5-1	1.9 ± 0.3	4.7 ± 1.1	66 ± 19	13 ± 0.3
	1-2	1.3 ± 0.2	3.6 ± 1.0	55 ± 13	13 ± 0.1
	2-3	1.7 ± 0.5	3.4 ± 0.8	79 ± 16	13 ± 0.3
	3-5	1.3 ± 0.1	4.5 ± 0.9	82 ± 25	13 ± 0.1
	5-7	1.3 ± 0.2	3.8 ± 1.0	90 ± 20	13 ± 0.2
Final-NRC[d]	0-0.5	1.3 ± 0.4	4.3 ± 0.4	24 ± 1.0	14 ± 0.3
	0.5-1	1.2 ± 0.6	3.9 ± 0.6	57 ± 13	13 ± 0.1
	1-2	1.1 ± 0.3	3.0 ± 0.6	58 ± 11	13 ± 0.2
	2-3	1.6 ± 0.7	2.8 ± 0.6	73 ± 13	13 ± 0.3
	3-5	1.5 ± 0.6	3.3 ± 0.4	81 ± 6.2	13 ± 0.3
	5-7	1.3 ± 0.4	3.5 ± 0.6	85 ± 3.4	12 ± 0.2

a: averages of duplicates run by ICP for THg and MeHg.
b and c: only one core was used for the initial condition.
d: the rest of samples are presented in averages of all three replicate tanks run by both ICP and CVAFS (see the text for details).

3.3.2.2. Mercury methylation

Percent methylation in the initial cores showed a peak in the 0.5-1 cm of the sediment layers, averaging 0.4 ± 0.003 % (Fig. 3.4a). In the RC tank, % methylation in the final cores was highest in deeper sediments (1-2 cm), averaging 0.8 ± 0.2 % (Fig. 3.4b). In the NRC tank, % methylation showed a peak in 0.5-1 cm sediment layer, with an average methylation of 0.9 ± 0.5 % (Fig. 3.4c). Compared to experiment 1, there was a distinct peak in both systems and less variability was found between the duplicates. A similar pattern was found in both RC and NRC tanks except that the peak in % methylation was found in deeper sediments of the RC tank. Although we did not collect pore water samples, our results likely suggest that there was optimum conditions for Hg methylation at these depths. Optimum conditions would be found in anoxic sediments with low concentrations of sulfide in pore water, as well as the presence of enriched biodegradable organic content and nutrients (Parks et al., 1989). In addition, the presence of hard clams in experiment 2 may have influenced Hg methylation. Hard clams are moderately rapid burrowers and adjust burrowing depth with the posterior tip positioned within 1-2 cm of the sediment surface (Harte, 2001). Burrowing activity is known to enhance transport of dissolved oxygen in sediments, thereby resulting in a local oxidation of reduced sediment compounds (Oenema et al., 1988), and a potential decrease in sulfate reduction activity, and by association, Hg methylation.

Figure 3.4. Percent methylation in sediment cores (experiment 2): (a) initial cores; (b) RC tank (T2); (c) NRC tank (T5).

Duplicate core IDs are presented in parenthesis for each time point (see text for details).

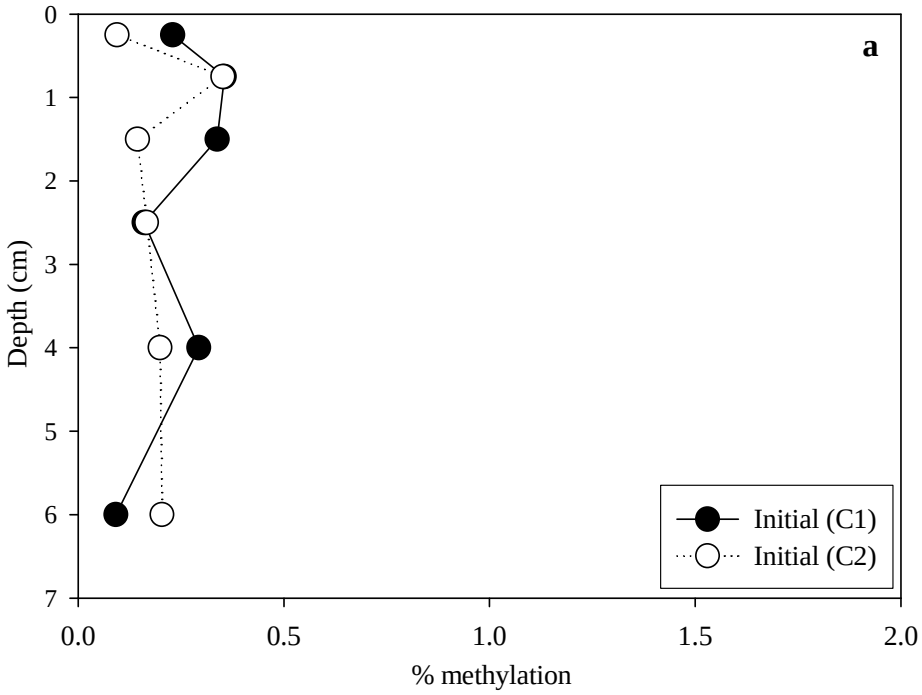
a
Depth (cm)
0
1
2
3
4
5
6
7
0.0
0.5
1.0
1.5
2.0
% methylation
Initial (C1)
Initial (C2)

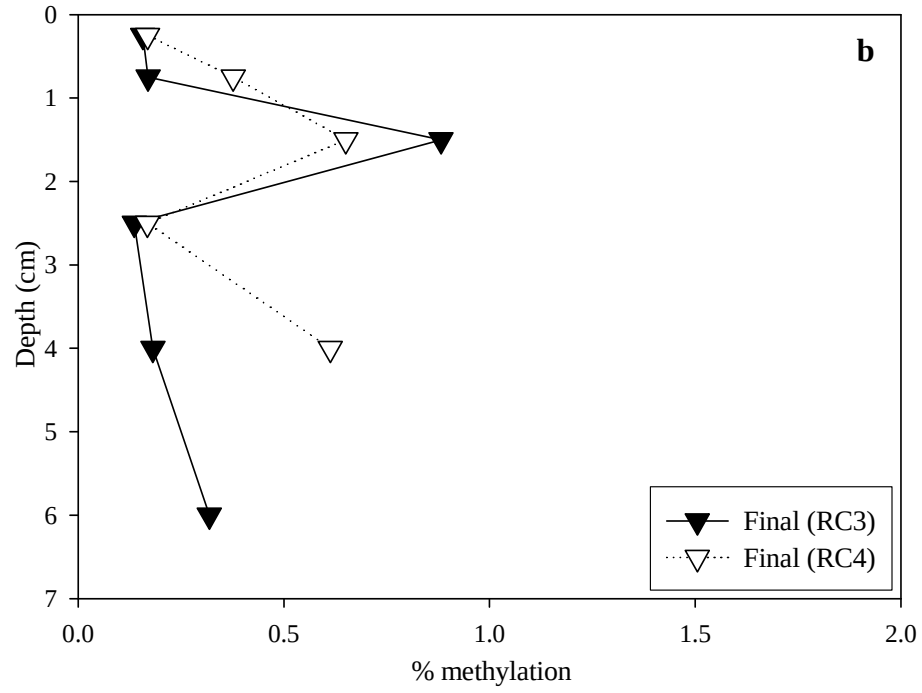
b
Depth (cm)
0
1
2
3
4
5
6
7
0.0
0.5
1.0
1.5
2.0
% methylation
Final (RC3)
Final (RC4)

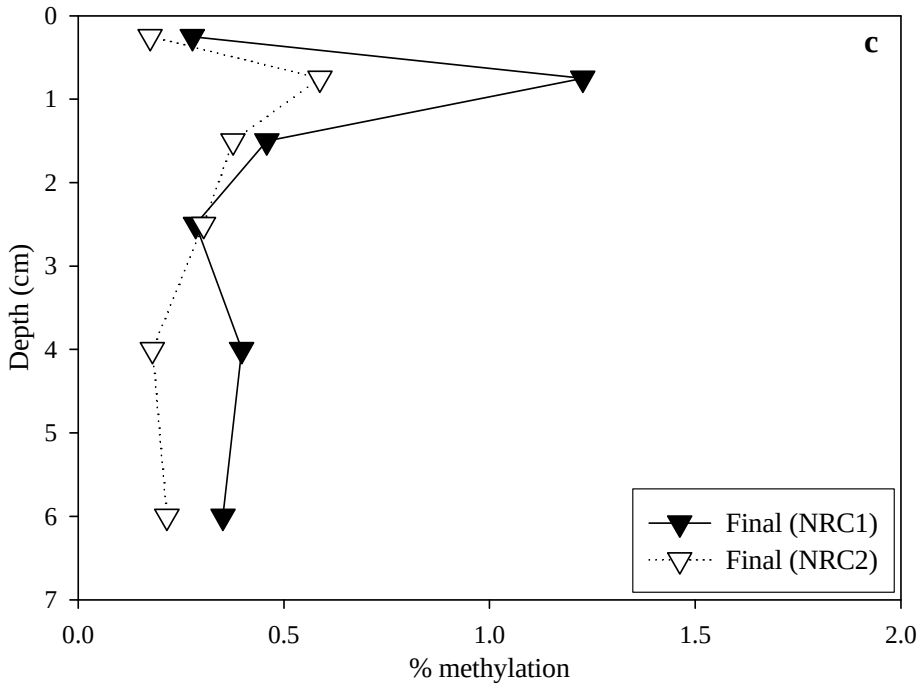
c
Depth (cm)
0
1
2
3
4
5
6
7
0.0
0.5
1.0
1.5
2.0
% methylation
Final (NRC1)
Final (NRC2)

There was a significant positive correlation between $Me^{199}Hg$ produced in 2 h and sediment MeHg ($r = 0.6$, $n = 36$), as seen in experiment 1 (Fig. 3.5a). The RC tank MeHg concentrations were in a higher range than the NRC tank, which showed a similar pattern to that of the mid point cores in experiment 1 (Fig. 3.2a). There was no correlation found between % methylation and sediment MeHg (Fig. 3.5b). Methylation rate constants in the initial cores were higher in the 0.5-1 cm of sediments ($0.04 \pm 0.0003\ d^{-1}$) than deeper layers. The NRC tank had a methylation maximum in the 0.5-1 cm of sediment ($0.1 \pm 0.05\ d^{-1}$), while methylation rate in the RC tank showed a peak in deeper sediment (1-2 cm), averaging $0.09 \pm 0.02\ d^{-1}$.

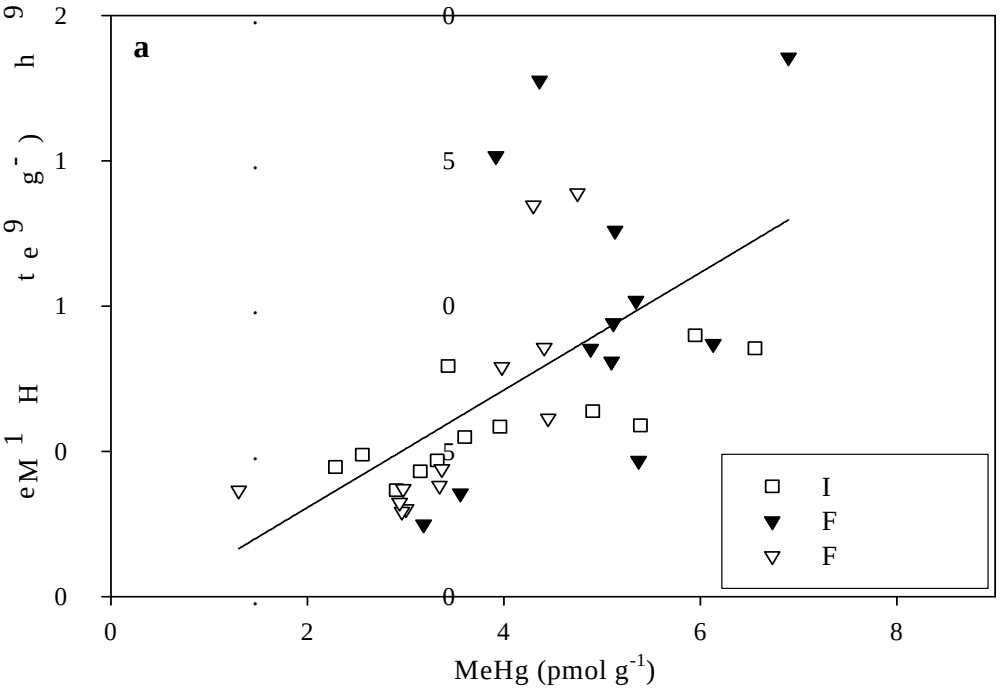
a
I
F
F
MeHg (pmol g-1)

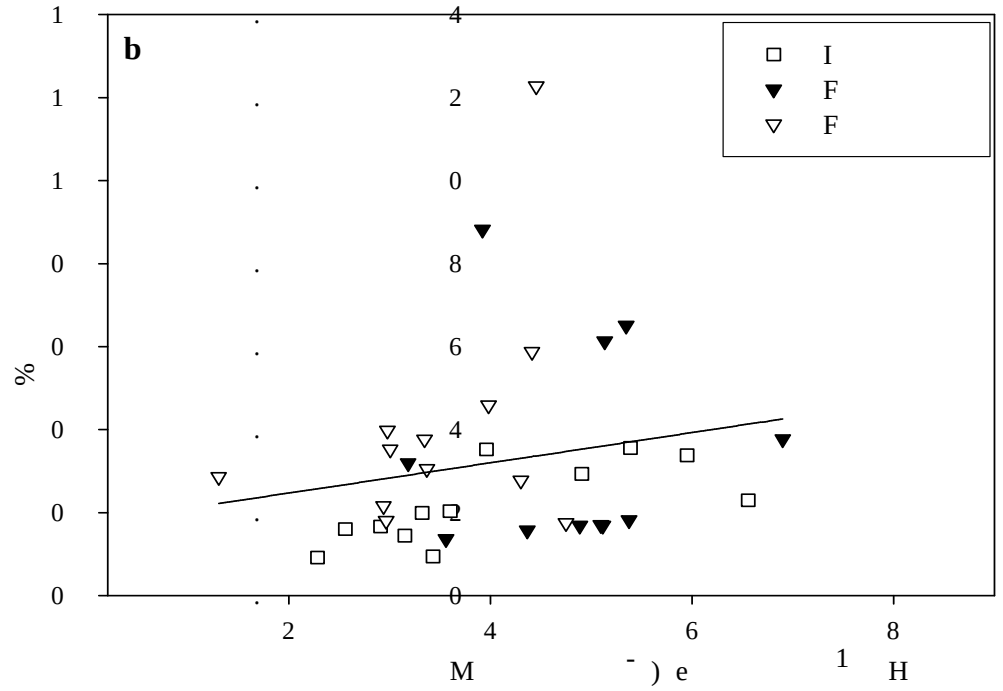
b
I
F
F

3.3.2.3. Methylmercury demethylation

There was only one initial core used for demethylation. As seen in Fig. 3.6a, demethylation showed a peak in the 2-3 cm of sediment (> 90 %) and more than 60 % of the added MeHg was demethylated at all depths. Both RC and NRC tanks showed a similar pattern for % demethylation that was lower in the top 0.5 cm and remained relatively constant in the deeper sediments (Fig. 3.6b, c). As seen in experiment 1, demethylation rates were substantially higher than methylation rates (i.e. ratio of methylation/ demethylation << 1). For example, the demethylation rate constant for the RC tank in the 1-2 cm of sediments was 24 ± 0.03 d^{-1} and 29 ± 10.3 d^{-1} for the NRC tank in the 0.5-1 cm of sediments, where the peaks in Hg methylation were observed. However, as mentioned earlier, MeHg concentration did not markedly decrease at the end of both experiments, compared to the initial condition.

Figure 3.6. Percent demethylation in sediment cores (experiment 2): (a) initial cores; (b) RC tank (T2); (c) NRC tank (T5).

Duplicate core IDs are presented in parenthesis for each time point (see text for details).

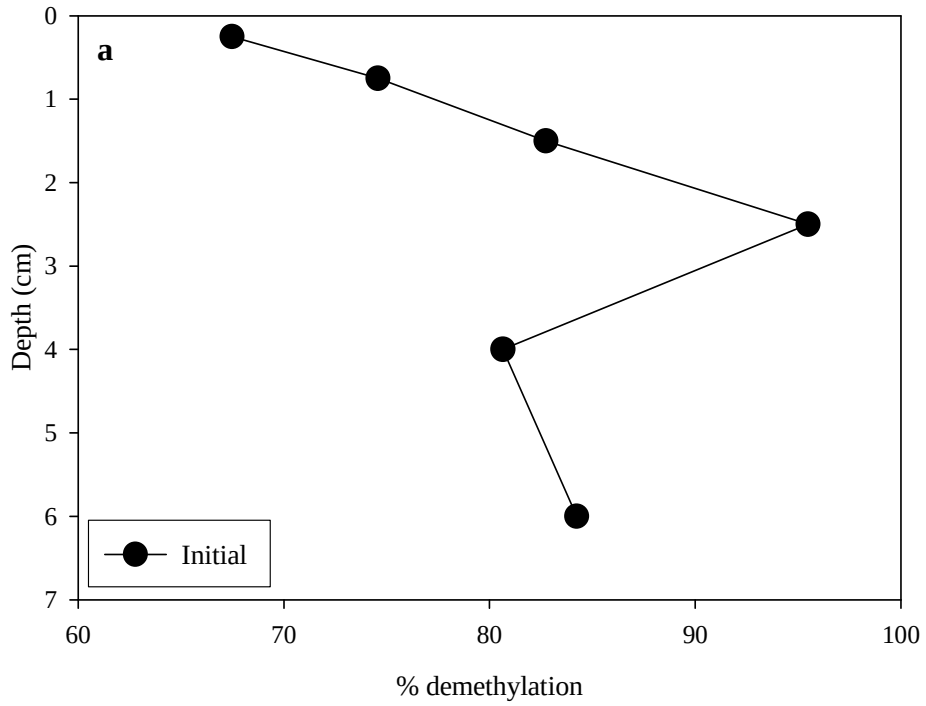
a
Depth (cm)
0
1
2
3
4
5
6
7
60
70
80
90
100
% demethylation
Initial

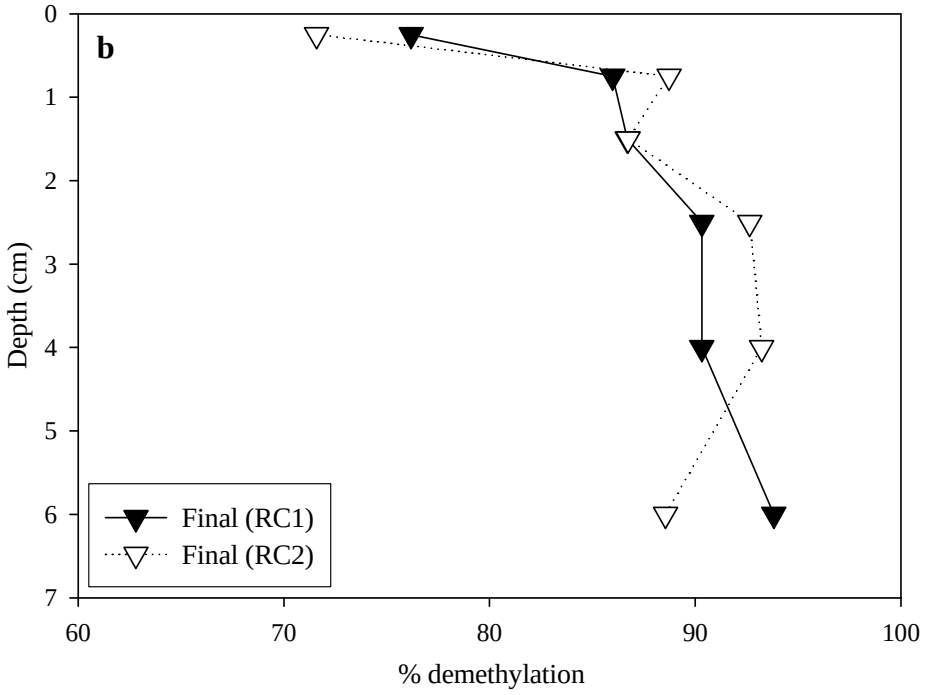
b
Depth (cm)
0
1
2
3
4
5
6
7
60
70
80
90
100
% demethylation
Final (RC1)
Final (RC2)

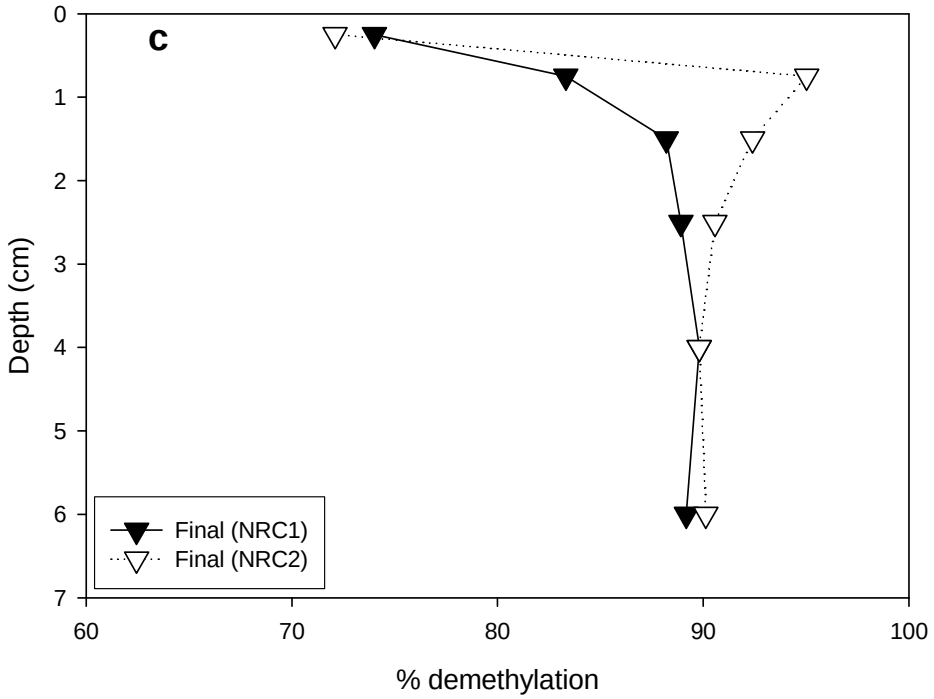
c
Depth (cm)
0
1
2
3
4
5
6
7
60
70
80
90
100
% demethylation
Final (NRC1)
Final (NRC2)

The ratio between the two rate constants (k_1/k_2) was comparable to the ratio of sediment Hg and MeHg concentrations, as seen in experiment 1 (Table 3.2). In addition, Table 3.4 presents methylation/demethylation rates and ratios of the two constants and *in situ* Hg/MeHg concentrations across ecosystems for comparisons. As seen in Table 3.4, the ratio between methylation and demethylation are generally in good agreement with the ratios of *in situ* Hg concentrations (e.g. within a factor of two) especially for estuarine systems. Stable isotope addition experiments seem to give better agreement in comparison of methylation/demethylation rates and sediment Hg concentration, compared to approaches where radioisotopes are used perhaps because of the necessity for longer incubations when radioisotopes are used especially for demethylation studies. It should, however, be noted that since the stable isotope ($Me^{199}Hg$ or ^{199}Hg) was added in solution, there is the possibility that the spiked isotope could have been more quickly methylated/demethylated when it was injected into cores, compared to the *in situ* Hg or MeHg. Others have expressed similar concerns with the short term rate measurements (e.g. Hintelmann, 2000; Benoit et al., 2003) but the results of this study suggest that the relative rates of methylation and demethylation measured using stable isotope spike experiments reflect relatively well the relative rates of methylation and demethylation *in situ*.

Table 3.4. Comparison of methylation and demethylation rates across ecosystems.

Location Type and Method[a]	k_1 ($\times 10^{-2}$) (d^{-1})	k_2 (d^{-1})	k_1/k_2 ($\times 10^{-3}$)	$[MeHg]_{tot}/[Hg]_{tot}$ ($\times 10^{-3}$)	**References.**
Hudson River (E/S)					
Bay of Fundy (E/S)	**0.4**	**11.9**	**0.2**	**0.2**	**Heyes et al., 2004**
Mesocosm Studies (E/S)	**4.2**	**5.5**	**7.6**	**5.8**	**Sunderland et al., 2004**
San Pablo Bay (EW/R)	**3.1**	**16.4**	**2.3**	**2.8**	**This study[b]**
115 Wetland (FW/S)	**1.4**	**0.3**	**56**	**18**	**Marvin- Dipasquale, 2003**
Ontario Lakes (L/S)	**3.2**	**5.0**	**6.4**	**78**	**Heyes (unpublished data)**
Everglades (W/S+R)	**1.3**	**0.5**	**28**	**16**	**Hintelmann et al., 2000**
Lake Sediment (L/R)	**1-4**	**0.04**	**250-1000**	**1-40**	**Benoit et al., 2003/Marvin-Dipasquale & Oremland, 1998[c]**
	0.2	**1-3**	**0.7-1**	**-**	**Pak & Bartha, 1998**

a: Type-- E = Estuarine; L = Lake; F = Freshwater; W = Wetland;
Method -- S = Stable isotopes used; R = Radioisotopes used.
(Time to equilibrium is hours to days.)

b: average values for both R and NR systems in the top sediment layer (0-0.5 cm).

c: methylation study used stable isotopes; demethylation study used radioisotopes.

3.3.2.4. Trace metals

Table 3.5 shows correlation coefficients (r) between metals including THg and MeHg in sediments (n = 48). THg concentration was positively and significantly correlated with most of the other metals except Cd, while MeHg had a significant positive correlation with As, Cu, and Zn only. It is surprising that there was no significant relation between AVS and other metals, especially Fe. However, when the data from the top sediment (1 cm) were excluded, p-values were improved, being near the significant level ($p \leq 0.05$) in most cases. Thus, as found by others (Gobeil and Cossa, 1993; Gagnon et al., 1997), trace metals are likely associated with other matrices such as iron oxides, organic matter, and oxide/organic matter associations, and not only AVS, in these surface sediments. Under highly anoxic conditions, however, AVS and organic matter are important scavengers for Hg species and other trace metals.

Table 3.5. Correlation table for experiment 2; values listed are Pearson's product-moment correlation coefficients (r)[a].

	Ag	As	Cd	Co	Cu	Fe
Ag	1	0.95	0.60	0.96	0.98	0.79
As		1	0.48	0.98	0.97	0.87
Cd			1	0.46	0.49	NS
Co				1	0.99	0.86
Cu					1	0.86
Fe						1
	Ni	Pb	Se	Zn	THg	MeHg
Ag	0.97	0.88	0.98	0.97	0.52	NS
As	0.97	0.87	0.93	0.99	0.47	0.47
Cd	0.48	NS	0.63	0.50	NS	NS
Co	0.99	0.90	0.96	0.98	0.51	NS
Cu	0.99	0.91	0.98	0.98	0.52	0.42
Fe	0.84	0.80	0.80	0.88	0.49	NS
Ni	1	0.90	0.96	0.97	0.49	NS
Pb		1	0.85	0.88	0.55	NS
Se			1	0.96	0.55	NS
Zn				1	0.52	0.48
THg					1	NS
MeHg						1

a: correlation coefficients are significant at a level of $p < 0.05$; NS = not significant.

3.3.3. Impact of resuspension on Hg methylation/demethylation

Overall, sediment resuspension seems to have a complex effect on the association of Hg with binding phases as well as Hg methylation and demethylation in surface sediments. It was observed in experiment 1 that AVS in the R tanks initially decreased in surface sediments, suggesting the oxidation of AVS due to resuspension. However, sediment AVS did not continuously decrease in the R tanks throughout the experiment, as was expected. In fact, the final AVS concentration in the R tanks was higher than in the NR tank. As mentioned above, the R system was accidentally shut down overnight near the end of experiment 1 and this may have resulted in the surface sediment possibly becoming more anoxic temporally due to the lack of oxygen penetration. However, we consider this unlikely given its relatively short duration compared to the overall experiment. More likely, during summer, the suboxic and anoxic boundary layer is closer to the sediment-water interface because of the higher sediment temperature and the input of freshly deposited organic matter, and its increased degradation. It should be noted that sediment resuspension did not inhibit primary productivity in the mesocosms (Chapter 2, Kim et al., 2004), as may have been expected. The enhanced supply of nutrients from the sediments, as a result of resuspension, led to an overall comparable or higher Chl *a* (Chlorophyll *a*) concentration in the resuspension tanks compared to the NR tanks, and a bloom in the mid period of the experiment. Settling of this organic matter may have resulted in the noted shift in surface sediment AVS. Thus, a combination of the seasonal influence and the accidental shutoff of the resuspension stirring mechanism is the likely

explanation for the AVS increase in the surface sediment of the R tanks at the end of the experiment.

As proposed by Gagnon et al. (1997), the oxidation of AVS could produce stable, soluble Hg complexes in the pore water. This released Hg could then be adsorbed onto or co-precipitated with iron oxides or organic matter. As mentioned above, sulfate reducing bacteria are the primary agents for methylating Hg. Maximal methylation occurs in environments where sulfate is sufficient to stimulate sulfate reduction and, as a result, Hg methylation but where there is relatively low sulfide, so that methylation is not limited (Choi and Bartha, 1994; Benoit et al., 1998). Bioavailability of Hg is an important factor in Hg methylation. Benoit et al. (1999a) developed a chemical equilibrium model to test the hypothesis that the bioavailability of Hg to sulfate reducing bacteria is a function of the concentration of neutral Hg sulfide complexes that can readily diffuse across the bacterial membrane. The model results suggest that as sulfide increases, the dominant Hg speciation changes from neutral dissolved Hg complexes (e.g. HgS (aq)) to charged sulfide complexes. Octanol-water partition experiments (Benoit et al., 1999b) and culture experiments (Benoit et al., 2001) have confirmed this hypothesis.

The results in experiment 1 showed that *in situ* MeHg production had an opposite pattern to changes in AVS concentration, especially in the top sediment layers. Although there was no attempt to analyze dissolved Hg species and sulfate/sulfide concentration in the pore water, our results from experiment 1 showed that Hg methylation was likely enhanced by resuspension, tightly coupled with the oxidation of AVS and the assumed associated change in redox state. In experiment 2,

however, the relationship between MeHg production and AVS concentration was found to be less clear. The situation is complex as while some sediment oxidation may lower sulfide levels and enhance Hg methylation, too much oxidation may hinder bacterial activity.

The demethylation of MeHg has received relatively less attention until recently, compared to Hg methylation. MeHg demethylation can proceed by biotic and abiotic pathways. Abiotic pathways such as photodegradation have been reported in the water column (Sellers et al., 1996; Weber, 1993). Biotic pathways include reductive (RD) and oxidative demethylation (OD), which produce different end products (e.g. CH_4 and Hg(0) for reductive demethylation; CO_2 and Hg(II) for oxidative demethylation) (Marvin-Dipasquale and Oremland, 1998; Hintelmann et al., 2000) and which occur in different regions of the redox zone. Although environmental factors controlling demethylation rates are not yet fully understood, Marvin-Dipasquale et al. (2000) found that RD was a major pathway in extremely contaminated sediments (i.e. ppm levels of THg concentration), while OD was dominant in less contaminated sediments (natural environments). In addition, both sulfate reducing bacteria and methanogens have been shown to be the primary agents for OD (Oremland et al., 1991; Oremland et al., 1995; Pak and Bartha, 1998). Thus, in environments where OD dominates, the end product, Hg(II) may be re-methylated or associated with reduced sulfur species. Recycling of Hg appears to be important and the balance between methylation/demethylation ultimately determines MeHg concentration in sediments.

It appears that our demethylation experiments in both experiment 1 and 2 gave a consistent relative comparison between the two experimental systems and also showed less variability between the R and NR tanks, compared to the methylation studies. Both sets of tanks showed a similar pattern in that demethylation rate was lower in the top sediment, while it remained fairly constant in deeper sediments. Therefore, our experiments seem to suggest that Hg methylation played a key role in maintaining a low MeHg pool in sediments while resuspension changed the sediment chemistry to favor relatively more Hg methylation.

3.3.4. Impacts of clams on plankton and mercury dynamics in the water column

This dissertation work is mostly focused on experiments 1 and 2. However, there were two more experiments conducted in summer of 2002 and 2003 (experiments 3 and 4; see Appendix I for more in detail). The later two experiments were designed to examine the effects of clam existence (RC vs. RNC) and density (RHC vs. RLC) on TSS levels, phytoplankton and zooplankton biomass, as well as Hg dynamics. Although experiments 3 and 4 are not discussed in detail here, some of data are shown in Appendix I for comparison.

Overall, the ratio of phytoplankton and POM was higher without clams (RNC) than with clams (RC) in experiment 3, averaging 0.3 ± 0.09 and 0.05 ± 0.02, respectively (Fig. A in Appendix I). Similarly, in experiment 4, the ratio between phytoplankton and POM was higher with low density clams (RLC) than wth high density clams (RHC), averaging 0.3 ± 0.1 and 0.1 ± 0.2, respectively (Fig. A in Appendix I). The results indicate that clams played an important role in controlling

phytoplankton biomass as phytoplankton served as a primary food source. Studies have found that phytoplankton biomass is reduced significantly due to filter feeder grazing (Padilla et al., 1996; Caraco et al., 1997; Descy et al., 2003). The ratio of zooplankton and POM showed a similar pattern that zooplankton biomass increased with decreasing clam density (Fig. B in Appendix I). It may have been due to a decrease in phytoplankton biomass, which is an important food source to zooplankton, and/or due to zooplankton being grazed by filter feeders. Viroux (2000) found that small zooplankton decreased with high zebra mussel density. To examine the clam-zooplankton interaction, modeling studies examined the effects of clams on plankton biomass and subsequent MeHg bioaccumulation (Chapter 4).

Tables A and B in Appendix I show water column data including THg and MeHg concentrations for all experiments for comparison. It appears that TSS concentration was higher with clams. Increasing TSS concentration was likely ascribed to sediment destabilization by clam presence (Porter et al., in preparation). Average concentrations of dissolved THg were not significantly different between RC and RNC (experiment 3) as well as RHC and RLC (experiment 4). A similar pattern was observed for dissolved MeHg in experiments 3 and 4, suggesting that clam presence or changes in clam density did not play a major role in Hg partitioning in the water column.

3.3.5. Mercury bioaccumulation

Total Hg concentration in zooplankton is shown in Fig. 3.7a. Unfortunately, zooplankton samples were not collected for THg on day 15. THg concentration was not significantly different between the two treatments (RC vs. NRC). There was no significant interaction between time and the treatments. However, THg concentration in zooplankton decreased significantly after day 2 and then remained relatively constant. Recall that in the beginning of the experiment ambient water from the Patuxent River, mixed with concentrated seawater, was added to the tanks, and the zooplankton in this water was the source of zooplankton in the mesocosms, and that the first sampling was made on day 2 of the experiment. Thus, zooplankton THg likely represented the concentration and reflected conditions in the Patuxent River for the first week until the zooplankton growth, uptake and depuration lead to the concentration being reflective of the *in situ* concentrations during the experiments. A sharp decrease in THg appeared to be linked to a zooplankton biomass increase. Zooplankton biomass (> 210 µm) on day 8 increased about a factor of two in the RC tanks and a factor of 3.5 in the NRC tanks, compared to day 2 (Fig. 3.7c).

As seen in zooplankton THg concentration, MeHg concentration showed no significant difference between the RC and NRC tanks (Fig. 3.7b). There was no significant interaction found between time and the treatments. In the RC tanks, MeHg in zooplankton increased significantly on day 15 and 22, compared to day 2. However, a MeHg increase in the NRC tanks was not significantly different over time. Changes in zooplankton concentration did not mirror water column MeHg concentration that was relatively constant over time, and that did not significantly

differ between experimental systems (Chapter 2, Kim et al., 2004). In the RC tanks, the average concentration of MeHg was 1.3 times higher than the NRC tanks. However, zooplankton biomass in the NRC tanks was 1.3 times higher, on average, than the RC tanks, suggesting that biomass dilution likely led to slightly lower concentration of MeHg in the NRC tanks.

Fig. 3.7. (a) THg in zooplankton; (b) MeHg in zooplankton; (c) zooplankton biomass (> 210 µm) (experiment 2).
Error bars show standard deviations of 3 replicates in each system.

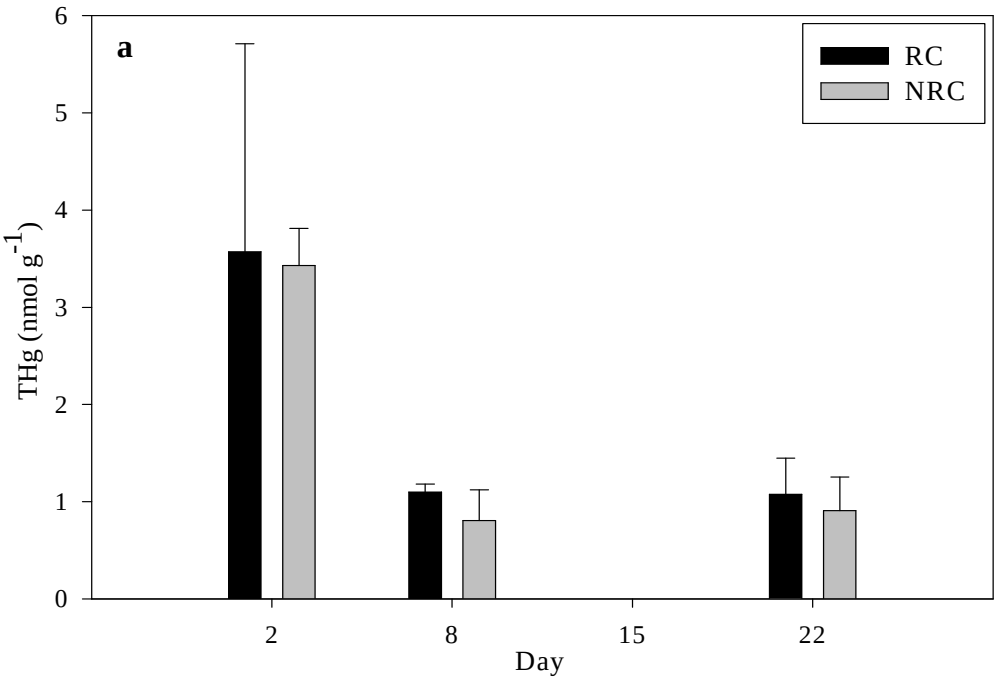
a
RC
NRC
THg (nmol g-1)
0
1
2
3
4
5
6
2
8
15
22
Day

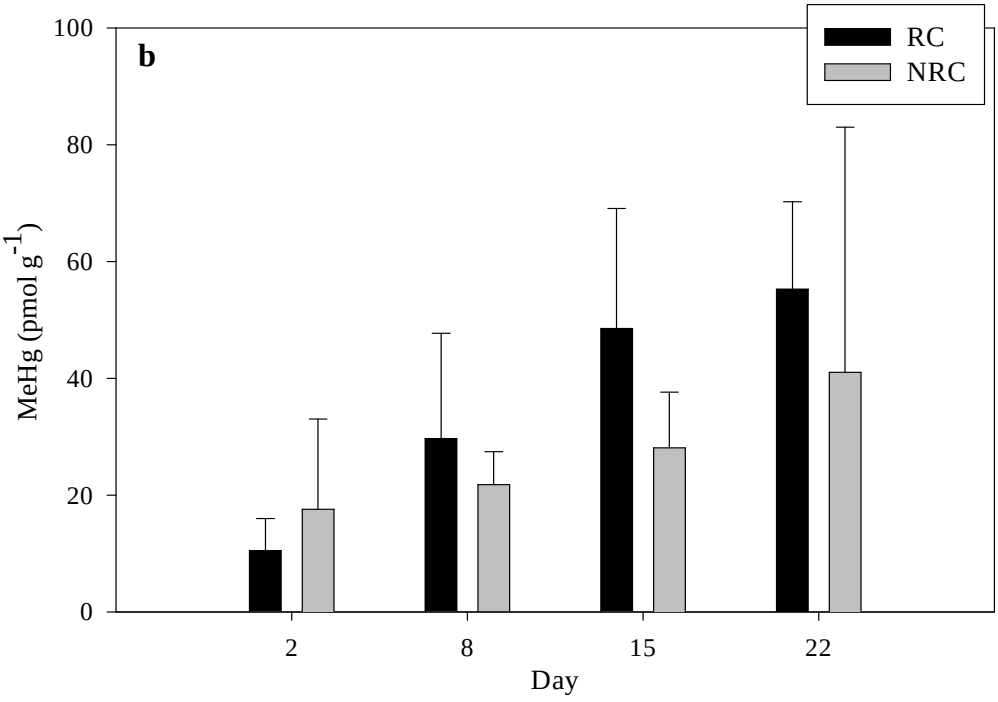
b
RC
NRC
MeHg (pmol g-1)
0
20
40
60
80
100
2
8
15
22
Day

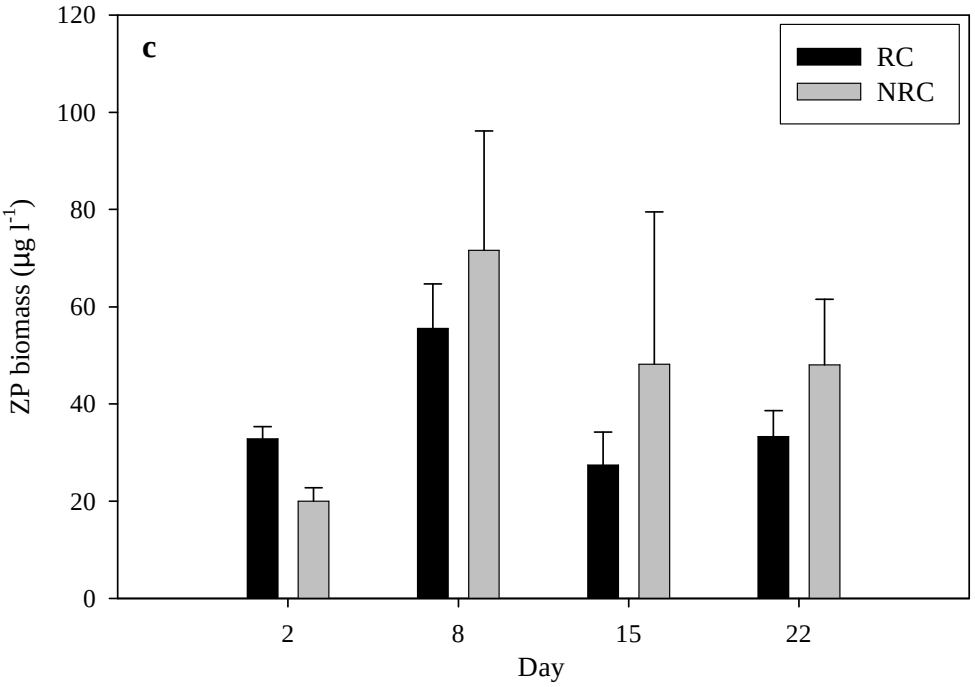
c
RC
NRC
ZP biomass (µg l-1)
120
100
80
60
40
20
0
2
8
15
22
Day

Based on the Chl a concentration in the mesocosm tanks and some reasonable assumptions about phytoplankton size and growth rate, the data in Mason et al. (1996) was used to estimate the steady state phytoplankton Hg burden under the experimental conditions (experiment 2) (Chapter 2, Kim et al., 2004). The estimated phytoplankton THg was in a similar range for both systems (about 0.3 to 0.5 nmol g^{-1}), being lower than the THg concentration in zooplankton and THg in the sediment. Calculation for MeHg gave a range of 5-30 pmol g^{-1} for both RC and NRC tanks, which was higher than MeHg concentrations in the sediment. Compared to the estimated MeHg in phytoplankton, zooplankton MeHg showed an increase by a factor of 2-3. A similar range in biomagnification has been found between phytoplankton and zooplankton by other investigators (Mason and Sullivan, 1997; Watras and Bloom, 1992).

The concentration of THg and MeHg in clams is presented in Table 3.6. There was no significant difference found in THg and MeHg concentration between the treatments. No significant interaction between time and the treatments was also found. However, the final concentration of THg significantly increased in the RC tanks, compared to the initial concentration. In contrast, the increase in the NRC tanks was not significant, compared to the initial concentration. As mentioned earlier, there were 5 suspended clams in each tank and a similar trend was observed to clams in sediments, indicating that the clams, although residing in the sediment, were reflecting the water column conditions as expected for filter feeders. Compared to the initial concentration, MeHg concentration in clams significantly increased in both RC and NRC tanks. A similar pattern was observed with the suspended clams. MeHg in

clams accounted for 71 ± 12 % of THg concentration, on average. There are very few data available on MeHg or % MeHg concentration in clams in field populations. MeHg, however, generally accounts for 20-80 % of THg in invertebrates while it is 10-30 % in plants and 80-100 % in fish and higher predators (Claisse et al., 2001). Our result falls within the range of % MeHg in oysters (*Crassostrea gigas*) and mussels (*Mytilus spp*) from the French Coast (11 to 88 % with a median of 43 %) (Claisse et al., 2001).

Table 3.6. Average concentrations of THg and MeHg in clams, *Mercenaria mercenaria*, with standard deviations at the beginning and the end of experiment 2.

	THg (nmol g^{-1} dw)	MeHg (nmol g^{-1} dw)	% MeHg
Initial	0.18	0.13	72
RC tanks	0.25 ± 0.04	0.16 ± 0.006	65 ± 11
S[a] – RC tanks	0.24 ± 0.08	0.18 ± 0.06	74 ± 12
NRC tanks	0.23 ± 0.04	0.15 ± 0.01	64 ± 5.9
S[a] – NRC tanks	0.20 ± 0.1	0.17 ± 0.05	86 ± 10

a: suspended clams in the RC and NRC tanks (see the text for details).

As discussed in Chapter 2 (Kim et al., 2004), average water temperature during the course of experiment 2 was 20 ± 2.0 °C and salinity for all the tanks was 19 ± 0.2 ppt. Within these ranges of temperature and salinity, there are generally no detrimental effects on pumping rate and growth of these clams (Grizzle et al., 2001 and references therein.). The RC tanks seem to be beneficial to feeding of clams in that Chl *a* concentration was higher and there was less zooplankton biomass (i.e. less competition), compared to the NRC tanks. Moreover, in experiment 3, a clam gape monitor (Porter et al., in preparation) was developed and used to measure clam gape

activity (closing/opening). It was found that clams in the RC tanks were open 62 % of time at TSS levels of 110 mg l^{-1}, suggesting that hard clams were coping with the turbid environment and were actively feeding. This observation is in contrast to what had been previously found (Bricelj and Malouf, 1984; Turner and Mills; 1991). However, it is not clear whether or not there was a strong correlation between valve gape and filtration rates, as suggested by Riisgård et al. (2003). They found that filtration rates of clams, *Mya arenaria*, decreased with reduced siphon opening but opening degree of siphons and valve gape might not be always correlated. Nevertheless, our data showed that the ratio between phytoplankton and POM was lower with increasing clam density, suggesting that phytoplankton was removed by clams (Fig. A in Appendix I).

Riisgård et al. (2003) found that filter feeding bivalves reduced their opening state and finally ceased filtering within a few hours when bivalves experienced algal concentration below a certain threshold (e.g. 0.5 μg l^{-1}). As discussed in Chapter 2 (Kim et al., 2004), Chl *a* was significantly higher in the RC tanks than NRC tanks, averaging 6.7 ± 0.3 and 3.6 ± 0.1 μg l^{-1}, respectively. In addition, Chl *a* concentration in both systems was lower, by 72 % (likely due to combination effects of lower temperature and clam presence), compared to experiment 1. Under the experiment condition, it is likely that filtration rates of clams in both systems were not dramatically different. Clams in the RC tanks were in the turbid environment where filtration rates may have been negatively affected but food concentration was relatively higher (compared to the NRC tanks). In contrast, clams in the NRC tanks likely faced food limitation due to a lower standing stock of phytoplankton. Overall,

resuspension of sediment has a complex effect of system productivity – it appears to enhance phytoplankton growth, but not zooplankton biomass, or that of clams (Porter et al., in preparation). The MeHg concentrations in the RC tanks in the clams were somewhat higher than those in the NRC tanks at the end of the experiment, with the likely explanation for this trend being differences in filtration and feeding rather than differences in concentration at the base of the food chain. A detailed ecosystem modeling study would be needed to reinforce this conclusion and this is examined in Chapter 4 where the effects of clams on phytoplankton and zooplankton biomass and the resulting MeHg bioaccumulation are modeled.

3.4. Summary

Our results suggest that sediment resuspension has a complex effect on Hg sedimentary chemistry (e.g. changes in the association of Hg with binding phases). Furthermore, resuspension appeared to enhance Hg methylation in surficial sediments. Demethylation was found to be similar between the R and NR systems with less variability, suggesting that Hg methylation played a key role in maintaining the MeHg pool in sediments. The results from measurements of the THg and MeHg concentration in the biota indicate that there is no simple relationship between the concentrations in the suspended particles and phytoplankton and the herbivores in these systems. In addition, clams did not seem to affect THg and MeHg concentrations in the water column.

Chapter 4: A modeling study on important factors in controlling methylmercury bioaccumulation into benthic and pelagic organisms

4.1. Introduction

There have been extensive efforts in modeling mercury (Hg) transport, speciation, and bioavailability in aquatic environments. Hg models have included various processes and biogeochemical reactions (e.g. atmospheric deposition, diffusive flux, biogeochemical transformation, sorption processes with particles, deposition/resuspension, and biouptake) to simulate Hg cycling in aquatic ecosystems. Existing Hg models are well described by Bale (2000). Interest in bioaccumulation of Hg and methylmercury (MeHg) by benthic organisms stems from public health concerns because these organisms serve as the food for benthic predators such as fish and as larger invertebrates are consumed by humans. Most bioaccumulation models for trace metals including Hg are under steady-state conditions (Fisher, 2000). Kinetic models have been developed to effectively and quantitatively separate uptake pathways of contaminants by aquatic organisms (Thomann et al., 1995; Morrison et al., 1997; Wang et al., 1998; Fisher et al., 2000; Roditi et al., 2000). While Hg models are mostly focused on equilibrium speciation, models that incorporate Hg cycling into carbon flows within aquatic systems are rare. Additionally, the previous models did not include physically induced processes such

as resuspension that may be a significant factor in the bioaccumulation of Hg and MeHg into benthic and pelagic organisms.

Two STORM (high bottom *S*hear realistic water column *T*urbulence *R*esuspension *M*esocosm) experiments were conducted in July (experiment 1) and October (experiment 2) of 2001 (Chapters 2 and 3). Each experiment was conducted with 3 replicates of resuspension (R) and no resuspension (NR). Hard clams, *Mercenaria mercenaria*, were introduced into the sediment for the study of bioaccumulation during experiment 2. Resuspension cycles were simulated with 4 h-on / 2 h-off cycles. More details on experiment set-up and results are discussed in Kim et al. (2004) and Kim et al. (submitted) (Chapters 2 and 3). It was found from the STORM experiments that dissolved MeHg was not significantly different between the two systems (R vs. NR). This suggests that release from sediment due to oxidation of sulfide phases, or other processes enhancing desorption, were not significant. Overall, the results from the experiments suggest that the impact of resuspension on MeHg bioaccumulation was likely indirect.

Increasing turbidity due to resuspension can limit light penetration and reduce primary production (Kirk, 1985; Ryan, 1991; Hoetzel and Croome, 1994). On the other hand, Schallenberg and Burns (2004) found that sediment resuspension stimulated phytoplankton production mainly through enhancing available nutrients even though light levels were more limited with resuspension. Light limitation due to resuspension rarely occurred in shallow lake systems (Schallenberg and Burns, 2004). The results of the STORM experiments showed that chlorophyll *a* (Chl *a*) concentration was higher and inorganic nutrients increased with resuspension

(Chapter 2; Porter et al., in preparation). The results indicated that phytoplankton growth was not substantially affected by light limitation due to resuspension.

Ashley (1998) proposed from his modeling results that as productivity increased, the algal contaminant concentration decreased due to growth dilution effects (i.e. the algal bioaccumulation factor (BAF) decreased). In addition, as the filter feeders increased their feeding rate with increasing productivity, the filter feeder BAF increased. However, once the feeding rate reached a maximum, the BAF began to decrease with decreasing algal BAF. Thus, the net effect of increased suspended material on the BAF of filter feeders was complex and could result in either an increase or decrease in the contaminant burden in filter feeders as a result of resuspension. It has been found from the STORM experiments that MeHg concentration in biota was not different between the resuspension and no-resuspension systems (Chapter 3, submitted). It appeared that food availability (phytoplankton stock in the water column) and food ingestion rates were the important factors in influencing accumulation of MeHg into herbivores (e.g. zooplankton and clams). To further investigate these interactions and processes, multi-compartment bioaccumulation model was developed in order to reinforce this conclusion and examine indirect effects.

As mentioned in Chapter 3 (Kim et al., submitted), Hg methylation is controlled by organic carbon content, microbial activity, and Hg bioavailability to methylating organisms (i.e. sulfate reducing bacteria; SRB). Relatively low sulfate concentration was found to stimulate both sulfate reduction and Hg methylation by SRB (Gilmour and Henry, 1991). Sediment resuspension can cause a change in sediment redox

status and influence Hg methylation in sediments. The STORM experiment results showed that resuspension appeared to enhance Hg methylation especially in summer when sediment temperature was high, which resulted in the increased degradation of freshly deposited organic matter (Chapter 3, submitted). In addition, demethylation rate was lower in the top sediment, while it remained fairly constant in deeper sediments. Demethylation also showed less variability between the treatments (resuspension vs. no resuspension) and with the different seasons, compared to methylation (Chapter 3, submitted). Thus, overall results of the methylation/ demethylation studies suggest that Hg methylation played a key role in maintaining a low MeHg pool in sediments while resuspension changed the sediment chemistry to favor relatively more Hg methylation. In this modeling study, Hg methylation and MeHg demethylation rates in the sediment were included as empirically-derived parameters. Methylation/demethylation rates were measured over the sediment depth in both experiments 1 and 2 using stable isotope spike addition incubation techniques (Chapter 3, submitted).

The objectives of this modeling study were a) to develop a carbon-based bioaccumulation model for MeHg within a shallow estuarine system with resuspension and b) to determine the most important parameters controlling MeHg bioaccumulation into benthic and pelagic organisms in shallow estuarine environments. This study also attempted to use the model as a diagnostic tool to examine and provide insight into the role of sediment resuspension in MeHg transfer and accumulation into benthic and pelagic organisms.

4.2. Methods

4.2.1. Model structure

Ashley (1998) incorporated a carbon-based benthic-pelagic food chain model that tracked the transfer and accumulation of organic carbon among numerous biotic and abiotic pools over time into an organic contaminant (HOC) model. In the Ashley model, contaminant flow and accumulation was subsequently modeled in response to the dynamic changes within the carbon-based model. The model consisted of five trophic levels (bacteria, protozoa, phytoplankton, zooplankton, zooplanktivores, and piscivores) within the water column and three benthic and epi-benthic trophic groups (deposit feeders, filter feeders, and benthivores/forage feeders). Chang (2001) refined the Ashley model with mass balance adjustments, variable depth, and bioenergetics terms. In this study, the formulation of Chang (2001) is adjusted to make it representative of the bioaccumulation of MeHg.

The basic structure of the model is similar to that of Ashley (1999) and Chang (2001), with some modifications. Trophic levels are simplified compared to the previous models (Ashley. 1999; Chang, 2001) in order to simulate experiment 2, as mentioned above. The carbon model consists of 6 state variables in the water column and sediment respectively (Fig.1a). The model includes phytoplankton (PP) and two different size groups of zooplankton (ZP): ZP1 (> 210 µm) and ZP2 (63 - 210 µm) in the water column. In experiment 2, ZP samples were collected using mesh sizes of 63 and 210 µm. However, only one group of ZP (>210 µm) was used for Hg analysis. Thus, two groups of ZP were modeled for comparison with the experimental data. The two groups of ZP feed on PP, as a primary food, and resuspended

microphytobenthos (MPB), as it has been found that MBP could serve as a food source for ZP in estuarine environments (Kibirige et al., 2003). The model also included predation on small ZP (ZP2) by ZP1 as found in other modeling studies (Verity, 2000; Griffin et al., 2001). MPB and filter feeders (FF) (clams) were included in the sediment. FF consumes PP, resuspended particulate organic carbon (RPOC), and MPB. There are two sediment layers in the model: the surface sediment (top 2 cm) and a deeper layer (> 2 cm). The final sediment depth in the STORM experiments was about 10 cm. The water column was 1 m deep with a surface area of 1 m^2 (total volume of 1000 L).

Particulate organic carbon (POC) in the water column was divided into two pools of carbon, RPOC and WPOC (water column particulate organic carbon) (Fig. 4.1a). While RPOC was derived from sediment organic carbon (SPOC) during resuspension events, sources of WPOC were PP and ZP mortality as well as bacterial uptake. WPOC and PP sinking were connected to SPOC pool. Both WPOC and SPOC consisted of living (e.g. bacteria) and non-living organic matter in the model. The DOC pool in the water column gained carbon from excretion of biota and degradation of both WPOC and RPOC and lost DOC to these fractions due to bacterial uptake. POC degradation in both the water column and sediment was assumed to be the first-order reaction. Decay constants were obtained from Wainright and Hopkinson (1997). Overall, the model included vertical carbon exchange between the water column and sediment such as a) FF ingestion of PP, resuspended MPB and RPOC; b) sinking WPOC and PP; c) resuspension/deposition of SPOC to the water

column; d) porewater DOC (SDOC) diffusion between the water column and the sediment (Fig. 4.1a).

It was assumed that the water column was well mixed (e.g. no stratification) and also that the system was spatially homogeneous. After initiating the system with unfiltered Patuxent River water, there was no particle input in experiment 2. In other words, the sediment and *in situ* plankton (derived from PP and ZP in the "seed" water) were the direct sources of particles in the water column. There were, however, dissolved inputs as filtered seawater was daily exchanged at 10 % of the total volume during experiment 2. Water exchange was always done during the off-cycle to minimize particle loss and it was modeled that losses of all the variables in the water column occurred only during the off-cycles. Since 10 % of the total water volume was flushed out every day, PP and ZP were also set to be lost at 10 % of their biomass per day in the model. In addition, the model assumed negligible bioturbation/ bioirrigation effects for simplicity as the sediments used in experiment 2 was defaunated prior to the beginning of the experiments.

MeHg flows and accumulation was incorporated into the carbon model. There were additional state variables (e.g. dissolved MeHg in the water column and pore water) and processes such as adsorption/desorption in both the water column and sediment and methylation/ demethylation in the sediment (Fig. 4.1b). Gas exchange at the air-water interface was assumed to be negligible. Our results (Lawson, unpublished) and that of others (Sellers et al. 1996) suggest that, in the water column, photodemethylation is only important in clear oligotrophic fresh waters, with the photodemethylation rate being much lower in saline waters. Thus, photo-

demethylation was assumed to be negligible in the model. No evidence has been found of water column methylation in oxic seawater. Thus, these processes were not included in the model.

All the state inventories in the sediments were normalized to the volume of the water column. All the standing stocks are in units of g m^{-3}, flows are in g m^{-3} h^{-1}. Initial PP biomass was estimated by the measurement of Chl *a* at the beginning of experiment 2. A carbon to Chl *a* ratio of 50:1 was assumed, as used in other studies (Bougis, 1976; Dagg and Wyman, 1983; Griffin et al., 2001; Harding et al., 2002). Dry weight of ZP and FF was obtained from published equations, based on length-weight relationships (White & Roman 1992; Grizzle, 2001). The carbon content (dry weight) of ZP and FF was assumed to be 40 % (Gorsky, et al., 1988; Jerling and Wooldridge, 1995; Froneman, 2000; Siokou-Frangou et al., 2002). Model simulations were carried out for 576 hours (24 days) using STELLA II®. The time step used in the model was 0.25 hour with the Rung-Kutta Type II integration method. Input parameters and equations for standing stocks and flows in the model are summarized in Appendix II.

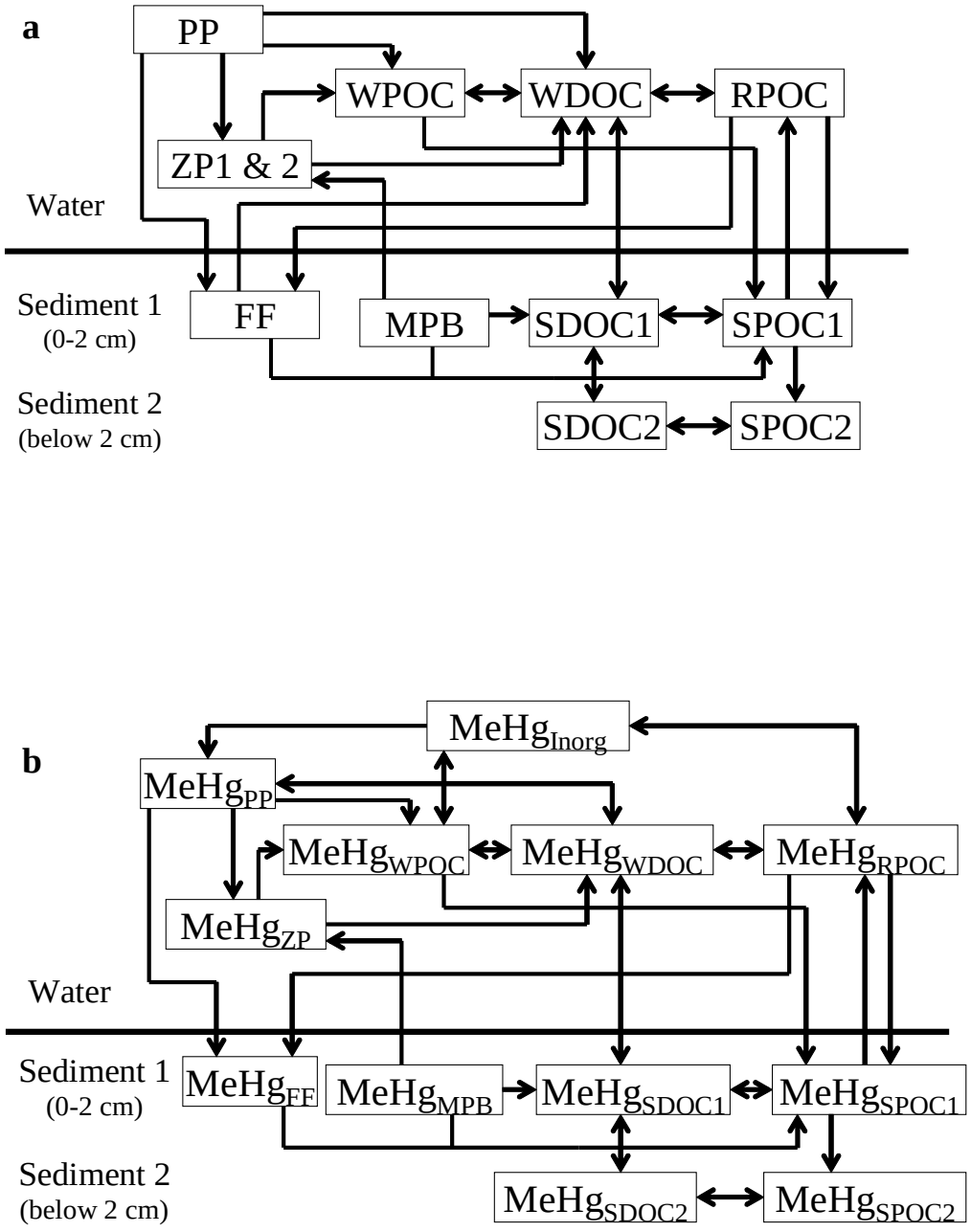

Figure 4.1. A model schematic: a) carbon flows; b) MeHg flows.

4.2.2 Model Formulation

4.2.2.1. Carbon flow model

In this study, the carbon model consists of 6 variables (PP, ZP1, ZP2, WPOC, RPOC, DOC) within the water column and 6 variables (MPB, FF, SDOC1, SDOC2, SPOC1, and sediment SPOC2) in the sediment. In general, each state variable is calculated as the difference between all the gain terms minus all the loss terms at each time step. For instance, the change in phytoplankton biomass is modeled using the following equation (Ashley, 1998):

$$d(PP) = PP(t - dt) + (Growth - Sinking - Respr - Excret - Mort - Graz_{ZP} - Graz_{FF} - Out) \times dt$$

where PP = phytoplankton biomass (g C m^{-3}),
Growth = phytoplankton growth (g C m^{-3} h^{-1}),
Sinking = sinking of phytoplankton to the sediment layer (g C m^{-3} h^{-1}),
Respr = phytoplankton respiration (g C m^{-3} h^{-1}),
Excret = phytoplankton excretion (g C m^{-3} h^{-1}),
Mort = phytoplankton mortality (g C m^{-3} h^{-1}),
Gra z_P = grazing on PP by ZP (g C m^{-3} h^{-1}),
$Graz_{FF}$ = grazing on PP by FF (g C m^{-3} h^{-1}),
Out = phytoplankton loss due to water exchange (g C m^{-3} h^{-1}).

PP growth is based on light, temperature, and nutrients in the model. Although light availability is an important factor in photosynthesis, the light influence on PP growth was modeled here as only the duration of the day light time (10 hours per day), not light intensity. Thus, in this model, growth rate is not a function of light intensity. As the system is well-mixed, PP is not stratified and thus spends some portion of their time in the upper waters where light limitation is minimal. Similarly, Verity (2000) assumed that the effect of light intensity on PP growth was negligible in their

modeling study. PP growth rate was modeled using the following equation and was a function of temperature (modified from Angelini and Petrere, Jr., 2000):

$$G = G_{max} * e^{(0.0693*Temp)}$$

where G = growth rate (h^{-1}),
G_{max} = maximal growth rate of PP (h^{-1}),
Temp = temperature data (°C).

The effect of nutrients was expressed as a Michaelis-Menten equation:

$$Nutrient = nut/(K + nut)$$

where nut = nutrient data (nitrate & nitrite),
K = half-saturation constant.

Thus, the overall PP growth was expressed as Growth = G * Nutrient * light * PP. The measurements of temperature and nutrients every 2-3 days from experiment 2 were used in this model. Similar approaches to model PP growth have been used by Griffin et al. (2001) and Darrow et al. (2003). MPB growth was modeled using the same equations as PP in the water column. In experiment 2, secchi depth data showed that light did not reach to the sediment surface during resuspension cycles, suggesting that MPB growth may be lower than PP growth due to light limitation. Darrow et al. (2003) used 0.5 $d^{-1}$of MPB G_{max} and 1.5 d^{-1} of PP G_{max} in their modeling study, based on field measurements and taking light limitation into account. Thus, a similar ratio was adopted to set MPB G_{max} in this model.

For organisms gaining carbon through food ingestion, carbon consumption was modeled using the following equation:

$$\text{Grazing} = ZP \text{ (or FF)} * FR * PP * AE * f$$

where ZP (or FF) = zooplankton (or filter feeder) biomass (g C m^{-3}),
FR = weight-specific filtration rate
(often referred as clearance rate, $m^3\ h^{-1}\ g\ C^{-1}$),
PP = phytoplankton (or microphytobenthos) biomass (g C m^{-3}),
AE = carbon assimilation efficiency (unitless),
f = fraction of diet from a particular source (unitless).

Filtration rate was represented using the equation modified from White and Roman (1992):

$$FR = FR_{max}\ (1 - e^{-kTemp})$$

where FR = weight specific filtration rate ($m^3\ h^{-1}\ g\ C^{-1}$),
k = 0.009 (White & Roman, 1992),
Temp = temperature.

A different FR_{max} was used for ZP1 and ZP2 as carbon-specific ingestion rate increased with temperature but decreased with body size (White and Roman, 1992; Griffin et al., 2001). Carbon-specific FR_{max} values were determined from model calibration. Those values used in the model fell within the range of filtration rates for ZP found in the Chesapeake Bay (White and Roman, 1992). Similarly, FR_{max} for FF used in the model was within the range of filtration rates found in Grizzle et al. (2001).

For ZP and FF, carbon assimilation efficiencies (AE) used in the model were 0.7 and 0.8, respectively (Halvorsen et al., 2001; Grizzle, 2001). It was assumed that ZP1 fed on PP, ZP2, and MPB with fractions of diet of 0.9, 0.05 and 0.05, respectively, while ZP2 consumed PP and MPB with fractions of 0.9 and 0.1. Although a carbon stock of resuspended MPB was not included explicitly in the model, consumption of resuspended MPB by ZP and FF was included. Studies have shown that ZP feed on

resuspended MPB (Baillie and Welsh, 1980; de Jonge and van Beusekom, 1992). Kim et al. (2004, Chapter 2) found from the STORM experiments that MPB was not substantially resuspended to the water column. Similarly, a mesocosm experiment by Sloth et al. (1996) found that a small amount of MPB (< 2 %) was transported to the water column for a 2-h resuspension period. After the model was calibrated and compared with the data in experiment 2, it was assumed that 5 % of MPB was resuspended and consumed by both ZP and FF. It was modeled that FF filter PP, RPOC, and resuspended MPB in the water column with fractions of diet of 0.6, 0.3, and 0.1, respectively. Assimilation efficiency (AE) for carbon for RPOC was assumed to be 0.2, lower than that for PP and MPB.

Porter et al.(in preparation) found from clam gape experiments that clams feed about 62 % of the time, even during resuspension. Thus, in the model the multiplier of 0.62 was included to take non-constant clam feeding into account. Another modeling study has also used a similar value (0.67; Padilla et al., 1996). Similarly, it was found that filter feeders such as zebra mussels filter about 50 to 67 % of the time (Morton, 1969; Walze, 1978). In addition, filter feeders may cease filtering when algal concentration decreases below the threshold level of approximately 0.025 mg C L^{-1} (Riisgård et al., 2003). Thus, in the model, herbivores were set to stop filtering when PP concentration reached below the threshold level.

4.2.2.2. Modeling resuspension

Physical processes (i.e. resuspension (erosion, E) and deposition, D) were modeled using the following equation (Sanford and Halka, 1993; Chang, 1999):

$$D = W_s * C$$

where D = deposition rate (g m^{-2} h^{-1})
W_s = settling speed (m h^{-1})
C = particle concentration in the water column (g m^{-3})

When erosion occurs, it is assumed that deposition rate equals to erosion rate at equilibrium. Then, E = D, so $E = W_s * C_{eq}$. By rearranging the equation, the following equation is obtained:

$$E - D = W_s * (C_{eq} - C(t))$$

where C_{eq} = 0 during the off-cycles and
C_{eq} = observed concentration during the on-cycles.

In order to determine a settling speed of particles, data from particle settling experiments were used (Porter et al. in preparation). Changes in TSS concentration over time were measured during the off-cycles. From the relationship between TSS and time, a settling speed of 1.66 m h^{-1} was obtained. In the model, a similar approach to Wainright and Hopkinson (1997) was adopted such that resuspension cycles were modeled using a resuspension timing parameter (either 1 or 0). In their model, resuspension and deposition did not occur simultaneously (e.g. when resuspension time was 1, deposition time was 0). However, in this model, continuous deposition was assumed. Modeling studies have shown that a continuous deposition assumption

results in better agreement of models with data (Sanford and Halka, 1993; Sanford and Chang, 1997).

4.2.2.3. Modeling bioaccumulation of MeHg

As seen in Fig. 4.1b, each state variable was represented as the time-variable MeHg inventory in response to each carbon state variable. There were two additional state variables, dissolved MeHg and dissolved porewater MeHg. Since dissolved MeHg is mostly associated with DOC (Mason et al., 1999; Ravichandran 2004), two fractions of dissolved MeHg were defined in the model, dissolved MeHg bound to DOC and MeHg bound to inorganic species or in the free MeHg form in both water and porewater. These fractions have different bioavailability to PP. The fractions of each species were calculated based on initial concentrations of MeHg and DOC, assuming that the species were at thermodynamic equilibrium. MeHg accumulation into PP was only from the dissolved phase. It was assumed that MeHg bound to DOC was available to PP with a lower uptake rate. Thus, the following equation was used to model MeHg accumulation in PP:

$$d(MeHg_{PP}) = MeHg_{PP}(t - dt) + (MeHg_{inorg\ du} + MeHg_{DOC\ du} - MeHg_{ZP} - MeHg_{FF} - MeHg_{excrt} - MeHg_{WPOC} - MeHg_{sink} - MeHg_{out}) \times dt$$

where $MeHg_{PP}$ = MeHg concentration in phytoplankton (g m^{-3})
$MeHg_{inorg\ du}$ = dissolved $MeHg_{inorg}$ transfer to phytoplankton (g m^{-3} h^{-1}),
$MeHg_{DOC\ du}$ = dissolved $MeHg_{DOC}$ transfer to phytoplankton (g m^{-3} h^{-1}),
$MeHg_{ZP}$ = MeHg transfer to zooplankton by grazing on phytoplankton (g m^{-3} h^{-1}),
$MeHg_{FF}$ = MeHg transfer to filter feeder by feeding on phytoplankton (g m^{-3} h^{-1}),
$MeHg_{excrt}$ = MeHg excretion (g m^{-3} h^{-1}),

$MeHg_{WPOC}$ = MeHg transfer to WPOC by mortality (g m^{-3} h^{-1}),
$MeHg_{sink}$ = MeHg transfer to SPOC by sinking (g m^{-3} h^{-1}),
$MeHg_{out}$ = MeHg loss by water exchange (g m^{-3} h^{-1}).

Dissolved MeHg uptake into PP was modeled using the following equation:

$$MeHg_{inorg\ du}(MeHg_{DOC\ du}) = K * \text{dissolved } MeHg_{inorg}(MeHg_{DOC})$$

where K = uptake rate (m^3 h^{-1} $cell^{-1}$) * PP (g m^{-3}) / mass of cell (g $cell^{-1}$).

Uptake rate of MeHg into PP was estimated from experimental data in Mason et al., (1996). It was assumed that PP was spherical and its radius was 5 μm. Most filter feeders have been found to be able to retain particles > 5 μm with maximum efficiency (Young et al., 1996; Grizzle et al., 2001).

4.2.2.4. Sorption processes for MeHg

Chang (1999) developed a 1-D numerical time and depth dependent water quality model in order to include reversible sorption processes for a hydrophobic organic contaminant (HOC). Most models to date have assumed equilibrium partitioning between the dissolved and particulate phases but this is unrealistic for strongly bound contaminants such as HOCs and Hg. Sorption processes were modeled here using the same approach as Chang (1999). A linear-reversible model for sorption processes was used:

$$R_{sd} = k_1 C_d - k_{-1} C_s = - R_{ds}$$

where R_{sd} = net adsorption rate (g m^{-3} h^{-1}),
R_{ds} = net desorption rate (g m^{-3} h^{-1}),
C_d = dissolved concentration (g m^{-3}),
C_s = particulate concentration (g m^{-3}),
k_1 = adsorption rate constant (m^3 g^{-1} h^{-1}),
k_{-1} = desorption rate constant (h^{-1}).

STORM experiments showed that dissolved MeHg concentration did not change in concert with particulate MeHg in both the R and NR systems, indicating non-equilibrium partitioning for MeHg. The desorption rate constant was calculated using the formulation outlined by Chang (1999) where k_{-1} is a function of distribution coefficient (K_d) and the particle /sediment physical properties. Effectively, k_{-1} increases as particle size decreases. Then, k_1 is estimated as K_d k_{-1}. A more detailed model description is given in Chang (1999). The desorption rate constant was obtained from Hintelmann and Harris (2004) and the organic-carbon based K_d from the actual data. In the model, sorption processes included adsorption and desorption between dissolved $MeHg_{inorg}$ and WPOC as well as RPOC. There were adsorption and desorption processes between dissolved $MeHg_{DOC}$, and WPOC as well as RPOC.

4.2.2.5. Modeling methylation/demethylation in the sediment

In the model, methylation/demethylation processes were treated as psuedo-first order reactions. Sediment total Hg (THg) concentration was used as a constant source to the MeHg pool in this model. As mentioned earlier, the rate constants were obtained from the measurements made in experiment 2 (Chapter 3, submitted). Thus, the model includes methylation/ demethylation in the sediment using the following equation:

$$d[MeHg]/dt = k_1[Hg] - k_2 [MeHg]$$

where [MeHg] = sediment MeHg concentration ($MeHg_{SPOC1}$, $MeHg_{SPOC2}$) (g m^{-3}),
[Hg] = sediment THg concentration (g m^{-3}),
k_1 = methylation rate (h^{-1}),
k_2 = demethylation rate (h^{-1}).

No attempt was made to model how resuspension changed methylation/demethylation rates over time as there were uncertainties in parameterizing microbial activity, sulfate reduction rate, bioavailable fraction of Hg, etc. However, methylation rate was varied during the model runs to examine the sensitivity of MeHg accumulation in biota to this parameter.

4.2.2.6. Modeling MeHg flows in the sediment

The overall formulation of MeHg concentration in the sediment (SPOC) is given by:

$$d[MeHg_{SPOC1}] = MeHg_{SPOC1}\,(t - dt) + (MeHg_{\text{fr WC}} + meth1 + ads\ PWMeHg_{DOC1} + ads\ PWMeHg_{inorg1} + MeHg_{MPB\ to\ SPOC1} + MeHg_{\text{fr RPOC}} - MeHg_{\text{to WC}} - demeth1 - MeHg_{\text{to SPOC2}} - des\ PWMeHg_{DOC1} - des\ PWMeHg_{inorg1} - MeHg_{degrad}) \times dt$$

where $MeHg_{SPOC1}$ = sediment MeHg concentration (g m^{-3}),
$MeHg_{\text{fr WC}}$ = $MeHg_{PP}$ and $MeHg_{WPOC}$ sinking from the water column (g m^{-3} h^{-1}),
meth1 = Hg methylation (g m^{-3} h^{-1}),
ads $PWMeHg_{DOC1}$ = adsorption of porewater MeHg bound to DOC (g m^{-3} h^{-1}),
ads PW $MeHg_{inorg1}$ = adsorption of porewater MeHg (g m^{-3} h^{-1}),
$MeHg_{MPB\ to\ SPOC1}$ = $MeHg_{MPB}$ mortality (g m^{-3} h^{-1}),
$MeHg_{\text{fr RPOC}}$ = $MeHg_{RPOC}$ deposition (g m^{-3} h^{-1}),
$MeHg_{\text{to WC}}$ = resuspended MeHg (g m^{-3} h^{-1}),
demeth1 = MeHg demethylation (g m^{-3} h^{-1}),
$MeHg_{\text{to SPOC2}}$ = MeHg burial to SPOC2 (g m^{-3} h^{-1}),
des $PWMeHg_{DOC1}$ = desorption of $MeHg_{SPOC1}$ (g m^{-3} h^{-1}),
des PWMeHginorg1 = desorption of $MeHg_{SPOC1}$ (g m^{-3} h^{-1}),
$MeHg_{degrad}$ = $MeHg_{SPOC1}$ degradation(g m^{-3} h^{-1}).

The sources of $MeHg_{SPOC1}$ were particle sinking (e.g. PP and WPOC), deposition of RPOC, Hg methylation in the top sediment (2 cm), adsorption of porewater MeHg (both fractions, porewater MeHg bound to DOC and MeHg bound to inorganic species), MeHg from MPB mortality, and MeHg from RPOC deposition. The loss terms of $MeHg_{SPOC1}$ were sediment resuspension, burial to the deeper layer (SPOC2), desorption, and organic carbon degradation. A similar formulation was used for the deeper sediment layer (SPOC2).

Processes involving changes in porewater MeHg was modeled by the following equation:

$$d(PW\ MeHg_{DOC1}) = PW\ MeHg_{DOC1}\ (t - dt) + (\text{diffusive flux1} + \text{diffusive flux2} + \text{des } MeHg_{DOC1} + MeHg_{SPOC1degrad} + MeHg_{MPBexcrt} - \text{ads to SPOC1}) \times dt$$

where $PW\ MeHg_{DOC1}$ = porewater MeHg bound to DOC (in the top sediment layer) ($g\ m^{-3}$),
diffusive flux1 = diffusive flux in or out of the sediment layer 1 ($g\ m^{-3}\ h^{-1}$),
diffusive flux 2 = diffusive flux in or out of the sediment layer 2 ($g\ m^{-3}\ h^{-1}$),
des $MeHg_{DOC1}$ = desorption ($g\ m^{-3}\ h^{-1}$),
$MeHg_{SPOC1degrad}$ = MeHg gain from SPOC1 degradation ($g\ m^{-3}\ h^{-1}$),
$MeHg_{MPBexcrt}$ = MeHg gain from MPB excretion ($g\ m^{-3}\ h^{-1}$),
ads to SPOC1 = adsorption ($g\ m^{-3}\ h^{-1}$).

Diffusive flux was modeled as a bi-direction flow system where the direction of flows was determined by concentration gradients between the water column and the sediment as well as the two sediment layers. Diffusion coefficients for MeHg and organic matter were obtained from the literature (Gill et al., 1999). Details of the formulation and the parameters are listed in Appendix II.

4.2.3. Model calibration and sensitivity analysis

The carbon model was calibrated by variation of physiological parameters for biota within reasonable bounds based on the literature to find the best fit to the observed data from experiment 2. Calibration of the bioaccumulation model was performed in a similar manner. A sensitivity analysis was performed to examine the effect of changes in key parameters on the state variables of interest in the model (Jorgensen, 1994). The following equation was used for the sensitivity analysis (Simas et al., 2001):

$$S = \Delta V / V$$

where S = sensitivity of each state variable to a chosen parameter,
V = state variable under standard condition,
ΔV = variation in the state variable due to changes in the chosen parameter.

Each parameter was changed at ± 20 % of its default value while keeping all other parameters the same as the standard condition. In the comparison, for variables that have a diurnal cycle, the maximum value of state variables of interest that occurred during the 24-day simulation were used within the model run.

4.2.4. Simulations of different scenarios

After the model was calibrated, it was used to simulate other conditions such as a different season and different clam biomass. There were two more STORM experiments, which were conducted in July of 2002 and 2003 (experiments 3 and 4; see appendix I for details). The treatment of experiment 3 was R with FF vs. R without FF. The model simulations were aimed at examining the effect of FF on PP

and ZP growth and MeHg accumulation and examining how well the model, as developed, was capable of reproducing the results from these experiments.

4.3. Results and discussion

4.3.1. Model outputs and comparison with observations

4.3.1.1 Biota results

The measured and modeled variations of the biomass in the water column and the benthic environment over time are shown in Fig. 4.2a-b. The oscillation of PP biomass in the model is due to the lack of growth at night. Modeled PP and ZP biomass was in relatively good agreement with the observed data. FF biomass slightly decreased with time. During experiment 2, there was no attempt to estimate the growth rate of FF or to measure changes in individual shell length. However, ash-free dry weight (AFDW) measurements of selected clams showed that clams did not grow substantially during the course of experiment (Porter et al., in preparation). Thus, the model results are in agreement with observation. Modeled MPB biomass increased over time, which showed a similar pattern with the data.

Modeled and measured concentrations of MeHg in biota are presented in Fig. 4.2c-d. Modeled MeHg concentration in PP reached a plateau after the first week and decreased slightly toward the end of the model run (Fig. 4.2c). A similar pattern was found in model results of dissolved MeHg (shown as $MeHg_{DOC}$ + $MeHg_{inorg}$) (Fig. 4.3d) as MeHg uptake for PP was only from the dissolved MeHg pools. Modeled MeHg in both small and larger ZP (ZP1 & 2) increased gradually over time (Fig. 4.2c). As mentioned above, MeHg in only ZP1 was determined during experiment 2

and the concentration compared well with the model results. Modeled MeHg in ZP1 fell within the range of the observed data. Model results showed that MeHg concentration in FF and MPB slightly increased over time (Fig. 4.2d). Additionally, the model result was similar to the measured MeHg concentration in FF. Modeled MeHg accumulation in ZP and FF was mostly from food ingestion (> 95 %), not from dissolved MeHg uptake. Other studies have also shown that aquatic invertebrates accumulated contaminants mainly from food ingestion (Luoma et al., 1992; Wang et al., 1996; Lawrence and Mason, 2001; Chang and Reinfelder, 2002; Tsui and Wang, 2004).

Figure 4.2. Model outputs: a) Biomass in the water column; b) Biomass in the sediment; c) MeHg in water column biota; d) MeHg in benthic biota.

Lines and symbols represent the model outputs and the data from experiment 2, respectively. Error bars show standard deviations of 3 replicates.

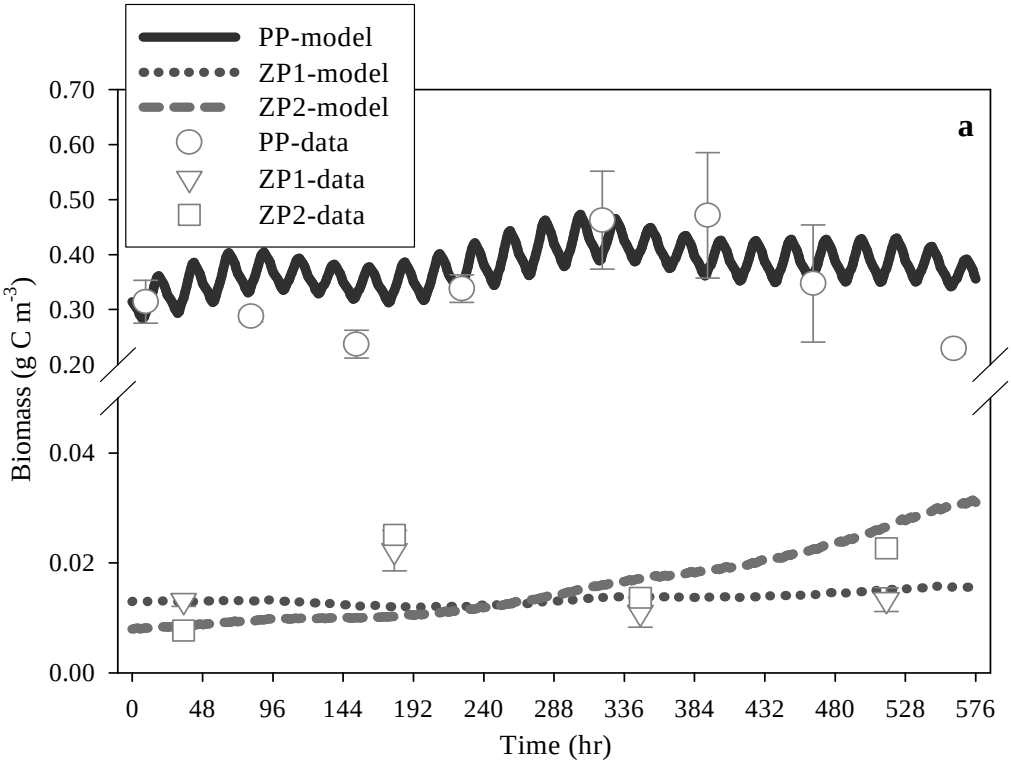
PP-model
ZP1-model
ZP2-model
PP-data
ZP1-data
ZP2-data
a
Biomass (g C m-3)
0.70
0.60
0.50
0.40
0.30
0.20
0.04
0.02
0.00
0
48
96
144
192
240
288
336
384
432
480
528
576
Time (hr)

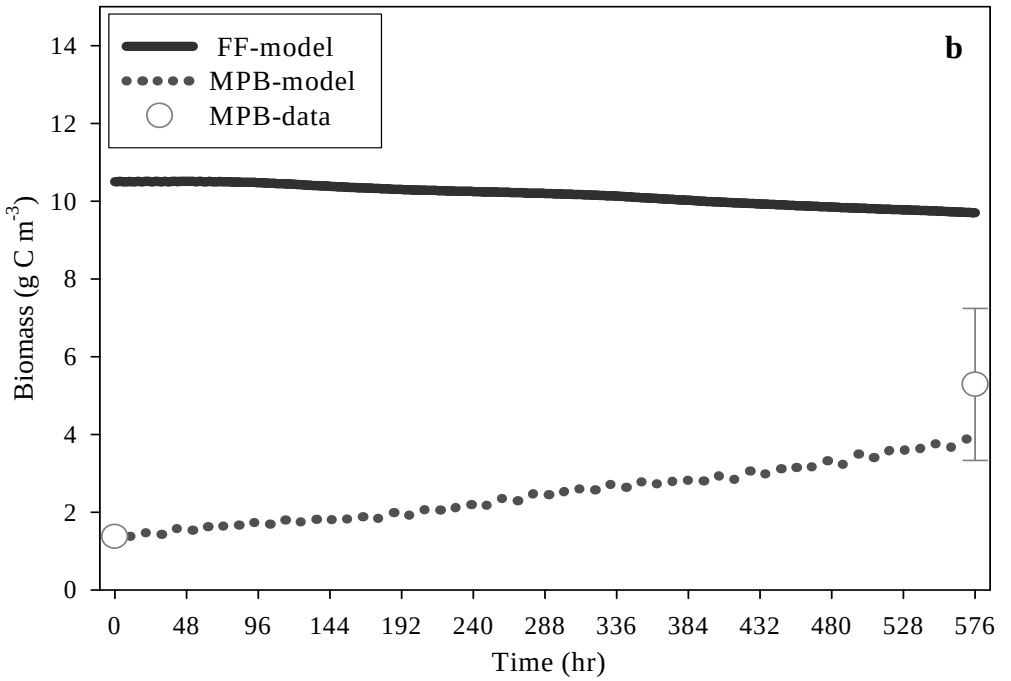
FF-model
MPB-model
MPB-data
b
Biomass (g C m-3)
14
12
10
8
6
4
2
0
0
48
96
144
192
240
288
336
384
432
480
528
576
Time (hr)

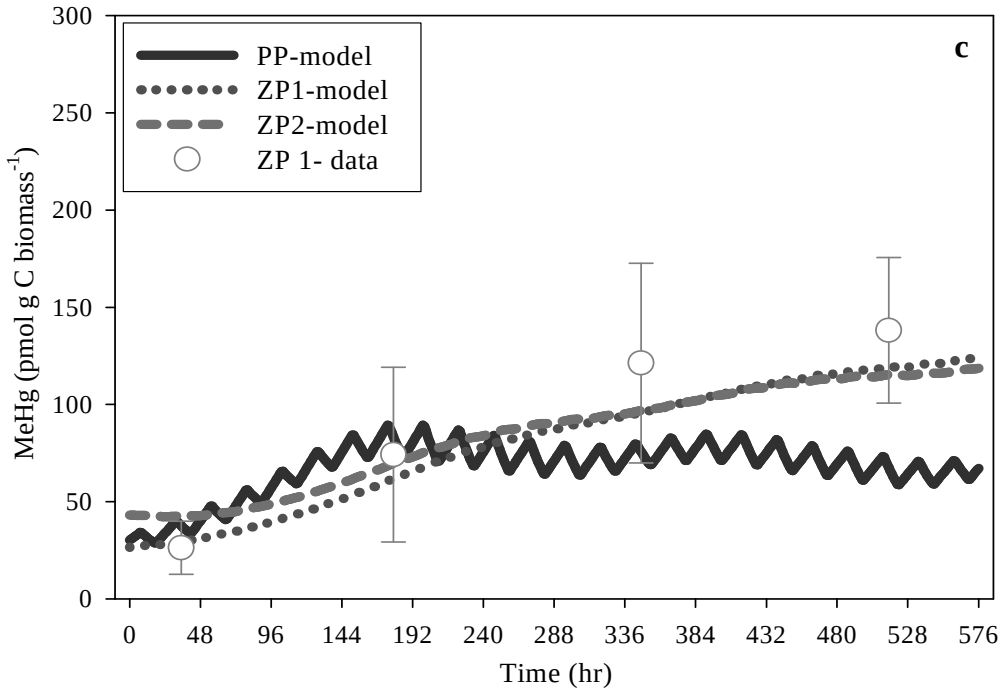
c
PP-model
ZP1-model
ZP2-model
ZP 1- data
MeHg (pmol g C biomass-1)
Time (hr)
0
50
100
150
200
250
300
0
48
96
144
192
240
288
336
384
432
480
528
576

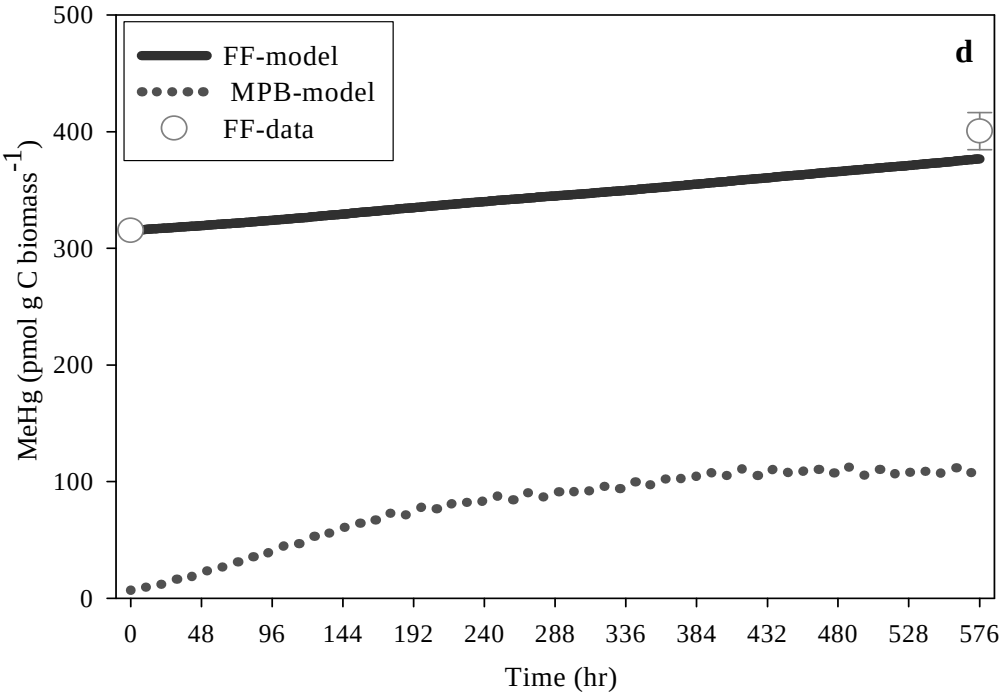
d
FF-model
MPB-model
FF-data
MeHg (pmol g C biomass-1)
Time (hr)
0
100
200
300
400
500
0
48
96
144
192
240
288
336
384
432
480
528
576

4.3.1.2. POC and DOC results

Fig. 4.3 shows a comparison of modeled POC and DOC in the water column with the data. Since the measured values contained all the different particles types, water column POC pools in the model (e.g. PP, ZP, WPOC, and RPOC stocks) were added together for a direct comparison at each time step. As seen in Fig. 4.3a, model outputs were in good agreement with the observed data. POC in the model responds to the resuspension cycles (4 times a day). On average, POC in the water column consisted of 49 % RPOC, 42 % WPOC, 9 % PP and ZP, showing that sediments accounted for a significant amount of POC in the water column. In comparison, the data showed that 12 % of POM, on average, was PP and ZP (Appendix I). In experiment 2, total suspended solids (TSS) and particulate organic matter (POM) were significantly higher in the R tanks than in the NR tanks (Chapter 2, Kim et al., 2004). Modeled DOC was in agreement with the measured DOC (within a factor of two) (Fig. 4.3b).

The model results for particulate MeHg are given in Fig. 4.3c. MeHg concentration in the model decreased slightly over time and varied in response to resuspension cycles. Observed MeHg concentrations were more variable compared to the model results. Dissolved MeHg in the model showed an increase in the beginning and a slight decrease over time (Fig. 4.3d). The model results were more comparable to the observed MeHg concentration in the later stages of the model run. From the STORM experiments, it was found that MeHg on particles per gram was higher during non-resuspension cycles compared to resuspension cycles (Chapter 2, Kim et al., 2004). The discrepancy between the model and the observed data is likely

explained by different particle sizes and settling speeds. This model did not include different sizes of particles and the same settling speed was used for all POC in the water column. In addition, dissolved MeHg flux from sediments was trivial. Flux experiments with Baltimore Harbor sediment showed that release of MeHg to the water column occurred only under anoxic conditions (Mason et al., submitted). Similarly, it has been shown that there is little flux of MeHg from sediments under oxic conditions (Covelli et al., 1999; Gill et al., 1999). Thus, the flux of MeHg from the sediment during resuspension is unlikely.

4.3.2. Effects of sediment Hg methylation rate

In order to examine how sediment methylation may influence MeHg in biota, methylation rate were varied by ± 20 % of its fixed value in the model. As mentioned earlier, there was no attempt made to model resuspension effects on Hg methylation even though several factors such as sulfide levels, organic carbon, and temperature could be involved in influencing Hg methylation in sediments. For instance, Hammerschmidt and Fitzgerald (2004) found that methylation potential was negatively related to organic carbon content of surface sediment in Long Island Sound, a large coastal embayment in the northeastern US. The model results are presented in Fig. 4.4. MeHg in PP and ZP1 varied approximately 12 % in accordance with the 20 % changes in methylation rate in the sediment (Fig. 4.4a-b and Table 4.1a). MeHg in FF were less affected by varying sediment methylation rates (about 3 % change of MeHg concentration), compared to MeHg in PP and ZP1 (Fig. 4.4c).

From the initial evaluation of the STORM experiment data, it was concluded that resuspension did not increase dissolved MeHg, suggesting that MeHg desorption was not important (Chapter 2, Kim et al., 2004). The model results, however, showed that increased sediment MeHg, which was resuspended, resulted in higher dissolved MeHg even though the desorption rate was the same (Table 4.1b). As a result, MeHg in PP increased and this led to higher MeHg in the herbivores. The effect of methylation rate is more profound on MeHg in ZP than in FF because FF biomass is dominant in the system and it requires a substantial change in sediment methylation or a longer run time to have a significant impact on MeHg burden in FF. Nonetheless, the model results seem to suggest an important implication that was not evident from the experimental results, that sediment resuspension may play a role in transferring sediment MeHg to aquatic food chains. Both ZP and FF can be an essential link in the trophic transfer of contaminants as they serve an important food source to upper levels of the food chain (Roper et al., 1996; Paterson et al., 1998; Cope et al., 1999; Fisher et al., 2000; Ni et al., 2000).

Figure 4.3. Model outputs: a) POC in the water column; b) DOC in the water column; c) particulate MeHg in the water column; d) dissolved MeHg in the water column. Lines and symbols represent the model outputs and the data from experiment 2, respectively. Error bars show standard deviations of 3 replicates.

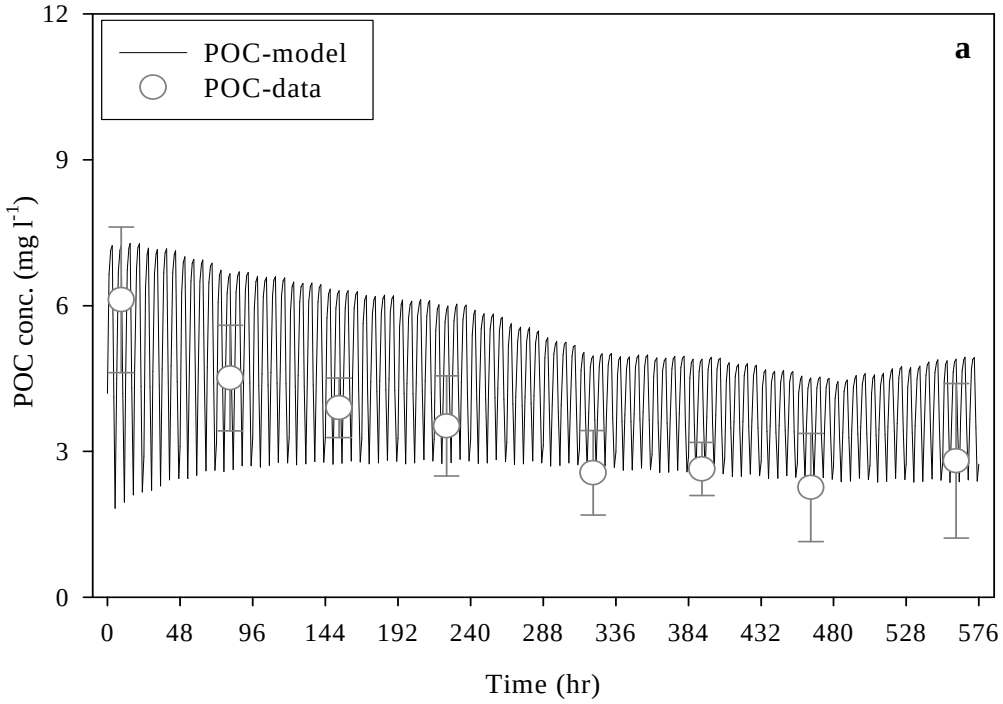
POC-model
POC-data
a
POC conc. (mg l-1)
0
3
6
9
12
0
48
96
144
192
240
288
336
384
432
480
528
576
Time (hr)

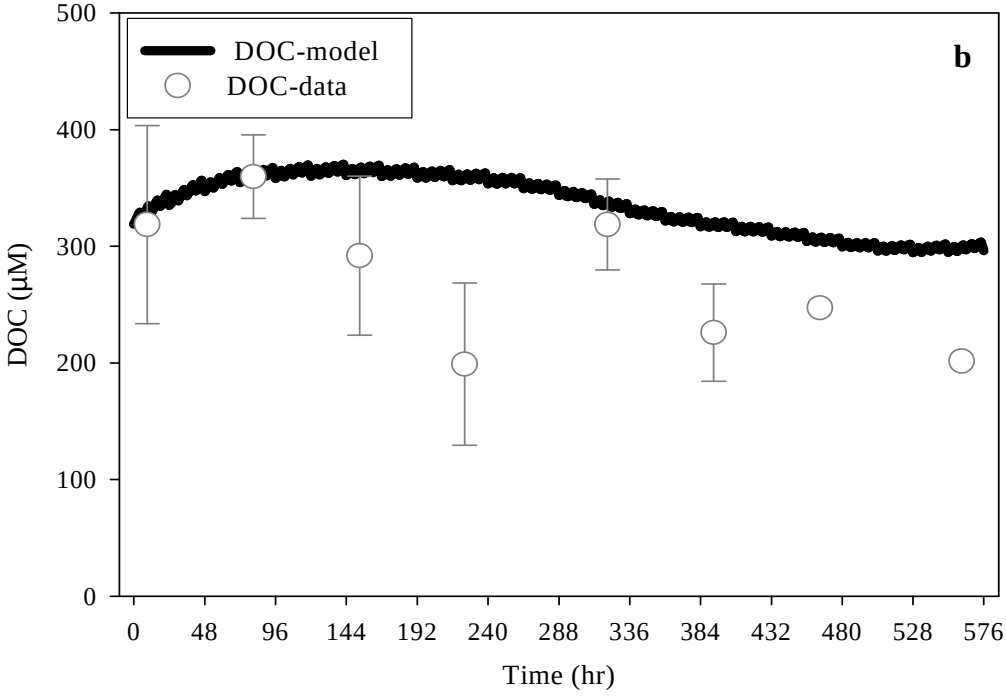
DOC-model
DOC-data
b
DOC (µM)
0
100
200
300
400
500
0
48
96
144
192
240
288
336
384
432
480
528
576
Time (hr)

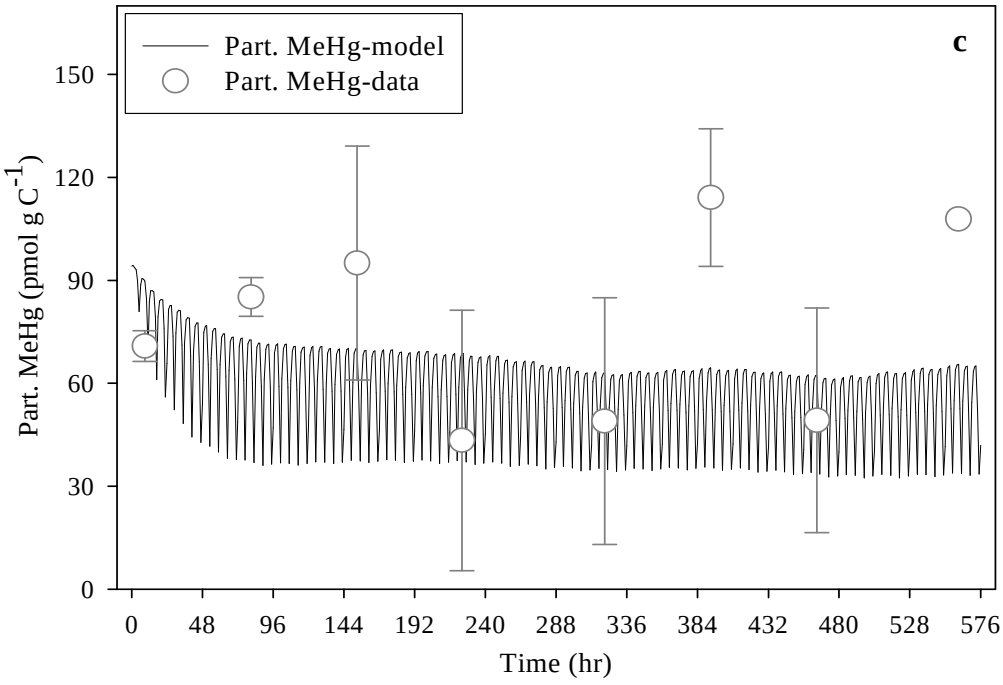
Part. MeHg-model
Part. MeHg-data
c
Part. MeHg (pmol g C-1)
150
120
90
60
30
0
0
48
96
144
192
240
288
336
384
432
480
528
576
Time (hr)

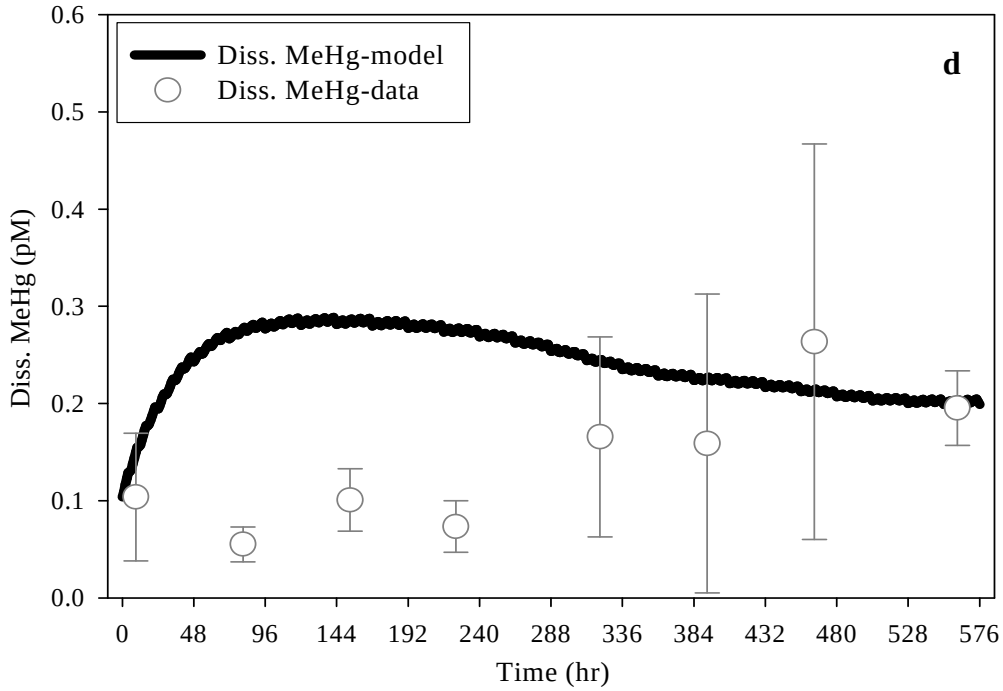
Diss. MeHg-model
Diss. MeHg-data
d
Diss. MeHg (pM)
0.6
0.5
0.4
0.3
0.2
0.1
0.0
0
48
96
144
192
240
288
336
384
432
480
528
576
Time (hr)

Figure 4.4. Model outputs: effect of methylation rate in a) PP; b) ZP1; c) FF. M is the methylation rate determined from Hg stable isotope spike addition incubation experiments (experiment 2).

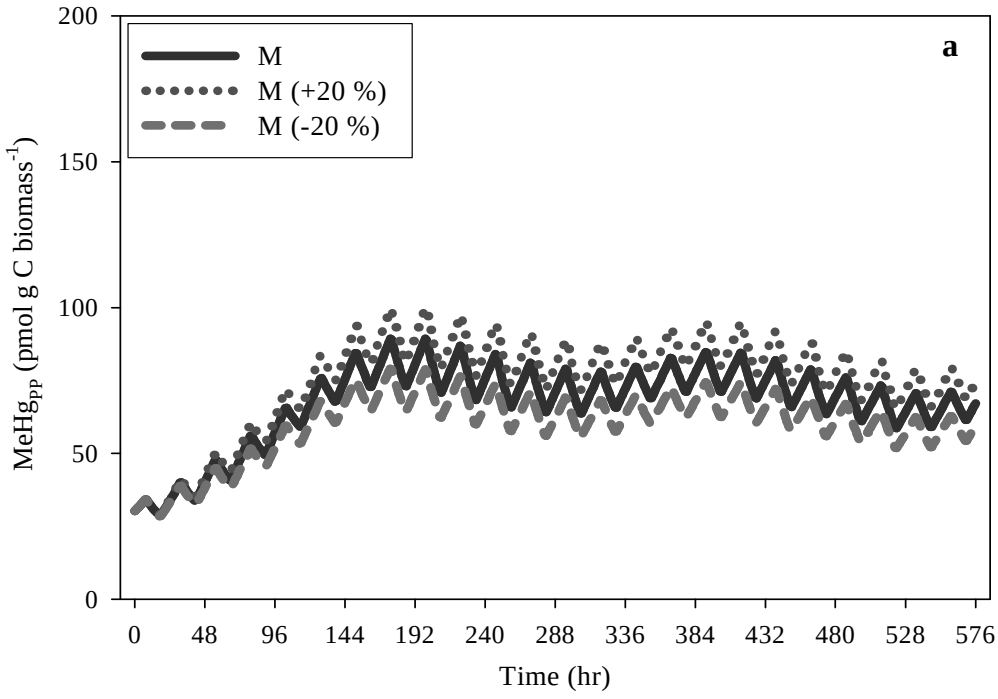
a
M
M (+20 %)
M (-20 %)
MeHg$_{pp}$ (pmol g C biomass^{-1})
0
50
100
150
200
0
48
96
144
192
240
288
336
384
432
480
528
576
Time (hr)

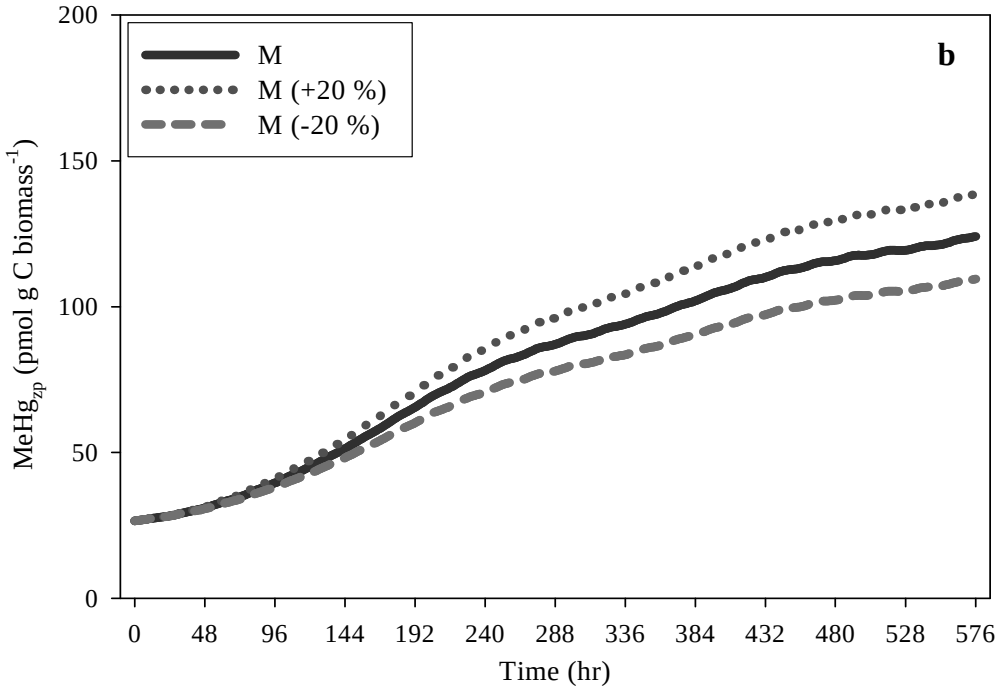
b
M
M (+20 %)
M (-20 %)
MeHg$_{zp}$ (pmol g C biomass^{-1})
0
50
100
150
200
0
48
96
144
192
240
288
336
384
432
480
528
576
Time (hr)

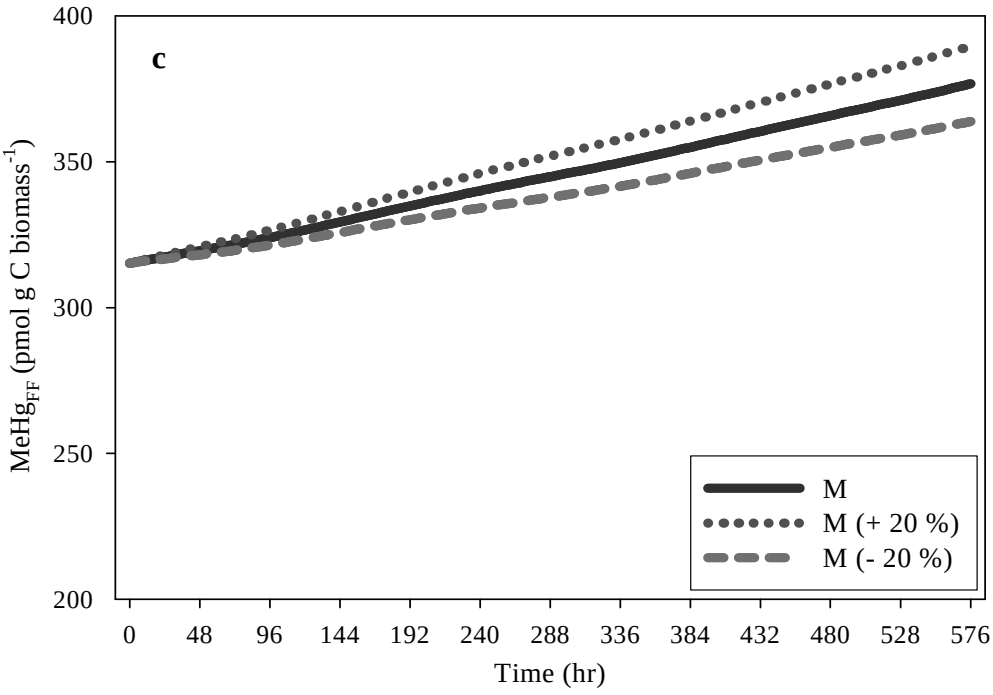
c
400
350
300
250
200
MeHg$_{FF}$ (pmol g C biomass^{-1})
0
48
96
144
192
240
288
336
384
432
480
528
576
Time (hr)
M
M (+ 20 %)
M (- 20 %)

4.3.3. Simulations of different scenarios

4.3.3.1. Model runs under a different season (experiment 3)

As mentioned above, different scenarios were simulated with some changes in inputs from the previous model run. These scenarios were modeled to explore the results of the other experiments and to ascertain how well the model could simulate these conditions. Firstly, the model was run with inputs used from the data in experiment 3, which was conducted in summer (July), but in all other aspects was similar to experiment 2. The initial biomass of PP, ZP and MPB were used from the data in experiment 3. The same FF biomass was used because of the same density of FF in both experiment 2 and 3. Average temperature (27 ± 1.5°C) was higher in experiments 3, compared to experiment 2 (20 ± 1.9 °C). Initial concentrations of dissolved MeHg, DOC, POC and nutrient data were also obtained from experiment 3 data. The organic-carbon based K_d for MeHg was used based on measurements from experiment 3. The results of this simulation are shown in Fig. 4.5.

It is likely that FF have a significant impact on PP and ZP biomass due to their being the dominant biomass in the system. In order to examine the effect of FF, the model was run with half the biomass of FF and without FF. These conditions were comparable to those of experiments 4. The model results and the observed data available are presented in Fig. 4.6.

Comparison of the model results with data from experiment 3 shows the model results of PP biomass were in relatively good agreement with the data in the early stage of the run. The model, however, failed to simulate the later PP bloom seen in the observed data (Fig. 4.5a). Actual ZP biomass showed a similar pattern to that of

the model, but showed a better agreement with the data in the early stage of the model run. It should be noted that measured PP biomass in experiment 3 (average Chl *a* of 6.9 µg L^{-1}) was comparable to that in experiment 2 (average Chl *a* of 6.7 µg L^{-1}) despite seasonal effects (mainly the higher water temperature in summer). Compared to the other experiments conducted in summer (experiments 1 and 4), the standing stock of PP was lower in experiment 3. This indicates that biomass was kept low by the likely competition between ZP and FF for limited food. The model results showed that ZP biomass varied in accordance with PP biomass (e.g. decreasing ZP biomass at the end of the model run).

The modeled FF biomass did not change substantially despite the PP biomass crash at the end of the model run. MPB biomass in the model increased over time. The observed data showed a similar pattern but increased to only about 2/3 of the modeled biomass (Fig. 4.5b). Although the same G_{max} was used for both experiment 2 and 3 conditions, it is likely that MPB production may have been different between the two experiments. Average concentration of TSS in experiment 3 (120 ± 45 mg L^{-1}) was about twice that of experiment 2 (63 ± 22 mg L^{-1}). Thus, one would expect that MPB production in experiment 3 might have been probably lower as MPB likely faced a more light-limited environment. However, this was not the case for experiment 3, suggesting that light limitation was likely not as important in MPB growth as initially expected.

The modeled MeHg in ZP showed a continuous increase over time while the observed data were in the lower range of the model results (Fig. 4.5c). One explanation for the discrepancy between the model and the observed data is likely

that the model did not simulate the later PP bloom and the corresponding increase in ZP2 at the end of the experiment. MeHg concentration in PP would have decreased as PP biomass increased. Pickhardt et al. (2002) found that an algal bloom reduced MeHg uptake by ZP because increasing algae decreased MeHg accumulation, resulting in a lower dietary inputs to ZP. Other studies have found similar results in that contaminant burden in algae decreased as biomass increased (Ashley, 1998; Winkels et al., 1998). Additionally, dissolved MeHg concentration was higher and more variable in experiment 3 (0.3 ± 0.1 pM), compared to experiment 2 (0.2 ± 0.05 pM). Although uptake by ZP from dissolved MeHg was not significant, compared to food ingestion, a higher concentration of dissolved MeHg likely contributed to higher MeHg in ZP. The model results fell within the range of MeHg in ZP found in other field measurements with a broad range from 88 pmol g C^{-1} to 14 nmol g C^{-1} (Plourde, et al., 1997; Paterson et al., 1998; Tremblay et al., 1998; Kainz et al., 2002). The model results of MeHg in FF slightly increased (by 37 %) with time and this was in good agreement with the observation (Fig. 4.5d).

Figure 4.5. Model outputs: a) biomass in the water column; b) biomass in the sediment; c) MeHg in water column biota; d) MeHg in benthic biota.

Lines and symbols represent the model outputs and the data from experiment 3, respectively. Error bars show standard deviations of 3 replicates.

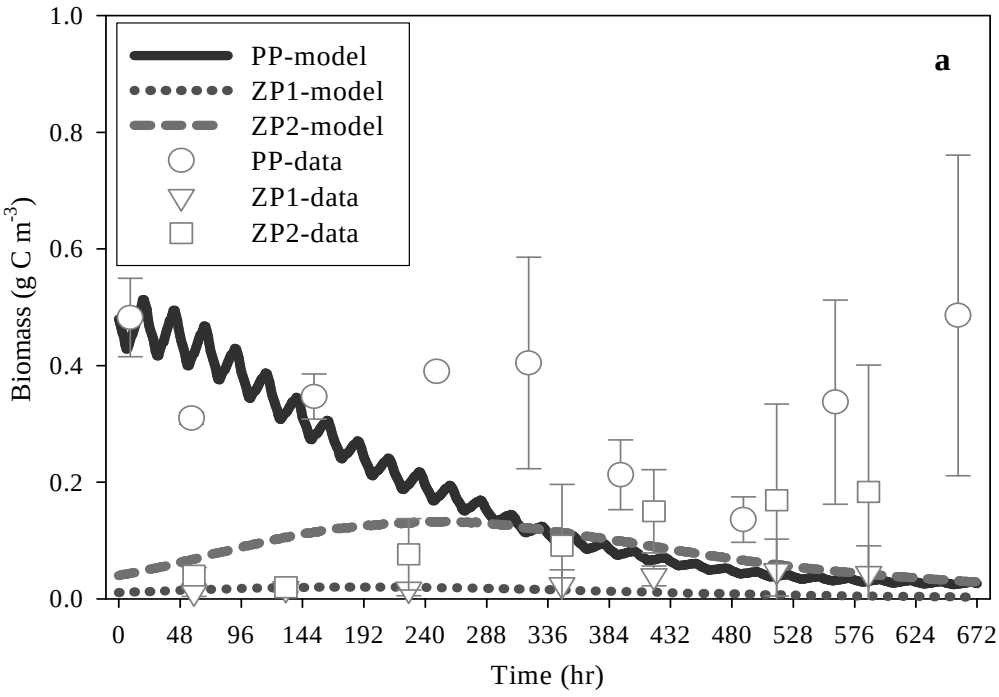
PP-model
ZP1-model
ZP2-model
PP-data
ZP1-data
ZP2-data
a
Biomass (g C m-3)
Time (hr)
0.0
0.2
0.4
0.6
0.8
1.0
0 48 96 144 192 240 288 336 384 432 480 528 576 624 672

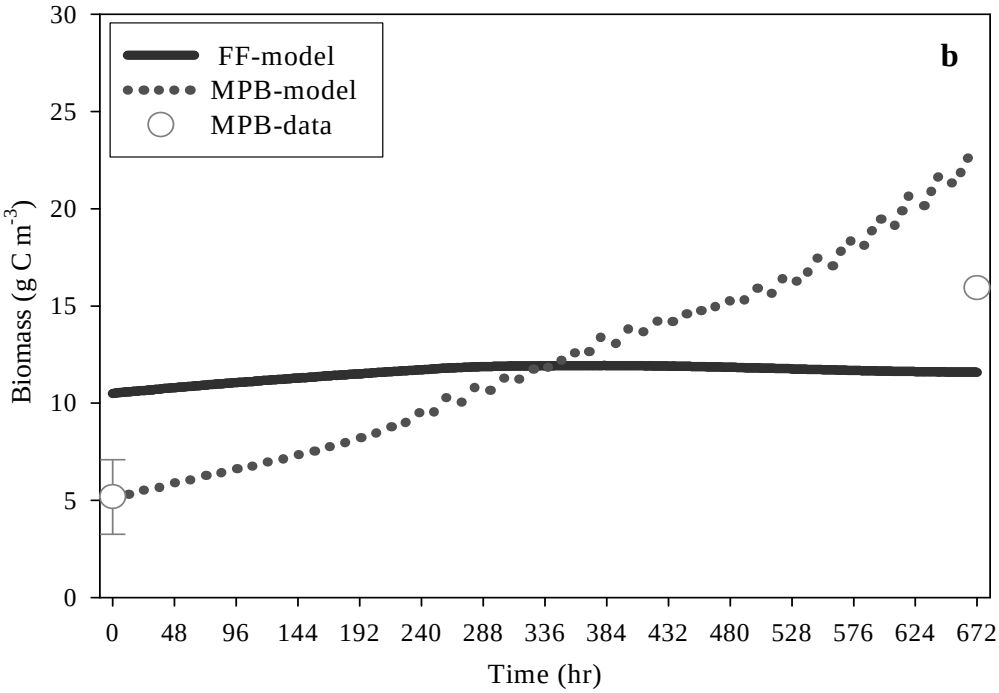
FF-model
MPB-model
MPB-data
b
Biomass (g C m-3)
Time (hr)
0
5
10
15
20
25
30
0 48 96 144 192 240 288 336 384 432 480 528 576 624 672

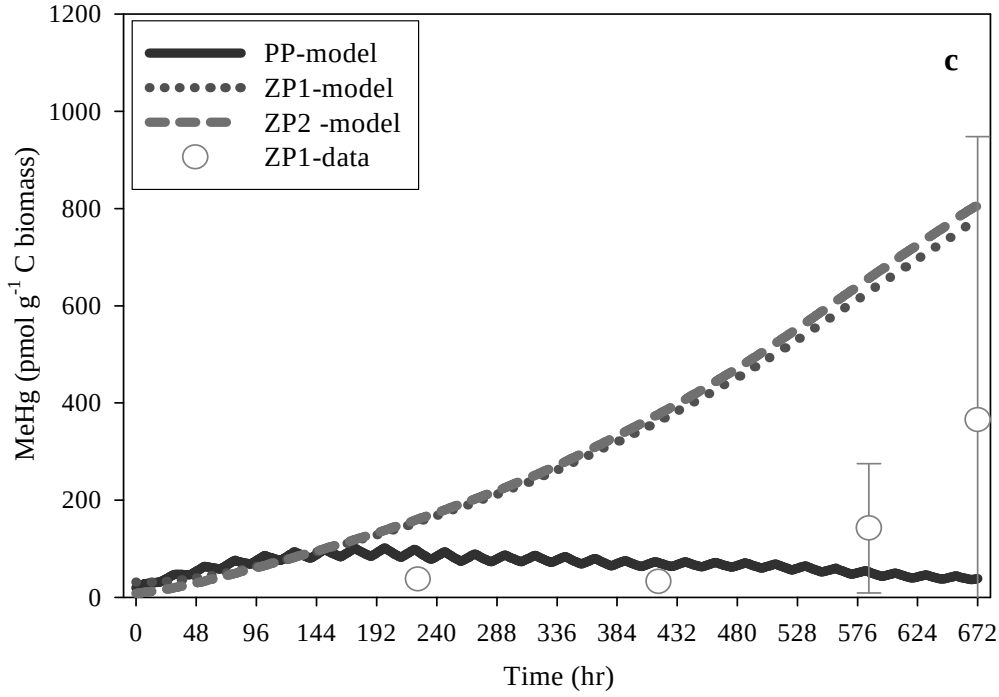
PP-model
ZP1-model
ZP2 -model
ZP1-data
c
MeHg (pmol g-1 C biomass)
Time (hr)
0
200
400
600
800
1000
1200
0
48
96
144
192
240
288
336
384
432
480
528
576
624
672

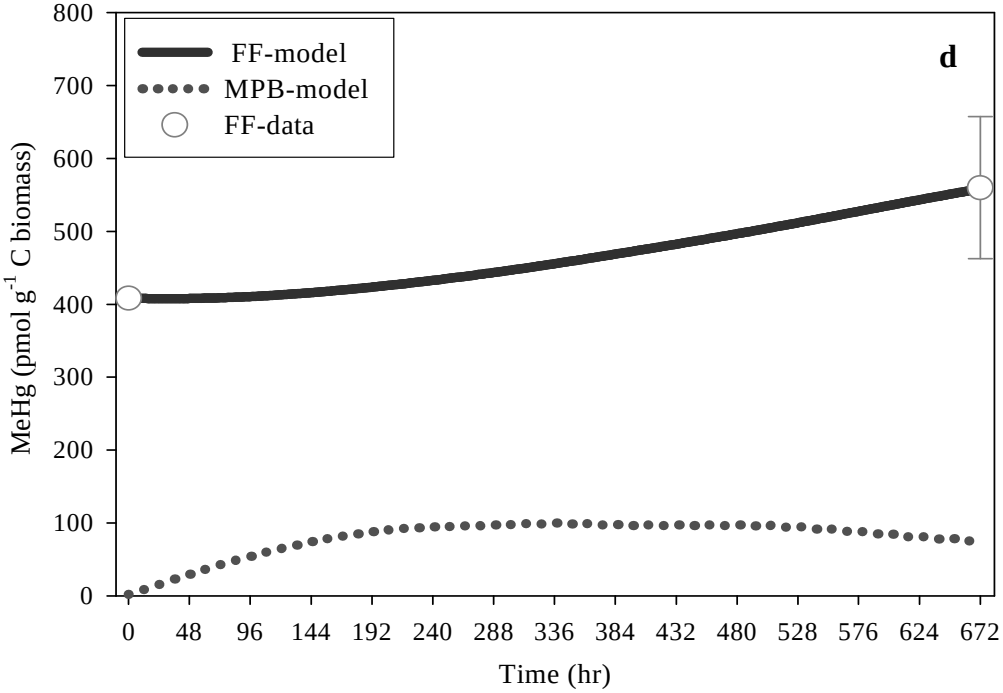
FF-model
MPB-model
FF-data
d
MeHg (pmol g-1 C biomass)
Time (hr)
0
100
200
300
400
500
600
700
800
0
48
96
144
192
240
288
336
384
432
480
528
576
624
672

4.3.3.2. Effects of filter feeder biomass

Fig. 4.6 shows the effects of FF on PP and ZP biomass and MeHg concentration. As seen in Fig. 4.6a, changes in FF biomass had a significant impact on PP biomass, especially in the early stage of the model run. As FF biomass increased, PP biomass dramatically decreased. A similar pattern was observed in the model for ZP biomass, which increased with decreasing FF biomass (Fig. 4.6b). This is because PP became more available to ZP as FF biomass decreased (i.e. reduction in FF filtering activity). Thus, the effect of changes in FF biomass on ZP is likely indirect. There was a time lag between PP and ZP peaks during the model runs probably because the grazing rate by ZP was slower than the PP growth rate. Although changes in FF biomass showed a great impact on PP and ZP biomass, MeHg burden in PP and ZP was affected by varying FF biomass to a lesser degree (Fig.4.6c-d). Similarly, model sensitivity analysis showed that increasing FF filtration rate by 20 % reduced PP biomass by 24 % while MeHg concentration in PP changed very little. It was also shown that MeHg burden in PP was governed more directly by dissolved MeHg uptake rate and PP growth compared to FF filtration rate (Table 4.1a). A similar pattern was found that MeHg in ZP was less affected by changes in FF biomass compared to ZP biomass.

Other modeling studies have shown that benthic filter feeders (e.g. zebra mussels) had a great impact on PP biomass. It was found that PP biomass decreased significantly due to grazing by filter feeders (Padilla et al., 1996; Caraco et al., 1997; Descy et al., 2003). Additionally, high zebra mussel density resulted in a decrease in small zooplankton such as rotifers especially in summer when mussels actively filter

(Viroux, 2000). However, in this model, grazing of ZP by FF was not included. Benthic filter feeders may not have impacts on different plankton communities in the same way. Padilla et al., (1996) found from their modeling study that mussel impact was greater on large PP than on small PP. It was likely that small PP compensated for grazing losses by enhanced growth due to increasing nutrient cycling and water clarity. As a result, ZP that consumed mainly small PP was less affected by mussels. Overall, the relation between benthic filter feeders and plankton can be more complicated than modeled here because of differences in size classes of prey and feeding preferences of ZP and FF and governed by other factors. PP biomass may not compensate by enhanced growth if there are nutrient-limited conditions and/or lower temperature. Filtration rate of FF can be affected by temperature, size of FF, hydrodynamic processes, and food availability (Riisgard, 1998; Grizzle et al., 2001; Riisgard et al., 2003; Newell, 2004). Those factors may influence MeHg accumulation in plankton as well as benthic filter feeders.

Figure 4.6. Model outputs: effects of FF biomass on a) PP biomass; b) ZP biomass; c) MeHg in PP; d) MeHg in ZP.

FF: the model run with biomass used in experiments 2 and 3; ½ FF: the model run with half the biomass; no FF: the model run without FF.

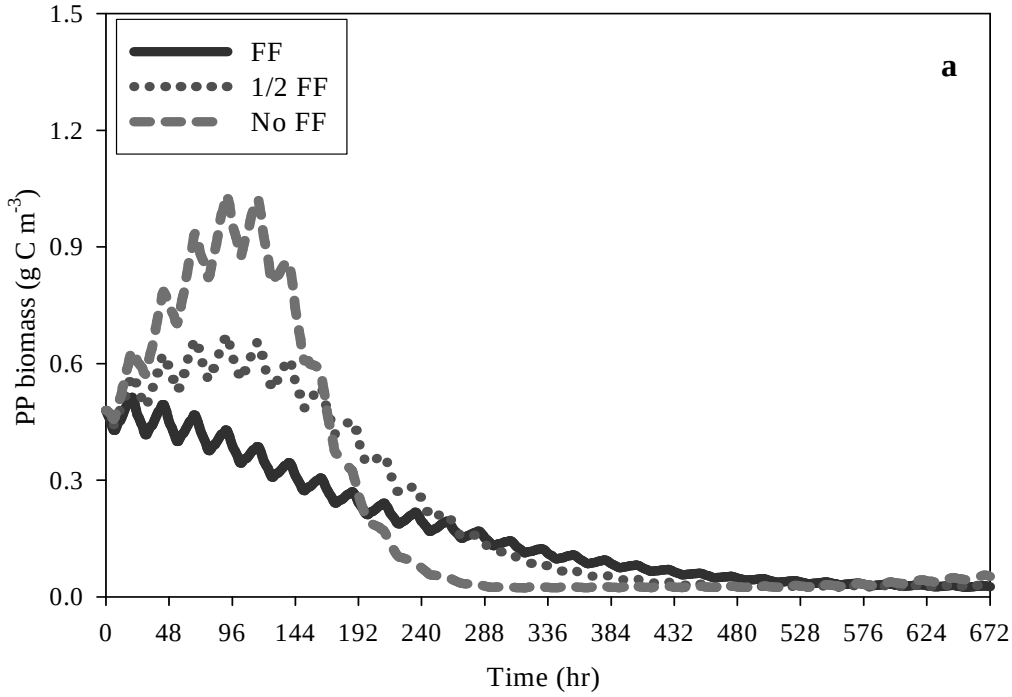
FF
1/2 FF
No FF
a
PP biomass (g C m-3)
1.5
1.2
0.9
0.6
0.3
0.0
0
48
96
144
192
240
288
336
384
432
480
528
576
624
672
Time (hr)

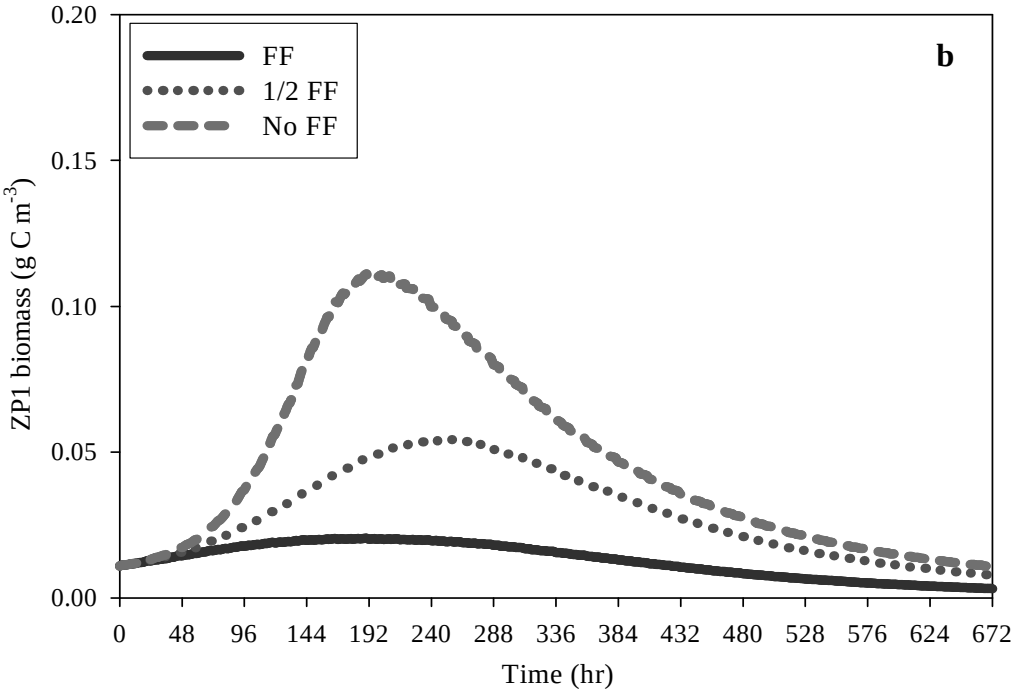
FF
1/2 FF
No FF
b
ZP1 biomass (g C m-3)
0.20
0.15
0.10
0.05
0.00
0
48
96
144
192
240
288
336
384
432
480
528
576
624
672
Time (hr)

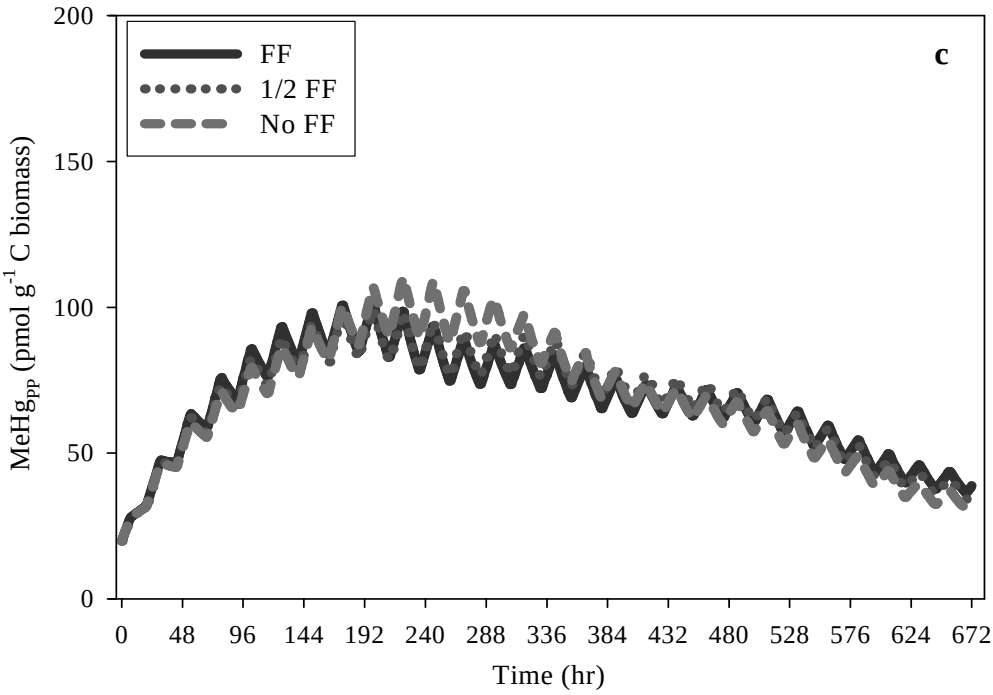
FF
1/2 FF
No FF
c
MeHg$_{PP}$ (pmol g^{-1} C biomass)
200
150
100
50
0
0 48 96 144 192 240 288 336 384 432 480 528 576 624 672
Time (hr)

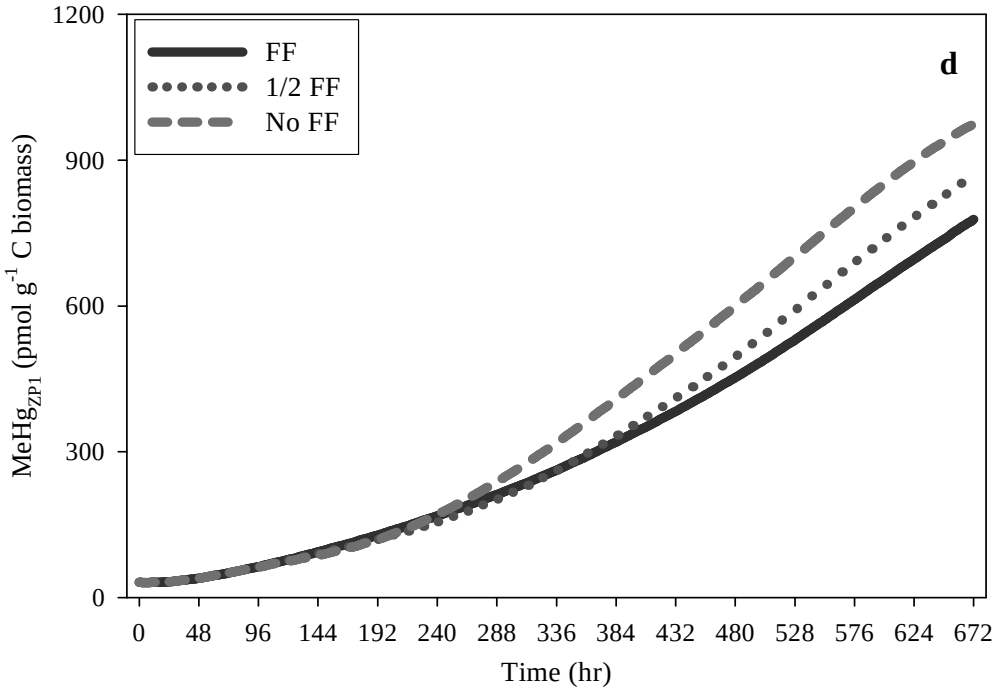
FF
1/2 FF
No FF
d
MeHg$_{ZP1}$ (pmol g^{-1} C biomass)
1200
900
600
300
0
0 48 96 144 192 240 288 336 384 432 480 528 576 624 672
Time (hr)

4.3.4. Sensitivity analysis results

The results of sensitivity analysis are presented in Table 4.1. It appears that PP growth rate was a highly sensitive parameter to plankton biomass but less so to FF biomass. In another modeling study, it was shown that G_{max} was the most sensitive component in the model, substantially altering the state variables (Angelini and Petrere Jr., 2000). Filtration rates of FF had also a great impact on plankton biomass and resulting MeHg burden in biota. Similarly, carbon AE for FF was a highly sensitive parameter in determining biomass and influencing MeHg accumulation more profoundly in ZP, compared to PP and FF. Increasing MeHg AE for ZP resulted in increasing MeHg burden in ZP. In addition, the results clearly show that increasing biomass leads to decreasing MeHg concentration in biota (dilution effect). The ZP biomass is two orders magnitude less than FF, resulting in ZP having a more sensitive response to varying parameters, compared to FF. For example, 20 % increase of PP growth rate changed ZP biomass to a large degree while the variation in FF biomass was very small. In addition, filtration rate of FF was one order magnitude lower than that of ZP. Thus, it would take longer time for FF biomass to change in response to food concentration. The model was run only for about a 4-week period (24-28 days) and this would be one explanation for the lesser impacts of PP growth on FF biomass.

Highly sensitive parameters to the dissolved MeHg state variable were organic carbon degradation rate in the water column, and sediment methylation rate (Table 4.1b). Dissolved MeHg concentration in the water column increased as POC degradation rate increased due to MeHg associated with POC (both WPOC & RPOC) recycling between dissolved MeHg and MeHg in POC pools. Increasing methylation

rate in the sediment contributed to higher dissolved MeHg in the water column as elevated MeHg concentration in sediments was transported to the water column. As mentioned earlier, from the STORM experiments, it was found that sediment resuspension did not increase dissolved MeHg in the water column to a significant degree (Chapter 2, Kim et al., 2004). This could just reflect the fact that the change predicted by the model (~ 13 %) was not substantially greater than the inherent variability in the MeHg concentration due to both analytical error and variability between the three tanks in the experiments. However, the model results suggest that sediment resuspension can play a role in transferring elevated MeHg on particles to the water column, resulting in increasing dissolved MeHg. The model results showed that MeHg concentration in plankton increased as uptake rate of dissolved MeHg by PP increased (Table 4.1). MeHg accumulation in FF was less affected by varying MeHg uptake rate by PP and a similar pattern was found for MPB, likely due to larger biomass relative to PP and ZP.

Table 4.1. Model sensitivity analysis.

Table 4.1a. Results are shown in percent.

		PP	ZP1	ZP2	FF	**MPB**
PP growth rate	+ 20 %	130	830	1300	2.8	**- 0.9**
	- 20 %	- 30	- 17	- 72	NC	**0.2**
ZP1 filtration rate	+ 20 %	- 3.4	96	- 18	NC	**NC**
	- 20 %	2.5	- 17	14	NC	**NC**
ZP2 filtration rate	+ 20 %	- 4.6	- 16	100	NC	**- 0.1**
	- 20 %	3.1	17	- 61	NC	**NC**
FF filtration rate	+ 20 %	- 24	- 17	- 71	0.7	**- 0.7**
	- 20 %	55	380	620	- 0.1	**0.5**
PP AE for ZP	+ 20 %	- 7.7	52	67	NC	**- 0.1**
	- 20 %	5.7	- 17	- 55	NC	**NC**
PP AE for FF	+ 20 %	- 24	- 17	- 71	0.2	**- 0.6**
	- 20 %	53	350	580	- 0.1	**0.5**
RPOC AE for FF	+ 20 %	- 1.8	- 6.7	- 9.2	0.4	**NC**
	- 20 %	1.8	7.8	10	- 0.1	**NC**
MeHg AE for FF	+ 20 %	NC	NC	NC	NC	**NC**
	- 20 %	NC	NC	NC	NC	**NC**
MeHg AE for ZP	+ 20 %	NC	NC	NC	NC	**NC**
	- 20 %	NC	NC	NC	NC	**NC**
		$MeHg_{PP}$	$MeHg_{ZP1}$	$MeHg_{ZP2}$	$MeHg_{FF}$	**$MeHg_{MPB}$**
PP growth rate	+ 20 %	- 15	- 7.3	- 5.7	- 6.0	**- 11**
	- 20 %	26	78	94	7.0	**6.8**
ZP1 filtration rate	+ 20 %	0.1	2.1	4.0	0.5	**0.2**
	- 20 %	- 0.1	- 0.2	- 2.3	- 0.3	**- 0.1**
ZP2 filtration rate	+ 20 %	0.2	7.6	6.7	0.8	**0.1**
	- 20 %	- 0.1	- 4.0	- 1.5	- 0.5	**- 0.1**
FF filtration rate	+ 20 %	1.1	31	36	3.3	**- 0.9**
	- 20 %	- 1.0	- 13	- 13	- 2.1	**- 0.5**
PP AE for ZP	+ 20 %	0.9	- 7.4	- 7.1	1.2	**0.4**
	- 20 %	- 0.6	18	19	- 0.9	**- 0.3**
PP AE for FF	+ 20 %	1.0	29	33	2.8	**- 0.8**
	- 20 %	- 0.9	- 13	- 13	- 1.7	**- 0.3**
RPOC AE for FF	+ 20 %	NC	1.5	1.6	- 1.8	**- 0.2**
	- 20 %	NC	- 1.4	- 1.6	1.8	**0.2**
MeHg AE for FF	+ 20 %	- 7.6	- 7.2	- 7.4	3.1	**- 3.9**
	- 20 %	9.7	8.7	9.0	- 3.2	**4.4**
MeHg AE for ZP	**+ 20 %**	**- 0.5**	**19**	**19**	**NC**	**- 0.1**
	- 20 %	**0.5**	**- 19**	**- 19**	**NC**	**0.1**

NC: no change.

Table 4.1b. Results are shown in percent.

	Diss. MeHg	DOC	MeHg $_{PP}$	MeHg $_{ZP1}$	MeHg $_{ZP2}$	MeHg $_{FF}$	**MeHg $_{MPB}$**
POC degradation rate							
+ 20 %	11	13	11	9.9	9.9	1.0	**10**
- 20 %	- 11	- 11	- 10	- 9.8	- 9.8	- 1.0	**- 10**
Uptake by Bacteria							
+ 20 %	- 1.2	- 8.9	- 1.1	- 0.9	- 0.8	- 0.1	**- 0.9**
- 20 %	1.5	12	1.3	1.1	1.1	0.1	**1.2**
Methylation rate							
+ 20 %	13	NC	12	12	12	3.4	**12**
- 20 %	-13	NC	- 12	- 12	- 12	- 3.4	**-12**
Dissolved MeHg$_{DOC}$ uptake rate by PP							
+ 20 %	**- 1.4**	**NC**	**18**	**9.4**	**9.5**	**0.4**	**- 1.7**
- 20 %	**1.5**	**NC**	**- 18**	**- 9.8**	**- 9.8**	**- 0.4**	**1.8**

NC: no change.

4.4. Summary

The model derived produced comparable results with the observed data for both biomass and MeHg burden under varying scenarios. Sediment resuspension can induce changes in sediment chemistry to favor Hg methylation, resulting in the transport of elevated sediment MeHg to the water column. The modeling result showed that dissolved MeHg in the water column was increased by elevated sediment MeHg transported to the water column. As a result, MeHg burden in plankton increased. Benthic filter feeders with dominant biomass, however, were less affected than plankton in the water column likely as a result of the limited duration of the simulation. Changes in filter feeder biomass had a great impact on plankton biomass but less on MeHg burden in plankton but it still was an important parameter. Model outputs were highly sensitive to phytoplankton growth and filtration rate of filter feeders. While the model provides a reasonable simulation of the conditions in the mesocosms, the model could be expanded to include a longer simulation period to further investigate effects of sediment resuspension on the MeHg burden in biota.

Chapter 5: Studies on controlling factors in the distribution of total mercury and methylmercury in estuarine sediments and on model applications of methylmercury bioaccumulation into benthic and pelagic organisms

5.1. Introduction

Estuaries provide an essential link in the global biogeochemical cycling of mercury (Hg) between the terrestrial and the marine environment. It has been reported that only a small fraction of the Hg transported in rivers is exported to the ocean due to the high retention of Hg in estuarine environments (Cossa et al., 1996; Benoit et al., 1998; Mason et al., 1999). Estuarine sediments serve as the principal location for Hg methylation (Gilmour and Henry, 1991; Benoit et al., 1998). As mentioned earlier, Hg is transformed to MeHg by sulfate reducing bacteria (SRB) in anaerobic environments. MeHg, a persistent and highly toxic contaminant, readily accumulates in aquatic food chains. Adverse effects of MeHg on higher trophic level organisms have been found such as neurological effects, reproductive effects, and behavioral effects (US EPA, 1995). MeHg accumulation into higher levels of food chains (e.g. fish) is of great concern for human health as humans are principally exposed to MeHg by fish consumption (Clarkson, 1990; Fitzgerald and Clarkson, 1991).

It has been shown that inorganic Hg, organic matter and sulfide were the most important factors in controlling MeHg levels in surface sediments (Benoit et al., 1998; Mason and Lawrence, 1999; Conaway et al., 2003; Hammerschmidt and Fitzgerald, 2004). In oxidized sediments, Hg tends to associate with sediment organic matter or iron/manganese oxides through adsorption/coprecipitation reactions (Benoit et al., 1998; Mason and Lawrence, 1999). When metal oxides are reduced Hg can be released into porewater (and eventually to overlying water via diffusion) or be removed by adsorption and coprecipitation with sulfide minerals under anoxic conditions (Gobeil and Cossa, 1993; Gagnon et al., 1997). In surface sediments, however, it is likely that both the oxidized solid iron (Fe) phases and reduced (e.g. FeS/AVS) coexist and thus the association of Hg and MeHg is complicated and depends on the relative concentrations of Fe, acid volatile sulfide (AVS), and organic carbon (Mason and Lawrence, 1999). Thus, the mobility and bioavailability of Hg and MeHg depends on the nature and concentration of the binding phases in the sediment, which appear to be controlled by sediment redox status. In addition, sediment-water partitioning of Hg and MeHg was positively related to organic matter in surface sediments with low levels of AVS (Hammerschmidt and Fitzgerald, 2004).

Benoit et al. (1999a; 1999b; 2001) demonstrated that sulfide influenced Hg methylation in sediment by controlling Hg speciation and its bioavailability to SRB. Additionally, it was found that organic matter and AVS had an inhibitory effect on Hg methylation in surface sediments by controlling the partitioning and subsequent availability of inorganic Hg in the pore water (Hammerschmidt and Fitzgerald, 2004). Temperature can be a controlling factor in Hg methylation and SRB activity (Korthals

and Winfrey, 1987; Winfrey and Rudd, 1990; Skyring, 1987). It was observed that Hg methylation was enhanced in August, compared to March and June, likely due to the effect of temperature influencing SRB activity (Hammerschmidt and Fitzgerald, 2004). Similarly, the results from mesocosm experiments showed that *in situ* MeHg production was higher, especially in the top sediment layers, in July, compared to October, and that *in situ* production was negatively related to AVS concentration in July (Chapter 3, submitted). As discussed earlier, sediment resuspension can play a role in enhancing Hg methylation and subsequent MeHg accumulation into benthic and pelagic organisms (Chapters 3 and 4). It has shown that there was a strong correlation between sediment MeHg concentration and biota concentration for both benthic invertebrates and zooplankton in Lavaca Bay, Texas, USA, a shallow estuary, where resuspension frequently occurred (Bloom et al., 1999).

Sediment organic carbon has an influence on controlling bioavailability of Hg and MeHg and subsequent their bioaccumulation into benthic organisms. It was observed from field studies and laboratory exposure experiments that bioaccumulation factors (BAF) decreased with increasing sediment organic matter (Mason et al., 1998; Mason and Lawrence, 1999; Lawrence and Mason, 2001). Furthermore, digestive fluid solubilization studies with the intestinal fluid of benthic organisms have shown that sediment organic matter played an important role in Hg and MeHg bioavailability to benthic invertebrates (Lawrence et al., 1999). Similarly, Hg concentration in benthic organisms was negatively related to levels of Fe/manganese (Mn) oxides, and organic content in the lake sediment (Jackson, 1988). In addition to geochemical factors, Hg and MeHg bioaccumulation into benthic and

pelagic organisms can be influenced by their feeding rate, food availability, and Hg and MeHg concentrations in foods, as discussed in Chapters 3 and 4.

The objective of this study was to examine the spatial distribution of Hg and MeHg and the factors controlling THg and MeHg distribution in surface sediments of the Chesapeake Bay, a large and productive estuary in the east coast of USA. Sediment samples and clams, *Rangia cuneata* were collected from Hart-Miller Island (HMI; Dredge Material Contaminant Facility) to investigate the role of organic matter in THg and MeHg distribution and bioaccumulation into *R. cuneata*. Sediments were also analyzed from a transect down the mainstem. Furthermore, the MeHg bioaccumulation model developed in Chapter 4 was applied to field situations to investigate the potential impact of sediment resuspension on MeHg bioaccumulation into benthic and pelagic organisms for a longer period of the model run. The model applications also included the effects of changes in sediment organic matter and Hg methylation on MeHg burden in biota.

5.2. Material and Methods

5.2.1. Sample locations and collection

Sediment samples were collected using a Cedar type box corer from the mainstem Chesapeake Bay in May, 1993, as part of the NSF-LMER program. The location of sampling sites is shown in Fig.5.1a. Sediment samples were collected around HMI regions (September, 2000) as a part of a long-term monitoring program. The samples were taken using a standard Ponar grab sampler. Sampling stations are presented in Fig. 5.1b. Samples were stored in acid-cleaned plastic cups and transported on ice back to CBL. Clam samples were collected at stations where they were available and sieved on-board. The samples were placed in zip-lock bags and stored on ice until they were transported back to CBL. Clams were shucked immediately upon the return to the lab and homogenized in a blender. All samples were kept frozen until analysis.

Figure 5.1. Sampling stations (circled): a) the mainstem Chesapeake Bay; b) Hart-Miller Island.

Sites	Lat.	Long.	Sites	Lat.	Long.
NSS3	39 09.99	76 18.70	MDE-1	39 15.39	76 20.57
NSS2	39 04.87	76 19.49	MDE-3	39 15.54	76 19.90
MSS17	39 00.23	76 20.79	MDE-7	39 15.06	76 20.34
MSS18	38 59.92	76 22.67	MDE-9	39 14.76	76 20.58
MSS15	38 49.93	76 26.28	MDE-13	39 13.51	76 20.60
MSS16	38 49.07	76 24.63	MDE-16	39 14.54	76 21.45
MSS11	38 39.98	76 28.00	MDE-17	39 14.17	76 21.19
MSS12	38 39.97	76 24.82	MDE-22	39 13.19	76 22.47
MSS10	38 39.96	76 29.98	MDE-28	39 45.14	76 23.19
MSS9	38 30.02	76 22.42	MDE-34	39 15.76	76 20.54
MSS7	38 29.97	76 27.58	MDE-35	39 16.32	76 20.70
MSS4	38 20.03	76 22.18			
MSS6	38 19.96	76 17.92			
MSS1	38 09.97	76 18.84			
SSS27	38 00.01	76 06.41			
SSS25	37 59.99	76 12.49			
SSSE	37 55.00	76 09.98			
SSS21	37 49.97	76 13.52			
SSSD	37 45.08	76 10.10			
SSS19	37 39.96	76 03.37			
SSS20	37 39.96	75 57.40			
SSS17	37 39.94	76 16.45			
SSSC	37 34.98	76 07.50			
SSS14	37 30.02	76 07.58			
SSS13	37 30.01	76 12.52			
SSS15	37 29.99	76 02.89			
SSS8	37 20.05	76 14.49			
SSS10	37 20.03	76 07.47			
SSS11	37 19.97	76 03.45			
SSS9	37 19.91	76 10.65			
SSS5	37 10.02	76 12.40			
SSS7	37 10.00	76 00.42			
SSS6	37 09.99	76 07.52			
SSS4	37 09.97	76 15.51			
SSS1	37 00.00	76 09.84			
SSS2	36 59.86	76 04.95			

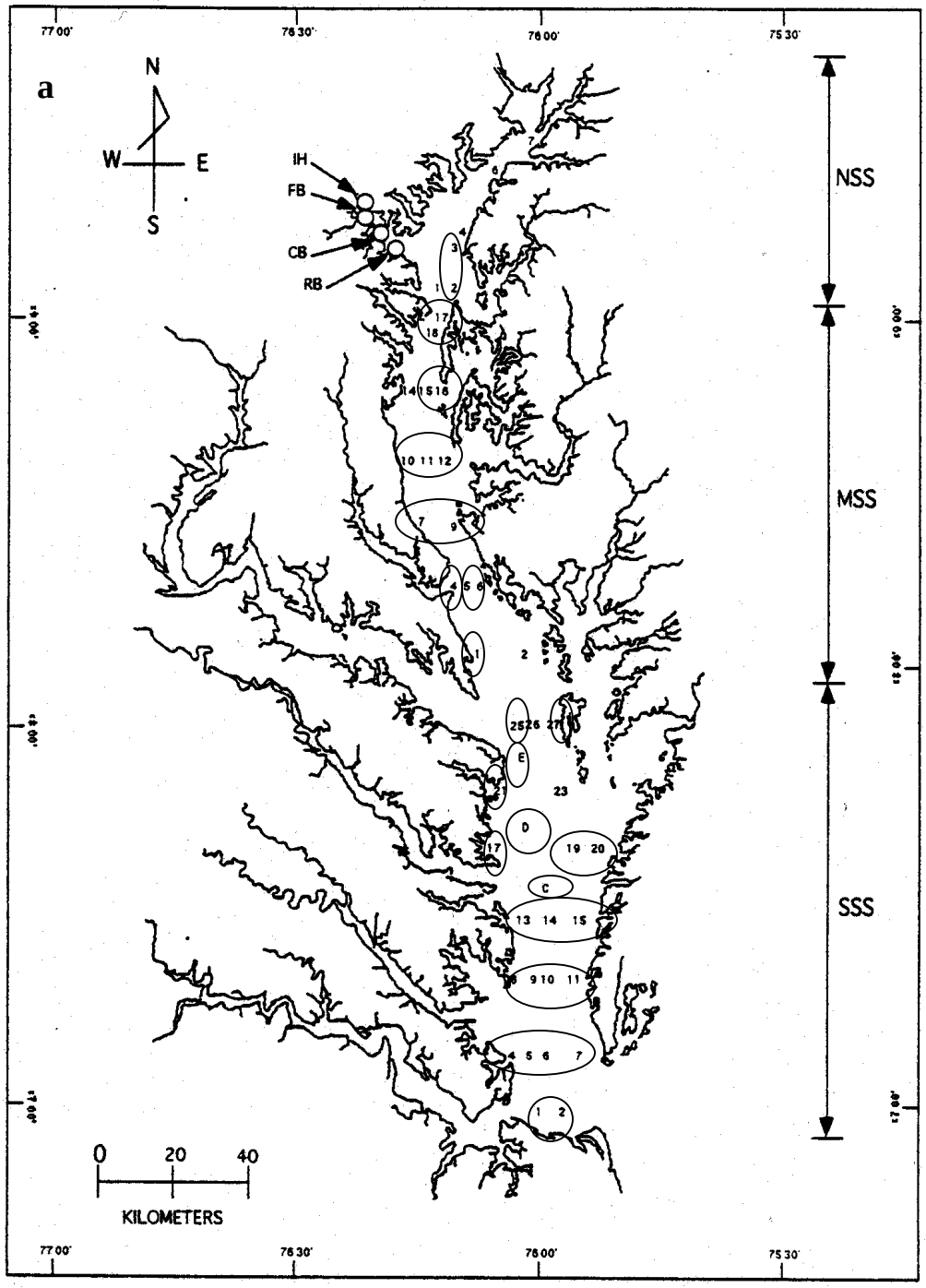
a
N
W
E
S
IH
FB
CB
RB
NSS
MSS
SSS
77°00'
76°30'
76°00'
75°30'
0 20 40
KILOMETERS

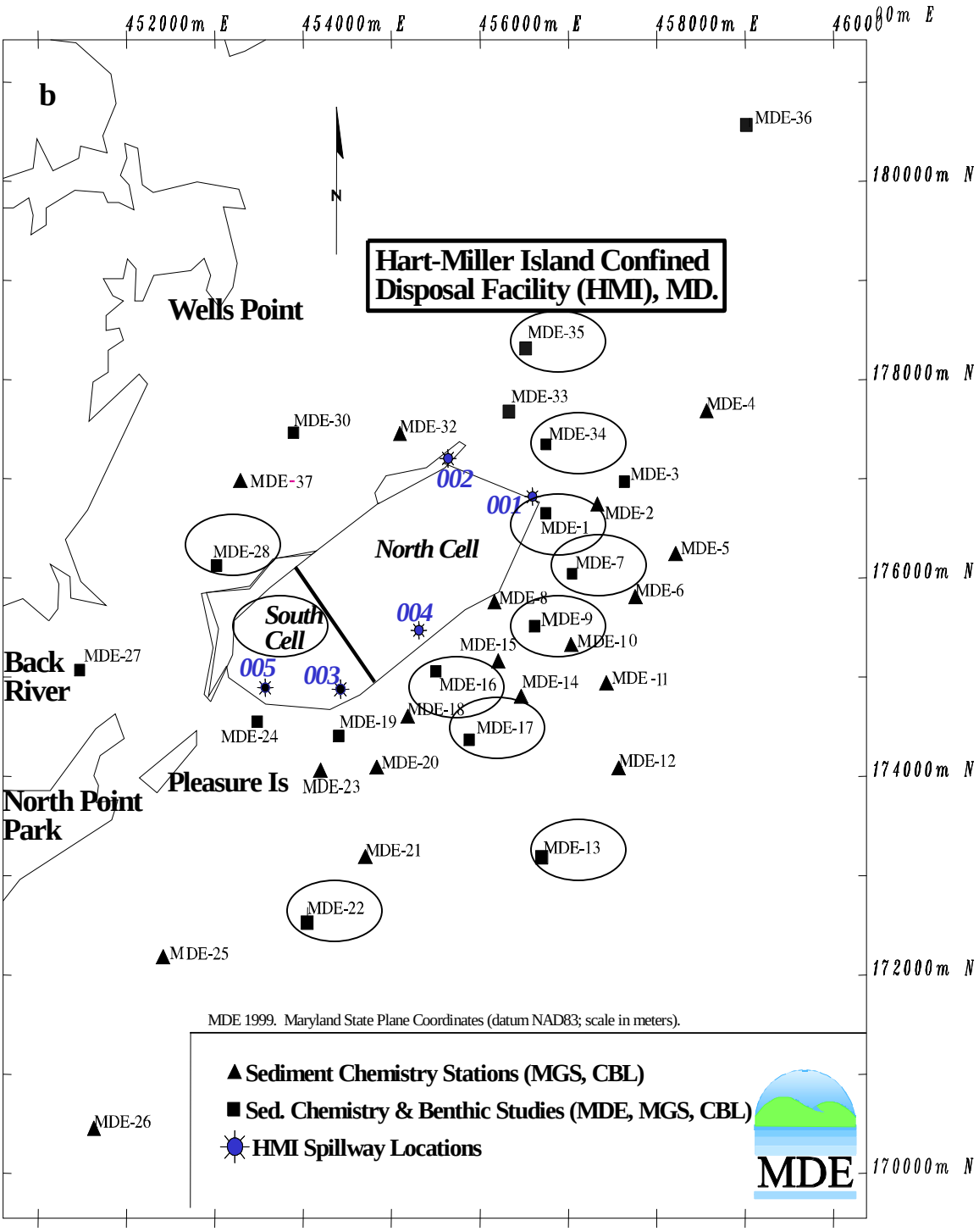
b
452000m E
454000m E
456000m E
458000m E
460000m E
180000m N
178000m N
176000m N
174000m N
172000m N
170000m N
N
Hart-Miller Island Confined Disposal Facility (HMI), MD.
Wells Point
Back River
North Point Park
Pleasure Is
North Cell
South Cell
001
002
003
004
005
MDE-1
MDE-2
MDE-3
MDE-4
MDE-5
MDE-6
MDE-7
MDE-8
MDE-9
MDE-10
MDE-11
MDE-12
MDE-13
MDE-14
MDE-15
MDE-16
MDE-17
MDE-18
MDE-19
MDE-20
MDE-21
MDE-22
MDE-23
MDE-24
MDE-25
MDE-26
MDE-27
MDE-28
MDE-30
MDE-32
MDE-33
MDE-34
MDE-35
MDE-36
MDE-37
MDE 1999. Maryland State Plane Coordinates (datum NAD83; scale in meters).
Sediment Chemistry Stations (MGS, CBL)
Sed. Chemistry & Benthic Studies (MDE, MGS, CBL)
HMI Spillway Locations
MDE

5.2.2. Sample analysis

5.2.2.1. Total Mercury

Both sediment and biota samples were thawed and digested in a solution of 7:3 sulfuric acid: nitric acid in Teflon vials in an oven at 60 °C overnight prior to BrCl oxidation (1/2-1 h). Then, excess oxidant was neutralized with 10 % hydroxylamine hydrochloride prior to analysis (Bloom and Crecelius, 1983). The samples were then reduced by tin chloride, sparged, and the elemental Hg trapped on gold traps. Quantification was done by dual-stage gold amalgamation/Cold Vapor Atomic Florescence detection (CVAFS) (Bloom and Fitzgerald, 1988) in accordance with protocols outlined in EPA method 1631 (EPA, 1995). Standard calibration curves with r^2 of > 0.99 for THg were achieved daily. THg concentration was determined by CVAFS. Analysis of standard reference material, estuarine sediments IAEA-405 (3.9 – 4.3 nmol g^{-1}), typically gave a 90 % recovery. Analysis of duplicate samples typically yielded a relative percent difference (RPD) of less than 15 %. Detection limits were based on 3 standard deviations of digestion blank measurements. Detection limits for THg were 1.1 pmol g^{-1} for sediments, and 0.1 pmol g^{-1} for biota.

5.2.2.2. Methyl mercury

Details of the analytical protocols are given elsewhere (Mason et al., 1999; Mason and Lawrence, 1999). Sediment and biota samples were distilled with a 50 % sulfuric acid and 20 % potassium chloride solution (Horvat et al., 1993). A sodium tetraethylborate solution was added to the distillate to convert the nonvolatile MeHg to gaseous methylethylmercury (Bloom, 1989). The volatile adduct was then purged

from solution and recollected on a graphitic carbon column at room temperature. The methylethylmercury was thermally desorbed from the column, and analyzed by isothermal gas chromatography with CVAFS. A calibration curve with an r^2 of > 0.99 was achieved on a daily basis. Analysis of duplicate samples typically gave a RPD of less than 20 %. Detection limits were based on 3 standard deviations of distillation blank measurements. Detection limits for MeHg were 0.02 pmol g^{-1} for sediments and 0.005 pmol g^{-1} for biota. Analysis of SRM IAEA-405 (25 - 30 pmol g^{-1}) generally gave a 90 % recovery.

5.2.2.3. Trace metals

A subsample of sediment or clams was placed in acid-cleaned flasks for digestion (EPA, 1996; Keith, 1991). Optima HNO_3 was added and the flasks were covered with watch glasses. The samples were then heated to 95°C and allowed to reflux for 15 min without boiling. Once the samples were cooled, HNO_3 was added, followed by refluxing for 30 min. This procedure was repeated in order to ensure complete oxidation. After the watch glasses were removed, the samples were allowed to evaporate to approximately 5 mL without boiling. When the samples were cooled, aliquots of 30 % H_2O_2 were added until the effervescence was minimal. Then, concentrated HCl and deionized water were added and the samples refluxed for 15 min. Finally, the samples were allowed to cool and diluted to 50 mL with deionized water. The digestates were analyzed for trace metals by ICP-MS using a quadrapole Hewlett-Packard 4500. A calibration curve with an r^2 of at least 0.99 was obtained daily. Analysis of duplicate samples generally gave a RPD of less than 10 %.

Detection limits for metals, based on 3 standard deviations of digestion blanks, were generally lower than 0.1 nmol g^{-1}. Analysis of standard reference material, estuarine sediment NIST 1646a, typically yielded a recovery of 84 %. Spike recovery averaged 83 %.

5.2.3. Model applications

The model developed in Chapter 4 was run for a longer period (May – October) with some modifications. Fig. 5.2 presents data for nutrients, temperature, and phytoplankton (PP) biomass in 2001 from three stations, CB5.1, CB5.2, and CB 6.4, chosen among stations for the Chesapeake Bay Program in the mainstem of the Chesapeake Bay (**www.chesapeakbay.net**). Average nutrients and temperature of the three stations were used in this model application. The stations chosen here were within the mesohaline-polyhaline regions of the Bay, as salinity in experiment 2 (19 ppt) was in a marginal range between the two regions. The three stations showed different ranges of sediment organic matter (e.g. low, medium, and high). Phytoplankton (PP) data was also presented for comparison with model results. Growth rate of PP was calibrated so that PP biomass in the model fell within the range of field data. As discussed in Chapter 4, the model results were highly sensitive to PP growth. Sediment resuspension was modeled in a similar way to the model developed in Chapter 4. However, the observed particle concentration in the water column was used a constant as total suspended solid (TSS) data showed a relatively constant pattern over time, averaging 6.9 ± 1.4 mg L^{-1}. TSS concentration was much lower than for the mesocosm studies (Chapter 2, Kim et al., 2004).

Figure 5.2. Data used in the model applications: a) average temperature and nutrients; b) average PP biomass in the Chesapeake Bay in 2001.

The data were obtained from three stations; CB5.1 (38º 32´ N), CB5.2 (38º 14´ N), and CB6.4(37º 24´ N).

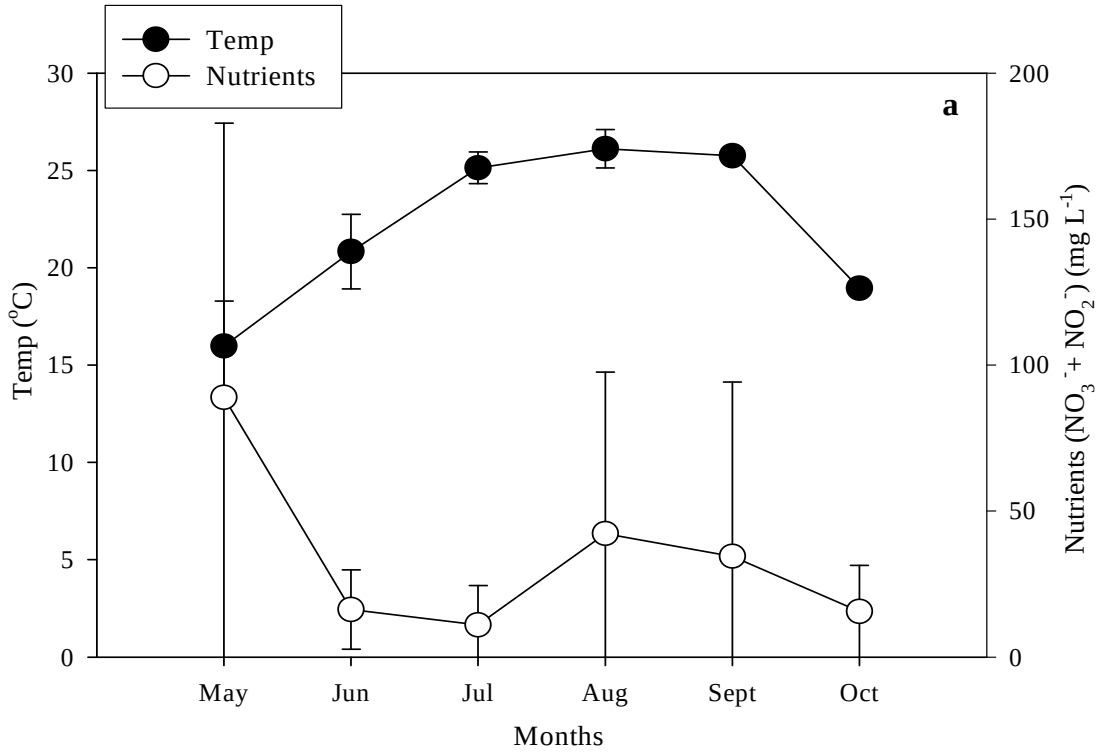
Temp
Nutrients
a
Temp (°C)
Nutrients (NO3- + NO2-) (mg L-1)
30
25
20
15
10
5
0
200
150
100
50
0
May
Jun
Jul
Aug
Sept
Oct
Months

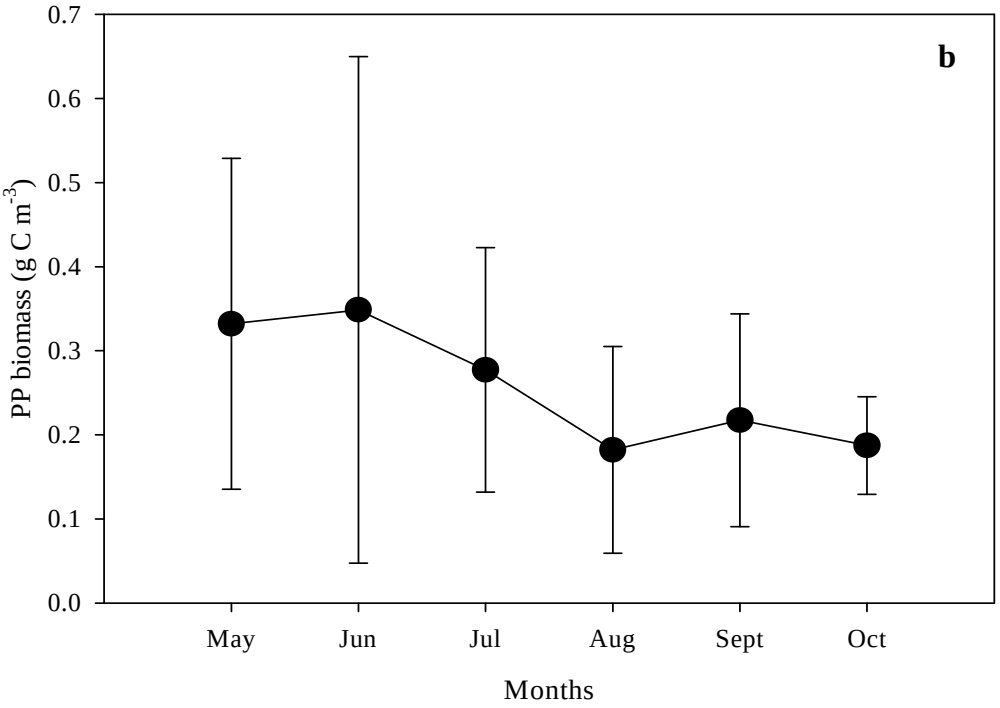
b
PP biomass (g C m-3)
0.7
0.6
0.5
0.4
0.3
0.2
0.1
0.0
May
Jun
Jul
Aug
Sept
Oct
Months

Additionally, as mentioned in Chapter 4, zooplankton (ZP1 and ZP2) and filter feeders (FF) fed on phytoplankton (PP) as the only food source in the model. Thus, loss terms for ZP and FF (e.g. excretion, respiration, and mortality) were decreased by 50 % from the values used in Chapter 4 to compensate for dramatic biomass reduction in ZP and FF due to food limitation during the longer period of model running, and to help the model stability. While the initial biomass of ZP1 and ZP2 was the same as the previous model, half the FF biomass was used in this study, which fell within a range typically found in the field (Grizzle et al., 2001). Additionally, predation terms for ZP, FF, and MPB were added to simulate consumption by higher trophic level organisms as the model was applied to field situations and a longer period of the model run. Changes made to the model application are summarized in Appendix III.

The model applications were aimed at examining the effects of varying organic matter content in the sediment with subsequent changes in Hg methylation on MeHg bioaccumulation into benthic and pelagic organisms. Given the wide range of organic matter in the Chesapeake Bay sediments, a range of organic matter content were chosen, high (12 %), medium (6 %), and low (3 %) for the modeling study. Field studies have shown that percent organic matter was negatively related to Hg methylation potential and this fact was used. By applying the linear relationship given by Hammerschmidt and Fitzgerald (2004), Hg methylation rate was estimated with different organic matter content. The Hg methylation rates used were 6.7×10^{-4}, 2.3×10^{-3}, and 3.1×10^{-3} h^{-1}, corresponding to organic matter content of 12, 6, and 3 %, respectively. Based on the relationship of organic matter with THg and MeHg found

in the samples collected from the Bay, the initial concentrations of THg and MeHg were determined corresponding to changes in sediment organic matter content. The distribution coefficient (K_d) for MeHg in sediments was also a function of % organic matter (Hammerschmidt and Fitzgerald, 2004; Bloom et al., 1999) and the relationship between the two variables was also obtained from Hammerschmidt and Fitzgerald (2004) to obtain the initial MeHg concentration in the porewater.

5.3. Results and discussion

5.3.1. Distribution and bioaccumulation of total mercury and methyl mercury

The overall general distribution of THg concentrations showed a decrease from the head of the Bay to the mouth of the Bay, with an average concentration of THg being 420 ± 530 pmol g^{-1} (Fig. 5.3a). THg concentrations fell within the range of those found in the previous investigation of Hg distribution in the Chesapeake Bay and tributaries (Mason et al., 1999; Benoit et al., 1998) and other estuarine systems (Conaway et al., 2003; Sunderland et al., 2004). MeHg concentrations were overall high in the upper bay but there were some sites with elevated levels of MeHg in the lower bay (Fig. 5.3b). Average concentration of MeHg was 2.2 ± 2.2 pmol g^{-1}, which was in a similar range of MeHg levels found by others (Mason et al., 1999; Conaway et al., 2003; Hammerschmidt and Fitzgerald, 2004; Sunderland et al., 2004). Percent organic matter in sediments showed, overall, a similar trend with THg and MeHg (Fig. 5.3c). Sediment organic matter was significantly correlated to THg ($r^2 = 0.60$, n = 36) and MeHg ($r^2 = 0.61$, n = 36) concentrations (Table 5.1).

Figure 5.3. The concentrations of a) THg; b) MeHg; c) organic matter in the mainstem Chesapeake Bay.

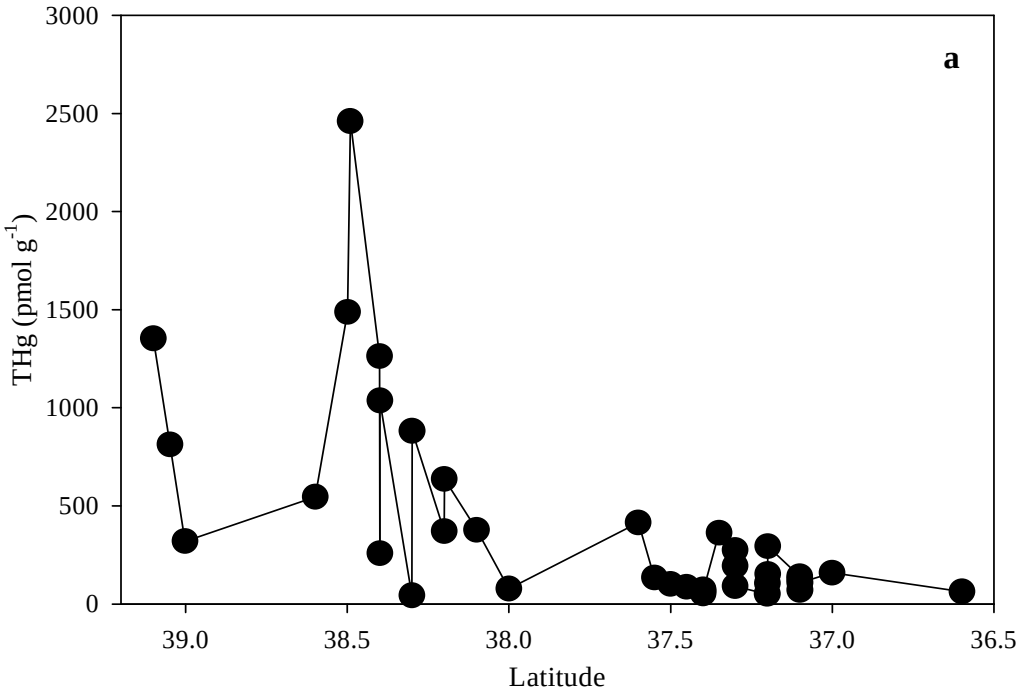
a
THg (pmol g-1)
3000
2500
2000
1500
1000
500
0
39.0
38.5
38.0
37.5
37.0
36.5
Latitude

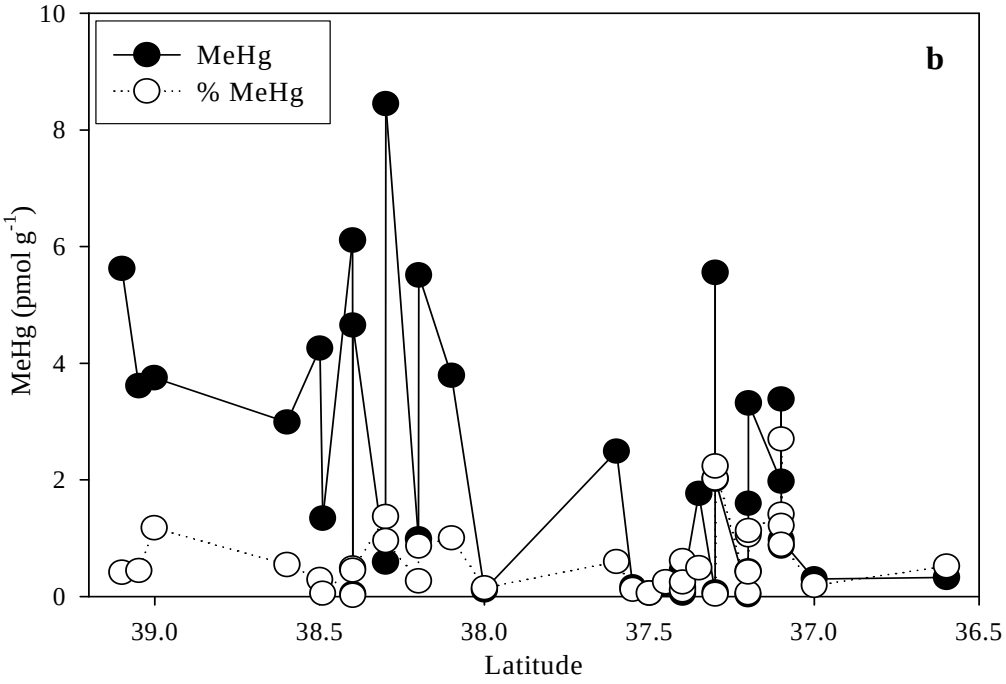
b
MeHg
% MeHg
MeHg (pmol g-1)
10
8
6
4
2
0
39.0
38.5
38.0
37.5
37.0
36.5
Latitude

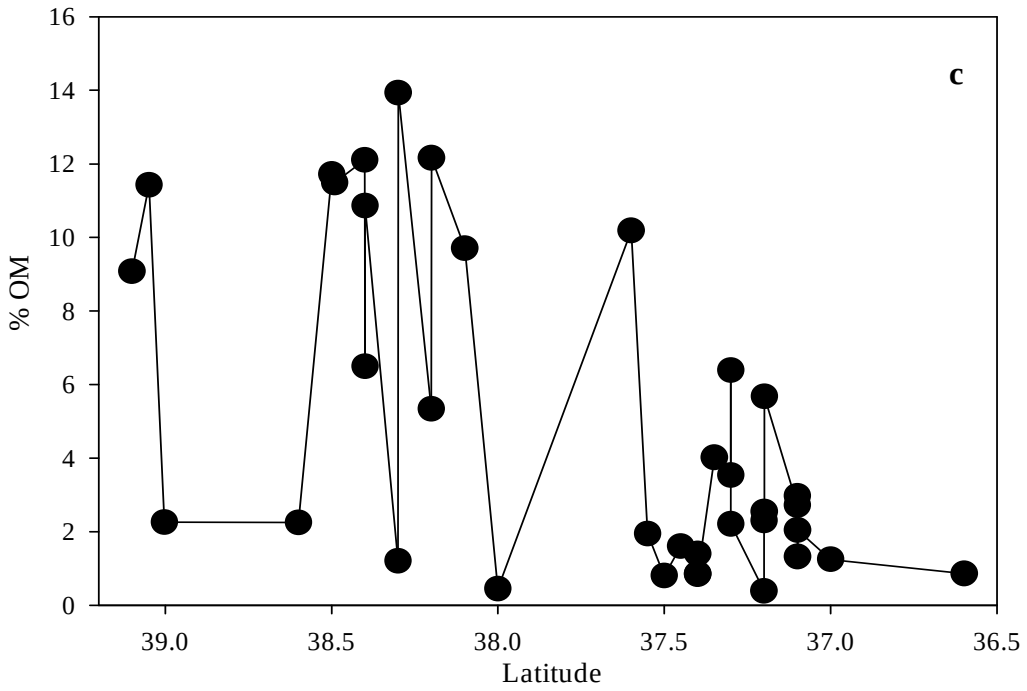
c
% OM
16
14
12
10
8
6
4
2
0
39.0
38.5
38.0
37.5
37.0
36.5
Latitude

Table 5.1. Correlation table for the mainstem of the Chesapeake Bay dataset.*

	Al	Fe	Mn	MeHg	THg	% OM
Al	-	0.71	0.40	0.45	0.56	0.74
Fe	0.71	-	0.50	0.31	0.79	0.64
Mn	0.40	0.50	-	0.21	0.32	0.26
MeHg	0.45	0.31	NS	-	0.29	0.61
THg	0.56	0.79	0.32	0.29	-	0.60
% OM	0.74	0.64	NS	0.61	0.60	-

* Regression values (r^2) are significant at $p < 0.01$. NS means 'not significant'.

Table 5.1 shows the correlations of THg, MeHg other metals, such as aluminum (Al), Fe, and Mn, as well as organic matter content that were found in samples collected from the Bay. In general, metal concentrations were significantly correlated to each other, suggesting an interaction or association of the oxide and organic matter phases. In comparison, however, the relationship between organic matter and Mn was weaker ($r^2 = 0.26$, $n = 36$). Given the much lower concentration of Mn relative to Fe and Al (data not shown), it is clear that these inorganic phases are more important than Mn in providing a substrate for organic matter coating, or for metal binding. It has been demonstrated that sediment organic matter can enhance the adsorption of metals to the solid phase relative to the pure oxide phases by the formation of tertiary complexes. The organic matter coats the Fe surface and the metals are complexed to the organic matter rather than directly to the oxide phases (e.g. Fe-OM-Hg). However, at high organic matter content in the porewater, the competition between the dissolved organic matter and the particulate organic matter for the metal can lead to a decrease in metal binding due to competitive binding to the dissolved ligands. However, as the distribution coefficient (K_d) for organic matter is 10-1000, typically,

for sediments, this interaction is unlikely to have a strong influence except for metals that bind strongly to organic matter, such as Hg.

There was no significant relationship between Hg and MeHg concentrations and AVS (data not shown). The AVS concentrations observed were < 0.5 μmole/g in most sites with some exceptionally higher concentrations in some locations (1.3 – 6.7 μmol/g). The lack of correlation between AVS and concentrations of Hg and MeHg is likely due to low AVS concentrations. There is a possibility that our AVS data could be affected by storage time. The AVS concentrations in other fresh and salt water systems ranged from 0.4 to 420 μmol/g (Hansen et al., 1996). Compared to our observation, Mason and Lawrence (1999) found higher AVS concentrations (1- 30 μmol/g) and a linear correlation between AVS and MeHg in Hart-Miller Island sediments. In Chapter 3 (Kim et al., submitted), the mesocosm experiments showed a broad range of AVS concentrations with sediment depths (0.03 to 130 μmol/g). In addition, AVS concentrations have shown a large vertical and temporal variability (Van den Berg et al., 1998). During summer, high sediment temperature and more freshly deposited, highly degradable organic matter result in more reducing environment and the boundary layer between the suboxic and the anoxic layer moves toward the sediment-water interface. As a result, the build-up of AVS was found closer to the sediment-water interface (Van den Berg et al., 1998). While Fe and organic matter concentrations do not vary significantly seasonally, AVS concentrations can vary with redox status and thus low AVS may reflect the season of collection. Given the high Fe and organic matter concentrations in the Chesapeake Bay sediments, there is sufficient binding capacity for Hg and MeHg even in the

absence of AVS. Thus, in this system, the influence of AVS on Hg and MeHg distribution in sediments could be less important than organic matter or Fe, although it is likely to impact the bioavailability of Hg and MeHg.

Fig. 5.4a presents the concentrations of THg and MeHg with % MeHg in HMI sediments. Organic matter was related to both MeHg ($r^2 = 0.57$, n = 11, $p < 0.01$) and THg ($r^2 = 0.91$, n = 11, $p < 0.01$). Average concentrations of THg and MeHg in HMI sediments were 790 ± 400 and 6.7 ± 3.9 pmol g^{-1}, respectively. Concentrations of Fe, Mn, Al, and AVS were not measured for the sampling time of 2000. Mason and Lawrence (1999) found a relationship between AVS and MeHg in HMI sediments collected in 1997, although the relationship was tenuous because it relied, to a large degree, on the one high data point. These authors suggested that *in situ* MeHg production might have not controlled the concentration in these surface sediments as MeHg production was likely inhibited due to high AVS concentrations.

Fig. 5.4b shows the concentrations of THg and MeHg with % MeHg in clams, *R. cuneata*, averaging 190 ± 70 (THg) and 18 ± 8.5 (MeHg) pmol g^{-1}, respectively. Similar MeHg concentration was found in clams (*Macoma*) collected from Baltimore Harbor where % carbon ranged from 0.2 to 3.5 (Mason and Lawrence, 1999). While THg concentration was comparable to the initial concentration in experiment 2 (overall average of 230 ± 57 pmol g^{-1}), MeHg in *R. cuneata* was much lower than that in *M. mercenaria* (overall average of 160 ± 37 pmol g^{-1}) (Chapter 3, submitted). Similarly, % MeHg in *R. cuneata* was lower (11 ± 6.7 %) than that in *M. mercenaria* (71 ± 12 %). MeHg typically accounts for 20-80 % of THg in invertebrates (Claisse et al., 2001). It has been shown that % MeHg in oysters and mussels collected in French

Coast ranged from 11 to 88 % (Claisse et al., 2001). Both species, *R. cuneata* and *M. mercenaria*, are suspension feeders (McConnell and Harrel, 1995; Grizzle et al., 2001) and feed on large quantities of detritus and phytoplankton, heterotrophic microorganisms in the water column (LaSalle and de la Cruz, 1985; Grizzle, 2001). *R. cuneata* is an estuarine species occurring where salinity varies between 1-18 ppt. However, the planktonic larval stage is more vulnerable to salinity and adult *R. cuneata* can be tolerant to freshwater or higher salinity water (Cain, 1975). In contrast, *M. mercenaria* behaviors (e.g. feeding rate, burrowing, growth, and survival of juveniles and adults) are affected negatively by salinities lower than 15 ppt. It should be noted that *M. mercenaria* was obtained from aqua farms and the initial concentration of MeHg, after their acclimation period (Chapter 3), was higher than MeHg in *R. cuneata* collected in the field. Thus, different habitat conditions for both species could account for the difference in MeHg burden.

BSAFs for MeHg and inorganic Hg (IHg) were calculated as the ratio between MeHg (IHg) concentration in the clam and MeHg (IHg) concentration in sediments. As discussed in Mason and Lawrence (1999), BSAF for inorganic Hg was calculated instead of BSAF for THg because % MeHg in sediment is typically lower (< 1 %) than that in invertebrate and vertebrate organisms (10 to 100 %). Thus, when BSAFs based on THg are compared to those for MeHg, this will lead to an overestimation of the bioaccumulation of IHg. As seen in Fig. 5.4c, it is clear that organic matter plays an important role in MeHg bioaccumulation. BSAF for MeHg decreased with increasing % OM in sediments. The BSAF values for *R. cuneata* were consistent with those found in the previous years (1996-1997) shown by Mason and Lawrence

(1999). Given that the clam is a suspension feeder, it could be expected that a relationship between BSAF and % OM may not be found. However, sediment resuspension is likely an explanation for this. HMI sampling sites are within the Chesapeake Bay ETM (Estuarine Turbidity Maximum Zone). The ETM is variably located between 39° 10′ and 39° 28′ N and usually extends 10 to 30 km along the N/S axis of the bay (Roman et al., 2001). Additionally, *R. cuneata* is a non-selective feeder (LaSalle and de la Cruz, 1985) and the clam likely feeds on resuspended particles.

As mentioned earlier, sediment organic content plays an important role in Hg methylation as it controls Hg distribution between particle and dissolved phases, resulting in determining Hg bioavailability to SRB. Hg methylaion was negatively correlated with K_d (Hammerschmidt and Fitzgerald, 2004). Thus, our observations give insight into the role of organic matter content in controlling Hg methylation and subsequent MeHg accumulation into benthic organisms. Additionally, sediment resuspension can play a role in not only changing redox state to favor Hg methylaion but also transporting elevated MeHg to the water column, leading to uptake MeHg into organisms, as discussed in Chapters 3 and 4.

Figure 5.4. The concentrations of THg and MeHg a) in HMI sediments; b) in clams, *R. cuneata* collected from the vicinity of HMI; c) bioaccumulation factors (BSAF) for clams (*R. cuneata*) collected from MHI for inorganic Hg and MeHg.

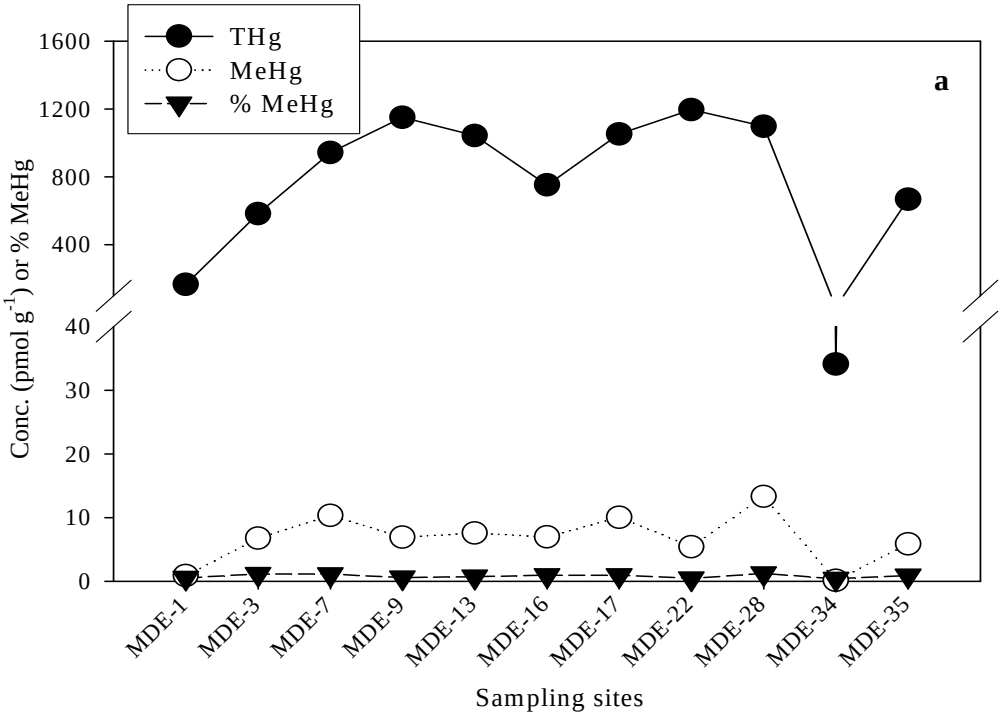
THg
MeHg
% MeHg
a
Conc. (pmol g-1) or % MeHg
1600
1200
800
400
40
30
20
10
0
MDE-1
MDE-3
MDE-7
MDE-9
MDE-13
MDE-16
MDE-17
MDE-22
MDE-28
MDE-34
MDE-35
Sampling sites

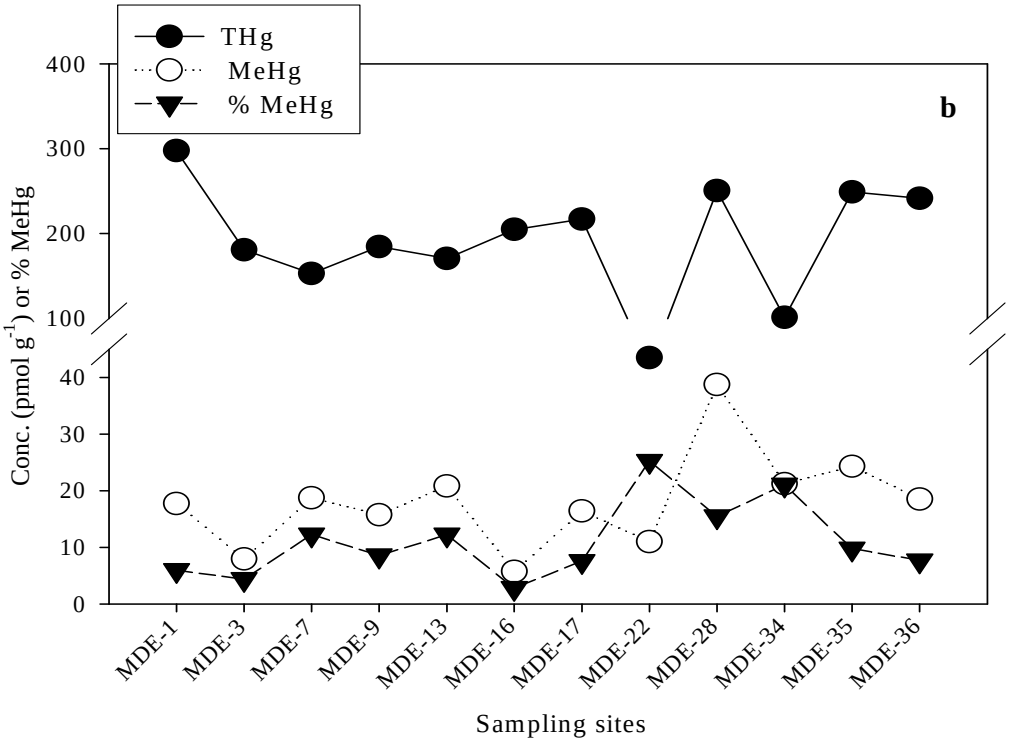
THg
MeHg
% MeHg
b
Conc. (pmol g-1) or % MeHg
400
300
200
100
40
30
20
10
0
MDE-1
MDE-3
MDE-7
MDE-9
MDE-13
MDE-16
MDE-17
MDE-22
MDE-28
MDE-34
MDE-35
MDE-36
Sampling sites

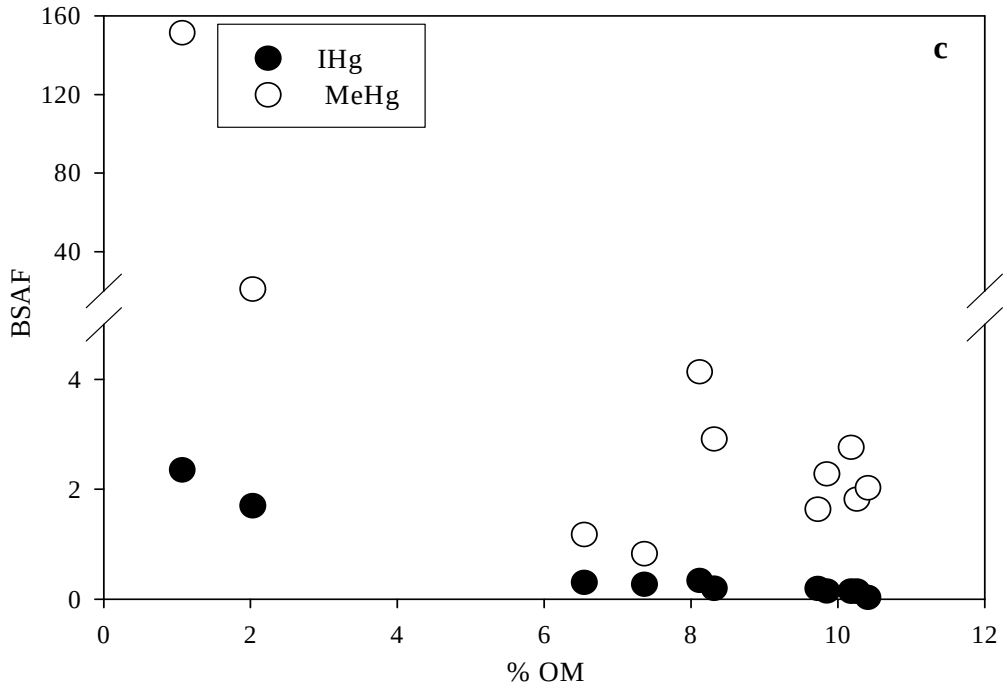
160
120
80
40
4
2
0
BSAF
IHg
MeHg
c
0
2
4
6
8
10
12
% OM

5.3.2 Modeling applications

5.3.2.1. Model results with a longer time simulation

Fig. 5.5 presents the model results of a longer time simulation with the same organic content and Hg methylation rate as the model developed in Chapter 4. A similar pattern was observed that PP biomass decreased from May to July between the observations (Fig. 5.2b) and the model output (Fig. 5.5a). However, the modeled PP biomass increased from July to September in response to increases in temperature and, more likely, nutrient concentration, followed by a substantial decrease in October. Meanwhile, the data showed a continuous decrease. The discrepancy is likely because ZP and FF are the only predators for PP in the model The structure of the community can be more complicated and variable in field situations. As seen in Fig. 5.2b, the PP data for the Bay have a relatively large standard deviation between the stations. Modeled ZP1 biomass remained relatively low throughout the model running time while model results of ZP2 showed an increase in accordance with an increase in PP biomass (Fig. 5.5a). As described in Chapter 4, the filtration rate for ZP2 was higher than that for ZP1 and, as a result, the response for ZP2 to increasing PP biomass was more immediate than ZP1. A time lag between the peaks in PP and ZP2 biomass was likely due to the difference in PP growth rate and ZP2 grazing rate, as mentioned in Chapter 4. It has been found that total zooplankton biomass in the mesohaline Chesapeake Bay is highest in March and October while lower in June and August (White and Roman, 1992). Thus, the model results showed a consistent pattern with the field data although the overall biomass was much lower than the field data. Zooplankton biomass was typically > 0.01 g C m^{-3} in the mesohaline

Chesapeake Bay (White and Roman, 1992). As seen in Fig. 5.5b, FF biomass decreased continuously and more substantially over time for a longer simulation time, compared to the model result in Chapter 4. MPB showed a similar pattern with PP in that changes in MPB biomass corresponded to changes in nutrient concentration (Fig. 5.5b).

Fig. 5.5c shows the modeled MeHg concentration in biota in the water column. The modeled MeHg concentration in PP was higher than the model results under the experiment 2 conditions in Chapter 4. MeHg concentration in ZP1 and ZP2 increased during the summer months when PP and ZP biomass were decreasing. MeHg burden in ZP was similar to that in the model simulation for experiment 3. As discussed in Chapter 4, low biomass of ZP results in higher MeHg burden in ZP. The concentration of dissolved MeHg was somewhat higher than the model result (experiment 2) in Chapter 4 but the difference was about a factor of two or less (Fig. 5e and Fig.3d in Chapter 4). Thus, the increase of MeHg burden in ZP was more likely due to the substantial decrease in ZP biomass during the summer months when PP biomass also decreased, which was a similar case for the model results (especially the later stage of the model run) under the experiment 3 condition (Fig. 5 in Chapter 4). In fact, the modeled ZP biomass in both cases was much lower than the field data in the Chesapeake Bay, as mentioned above, and other estuarine environments (Froneman, 2000).

MeHg concentration in copepods collected from the mid bay (around 38 º N) was lower in April than August of 1997, averaging 39 and 130 pmol g C^{-1}, respectively (Leaner, unpublished data). However, it is not clear weather higher

MeHg burden in ZP in April was related to lower ZP biomass at that time due to limited data. Dissolved MeHg concentration in the same sampling stations where ZP measurements were made averaged 0.09 and 0.04 pM in April and August of 1997, respectively (Leaner, unpublished data). Thus, given the lower concentration of dissolved MeHg and the findings that ZP biomass was typically lower in summer, higher MeHg burden in ZP in August may be likely attributed to low ZP biomass. Nonetheless, MeHg in ZP from the mesohaline bay (Leaner, unpublished data) was comparable to the data from experiment 2 as well as the model result in Chapter 4. MeHg burden in FF and MPB showed an opposite trend to their biomass (Fig. 5.5d). BSAF for FF in the model was obtained using a similar approach with BSAF for the clam, *R. cuneata*. The BSAF for FF in the model was 5.0, which was in the same order but slightly higher than BSAF values for *R. cuneata* at high organic matter content in sediments (12 %). As mentioned earlier, it is likely due to much higher MeHg concentration in FF (*M. mercenaria* in the model) than that in *R. cuneata*.

Fig. 5.5e presents the modeled MeHg concentrations in particulate and dissolved phases, which were in a similar range of the previous model results (Fig. 5.3c and d in Chapter 4). On average, particles in the water column were mostly RPOC (36 %) and WPOC (51 %), accounting for 13 % PP and ZP. In the previous model (Chapter 4), particles in the water column consisted of 49 % RPOC, 42 % WPOC, and 9 % PP and ZP. Percent RPOC in this model run was less than that in the previous one. It is likely that lower TSS concentration from the field data was applied to this model, compared to the previous model with higher TSS concentration. As mentioned in Chapter 4, water column particles included different particle types and MeHg on particles

presented here was normalized to the total particle concentration (MeHg pmol per Σ g C), not normalized to concentrations of each particle type. Total MeHg in the water column (particulate + dissolved MeHg) of the model was 0.3 pM and this was comparable to the average total MeHg, 0.3 ± 0.3 pM, found in the mainstem Chesapeake Bay (Mason et al., 1999).

The modeled dissolved MeHg increased in response to decreasing PP and MPB biomass during the summer months, as the dissolved MeHg was taken up by PP and MPB to a larger degree than ZP or FF. As mentioned in Chapter 4, resuspension can play a role in transferring sediment MeHg to the water column and in subsequent MeHg accumulation into benthic-pelagic organisms. When there was no sediment resuspension in the model (by shutting down all the flows in/out of the RPOC and MeHg in RPOC pools), the overall average concentration of dissolved MeHg decreased by about 70 %. A similar reduction (about 62 – 73 %) of MeHg burden in biota (PP, ZP1, ZP2, and MPB) was found while the effect was much less for FF (about 2 % decrease). This provides insight into why MeHg concentration in biota, especially the upper levels of food chains remains high even though Hg loadings to environments may be reduced. Sediment resuspension can play a role in reintroducing MeHg in sediments to the water column and food chains, as suggested by others (Sunderland et al., 2004; Sager, 2002).

Figure 5.5. Model outputs: a) biomass in the water column; b) biomass in the sediment; c) MeHg in water column biota; d) MeHg in benthic biota; e) particulate and dissolved MeHg in the water column.

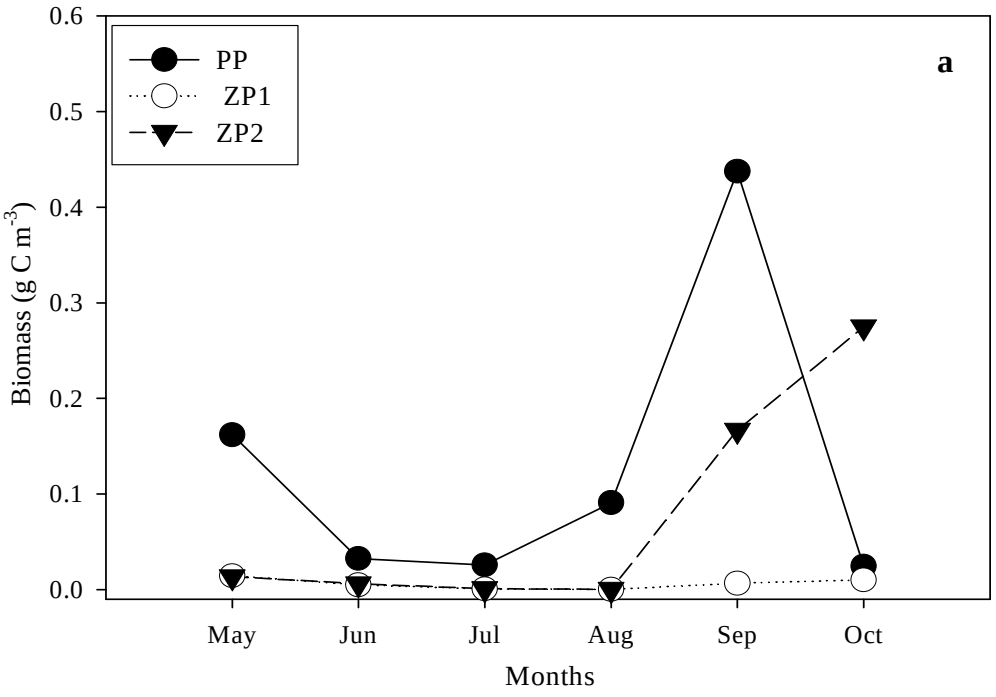
PP
ZP1
ZP2
a
Biomass (g C m-3)
0.6
0.5
0.4
0.3
0.2
0.1
0.0
May
Jun
Jul
Aug
Sep
Oct
Months

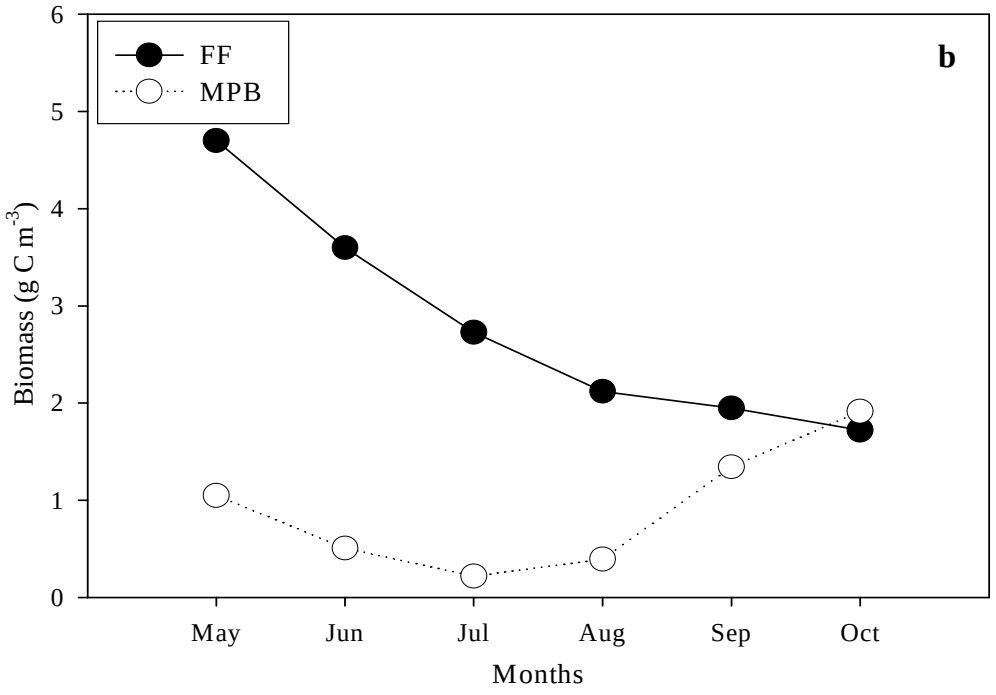
FF
MPB
b
Biomass (g C m-3)
6
5
4
3
2
1
0
May
Jun
Jul
Aug
Sep
Oct
Months

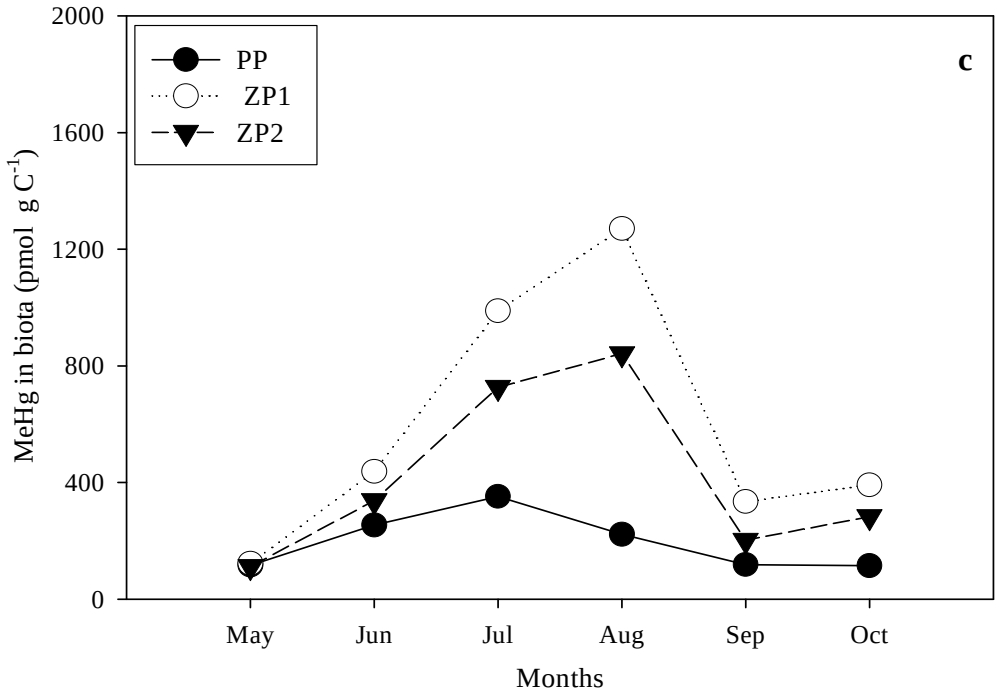
c
PP
ZP1
ZP2
MeHg in biota (pmol g C-1)
2000
1600
1200
800
400
0
May
Jun
Jul
Aug
Sep
Oct
Months

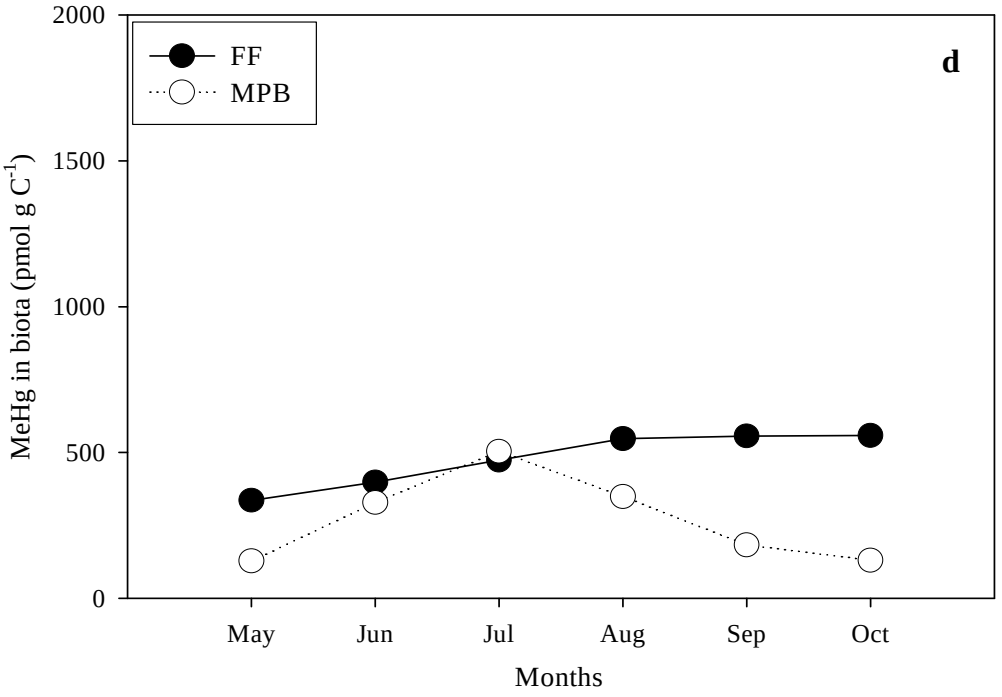
d
FF
MPB
MeHg in biota (pmol g C-1)
2000
1500
1000
500
0
May
Jun
Jul
Aug
Sep
Oct
Months

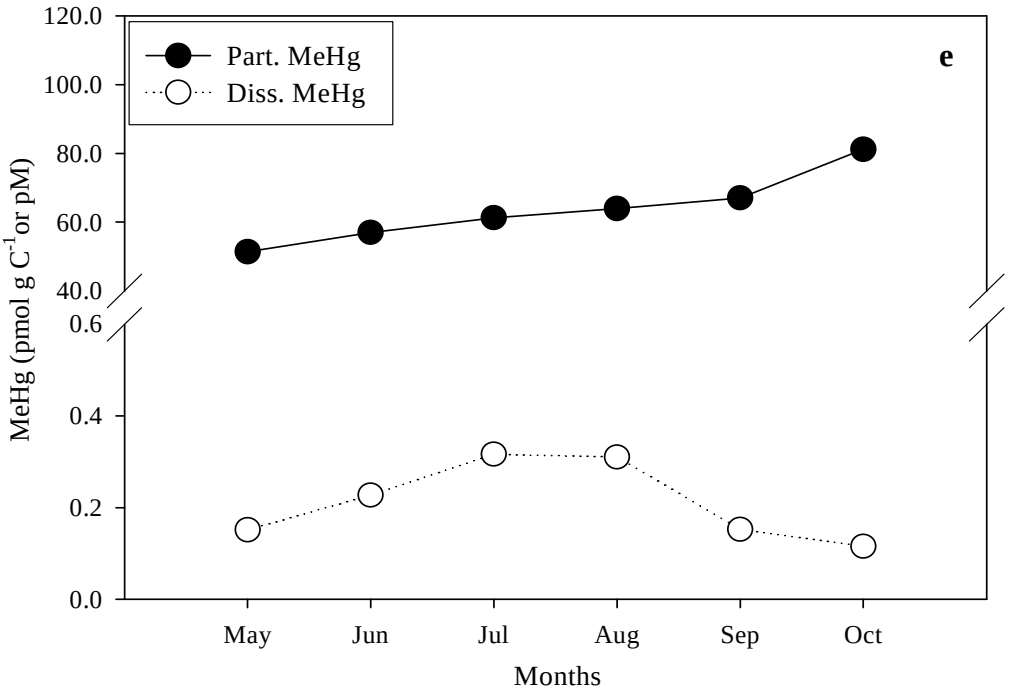
120.0
100.0
80.0
60.0
40.0
0.6
0.4
0.2
0.0
Part. MeHg
Diss. MeHg
e
MeHg (pmol g C-1 or pM)
May
Jun
Jul
Aug
Sep
Oct
Months

5.3.2.2. Effects of sediment organic matter and Hg methylation on MeHg burden in biota

In this section, the model was applied under conditions of varied sediment organic matter. This influenced both the concentration of THg and MeHg and the corresponding Hg methylaion. As mentioned earlier, it has been found that Hg methylation varied inversely with % organic matter (Hammerschmidt and Fitzgerald, 2004) and, as discussed above, THg and MeHg were found to increase with increasing % OM. As seen in Fig. 5.6a, the resulting sediment MeHg was lowest at 12 % organic matter content with an overall average of 22 pmol g C^{-1}. MeHg concentration in sediments averaged 61 and 84 pmol g C^{-1} at 6 % organic matter and 3 % organic matter, respectively. The model result clearly showed an increase in sediment MeHg per g C as % organic matter decreased. Similarly, particulate MeHg in the water column increased with decreasing % organic matter (Fig. 5.6b). MeHg concentration on particles presented in Fig. 5.6b was normalized to the total particle concentrations, as done previously. Overall, water column particles consisted of 36 % RPOC, 51 % WPOC, and 8 % PP, and 5 % ZP, on average and the proportions were relatively constant, regardless of changes in sediment organic matter content. While MeHg on RPOC was comparable to MeHg concentration in sediments, MeHg on particles per Σ g C in the water column appeared to be lower than sediment MeHg. The ratios between MeHg on particles in the water column and sediment MeHg were 0.67, 0.69, and 0.81 at 3 %, 6 %, and 12 % organic matter, respectively. A similar pattern was observed for dissolved MeHg in the water column (Fig. 5.6c), averaging 0.19, 0.14, and 0.07 pM at 3 %, 6 %, and 12 % organic matter content.

Figure 5.6. Model outputs: a) MeHg in the sediment; b) particulate MeHg in the water column; c) dissolved MeHg in the water column with changes in sediment organic matter.

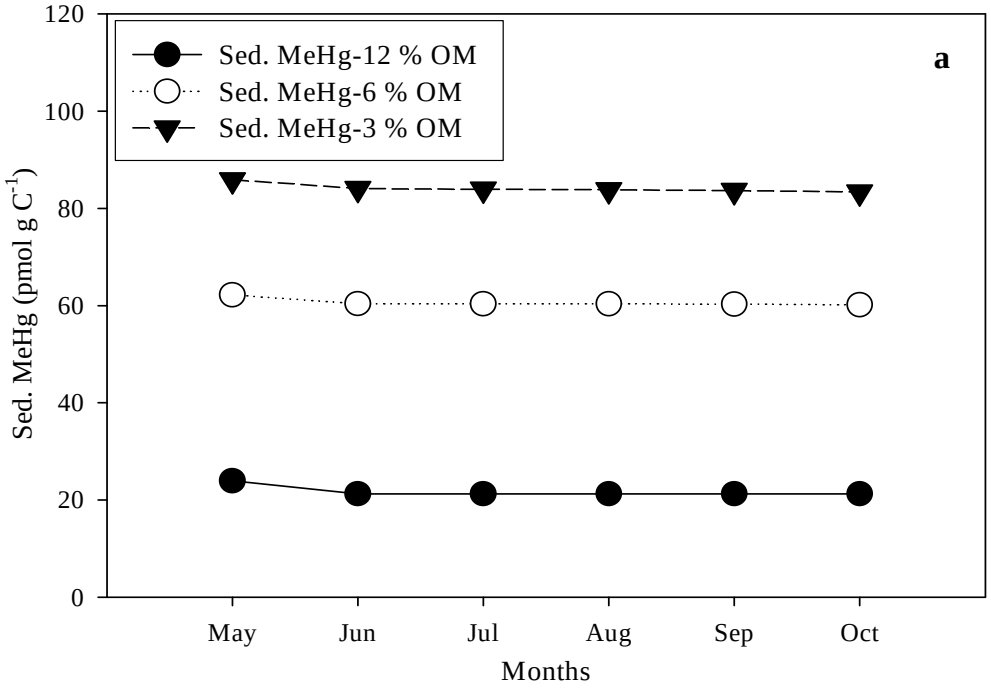
Sed. MeHg-12 % OM
Sed. MeHg-6 % OM
Sed. MeHg-3 % OM
a
Sed. MeHg (pmol g C-1)
120
100
80
60
40
20
0
May
Jun
Jul
Aug
Sep
Oct
Months

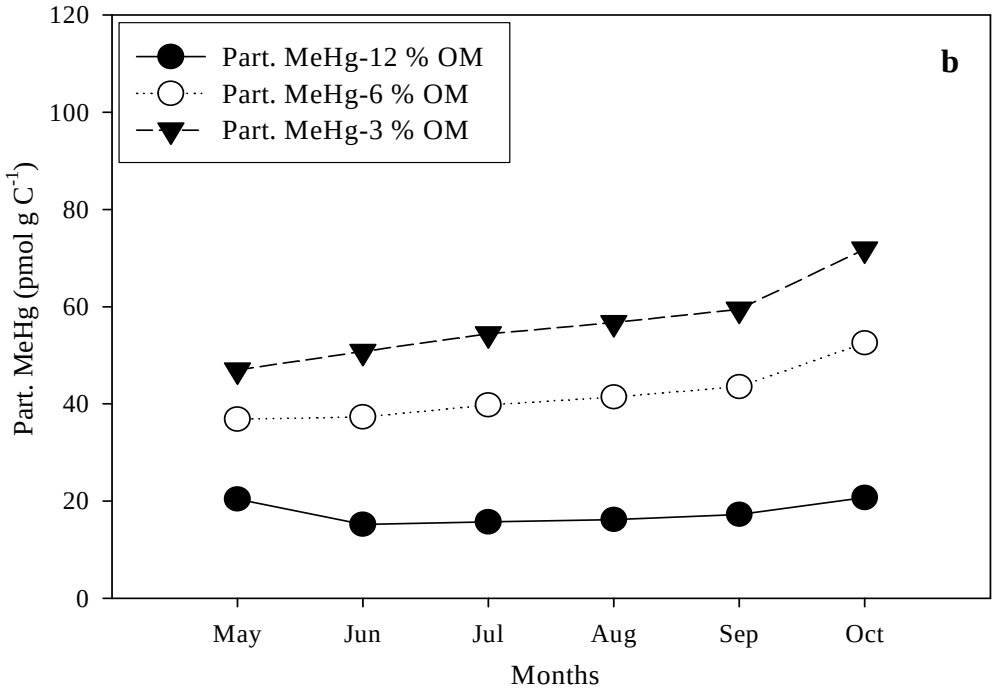
Part. MeHg-12 % OM
Part. MeHg-6 % OM
Part. MeHg-3 % OM
b
Part. MeHg (pmol g C-1)
120
100
80
60
40
20
0
May
Jun
Jul
Aug
Sep
Oct
Months

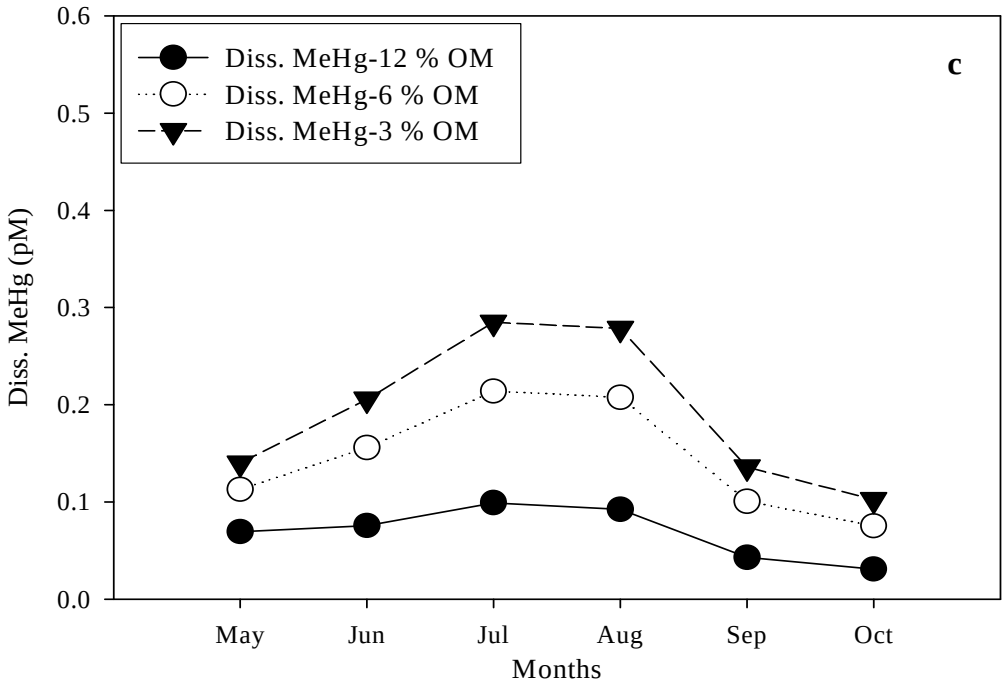
Diss. MeHg-12 % OM
Diss. MeHg-6 % OM
Diss. MeHg-3 % OM
c
Diss. MeHg (pM)
0.0
0.1
0.2
0.3
0.4
0.5
0.6
May
Jun
Jul
Aug
Sep
Oct
Months

MeHg burden in biota was influenced by changes in organic matter and the subsequent Hg methylation (Fig. 5.7). However, biomass did not change upon sediment organic matter. MeHg concentration in PP, overall, averaged 67, 140, and 180 pmol g C^{-1} at 12 %, 6 %, and 3 % organic matter, respectively (Fig. 5.7a). A similar trend was observed for ZP that MeHg burden increased with decreasing % organic matter (Fig. 5.6b,c), averaging 240, 430, and 540 pmol g C^{-1} for ZP1 and 170, 300, and 380 pmol g C^{-1} for ZP2 at 12 %, 6 %, and 3 % organic matter, respectively. The model results were somewhat higher than MeHg in ZP found from the mid bay in April, as stated above, but these concentrations were of the same order of magnitude. Overall average MeHg in FF was 360, 420, and 460 pmol g C^{-1} at 12 %, 6 %, and 3 % organic matter, respectively (Fig. 5.7d). The modeled MeHg concentration in FF was quite higher than observed in MeHg in *R. cuneata* collected from HMI sites. However, the initial concentration used in the model was based on the measurement of *M. mercenaria* in experiment 2 (Chapter 3, submitted). Thus, the model result could have been comparable to MeHg concentration in *R. cuneata*, if the initial concentration for *R. cuneata* used and other parameters were kept the same. MeHg burden in MPB was similar to that in PP, averaging 91, 190, and 250 pmol g C^{-1} at 12 %, 6 %, and 3 % organic matter (Fig. 5.7e).

Studies have shown that *in situ* production in sediments is a significant source of MeHg in estuarine environments (Mason et al., 1999; Hammerschmidt et al., 2004; Sunderland et al., 2004). Similarly, a preliminary mass balance for the mesocosm experiments showed that *in situ* MeHg production occurred and this was confirmed by the Hg methylation experiments (Chapter 2, Kim et al., 2004; Chapter 3,

submitted). Sager (2002) has suggested that continued Hg release, resuspension and/or bioturbation of buried sediments with enhanced Hg contributed to elevated Hg levels in the higher trophic organisms. Similarly, it was determined that most MeHg concentration in PP of Long Island Sound was likely attributed to sedimentary flux and this could contribute to MeHg accumulation in higher trophic levels (Hammerschmidt et al., 2004). The modeling study with varying organic matter and the subsequent MeHg production demonstrated that the enhanced MeHg was transported to the water column by sediment resuspension, resulting in higher biotic MeHg burden in organisms mainly through dietary uptake.

5.4. Summary

Organic matter content played an important role in the distribution of Hg and MeHg in surface sediments as well as bioaccumulation into biota. The SBAF values for MeHg and IHg varied inversely with sediment organic matter. The model results with a longer simulation time appeared to be in agreement with the field data. The modeling studies demonstrated that MeHg levels in sediments were closely related to varying organic matter content, as organic matter was an important controlling factor in Hg methylation. The enhanced MeHg can be transferred to the water column by sediment resuspension. Thus, higher MeHg burden in benthic-pelagic organisms can be attributed to enhanced MeHg in sediment.

Figure 5.7. Model outputs: a) MeHg in PP; b) MeHg in ZP1; c) MeHg in ZP2; d) MeHg in FF; e) MeHg in MPB with changes in sediment organic matter.

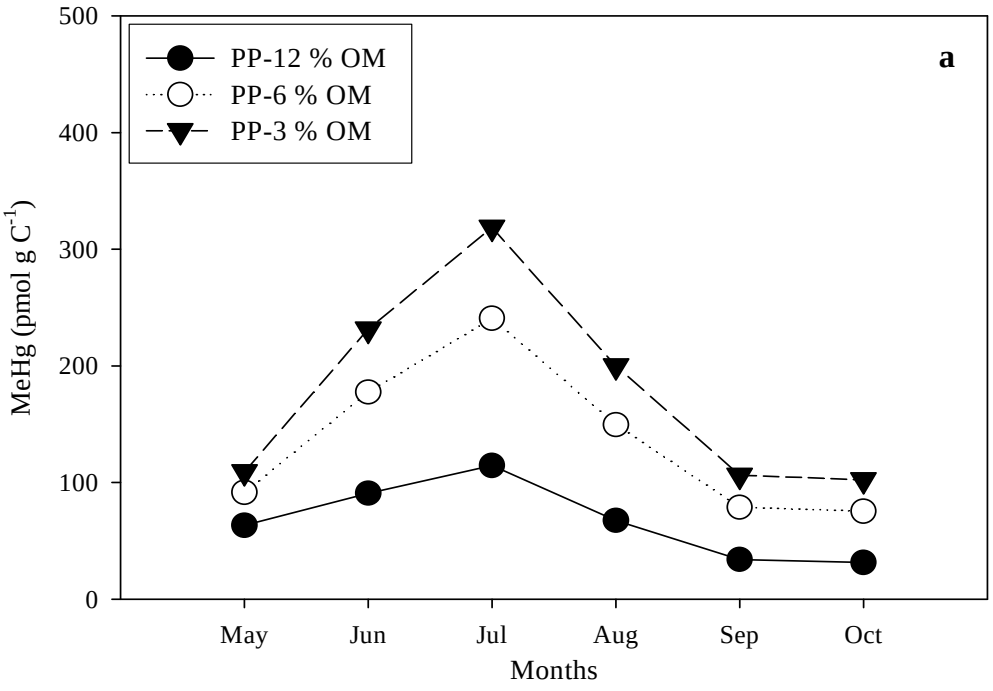
PP-12 % OM
PP-6 % OM
PP-3 % OM
a
MeHg (pmol g C-1)
500
400
300
200
100
0
May
Jun
Jul
Aug
Sep
Oct
Months

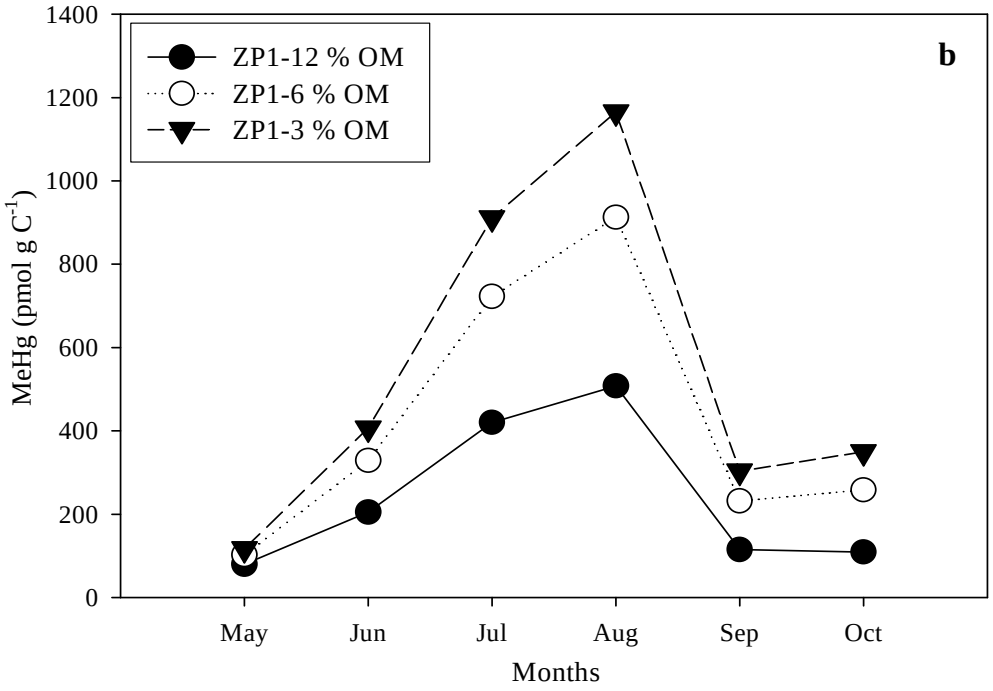
ZP1-12 % OM
ZP1-6 % OM
ZP1-3 % OM
b
MeHg (pmol g C-1)
1400
1200
1000
800
600
400
200
0
May
Jun
Jul
Aug
Sep
Oct
Months

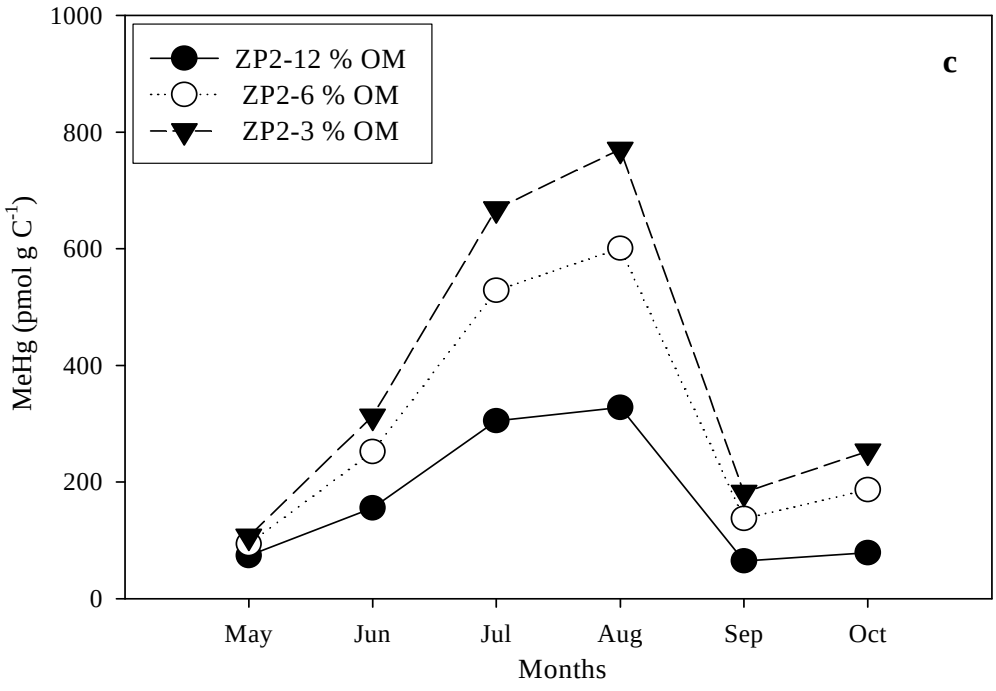
ZP2-12 % OM
ZP2-6 % OM
ZP2-3 % OM
c
MeHg (pmol g C-1)
1000
800
600
400
200
0
May
Jun
Jul
Aug
Sep
Oct
Months

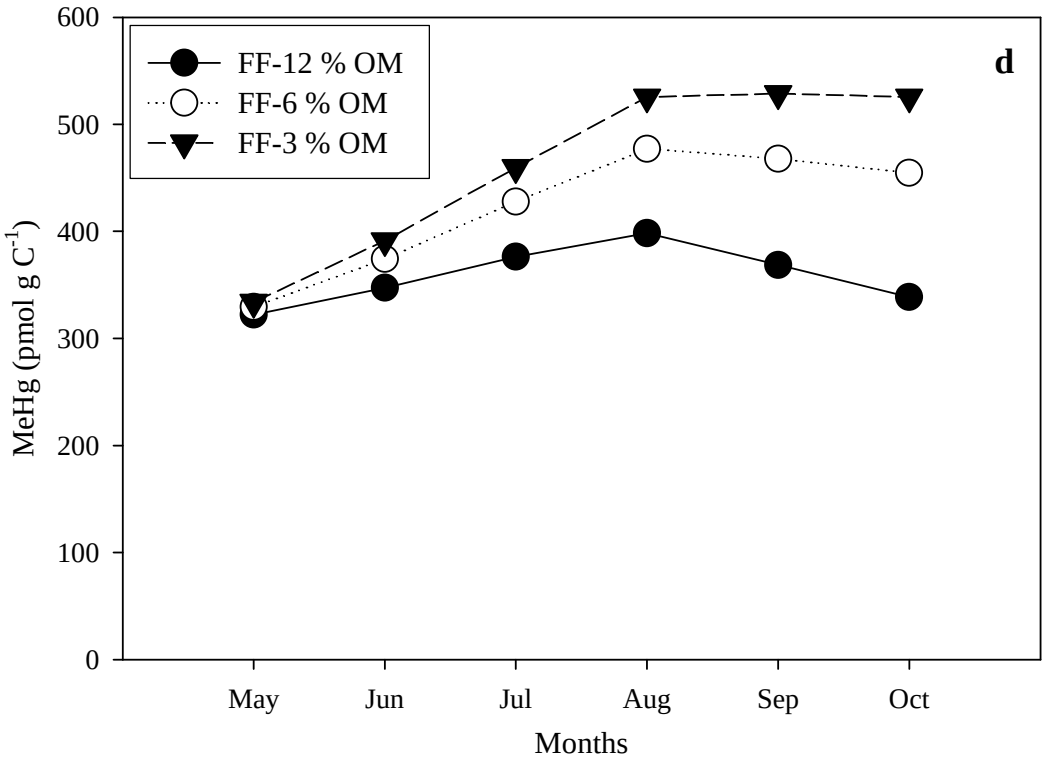
FF-12 % OM
FF-6 % OM
FF-3 % OM
d
MeHg (pmol g C-1)
600
500
400
300
200
100
0
May
Jun
Jul
Aug
Sep
Oct
Months

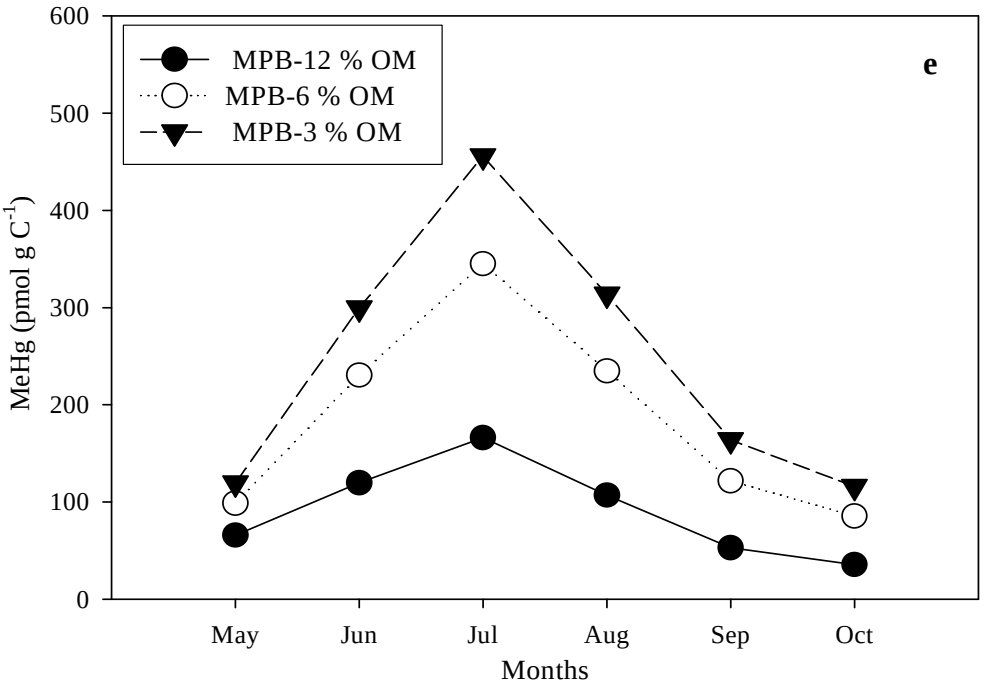
MPB-12 % OM
MPB-6 % OM
MPB-3 % OM
e
MeHg (pmol g C-1)
600
500
400
300
200
100
0
May
Jun
Jul
Aug
Sep
Oct
Months

Chapter 6: Summary, conclusions, and recommendations

6.1. Summary

The contamination of mercury (Hg) in estuaries is a concern as most estuarine and coastal environments are in close proximity to urban centers. Additionally, estuaries are productive ecosystems and provide an important food source for humans as well as being nursery areas for young fish (Benoit et al., 1998; Mason et al., 1999). Sediments are the major repository of Hg in estuarine environments and only a small fraction of the Hg transported in rivers is exported to the ocean due to the high retention of Hg in estuaries (Cossa et al., 1996; Benoit et al., 1998; Mason et al., 1999). Hg can be transformed to methyl mercury (MeHg) in anaerobic conditions by sulfate reducing bacteria (SRB), the principal mediators of Hg methylation (Gilmour and Henry, 1992). Hg in sediments constitutes an enriched pool potentially available to organisms. Interest in bioaccumulation of Hg and MeHg into lower trophic levels of benthic and pelagic organisms stems from public health concerns as these organisms provide essential links for higher trophic levels of food chains such as fish and larger invertebrates. Fish consumption is the major exposure route of MeHg to humans (Clarkson, 1990).

The mobility and bioavailability of Hg and MeHg is controlled by the nature and concentration of the binding phases in sediments. Hg associates with particulate

organic matter and iron (Fe)/manganese (Mn) oxides through adsorption and coprecipitation reactions in oxidized sediments. In contrast, Hg is adsorbed onto and coprecipitated with sulfide minerals in anoxic conditions (Gobeil and Cossa, 1993; Gagnon et al., 1997; Wang et al., 1998). When metal oxides are reduced Hg can be released into the porewater (or eventually to the overlying water via diffusion) or can be removed by adsorption and coprecipitation with sulfide minerals in anoxic environments. Additionally, Hg can be released as a result of the microbial degradation of organic matter and by chemical dissolution of sulfides due to redox changes during diagenesis.

Sediment resuspension plays an important role in reintroducing metals into the water column and in the cycling of particles and associated nutrients and contaminants at the sediment-water interface (Bloesch, 1995). It has shown that sulfide-associated trace metals could be a more bioavailable phase following a major oxidation event such as that caused by dredging, resuspension, and seasonal migration of the redoxcline (Copper and Morse, 1996). Sediment resuspension can be an important factor in controlling Hg methylation in sediments as resuspension can induce a change in sediment redox state. Recent studies have shown that *in situ* MeHg production is a significant source to estuarine environments (Mason et al, 1999; Sunderland et al., 2004; Hammerschmidt and Fitzgerald, 2004; Balcom et al., 2004). There is, however, a paucity of information on the effects of sediment resuspension on the fate, transport, and bioaccumulation of Hg and MeHg.

This dissertation research was, therefore, aimed at investigating a) direct and indirect effects of sediment resuspension in shallow systems on the fate, transport,

and bioavailability of Hg and MeHg; b) the importance of the various geochemical factors in contributing to the fate and bioavailability of Hg and MeHg. A model for MeHg bioaccumulation into benthic invertebrates was developed and tested using the results from these studies.

Two 4-week STORM experiments were conducted in July and October of 2001 (experiments 1 and 2) with two treatments of resuspension (R) and no-resuspension (NR) (Chapters 2 and 3). A bioenergetic-based model was used to study MeHg transport between the water column and the sediment as well as MeHg bioaccumulation into benthic and pelagic organisms in representative shallow estuarine environments (Chapter 4). The model was applied to field situations to assess the role of sediment resuspension with varying sediment organic matter and the resulting Hg methylaion on MeHg accumulation into benthic and pelagic organisms (Chapter 5). Additionally, this research examined the spatial distribution of Hg and MeHg in sediments from the mainstem Chesapeake Bay and the importance of controlling factors in determining Hg and MeHg concentrations and their bioaccumulation (Chapter 5).

The results of mesocosm experiments in Chapter 2 showed that sediment resuspension introduced significant amounts of particulate total Hg (THg) to the water column as total suspended solids (TSS) increased. THg was strongly bound to the sediment particles and cycled between the water column and sediments, with little release during resuspension. In contrast, particulate MeHg was significantly lower in the R tanks, compared to particulate MeHg in the NR tanks. The introduction of a large amount of sediment particles containing lower MeHg concentration was likely

attributed to the lower MeHg concentration on particles in the water column with resuspension. Dissolved THg and MeHg concentrations did not vary in response to changes in particulate load, suggesting that the dissolved and particulate phases for both THg and MeHg cannot be explained solely by equilibrium partitioning, on a resuspension time basis in the experiments.

A mass balance based on the mesocosm experiments (Chapter 2) suggested that resuspension could enhance MeHg production. Sediment oxygenation resulting from resuspension can reduce sulfide levels in surface sediment and in the porewater and thus stimulate Hg methylation by enhancing Hg bioavailability to SRB, as proposed by Benoit et al. (1999a). The results of mesocosm experiments showed that sediment resuspension had a complex effect on the association of Hg with binding phases as well as Hg methylation and demethylation in surface sediments (Chapter 3). The results in experiment 1 showed that *in situ* MeHg production was inversely related to acid volatile sulfide (AVS) concentration, especially in the top sediment layers and MeHg production was likely enhanced by resuspension. However, the results in experiment 2 showed a less clear relationship between AVS and MeHg production, suggesting that while some sediment oxidation may lower sulfide levels and enhance Hg methylation, too much oxidation may hinder bacterial activity. Demethylation experiments gave a consistent relative comparison between experiment 1 and 2 as well as showed less variability between the R and NR tanks. Demethylation rates were relatively lower in the top sediment layers and remained fairly constant in deeper layers.

The two experiments indicated that resuspension influenced system productivity and bioaccumulation indirectly (Chapters 2 and 3). Chl *a* concentration was significantly higher in the R tanks, compared to the NR tanks, which appeared to be counter-intuitive to expectation. Other studies have shown that planktonic microbial growth was stimulated by sediment resuspension (Wainright. 1987; Wainright, 1990). Zooplankton biomass (> 63 µm) was, overall, somewhat higher in the NR tanks, compared to the R tanks (Appendix I). In general, MeHg burden in zooplankton showed an increase over the course of experiment 2 and was slightly higher in the R tanks than the NR tanks (Chapter 3). MeHg concentration in phytoplankton was estimated based on Chl *a* data and some reasonable assumptions about phytoplankton size and growth rate (Mason et al., 1996) and ranged from 5 to 30 pmol g^{-1} for both R and NR tanks. Given that dissolved MeHg concentration and MeHg concentration in phytoplankton were comparable between the two systems (R and NR), the results suggested that higher MeHg burden in zooplankton in the R tanks was likely attributed to lower zooplankton biomass. The modeling study confirmed that increasing biomass resulted in a decrease in MeHg burden in biota (dilution effect) (Chapter 4), as proposed by Ashley (1998).

The model further examined what factors control planktonic biomass and MeHg accumulation into biota. The results of model sensitivity analysis showed that overall biomass and MeHg burden in biota were highly sensitive to varying phytoplankton production and the filtration of filter feeders, whose biomass was dominant in the system. The model demonstrated that changes in filter feeder biomass had a significant effect on phytoplankton biomass (Chapter 4). As filter feeder biomass

increased, phytoplankton biomass was significantly reduced. Changes in filter feeder biomass appeared to have an influence on zooplankton biomass. However, it was likely an indirect effect due to limited food because phytoplankton became more available to zooplankton as filter feeder biomass decreased. Despite a great impact of filter feeder biomass on planktonic biomass, MeHg burden in phytoplankton and zooplankton were affected by changes in filter feeder biomass to a lesser degree. MeHg burden in phytoplankton was governed more directly by dissolved MeHg uptake rate and phytoplankton growth. A similar pattern was observed for zooplankton.

As shown in Chapter 5, THg and MeHg concentrations were significantly related to organic matter content in sediments from the mainstem Chesapeake Bay. The overall AVS concentration was low and there was no correlation found between AVS and levels of THg and MeHg. Hammerschmidt and Fitzgerald (2004) showed that methylation potential was inversely related to varying organic matter content of surface sediment in Long Island Sound, a large coastal embayment in the northeastern US. The model results demonstrated that increasing Hg methylation resulted in higher MeHg burden in biota (Chapter 4). Thus, the model was applied to situations of varying organic matter and associated changes in Hg methylation to investigate how organic matter content and the resulting MeHg production affect MeHg burden in benthic and pelagic organisms (Chapter 5). The model results showed that the elevated MeHg was transported to the water column by resuspension and resulted in higher dissolved MeHg and subsequently in higher MeHg burden in biota even though the desorption rate was the same. The model studies clearly demonstrated that

increasing MeHg accumulation into benthic and pelagic organisms could be attributed to the enhanced MeHg production in sediments, as suggested by others (Hammerschmidt et al., 2004; Sager, 2002; Sunderland et al., 2004).

6.2. Conclusions

The dissertation research can draw the following conclusions:

1) Sediment resuspension has complex effects on system productivity and Hg and MeHg dynamics through direct and indirect interactions;
2) Sediment resuspension plays a significant role in transferring sediment MeHg to the water column, resulting in increasing MeHg bioaccumulation into benthic and pelagic organisms;
3) Organic matter content is an important factor in controlling the distribution of Hg and MeHg in surface sediments as well as their bioaccumulation into biota; and
4) System productivity is an important variable in determining MeHg bioaccumulation in shallow ecosystems.

It was hypothesized that resuspension would decrease MeHg sediment concentration through a series of direct and indirect interactions but increase MeHg flux at the sediment-water interface. However, the STORM experiment results showed that sediment resuspension had a complex effect on the association of Hg with binding phases and on *in situ* MeHg production. Additionally, other controlling factors (e.g.

temperature differences and organic matter content) can play a role in either decreasing or increasing MeHg concentration in sediments. The STORM experiments and modeling efforts clearly supported that resuspension could lead to an enhancement of MeHg accumulation into higher trophic level organisms.

6.3. Implications and recommendations for future study

The modeling studies gave intriguing results that sediment resuspension could play an important role in transporting the elevated MeHg to the water column and resulting in higher MeHg burden in biota. However, the model was developed to mimic experiment 2 conditions which did not include benthic deposit feeders and higher trophic level organisms. Additionally, bioturbation effects on *in situ* MeHg production need to be included. There have been evidence that bioturbation can increase Hg methylation in sediments (Hammerschmidt et al., 2004; Benoit et al., 2004). Impacts of Hg methylation on THg and MeHg bioaccumulation into deposit feeders can be critical as they are potentially exposed to THg and MeHg from both the porewater/overlying water and the sediments (solid phase).

In the model, the methylation rate was a function of THg concentration and the methylation rate, which was used as a constant. Although MeHg demethylation varied depending on a sediment MeHg pool, the demethylation rate was also used as a constant. As environmental factors such as temperature can play a role in controlling microbial activity involved in Hg methylation and MeHg demethylation, a better parameterization of both methylation and demethylation rates is necessary,

especially for a longer time of a model simulation. In the model applications, the effects of sulfide levels on Hg methylation were not included but the extension of the model to include such interactions would improve the predictive power of the model. Organic matter content in sediments was the principal control on MeHg production in low sulfide sediments (Hammerschmidt and Fitzgerald, 2004). However, the effects of sulfide may be as important as organic content in high sulfide sediments.

The modeling study gives insight into some potentialmanagement concerns. Firstly, the invasion of foreign species of filter feeder has been observed in many estuarine environments (Cope et al., 1997; Descy et al., 2003). Thus, these invaders likely influence phytoplankton productivity as well as may serve as an essential link in the trophic transfer of contaminants such as MeHg into the higher trophic levels of organisms. Secondly, changes in nutrient loadings could affect MeHg production by controlling the bioavailability of Hg in the sediment. Reduction in nutrient loadings could inadvertently lead to an enhancement of MeHg concentration in the sediments, as suggested by Hammerschmidt and Fitzgerald (2004).

The overall results of this research showed a significance of physical mixing and geochemical factors in biogeochemical cycling and bioaccumulation of Hg and MeHg within shallow estuarine environments. For sediment management aspects, the results can provide useful insight into THg and MeHg mobilization, sedimentary MeHg production, and bioaccumulation of THg and MeHg into benthic and pelagic organisms. In addition, this research helps understand the links between high MeHg concentration in organisms, system productivity and *in situ* MeHg production in sediments.

Appendices

List of appendices

Appendix I

There are four STORM experiments (experiment 1-4). Experiment 1 was conducted in July of 2001 without clams (R vs NR) and experiment 2 with clams (RC vs NRC) in October of 2001. Experiment 3 was conducted in July of 2002 with clams and without clams (RC vs RNC). Experiment 4 was performed in July of 2003 with high density clams (RHC) and low density clams (RLC). Experiments 3 and 4 were aimed at examining effects of clams on plankton as well as Hg cycling with resuspension. This dissertation is mostly focused on the first two experiments (experiments1 and 2). Details of experiments 3 and 4 will be in Christine Bergeron's MS dissertation. This appendix presents some of data from all the experiments in order to help understand ecological effects of clams on plankton biomass with/without resuspension. Phytoplankton (PP) biomass was obtained from Chl *a* data and the ratio between Chl *a* and carbon content, as stated in Chapter 4. Both phytoplankton and zooplankton (ZP) biomass are normalized to particulate organic matter (POM) in the water column.

Figure A. Average ratios of PP and POM (mg mg^{-1}): a) experiment 1; b) experiment 2; c) experiment 3; d) experiment 4. Error bars show standard deviations of 3 replicates in each system.

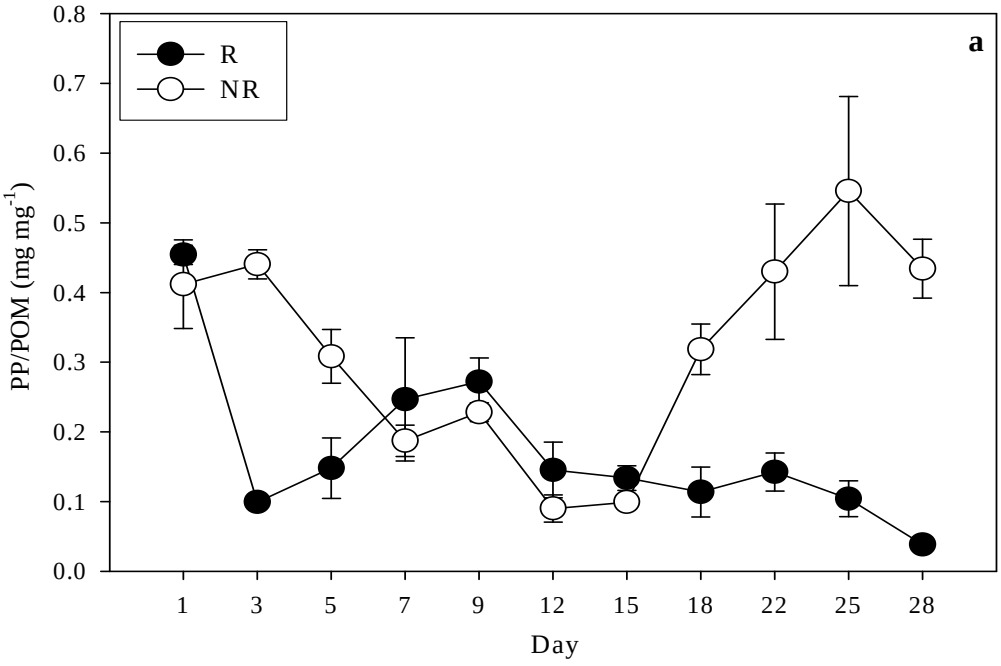
a
R
NR
PP/POM (mg mg-1)
0.0
0.1
0.2
0.3
0.4
0.5
0.6
0.7
0.8
1
3
5
7
9
12
15
18
22
25
28
Day

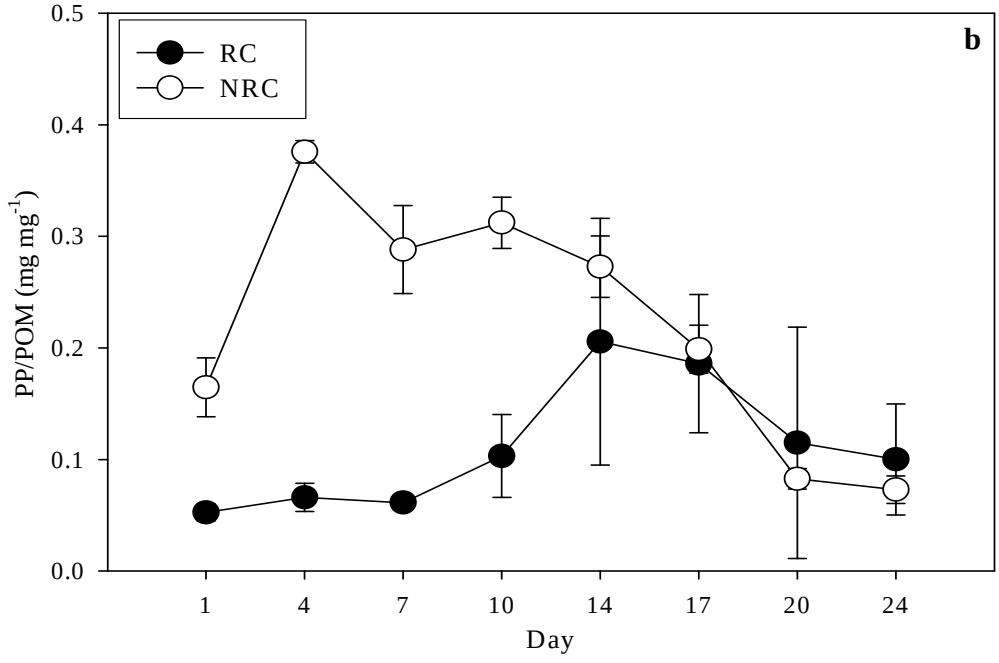
b
RC
NRC
PP/POM (mg mg-1)
0.0
0.1
0.2
0.3
0.4
0.5
1
4
7
10
14
17
20
24
Day

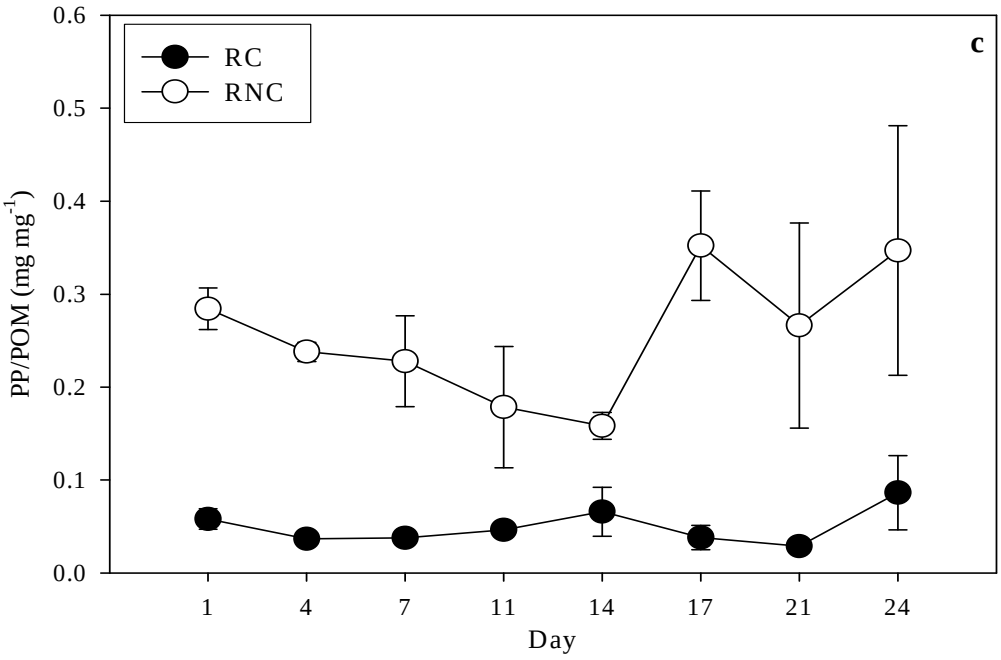
c
RC
RNC
PP/POM (mg mg-1)
0.0
0.1
0.2
0.3
0.4
0.5
0.6
1
4
7
11
14
17
21
24
Day

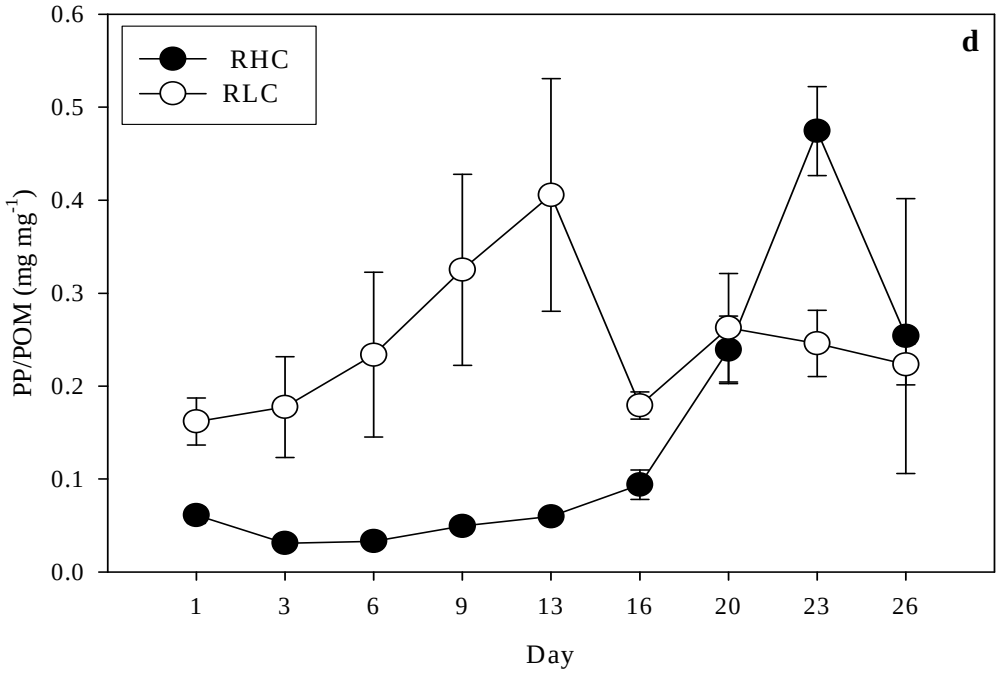
d
RHC
RLC
PP/POM (mg mg-1)
0.0
0.1
0.2
0.3
0.4
0.5
0.6
1
3
6
9
13
16
20
23
26
Day

Figure B. Average ratios of ZP (> 63 µm) and POM (mg mg^{-1}): a) experiment 1; b) experiment 2; c) experiment 3; d) experiment 4. Error bars show standard deviations of 3 replicates in each system.

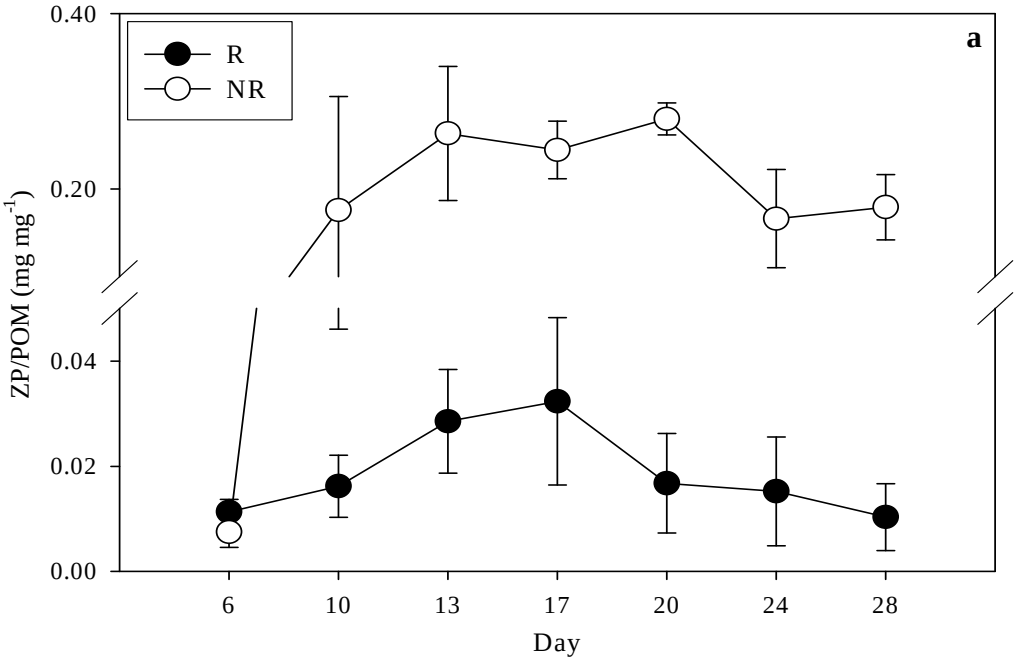
a
R
NR
0.40
0.20
0.04
0.02
0.00
ZP/POM (mg mg-1)
6
10
13
17
20
24
28
Day

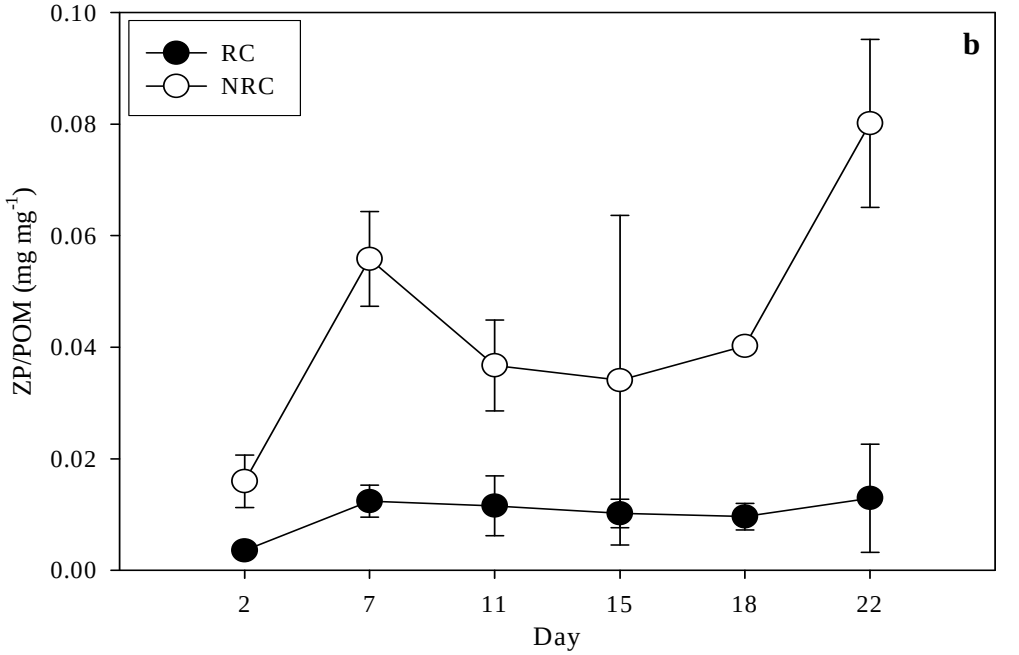
b
RC
NRC
0.10
0.08
0.06
0.04
0.02
0.00
ZP/POM (mg mg-1)
2
7
11
15
18
22
Day

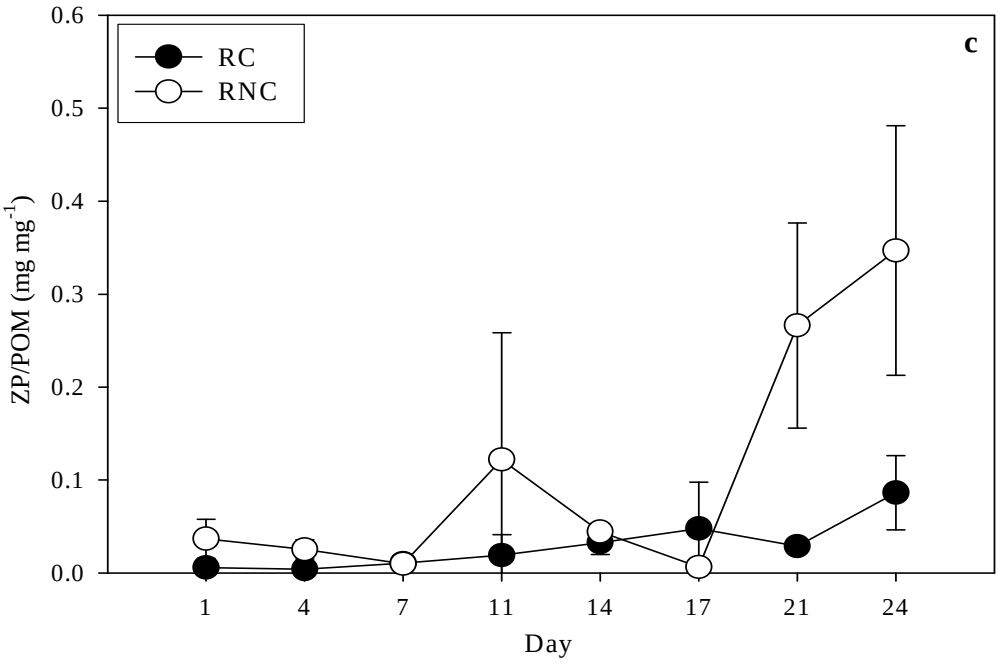
c
RC
RNC
ZP/POM (mg mg-1)
0.0
0.1
0.2
0.3
0.4
0.5
0.6
1
4
7
11
14
17
21
24
Day

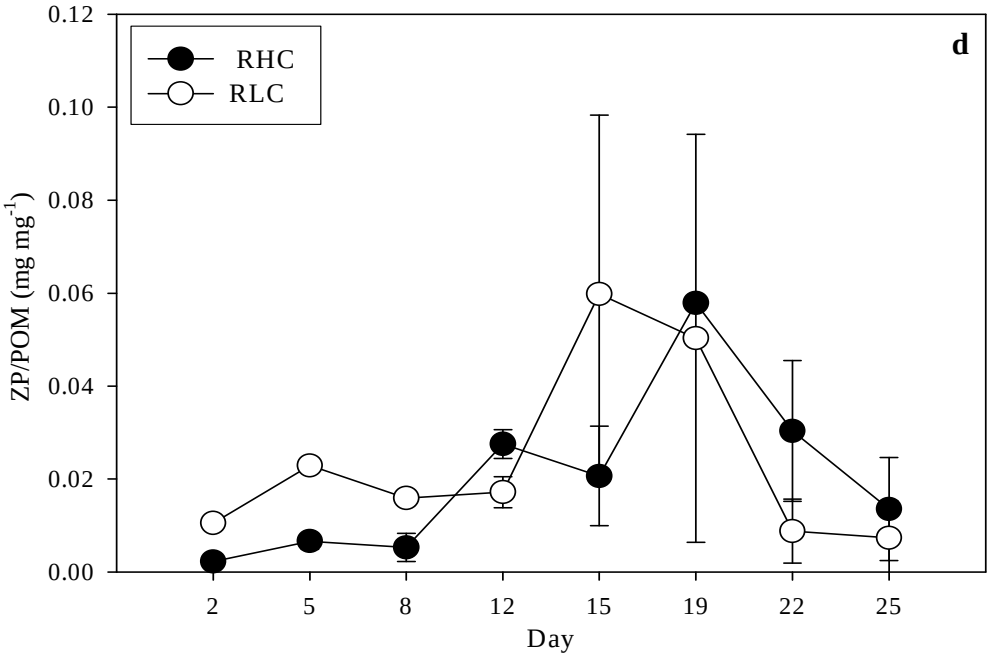
d
RHC
RLC
ZP/POM (mg mg-1)
0.00
0.02
0.04
0.06
0.08
0.10
0.12
2
5
8
12
15
19
22
25
Day

Table A. Water column data in experiments 1 and 2.

		Experiment 1	Experiment 2
Temperature	R (RC) NR (NRC)	25 ± 1.2 °C 25 ± 1.3 °C	20 ± 1.9 °C 20 ± 2.0 °C
Salinity	R(RC) NR (NRC)	14 ± 0.3 ppt 14 ± 0.3 ppt	19 ± 0.2 ppt 19 ± 0.2 ppt
TSS	R(RC) NR (NRC)	150 ± 27 mg/L 10 ± 0.2 mg/L	63 ± 22 mg/L 4.5 ± 0.6 mg/L
POM (% POM)	R(RC) NR (NRC)	22 ± 3 mg/L (18 ±0.9 %) 5.4 ± 0.1 mg/L (53 ± 1 %)	10 ± 4.2 mg/L (16 ±0.7 %) 2.0 ± 0.2 mg/L (46 ± 2.3 %)
DOC	R(RC) NR (NRC)	240 ± 8 µM 280 ± 3 µM	300 ± 54 µM 330 ± 10 µM
Chl *a*	R(RC) NR (NRC)	24 ± 2 µg/L 13 ± 0.9 µg/L	6.7 ± 0.3 µg/L 3.6 ± 0.1 µg/L
Part. THg	R(RC) NR (NRC)	2.3 ± 0.1 nmol/g 1.1 ± 0.05 nmol/g	2.3 ± 0.2 nmol/g 1.4 ± 0.05 nmol/g
Diss. THg	R(RC) NR (NRC)	5.5 ± 1.0 pM 5.5 ± 1.0 pM	8.0 ± 1.0 pM 6.0 ± 1.0 pM
Part. MeHg	R(RC) NR (NRC)	11 ± 2.0 pmol/g 34 ± 5.0 pmol/g	6.0 ± 1.0 pmol/g 26 ± 5.0 pmol/g
Diss. MeHg	R(RC) NR (NRC)	0.3 ± 0.2 pM 0.3 ± 0.1 pM	0.2 ± 0.05 pM 0.2 ± 0.05 pM

Table B. Water column data in experiments 3 and 4

		Experiment 3	Experiment 4
Temperature	RC (RHC) RNC(RLC)	26 ± 0.02°C 26 ± 0.01 °C	24 ± 0.1 °C 24 ± 0.08 °C
Salinity	RC (RHC) RNC(RLC)	18 ± 0.2 ppt 18 ± 0.3 ppt	18 ± 0.4 ppt 18 ± 0.6 ppt
TSS	RC (RHC) RNC(RLC)	130 ± 46 mg/L 49 ± 16 mg/L	90 ± 54 mg/L 52 ± 20 mg/L
POM (% POM)	RC (RHC) RNC(RLC)	17 ± 5.1mg/L (14 ± 1.4%) 9.2 ± 2.0 mg/L (20 ±4.3 %)	16 ± 7.4 mg/L (20 ± 5.7 %) 12 ± 3.8 mg/L (24 ± 5.3 %)
DOC	RC (RHC) RNC(RLC)	280 ± 43 µM 290 ± 42 µM	300 ± 33 µM 300 ± 48 µM
Chl *a*	RC (RHC) RNC(RLC)	6.9 ± 3.1 µg/L 19 ± 8.5 µg/L	12 ± 8.2 µg/L 23 ± 8.2 µg/L
Part. THg	RC (RHC) RNC(RLC)	NA	NA
Diss. THg	RC (RHC) RNC(RLC)	9.7 ± 3.8 pM 9.2 ± 6.5 pM	5.1 ± 0.8 pM 4.0 ± 1.2 pM
Part. MeHg	RC (RHC) RNC(RLC)	NA	NA
Diss. MeHg	RC (RHC) RNC(RLC)	0.3 ± 0.1 pM 0.3 ± 0.08 pM	0.3 ± 0.2 pM 0.3 ± 0.2 pM

NA: not analyzed.

Appendix II.

A. Model parameters.

Parameter	Value	Unit	**Reference**
Phytoplankton (PP)			
Maximum growth rate (G_{max})	**0.01**	**h^{-1}**	**Calibration**
Excretion rate	**0.000417**	**h^{-1}**	**Calibration**
Mortality rate	**0.000208**	**h^{-1}**	**Ashley (1998)**
Respiration rate	**0.00208**	**h^{-1}**	**Ashley (1998)**
Sinking rate	**0.00125**	**h^{-1}**	**Bienfang (1981)**
Half saturation constant for nutrients	**0.24**	**µmol L^{-1}**	**Schnoor (1996)**
Carbon assimilation efficiency (AE) for ZP	**0.7**	**Unitless**	**Halvorsen et al. (2001)**
Carbon assimilation efficiency (AE) for FF	**0.8**	**Unitless**	**Grizzle (2001)**
Fraction of PP ingestion by ZP1	**0.9**	**Unitless**	**Calibration**
Fraction of PP ingestion by ZP2	**0.95**	**Unitless**	**Calibration**
Fraction of PP ingestion by FF	**0.6**	**Unitless**	**Calibration**
Zooplankton (ZP)			
Maximum filtration rate (F_{max}) for ZP1	**0.19**	**m^3 hr^{-1} C g^{-1}**	**Calibration**
Maximum filtration rate for ZP2	**0.23**	**m^3 hr^{-1} C g^{-1}**	**Calibration**
Excretion rate	**0.00167**	**h^{-1}**	**Kiorbe (1985)**
Mortality rate	**0.000868**	**h^{-1}**	**Calibration**
Respiration rate	**0.00167**	**h^{-1}**	**Kiorbe (1985)**
Fraction of ZP2 ingestion by ZP1	**0.05**	**Unitless**	**Calibration**
ZP2 AE for ZP1	**0.3**	**Unitless**	**Calibration**
Filter feeder(FF)			
Maximum filtration rate for FF	**0.015**	**m^3 hr^{-1} C g^{-1}**	**Calibration**
Excretion rate	**0.00025**	**h^{-1}**	**Calibration**
Respiration rate	**0.00025**	**h^{-1}**	**Calibration**
Biodepostion rate	**0.000125**	**h^{-1}**	**Grizzle (2001)**
Microphytobenthos (MPB)			
Maximum growth rate	**0.003**	**h^{-1}**	**Calibration**
Excretion rate	**0.000417**	**h^{-1}**	**Calibration**
Mortality rate	**0.000208**	**h^{-1}**	**Ashley (1998)**
Respiration rate	**0.00208**	**h^{-1}**	**Ashley (1998)**
Fraction of MPB ingestion by ZP1	**0.05**	**Unitless**	**Calibration**
Fraction of MPB ingestion by ZP2	**0.05**	**Unitless**	**Calibration**
Fraction of MPB ingestion by FF	**0.1**	**Unitless**	**Calibration**

Parameter	Value	Unit	**Reference**
Particulate organic carbon in the water column (WPOC)			
WPOC degradation rate	**0.00917**	**h^{-1}**	**Wainright and Hopkinson (1997)**
Sinking rate	**0.0107**	**h^{-1}**	**Calibration**
Dissolved organic carbon in the water column (WDOC)			
Bacterial uptake	**0.0108**	**h^{-1}**	**Calibration**
Diffusion coefficient	**7.2E-7**	**$m^2 h^{-1}$**	**Gill et al.(1999)**
DOC in the pore water (PW DOC)			
Bacterial uptake	**0.0190**	**h^{-1}**	**Calibration**
Resuspended organic carbon (RPOC)			
RPOC AE for FF	**0.2**	**Unitless**	**Calibration**
Fraction of RPOC ingestion by FF	**0.3**	**Unitless**	**Calibration**
RPOC degradation rate	**0.00917**	**h^{-1}**	**Wainright and Hopkinson (1997)**
Deposition rate	**1.656**	**m h^{-1}**	**Data from experiment2**
Sediment organic carbon (SPOC)			
SPOC degradation rate	**0.0001**	**h^{-1}**	**Wainright and Hopkinson (1997)**
Burial rate	**8.33E-7**	**h^{-1}**	**Calibration**
Dissolved MeHg bound to DOC (MeHgDOC)			
Uptake rate by PP	**2.0E-12**	**$m^3 h^{-1} cell^{-1}$**	**Calibration**
Uptake rate by ZP	**0.000115**	**$m^3 hr^{-1} C g^{-1}$**	**Calibration**
Uptake rate by FF	**0.0001**	**$m^3 hr^{-1} C g^{-1}$**	**Calibration**
Uptake rate by MPB	**1.0E-12**	**$m^3 h^{-1} cell^{-1}$**	**Mason et al. (1996)**
Adsorption rate1	**0.00172**	**$m^3 hr^{-1} C g^{-1}$**	**Calculated using K_d and desorption rate**
Adsorption rate2	**0.00150**	**$m^3 hr^{-1} C g^{-1}$**	**"**
Desoprtion rate	**0.00180**	**h^{-1}**	**Hintelman and Harris (in press)**
Organic carbon based K_d	**0.834**	**$m^3 C g^{-1}$**	**Data from experiment2**
Fraction of MeHgDOC	**0.988**	**Unitless**	**Calculated**

Parameter	Value	Unit	**Reference**
Dissolved MeHg			
Uptake rate by PP	**1.0E-11**	**$m^3\ h^{-1}\ cell^{-1}$**	**Calibration**
Uptake rate by ZP	**0.000115**	**$m^3\ hr^{-1}\ C\ g^{-1}$**	**Calibration**
Uptake rate by FF	**0.0001**	**$m^3\ hr^{-1}\ C\ g^{-1}$**	**Calibration**
Uptake rate by MPB	**5.0E-12**	**$m^3\ h^{-1}\ cell^{-1}$**	**Calibration**
Diffusion coefficient	**4.68E-6**	**$m^2\ h^{-1}$**	**Gill et al. (1999)**
Sediment MeHg ($MeHg_{SPOC}$)			
Methylation rate1	**0.002**	**h^{-1}**	**Data from experiment2**
Methylation rate2	**0.0014**	**h^{-1}**	**Data from experiment2**
Demethylation rate	**0.7**	**h^{-1}**	**Data from experiment2**
Total Hg concentration1	**0.0098**	**$g\ m^{-3}$**	**Data from experiment2**
Total Hg concentration2	**0.0091**	**$g\ m^{-3}$**	**Data from experiment2**
Organic carbon based K_d	**0.0104**	**$m^3\ C\ g^{-1}$**	**Bloom et al. (1999)**
Adsorption rate	**0.0015**	**$m^3\ hr^{-1}\ C\ g^{-1}$**	**Calculated**
Desorption rate	**0.144**	**h^{-1}**	**Calculated**

B. Model equations.

PP: Phytoplankton,
ZP1: Zooplankton (> 210 µm),
ZP2: Zooplankton (63-210 µm),
WPOC: Water column particulate organic carbon,
WDOC: Water column dissolved organic carbon,
RPOC: Resuspended particulate organic carbon,
FF: Filter Feeder,
MPB: Microphytobenthos,
SPOC1: Sediment particulate organic carbon in sediment layer 1,
SPOC2 : Sediment Particluate organic carbon in sediment layer 2,
SDOC1 : Dissolved organic carbon in sediment layer 1,
SDOC2: Dissolved organic carbon in sediment layer 2,
$MeHg_{inorg}$: Dissolved MeHg bound to inorganic complexes or free dissolved MeHg,
$MeHg_{WDOC}$: Dissolved MeHg bound to WDOC (Dissolve MeHg = $MeHg_{inorg}$ + $MeHg_{WDOC}$),
$MeHg_{PP}$: MeHg in phytoplankton,
$MeHg_{ZP1}$: MeHg in zooplankton 1,
$MeHg_{ZP2}$: MeHg in zooplankton 2,
$MeHg_{WPOC}$: MeHg in water column particulate organic carbon,
$MeHg_{RPOC}$: MeHg in resuspended particulate organic carbon,
$MeHg_{FF}$: MeHg in filter feeder,
$MeHg_{MPB}$: MeHg in microphytobenthos,
$MeHg_{SPOC1}$: MeHg in sediment particulate organic carbon1,
$MeHg_{SPOC2}$: MeHg in sediment particulate organic carbon2,
$MeHg_{SDOC1}$: Dissolved MeHg bound to dissolved organic carbon in sediment layer1,
$MeHg_{SDOC2}$: Dissolved MeHg bound to dissolved organic carbon in sediment layer2,
$MeHg_{PW1inorg}$: Dissolved MeHg bound to inorganic complexes or free dissolved MeHg in sediment layer1,
$MeHg_{PW2inorg}$: Dissolved MeHg bound to inorganic complexes or free dissolved MeHg in sediment layer1.

Clams (FF)

FF(t) = FF(t - dt) + (C_fr_PP + fr_RPOC + C_FF_fr_MPB - clam_excret - biodeposit_to_SPOC1 - FF_respr) * dt

INIT FF = 10.50

INFLOWS:

C_fr_PP = PP_C_to_FF
fr_RPOC = to_FF
C_FF_fr_MPB = MPB_to_FF

OUTFLOWS:

clam_excret = FF*FF_excret_rate
biodeposit_to_SPOC1 = FF*biodeposition_rate
FF_respr = FF*FF_respr_rate

MeHg_FF(t) = MeHg_FF(t - dt) + (diff_uptake_FF + MeHg_FF_fr_PP + MeHg_RPOC_to_FF + diff_MeHgDOC_FF + MeHg_MPB_to_FF - MeHg_FF_excrt) * dt

INIT MeHg_FF = 6.62E-7

INFLOWS:

diff_uptake_FF = uptake_rate_FF*FF*diss_MeHg
MeHg_FF_fr_PP = MeHg_PP_to_FF
MeHg_RPOC_to_FF = RPOC_to_FF
diff_MeHgDOC_FF = uptake_rate_FF*FF*WMeHgDOC
MeHg_MPB_to_FF = MeHg_to_FF

OUTFLOWS:

MeHg_FF_excrt = clam_excret*MeHg_FF/FF
biodeposition_rate = 0.000125
FF_excret_rate = 0.03/24*0.2
FF_respr_rate = 0.03/24*0.2
MeHg_ng_per_g_C_FF = MeHg_FF/FF*1e9
uptake_rate_FF = 0.0001

Dissolved $MeHg_{inorg}$

$diss\_MeHg_{inorg}$ (t) = diss_MeHg(t - dt) + (MeHg_in + desorp_RMeHg + diff_flux_fr_PWMeHg1 + desorp_WMeHg - uptake_by_PP - uptake_by_ZP1 - uptake_by_ZP2 - MeHg_diss_out - adsorp_WMeHg - adsorp_RMeHg - uptake_by_FF - uptake_by_MPB) * dt

INIT diss_MeHg = 2.58E-10

INFLOWS:

MeHg_in = 3.46E-10*0.1/24
desorp_RMeHg = des_RMeHg
diff_flux_fr_PWMeHg1 = -(diff_const_MeHg/1*(diss_MeHg-PW_MeHg1))
desorp_WMeHg = des_WMeHg

OUTFLOWS:

uptake_by_PP = diff_uptake_PP
uptake_by_ZP1 = diff_MeHg_ZP1
uptake_by_ZP2 = diff_MeHg_ZP2
MeHg_diss_out = IF(resuspn_timing=0) then diss_MeHg*0.1/8{hr-1} else 0
adsorp_WMeHg = ads_rate1*WPOC*diss_MeHg
adsorp_RMeHg = ads_rate2*Resuspd_POC*diss_MeHg
uptake_by_FF = diff_uptake_FF
uptake_by_MPB = diff_WMeHg_MPB
ads_rate1 = 1.72E-03
ads_rate2 = 1.50E-03
diff_const_MeHg = 4.68E-06
diss_MeHg_in_ng_per_L = diss_MeHg*1e6

DOC

WDOC(t) = WDOC(t - dt) + (DOC_fr_ZP1 + DOC_fr_input_water + DOC_fr_PP + DOC_fr_WPOC + DOC_fr_ZP2 + DOC_fr_RPOC + diff_flux_fr_PW_DOC1 + DOC_fr_FF - DOCout - DOC_loss_to_bacteria) * dt

INIT WDOC = 3.83

INFLOWS:

DOC_fr_ZP1 = ZP1_excret
DOC_fr_input_water = 3.70*0.1/24{hr-1}
DOC_fr_PP = PP_excret
DOC_fr_WPOC = WPOC_degrad
DOC_fr_ZP2 = ZP2_excret
DOC_fr_RPOC = RPOC_degrad
diff_flux_fr_PW_DOC1 = -(DOC_diff_coeff/1{m2;SA}*(WDOC-PW_DOC1))
DOC_fr_FF = clam_excret

OUTFLOWS:

DOCout = IF(resuspn_timing=0) then WDOC*0.1/8{hr-1} else 0
DOC_loss_to_bacteria = WDOC*0.005417*2

Dissolved $MeHg_{DOC}$(t) = MeHgDOC(t - dt) + (MeHgDOC_in + diff_flux_fr_PWMeHgDOC1 + desorp_RMeHgDOC + desorp_WMeHgDOC +

fr_MeHgPOC + fr_MeHgRPOC + fr_ZP_excrt + fr_MeHg_PP_excrt + fr_MeHg_FF_excrt - MeHgDOC_out - PP_uptake - ZP2_uptake - ZP1_uptake - FF_uptake - adsorp_WMeHgDOC - adsorp_RMeHgDOC - MPB_uptake) * dt

INIT WMeHgDOC = 2.05E-08

INFLOWS:

MeHgDOC_in = 2.75E-08*0.1/24
diff_flux_fr_PWMeHgDOC1 = diff_flux_fr_PW_DOC1/(WDOC-PW_DOC1)*(WMeHgDOC-PW_MeHgDOC1)
desorp_RMeHgDOC = des_RMeHgDOC
desorp_WMeHgDOC = des_WMeHgDOC
fr_MeHgPOC = to_MeHgDOC
fr_MeHgRPOC = to__MeHgDOCa
fr_ZP_excrt = MeHgZP1_excrt+MeHg_ZP2_excrt
fr_MeHg_PP_excrt = MeHg_PP_excrt
fr_MeHg_FF_excrt = MeHg_FF_excrt

OUTFLOWS:

MeHgDOC_out = IF(resuspn_timing=0) then WMeHgDOC*0.1/8{hr-1} else 0
PP_uptake = diff_MeHgDOC_PP
ZP2_uptake = diff_MeHgDOC_ZP2
ZP1_uptake = diff_MeHgDOC_ZP1
FF_uptake = diff_MeHgDOC_FF
adsorp_WMeHgDOC = ads_rate1*WPOC*WMeHgDOC
adsorp_RMeHgDOC = ads_rate2*Resuspd_POC*WMeHgDOC
MPB_uptake = diff_WMeHgDOCMPB2
DOC_diff_coeff = 7.20E-07
MeHgDOC_ng_per_L = WMeHgDOC*1e6

Microphytobenthos (MPB)

MeHg_MPB(t) = MeHg_MPB(t - dt) + (diff_WMeHg_MPB + diff_WMeHgDOCMPB2 - MeHg_MPB_mort - MeHg_to_ZP1 - MeHg_to_ZP2 - MeHg_to_FF - MeHg_MPB_excrt) * dt

INIT MeHg_MPB = 1.9E-9

INFLOWS:

diff_WMeHg_MPB = K1'*diss_MeHg
diff_WMeHgDOCMPB2 = K2'*WMeHgDOC

OUTFLOWS:

MeHg_MPB_mort = MPB_mort/MPB*MeHg_MPB
MeHg_to_ZP1 = MPB_to_ZP1*MeHg_MPB/(MPB*0.05)*AE_ratio
MeHg_to_ZP2 = MPB_to_ZP2*MeHg_MPB/(MPB*0.05)*AE_ratio
MeHg_to_FF = (MPB_to_FF*MeHg_MPB/(MPB*0.05))*AE_ratio2

MeHg_MPB_excrt = MPB_excrt*MeHg_MPB/MPB

MPB(t) = MPB(t - dt) + (MPB_growth - MPB_excrt - MPB_respr - MPB_mort - MPB_to_FF - MPB_to_ZP1 - MPB_to_ZP2) * dt

INIT MPB = 1.37

INFLOWS:

MPB_growth = growth_max2*light*nut_effect*MPB

OUTFLOWS:

MPB_excrt = MPB*0.01/24
MPB_respr = MPB*0.05/24
MPB_mort = MPB*0.0002
MPB_to_FF = (MPB*0.05)*CR_FF*FF*AE_FF*MPB_frac_to_FF*clam_feeding
MPB_to_ZP1 = (MPB*0.05)*CR_ZP1*ZP1*PP_C_AE_ZP*MPB_frac_to_ZP1
MPB_to_ZP2 = (MPB*0.05)*CR_ZP2*ZP_2*PP_C_AE_ZP*MPB_frac_to_ZP2
growth_max2 = MPB_const*EXP(0.06933*temp)
K1' = uptake_rate_1'*MPB/mass_of_cell
K2' = uptake_rate_2'*MPB/mass_of_cell
MPB_const = 0.003
MPB_frac_to_FF = 0.1
MPB_frac_to_ZP1 = 0.05
MPB_frac_to_ZP2 = 0.05
ng_MeHg_per_g_C_MPB = MeHg_MPB/MPB*1e9
uptake_rate_1' = 1E-12*5
uptake_rate_2' = 1e-12

Phytoplankton

MeHg_PP(t) = MeHg_PP(t - dt) + (diff_uptake_PP + diff_MeHgDOC_PP - MeHg_PP_to_ZP1 - MeHg_PP_out - MeHg_PP_to_ZP2 - MeHg_PP_to_FF - MeHg_PP_to_WPOC - MeHg_PP_sinking - MeHg_PP_excrt) * dt

INIT MeHg_PP = 1.9E-9

INFLOWS:

diff_uptake_PP = K1*diss_MeHg
diff_MeHgDOC_PP = K2*WMeHgDOC

OUTFLOWS:

MeHg_PP_to_ZP1 = PP_C_to_ZP1*MeHg_PP/PP*AE_ratio
MeHg_PP_out = PP_out*MeHg_PP/PP
MeHg_PP_to_ZP2 = PP_C_to_ZP2*MeHg_PP/PP*AE_ratio

MeHg_PP_to_FF = PP_C_to_FF*MeHg_PP/PP *AE_ratio2
MeHg_PP_to_WPOC = PP_mort*MeHg_PP/PP
MeHg_PP_sinking = PP_sinking_to_SPOC1/PP*MeHg_PP
MeHg_PP_excrt = PP_excret*MeHg_PP/PP

PP(t) = PP(t - dt) + (PP_growth - PP_sinking_to_SPOC1 - PP_respr - PP_excret - PP_C_to_FF - PP_C_to_ZP1 - PP_mort - PP_out - PP_C_to_ZP2) * dt

INIT PP = 0.314

INFLOWS:

PP_growth = growth_max*nut_effect*light*PP

OUTFLOWS:

PP_sinking_to_SPOC1 = PP*settling_sp1
PP_respr = PP*0.05/24
PP_excret = PP*0.01/24
PP_C_to_FF = IF(PP>= 0.025) then FF*CR_FF*PP*AE_FF*clam_feeding*PP_frac_to_FF else 0
PP_C_to_ZP1 = IF(PP>= 0.025) then ZP1*CR_ZP1*PP*PP_C_AE_ZP*PP_frac_to_ZP1 else 0
PP_mort = PP*0.000208
PP_out = IF(resuspn_timing=0) then PP*0.1/8{hr-1} else 0
PP_C_to_ZP2 = IF(PP>= 0.025) then ZP_2*CR_ZP2*PP*PP_C_AE_ZP*PP_frac_to_ZP2 else 0
AE_FF = 0.8
AE_ratio = MeHg_AE_ZP/PP_C_AE_ZP
AE_ratio2 = MeHg_AE_FF/AE_FF
clam_feeding = 0.62
const = 0.01
CR_FF = 0.015*(1-EXP(-0.009*temp))
CR_ZP1 = 0.19*(1-EXP(-0.009*temp))
CR_ZP2 = 0.23*(1-EXP(-0.009*temp))
growth_max = const*EXP(0.06933*temp)
K1 = uptake_rate1*PP/mass_of_cell
K2 = uptake_rate2*PP/mass_of_cell
mass_of_cell = 524E-12
MeHg_AE_FF = 0.8
MeHg_AE_ZP = 0.6
ng_MeHg_per_g_C_PP = MeHg_PP/PP*1e9
nut_effect = nut_data/(0.24+nut_data)
PP_C_AE_ZP = 0.7
PP_frac_to_FF = 0.6
PP_frac_to_ZP1 = 0.9
PP_frac_to_ZP2 = 0.95
settling_sp1 = 0.00125
uptake_rate1 = 1E-12*10
uptake_rate2 = 1e-12*2

light = GRAPH(time_of_day)
(0.00, 0.00), (1.00, 0.00), (2.00, 0.00), (3.00, 0.00), (4.00, 0.00), (5.00, 0.00), (6.00, 0.00), (7.00, 0.00), (8.00, 1.00), (9.00, 1.00), (10.0, 1.00), (11.0, 1.00), (12.0, 1.00), (13.0, 1.00), (14.0, 1.00), (15.0, 1.00), (16.0, 1.00), (17.0, 1.00), (18.0, 0.00), (19.0, 0.00), (20.0, 0.00), (21.0, 0.00), (22.0, 0.00), (23.0, 0.00)
nut_data = GRAPH(TIME)
(0.00, 2.58), (80.0, 11.0), (160, 6.46), (240, 8.67), (320, 3.54), (400, 2.78), (480, 1.62), (560, 0.97)
temp = GRAPH(TIME)
(0.00, 20.7), (24.0, 22.0), (48.0, 22.3), (72.0, 20.2), (96.0, 17.7), (120, 15.8), (144, 16.5), (168, 18.2), (192, 20.6), (216, 20.6), (240, 21.2), (264, 21.2), (288, 20.8), (312, 19.8), (336, 17.4), (360, 16.5), (384, 17.2), (408, 18.7), (432, 20.1), (456, 20.5), (480, 20.6), (504, 21.5), (528, 21.7), (552, 18.9)

POC in the water column (WPOC)

MeHg_WPOC(t) = MeHg_WPOC(t - dt) + (MeHg_WPOC_fr_ZP1 + MeHg_WPOC_fr_ZP2 + ads_WMeHg + ads_WMeHgDOC + MeHg_WPOC_fr_PP - MeHg_WPOC_out - MeHg_WPOC_sinking - des_WMeHg - des_WMeHgDOC - to_MeHgDOC) * dt

INIT MeHg_WPOC = 1.85e-8

INFLOWS:

MeHg_WPOC_fr_ZP1 = MeHg_ZP1_to_WPOC
MeHg_WPOC_fr_ZP2 = MeHg_ZP2_to_WPOC
ads_WMeHg = adsorp_WMeHg
ads_WMeHgDOC = adsorp_WMeHgDOC
MeHg_WPOC_fr_PP = MeHg_PP_to_WPOC

OUTFLOWS:

MeHg_WPOC_out = WPOCout/WPOC*MeHg_WPOC
MeHg_WPOC_sinking = WPOC_sinking_to_SPOC1/WPOC*MeHg_WPOC
des_WMeHg = des_rate*MeHg_WPOC*(1-frac_MeHgDOC)
des_WMeHgDOC = des_rate*MeHg_WPOC*frac_MeHgDOC
to_MeHgDOC = WPOC_degrad*MeHg_WPOC/WPOC

WPOC(t) = WPOC(t - dt) + (ZP1_mort_to_WPOC + PP_mort_WPOC + uptake_by_bacteria + ZP2_mort_to_WPOC - WPOC_sinking_to_SPOC1 - WPOCout - WPOC_degrad) * dt

INIT WPOC = 0.83

INFLOWS:

ZP1_mort_to_WPOC = ZP1_mort
PP_mort_WPOC = PP_mort

uptake_by_bacteria = DOC_loss_to_bacteria
ZP2_mort_to_WPOC = ZP_2_mort

OUTFLOWS:

WPOC_sinking_to_SPOC1 = WPOC*settling_sp2
WPOCout = IF(resuspn_timing=0) then WPOC*0.1/8{hr-1} else 0
WPOC_degrad = WPOC*degrad_rate
degrad_rate = 0.22/24
MeHgWPOC_ng_per_g_WPOC = MeHg_WPOC/WPOC*1e9
MeHg_WPOC_ng_per_L = MeHg_WPOC*1e6
settling_sp2 = 0.02133*0.5

Porewater DOC1 (PW DOC1)

PW_DOC1(t) = PW_DOC1(t - dt) + (degrad_fr_SPOC1 + diff_flux_fr_WDOC + diff_flux_fr_PW_DOC2 + PW_DOC1_fr_MPB - PW_DOC1_uptake_by_bacteria) * dt

INIT PW_DOC1 = 7.81

INFLOWS:

degrad_fr_SPOC1 = SPOC1_degrad
diff_flux_fr_WDOC = DOC_diff_coeff*(WDOC-PW_DOC1)
diff_flux_fr_PW_DOC2 = -(DOC_diff_coeff/1*(PW_DOC1-PW_DOC2))
PW_DOC1_fr_MPB = MPB_excrt

OUTFLOWS:

PW_DOC1_uptake_by_bacteria = PW_DOC1*0.005417*3.5

PW_MeHgDOC1(t) = PW_MeHgDOC1(t - dt) + (diff_flux__fr_WMeHgDOC + diff_flux_fr_MeHgDOC2 + desorp_MeHgDOC1 + fr_SPOC1_degrad + fr_MeHg_MPB_excrt - adsorp_PWMeHgDOC1) * dt

INIT PW_MeHgDOC1 = 1.84E-06

INFLOWS:

diff_flux__fr_WMeHgDOC = diff_flux_fr_WDOC/(WDOC-PW_DOC1)*(WMeHgDOC-PW_MeHgDOC1)
diff_flux_fr_MeHgDOC2 = diff_flux_fr_PW_DOC2/(PW_DOC1-PW_DOC2)*(PW_MeHgDOC1-PW_MeHgDOC2)
desorp_MeHgDOC1 = des_PWMeHgDOC1
fr_SPOC1_degrad = to_PWMeHgDOC1
fr_MeHg_MPB_excrt = MeHg_MPB_excrt

OUTFLOWS:

adsorp_PWMeHgDOC1 = adsorp_rateS*SPOC1*PW_MeHgDOC1
adsorp_rateS = 1.5e-3
part_coeff_for_OC1 = (SPOC1/1.5e6)/PW_DOC1*1e3
PW_MeHgDOC1_ng_per_L = PW_MeHgDOC1*1e6

Porewater DOC2 (PW DOC2)

PW_DOC2(t) = PW_DOC2(t - dt) + (fr_SPOC2 + diff_flux_to_PW_DOC2 - PW_DOC2_degrad) * dt

INIT PW_DOC2 = 7.96

INFLOWS:

fr_SPOC2 = SPOC2_degrad
diff_flux_to_PW_DOC2 = DOC_diff_coeff/1*(PW_DOC1-PW_DOC2)

OUTFLOWS:

PW_DOC2_degrad = PW_DOC2*0.005417*3.5

PW_MeHgDOC2(t) = PW_MeHgDOC2(t - dt) + (diff_flux_to_MeHgDOC2 + desorp_MeHgDOC2 + fr_SPOC2_degrad - adsorp_MeHgDOC2) * dt

INIT PW_MeHgDOC2 = 1.24E-06

INFLOWS:

diff_flux_to_MeHgDOC2 = diff_flux_to_PW_DOC2/(PW_DOC1-PW_DOC2)*(PW_MeHgDOC1-PW_MeHgDOC2)
desorp_MeHgDOC2 = des_MeHgDOC2
fr_SPOC2_degrad = to_PW_MeHgDOC2

OUTFLOWS:

adsorp_MeHgDOC2 = adsorp_rateS*SPOC2*PW_MeHgDOC2
part_coeff_for_OC2 = (SPOC2/1.5e6)/PW_DOC2*1e3
PW_MeHgDOC2_ng_per_L = PW_MeHgDOC2*1e6

Porewater MeHg 1 (PW1 $MeHg_{inorg}$)

PW_MeHg1(t) = PW_MeHg1(t - dt) + (diff_flux_to_PW_MeHg1 + diff_flux_fr_PW_MeHg2 + desorpPWMeHg1 - adsorp_PWMeHg1) * dt

INIT PW_MeHg1 = 2.31E-08

INFLOWS:

diff_flux_to_PW_MeHg1 = diff_const_MeHg/1*(diss_MeHg-PW_MeHg1)
diff_flux_fr_PW_MeHg2 = -diff_const_MeHg/1*(PW_MeHg1-PW_MeHg2)
desorpPWMeHg1 = des_PWMeHg1

OUTFLOWS:

adsorp_PWMeHg1 = adsorp_rateS*SPOC1*PW_MeHg1
Kd_S1MeHg = MeHg_SPOC1/(SPOC1*(PW_MeHgDOC1+PW_MeHg1))*1e6
log_Kd_S1MeHg = LOG10(Kd_S1MeHg)
PW_MeHg1_ng_per_L = PW_MeHg1*1e6

Porewater MeHg2 (PW2 $MeHg_{inorg}$)

PW_MeHg2(t) = PW_MeHg2(t - dt) + (diff_flux_to_PW_MeHg2 + desorp_PW_MeHg2 - adsorp_PW_MeHg2) * dt

INIT PW_MeHg2 = 1.56E-08

INFLOWS:

diff_flux_to_PW_MeHg2 = diff_const_MeHg/1*(PW_MeHg1-PW_MeHg2)
desorp_PW_MeHg2 = des_PWMeHg2

OUTFLOWS:

adsorp_PW_MeHg2 = adsorp_rateS*SPOC2*PW_MeHg2
Kd_S2MeHg = MeHg_SPOC2/(SPOC2*(PW_MeHgDOC2+PW_MeHg2))*1e6
log_Kd_S2MeHg = LOG10(Kd_S2MeHg)
PW_MeHg2_ng_per_L = PW_MeHg2*1e6

Resuspended POC (RPOC)

MeHg_RPOC(t) = MeHg_RPOC(t - dt) + (MeHg_erosion_fr_SPOC1 + ads_RMeHg + ads_RMeHgDOC - MeHg_RPOC_out - RPOC_to_FF - MeHg_to_SPOC1 - des_RMeHgDOC - des_RMeHg - to__MeHgDOCa) * dt

INIT MeHg_RPOC = 5.85E-08

INFLOWS:

MeHg_erosion_fr_SPOC1 = MeHg_to_water_col
ads_RMeHg = adsorp_RMeHg
ads_RMeHgDOC = adsorp_RMeHgDOC

OUTFLOWS:

MeHg_RPOC_out = RPOCout/Resuspd_POC*MeHg_RPOC
RPOC_to_FF = to_FF*MeHg_RPOC/Resuspd_POC*MeHg_AE_FF/AE3
MeHg_to_SPOC1 = depositon/Resuspd_POC*MeHg_RPOC
des_RMeHgDOC = des_rate*MeHg_RPOC*frac_MeHgDOC
des_RMeHg = des_rate*MeHg_RPOC*(1-frac_MeHgDOC)
to__MeHgDOCa = RPOC_degrad*MeHg_RPOC/Resuspd_POC

Resuspd_POC(t) = Resuspd_POC(t - dt) + (erosion - depositon - to_FF - RPOCout - RPOC_degrad) * dt

INIT Resuspd_POC = 3.03

INFLOWS:

erosion = SPOC1_to_water_column

OUTFLOWS:

depositon = RPOC_settling_rate/water_depth*Resuspd_POC
to_FF = FF*CR_FF*Resuspd_POC*AE3*clam_feeding*RPOC_frac_to_FF
RPOCout = IF(resuspn_timing=0) then Resuspd_POC*0.1/8{hr-1} else 0
RPOC_degrad = Resuspd_POC*degrad_rate
AE3 = 0.2
des_rate = 1.8e-3
Kd_RMeHg = (MeHg_RPOC+MeHg_WPOC)/((Resuspd_POC+WPOC)*(WMeHgDOC+diss_MeHg))*1e6
log_Kd_RMeHg = LOG10(Kd_RMeHg)
MeHg_ng_per_g_RPOC = MeHg_RPOC/Resuspd_POC*1e9
RPOC_frac_to_FF = 0.3
time_of_day = MOD(time, 24)
water_depth = 1

Sediment POC 2 (SPOC2; below 2 cm)

MeHg_SPOC2(t) = MeHg_SPOC2(t - dt) + (fr_SPOC1 + meth2 + ads_MeHgDOC2 + ads_PWMeHg2 - demeth2 - des_PWMeHg2 - des_MeHgDOC2 - to_PW_MeHgDOC2) * dt

INIT MeHg_SPOC2 = 1.96E-05

INFLOWS:

fr_SPOC1 = MeHg_burial_to_SPOC2
meth2 = meth_rate2*THg2
ads_MeHgDOC2 = adsorp_MeHgDOC2
ads_PWMeHg2 = adsorp_PW_MeHg2

OUTFLOWS:

demeth2 = MeHg_SPOC2*demeth_rate
des_PWMeHg2 = des_rate2*MeHg_SPOC2*(1-frac_MeHgDOC)
des_MeHgDOC2 = des_rate2*MeHg_SPOC2*frac_MeHgDOC
to_PW_MeHgDOC2 = SPOC2_degrad*MeHg_SPOC2/SPOC2

SPOC2(t) = SPOC2(t - dt) + (burial + fr_PW_DOC2 - SPOC2_degrad) * dt

INIT SPOC2 = 1492

INFLOWS:

burial = burial_to_SPOC2
fr_PW_DOC2 = PW_DOC2_degrad

OUTFLOWS:

SPOC2_degrad = SPOC2*SPOC__degrad
MeHg_ng_per_g_SPOC2 = MeHg_SPOC2/SPOC2*1e9
meth_rate2 = 0.0014
THg2 = 0.0091

Sediment POC1 (SPOC1; top 2 cm)

MeHg_SPOC1(t) = MeHg_SPOC1(t - dt) + (MeHg_sinking + meth1 + ads_PWMeHgDOC1 + ads_PWMeHg1 + MeHg_MPB_to_SPOC1 + MeHg_fr_RPOC - MeHg_to_water_col - demeth1 - MeHg_burial_to_SPOC2 - des_PWMeHgDOC1 - des_PWMeHg1 - to_PWMeHgDOC1) * dt

INIT MeHg_SPOC1 = 2.84E-5

INFLOWS:

MeHg_sinking = MeHg_PP_sinking+MeHg_WPOC_sinking
meth1 = THg1*meth_rate1
ads_PWMeHgDOC1 = adsorp_PWMeHgDOC1
ads_PWMeHg1 = adsorp_PWMeHg1
MeHg_MPB_to_SPOC1 = MeHg_MPB_mort
MeHg_fr_RPOC = MeHg_to_SPOC1

OUTFLOWS:

MeHg_to_water_col = SPOC1_to_water_column/SPOC1*MeHg_SPOC1
demeth1 = MeHg_SPOC1*demeth_rate
MeHg_burial_to_SPOC2 = burial_to_SPOC2/SPOC1*MeHg_SPOC1
des_PWMeHgDOC1 = des_rate2*MeHg_SPOC1*frac_MeHgDOC
des_PWMeHg1 = des_rate2*MeHg_SPOC1*(1-frac_MeHgDOC)

to_PWMeHgDOC1 = SPOC1_degrad*MeHg_SPOC1/SPOC1

SPOC1(t) = SPOC1(t - dt) + (POC_fr_PP&WPOC + deposition_fr_RPOC + fr_PW_DOC1 + MPB_to_SPOC1 + fr_clams_to_SPOC1 - SPOC1_degrad - SPOC1_to_water_column - burial_to_SPOC2) * dt

INIT SPOC1 = 1465

INFLOWS:

POC_fr_PP&WPOC = (WPOC_sinking_to_SPOC1+PP_sinking_to_SPOC1)
deposition_fr_RPOC = depositon
fr_PW_DOC1 = PW_DOC1_uptake_by_bacteria
MPB_to_SPOC1 = MPB_mort
fr_clams_to_SPOC1 = biodeposit_to_SPOC1

OUTFLOWS:

SPOC1_degrad = SPOC1*SPOC__degrad
SPOC1_to_water_column = erosion_rate*resuspn_timing*obs_WPOCeq
burial_to_SPOC2 = SPOC1*burial_rate1
burial_rate1 = 0.00002/24
demeth_rate = 0.7
des_rate2 = 1.44E-01
erosion_rate = RPOC_settling_rate/water_depth
frac_MeHgDOC = 9.88E-01
MeHg_ng_per_g_SPOC1 = MeHg_SPOC1/SPOC1*1e9
meth_rate1 = 0.002
RPOC_settling_rate = 1.656
SPOC__degrad = 0.0024/24
THg1 = 0.0098
obs_WPOCeq = GRAPH(TIME)
(0.00, 6.12), (80.0, 4.51), (160, 3.90), (240, 3.52), (320, 2.56), (400, 2.64), (480, 2.26), (560, 2.81)
resuspn_timing = GRAPH(time_of_day)
(0.00, 1.00), (1.00, 1.00), (2.00, 1.00), (3.00, 1.00), (4.00, 0.00), (5.00, 0.00), (6.00, 1.00), (7.00, 1.00), (8.00, 1.00), (9.00, 1.00), (10.0, 0.00), (11.0, 0.00), (12.0, 1.00), (13.0, 1.00), (14.0, 1.00), (15.0, 1.00), (16.0, 0.00), (17.0, 0.00), (18.0, 1.00), (19.0, 1.00), (20.0, 1.00), (21.0, 1.00), (22.0, 0.00), (23.0, 0.00)

Zooplankton 2 (ZP2; 63 - 210 um)

MeHg_ZP2(t) = MeHg_ZP2(t - dt) + (MeHg_fr_PP_to_ZP2 + diff_MeHg_ZP2 + diff_MeHgDOC_ZP2 + MeHg_MPB_to_ZP2 - MeHg_ZP2_out- MeHg_ZP2_to_WPOC - grazed_by_ZP1 - MeHg_ZP2_excrt) * dt

INIT MeHg_ZP2 = 6.90E-11

INFLOWS:

MeHg_fr_PP_to_ZP2 = MeHg_PP_to_ZP2
diff_MeHg_ZP2 = uptake_rate_ZP*ZP_2*diss_MeHg
diff_MeHgDOC_ZP2 = uptake_rate_ZP*ZP_2*WMeHgDOC
MeHg_MPB_to_ZP2 = MeHg_to_ZP2

OUTFLOWS:

MeHg_ZP2_out = (ZP2_out /ZP_2)*MeHg_ZP2
MeHg_ZP2_to_WPOC = ZP_2_mort/ZP_2*MeHg_ZP2
grazed_by_ZP1 = ZP2_grazing*MeHg_ZP2/ZP_2*MeHg_AE_ZP/AE_ZP2
MeHg_ZP2_excrt = ZP2_excret*MeHg_ZP2/ZP_2

ZP_2(t) = ZP_2(t - dt) + (ZP_2_C_fr_PP + C_fr_MPB_to_ZP2 - ZP2_excret - ZP_2_mort - ZP2_out - ZP2_respr - ZP2_grazing) * dt

INIT ZP_2 = 0.008

INFLOWS:

ZP_2_C_fr_PP = PP_C_to_ZP2
C_fr_MPB_to_ZP2 = MPB_to_ZP2

OUTFLOWS:

ZP2_excret = ZP_2*excrt_rate
ZP_2_mort = ZP_2*0.02/24
ZP2_out = IF(resuspn_timing=0) then ZP_2*0.1/8{hr-1} else 0
ZP2_respr = ZP_2*respr_rate
ZP2_grazing = ZP1*CR_ZP1*ZP_2*AE_ZP2*ZP2_frac
AE_ZP2 = 0.3
MeHg_ng_per_g__C_ZP2 = MeHg_ZP2/ZP_2*1e9
ZP2_frac = 0.05

Zooplankton1 (ZP1; > 210 um)

MeHg_ZP1(t) = MeHg_ZP1(t - dt) + (MeHg_fr_PP_ZP1 + diff_MeHg_ZP1 + diff_MeHgDOC_ZP1 + MeHg_MPB_to_ZP1 + fr_MeHg_ZP2 - MeHg_ZP1_out - MeHg_ZP1_to_WPOC - MeHgZP1_excrt) * dt

INIT MeHg_ZP1 = 6.90E-11

INFLOWS:

MeHg_fr_PP_ZP1 = MeHg_PP_to_ZP1

diff_MeHg_ZP1 = uptake_rate_ZP*ZP1*diss_MeHg
diff_MeHgDOC_ZP1 = uptake_rate_ZP*ZP1*WMeHgDOC
MeHg_MPB_to_ZP1 = MeHg_to_ZP1
fr_MeHg_ZP2 = grazed_by_ZP1

OUTFLOWS:

MeHg_ZP1_out = (ZP1_out/ZP1)*MeHg_ZP1
MeHg_ZP1_to_WPOC = ZP1_mort*MeHg_ZP1/ZP1
MeHgZP1_excrt = ZP1_excret*MeHg_ZP1/ZP1

ZP1(t) = ZP1(t - dt) + (ZP1_C_fr_PP + C_fr_MPB_to_ZP1 + fr_ZP2 - ZP1_mort - ZP1_respr - ZP1_excret - ZP1_out) * dt

INIT ZP1 = 0.013

INFLOWS:

ZP1_C_fr_PP = PP_C_to_ZP1
C_fr_MPB_to_ZP1 = MPB_to_ZP1
fr_ZP2 = ZP2_grazing

OUTFLOWS:

ZP1_mort = ZP1*0.02/24
ZP1_respr = ZP1*respr_rate
ZP1_excret = ZP1*excrt_rate
ZP1_out = IF(resuspn_timing=0) then ZP1*0.1/8{hr-1} else 0
excrt_rate = 0.04/24
MeHg_ng_per_g__C_ZP1 = MeHg_ZP1/ZP1*1e9
respr_rate = 0.04/24
uptake_rate_ZP = 0.00115*0.1

Not in a sector

Appendix III.

Model parameters.

Parameter	Value	Unit	**Reference**
Phytoplankton (PP)			
Maximum growth rate (G_{max})	**4.0×10^{-3}**	**h^{-1}**	**Calibration**
Fraction of PP ingestion by ZP1	**0.85**	**Unitless**	**Calibration**
Zooplankton (ZP)			
Excretion rate	**8.4×10^{-4}**	**h^{-1}**	**Calibration**
Mortality rate	**4.3×10^{-4}**	**h^{-1}**	**Calibration**
Respiration rate	**8.4×10^{-4}**	**h^{-1}**	**Calibration**
Predation rate	**1.0×10^{-3}**	**h^{-1}**	**Calibration**
Filter feeder(FF)			
Excretion rate	**1.3×10^{-4}**	**h^{-1}**	**Calibration**
Respiration rate	**1.3×10^{-4}**	**h^{-1}**	**Calibration**
Mortality rate	**2.1×10^{-4}**	**h^{-1}**	**Calibration**
Predation rate	**2.1×10^{-4}**	**h^{-1}**	**Calibration**
Microphytobenthos (MPB)			
Predation rate	**2.1×10^{-3}**	**h^{-1}**	**Calibration**
Fraction of MPB ingestion by ZP1	**0.1**	**Unitless**	**Calibration**
Sediment MeHg ($MeHg_{SPOC}$)			
Methylation rate (12 % OM)	**6.7×10^{-4}**	**h^{-1}**	**Calculated from**
Methylation rate (6 % OM)	**2.3×10^{-3}**	**h^{-1}**	**Hammerschmidt and**
Methylation rate (3 % OM)	**3.1×10^{-3}**	**h^{-1}**	**Fitzgerald (2004)**
Total Hg concentration (12 % OM)	**1.4×10^{-3}**	**$g\ m^{-3}$**	**Data from**
Total Hg concentration (6 % OM)	**3.1×10^{-3}**	**$g\ m^{-3}$**	**the Chesapeake Bay**
Total Hg concentration (3 % OM)	**6.5×10^{-3}**	**$g\ m^{-3}$**	**samples**
Organic carbon based K_d (12 % OM)	**0.010**	**$m^3\ C\ g^{-1}$**	**Calculated from**
Organic carbon based K_d (6 % OM)	**8.3×10^{-3}**	**$m^3\ C\ g^{-1}$**	**Hammerschmidt and**
Organic carbon based K_d (3 % OM)	**5.3×10^{-3}**	**$m^3\ C\ g^{-1}$**	**Fitzgerald (2004)**
Desorption rate (12 % OM)	**0.14**	**h^{-1}**	**Calculated**
Desorption rate (6 % OM)	**0.18**	**h^{-1}**	**Calculated**
Desorption rate (3 % OM)	**0.29**	**h^{-1}**	**Calculated**

Appendix IV.

22 November 2004

Our Ref: HG/jj/Nov04/J370
Your Ref:

Eun-Hee Kim
Graduate Research Assistant
Chesapeake Biological Lab
University of Maryland Center for Environmental Science
P.O. Box 38
1 Williams Street
Solomons, MD 20688
USA

Dear Eun-Hee Kim

MARINE CHEMISTRY, Vol 86, No 3-4, 2004, pp 121-127, Kim et al: "The effect of resuspension on the fate of total mercury and methyl …"

As per your letter dated 12 November 2004, we hereby grant you permission to reprint the aforementioned material at no charge **in your thesis** subject to the following conditions:

1. If any part of the material to be used (for example, figures) has appeared in our publication with credit or acknowledgement to another source, permission must also be sought from that source. If such permission is not obtained then that material may not be included in your publication/copies.

2. Suitable acknowledgment to the source must be made, either as a footnote or in a reference list at the end of your publication, as follows:

   "Reprinted from Publication title, Vol number, Author(s), Title of article, Pages No., Copyright (Year), with permission from Elsevier".

3. Reproduction of this material is confined to the purpose for which permission is hereby given.

4. This permission is granted for non-exclusive world **English** rights only. For other languages please reapply separately for each one required. Permission excludes use in an electronic form. Should you have a specific electronic project in mind please reapply for permission.

5. This includes permission for UMI to supply single copies, on demand, of the complete thesis. Should your thesis be published commercially, please reapply for permission.

Yours sincerely

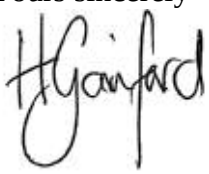

Helen Gainford
Rights Manager

Bibliography

Allen, H.E., Fu, G., Boothman, W., Di Toro, D.M. and Mahoney, J.D., 1991. Determination of acid volatile sulfide and selected simultaneously extractable metals in sediments. Office of water regulations and standards, US EPA, Washington, DC.

Allen, H.E., 1995. Metal contaminated aquatic sediments. Ann Arbor Press, Inc.

Angelini, R. and Petrere, M.J., 2000. A model for the plankton system of the Broa Reservoir, Sao Carlos, Brazil. Ecological Modeling, 126(2-3): 131-137.

Arfi, R., Guiral, D. and Bouvy, M., 1993. Wind induced resuspension in a shallow tropical lagoon. Estuarine Coastal and Shelf Science, 36: 587-604.

Ashley, J.T.F., 1998. Habitat use and trophic status as determinants of hydrophobic organic contaminant bioaccumulation within shallow systems. PhD Thesis, University of Maryland, College Park.

Babiarz, C.L., Hurley, J.P., Benoit, J.M., Shafer, M.M., Andren, A.W. and Webb, D.A., 1998. Seasonal influences on partitioning and transport of total and methylmercury in rivers from contrasting watersheds. Biogeochemistry, 41: 237-257.

Baillie, P.W. and Welsh, B.L., 1980. The effect of tidal resuspension on the distribution of intertidal epipelic alage in an estuary. Estuarine, Coastal and Shelf Science, 10: 165-180.

Balcom, P.H., Fitzerald, W.F., Vandal, G.M., Laamborg, C.H., Rolfhus, K.R., Langer, C.S., Hammerschmidt, C.R., 2004. Mercury sources and cycling in the connecticut river and long island sound. Marine Chemistry, 90(1-4): 53-74.

Bale, A.E., 2000. Modeling aquatic mercury fate in clear lake, Calif. Journal of Environmental Engineering-Asce, 126(2): 153-163.

Baumann, E.W., 1974. Determination of parts per billion sulfide in water with the sulfide-selective electrode. Analytical Chemistry, 46: 1345-1347.

Benoit, J.M., Gilmour, C.C., Mason, R.P., Riedel, G.S. and Riedel, G.F., 1998. Behavior of mercury in the Patuxent River estuary. Biogeochemistry, 40(2-3): 249-265.

Benoit, J.M., Gilmour, C.C., Mason, R.P. and Heyes, A., 1999a. Sulfide controls on mercury speciation and bioavailability to methylating bacteria in sediment pore waters. Environmental Science & Technology, 33(6): 951-957.

Benoit, J.M., Mason, R.P. and Gilmour, C.C., 1999b. Estimation of mercury-sulfide speciation in sediment pore waters using octanol-water partitioning and implications for availability to methylating bacteria. Environmental Toxicology and Chemistry, 18(10): 2138-2141.

Benoit, J.M., Gilmour, C.C. and Mason, R.P., 2001. The influence of sulfide on solid phase mercury bioavailability for methylation by pure cultures of desulfobulbus propionicus (1pr3). Environmental Science & Technology, 35(1): 127-132.

Benoit, J., Gilmour, C.C., Heyes, A., Mason, R. and Miller, C., 2003. Geochemical and biological controls over methylmercury production and degradation in aquatic systems. In: Y. Chai and O.C. Braids (Editors), Biochemistry of environmental important trace elements. American Chemical Society, Washington, DC, pp. 262-297.

Benoit, J.M. and Shull, D.H., 2004. Pattern of bioturbation, infaunal abundances and methylmercury accumulation in boston harbor sediments, 8th International Estuarine Biogeochemistry, Solomons, Maryland, USA.

Bienfang, P.K., 1981. Sinking rates of heterogeneous temperate phytoplankton population. Journal of Plankton Research, 3: 235-250.

Bloesch, J., 1995. Mechanisms, measurement and importance of sediment resuspension in lakes. Marine and Freshwater Research, 46(1): 295-304.

Bloom, N.S. and Crecelius, E.A., 1983. Determination of mercury in seawater at subnanogram per liter levels. Marine Chemistry, 14: 49-59.

Bloom, N. and Fitzgerald, W.F., 1988. Determination of volatile mercury species at the picogram level by low-temperature gas-chromatography with cold-vapor atomic fluorescence detection. Analytica Chimica Acta, 208(1-2): 151-161.

Bloom, N., 1989. Determination of picogram levels of methylmercury by aqueous phase ethylation, followed by cryogenic gas-chromatography with cold vapor atomic fluorescence detection. Canadian Journal of Fisheries and Aquatic Sciences, 46(7): 1131-1140.

Bloom, N.S. and Lasorsa, B.K., 1999. Changes in mercury speciation and the release of methyl mercury as a result of marine sediment dredging activities. The Science for the Total Environment, 237/238: 379-385.

Bloom, N.S., Gill, G.A., Cappellino, S., Dobbs, C., McShea, L., Driscoll, C., Mason, R. and Rudd, J., 1999. Speciation and cycling of mercury in Lavaca Bay, Texas, sediments. Environmental Science & Technology, 33(1): 7-13.

Bougis, P., 1976. Marine plankton ecology. North-Holland, Amsterdam, pp. 355.

Brassard, P., Kramer, J.R. and Collins, P.V., 1997. Dissolved metal concentration and suspended sediment in Hamilton Harbour. Journal of Great Lakes Research, 23(1): 86-96.

Bricelj, V.M. and Malouf, R.E., 1984. Influence of algal and suspended sediment concentraions on the feeding physiology of the hard clam *Mercenaria mercenaria*. Marine Biology, 84: 155-165.

Cain, T.D., 1975. Reproduction and recruitment of the brackish water clam *Rangia cuneata* in the James River, Vrginia. Fishery Bulletin, 73: 412-430.

Callister, S.M. and Winfrey, M.R., 1986. Microbial methylation of mercury in upper Wisconsin River sediments. Water Air and Soil Pollution, 29(4): 453-465.

Calvo, C., Donazzolo, R., Guidi, F. and Orio, A.A., 1991. Heavy metal pollution studies by resuspension experiments in Venice Lagoon. Water Research, 25(10): 1295-1302.

Caraco, N.F., Cole, J.J., Raymond, P.A., Strayer, D.L., Pace, M.L., Findlay, S.E.G. and Fischer, D.T., 1997. Zebra mussel invasion in a large, turbid river: Phytoplankton response to increased grazing. Ecology, 78: 588-602.

Chang, C.-W.A., 2001. Modeling the fate and trophic transfer of chemical contaminants in an urban estuary. MS Thesis, University of Maryland, College Park.

Chang, M.-L., 1999. Modeling the effects of resuspension and deposition on early diagenesis of nutrients and contaminants. PhD Thesis, University of Maryland, College Park.

Chang, S.I. and Reinfelder, J.R., 2002. Relative importance of dissolved versus trophic bioaccumulation of copper in marine copepods. Marine Ecology-Progress Series, 231: 179-186.

Choi, S.C. and Bartha, R., 1994. Environmental-factors affecting mercury methylation in estuarine sediments. Bulletin of Environmental Contamination and Toxicology, 53(6): 805-812.

Clarkson, T.W., 1990. Human health risks from methylmercury in fish. Environmental Toxicology and Chemistry, 9: 957-961.

Claisse, D., Cossa, D., Bretaudeau-Sanjuan, J., Touchard, G. and Bombled, B., 2001. Methylmercury in molluscs along the french coast. Marine Pollution Bulletin, 42(4): 329-332.

Compeau, G.C. and Bartha, R., 1983. Effects of sea salt anions on the formation and stability of methylmercury. Bulletin of Environmental Contamination and Toxicology, 31(4): 486-493.

Compeau, G. and Bartha, R., 1984. Methylation and demethylation of mercury under controlled redox, ph, and salinity conditions. Applied and Environmental Microbiology, 48(6): 1203-1207.

Compeau, G.C. and Bartha, R., 1987. Effect of salinity on mercury-methylating activity of sulfate-reducing bacteria in estuarine sediments. Applied and Environmental Microbiology, 53(2): 261-265.

Conaway, C.H., Squire, S., Mason, R.P., Flegal, A. R., 2003. Mercury speciation in the San Francisco Bay Estuary. Marine Chemistry, 80: 199-225.

Cooper, D.C. and Morse, J.W., 1996. The chemistry of Offatts Bayou, Texas: A seasonally highly sulfidic basin. Estuaries, 19(3): 595-611.

Cope, W.G. and Bartsch, M.R., 1999. Bioassessment of mercury, cadmium, polychlorinated biphenyls, and pesticides in the upper Mississippi River with zebra messels (*Dreissena polymorpha*). Environmental Science & Technology, 33: 4385-4390.

Coquery, M., Cossa, D., and Sanjuan, J., 1997. Speciation and sorption of mercury in two macro-tidal estuaries. Marine Chemistry, 58: 213-227.

Cossa, D., Coquery, M., Gobeil, C. and Martin, J.-M., 1996. Mercury fluxes at the ocean margins. In: W. Baeyens, R. Ebinghaus and O. Vasiliev (Editors), Global and regional mercury cycles: Sources, fluxes, and mass balances. NATO ASI Series. Kluwer cademic Publishing, Dordrecht, pp. 229-247.

Covelli, S., Faganeli, J., Horvat, M. and Brambati, A., 1999. Porewater distribution and benthic flux measurements of mercury and methylmercury in the gulf of Trieste (northern Adriatic sea). Estuarine Coastal and Shelf Science, 48(4): 415-428.

Crawford, S.M. and Sanford, L.P., 2001. Boundary shear velocities and fluxes in the MEERC experimental ecosystems. Marine Ecology-Progress Series, 210: 1-12.

Dagg, M.J. and Wyman, K.D., 1983. Natural ingestion rates of the copepods *Neocalanus plumchrus* and *N. cristatus* calculated from gut contents. Marine Ecology-Progress Series, 13: 37-46.

Darrow, B.P., Walsh, J.J., Vargo, G.A., Masserini, R.T., Fanning, K.A. and Zhang, J.Z., 2003. A simulation study of the growth of benthic microalgae following the decline of a surface phytoplankton bloom. Continental Shelf Research, 23(14-15): 1265-1283.

de Jonge, V.N. and van Beusekom, J.E.E., 1992. Contribution of resuspended microphytobenthos to total phytoplankton in the ems estuary and its possible role for grazers. Netherlands Journal of Sea Research, 30: 91-105.

Descy, J.-P., Everbecq, E., Gosselain, V., Viroux, L., Smitz, J.S., 2003. Modelling the impact of benthic filter-feeders on the composition and biomass of river plankton. Freshwater Biology, 48: 404-417.

Driscoll, C.T., Yan, C., Schofield, C.L., Munson, R., Holsapple, J., 1994. The mercury cycle and fish in the Adirondack Lakes. Environmental Science & Technology, 28(3): 136(A)-143(A).

Driscoll, C.T., Blette, V., Yan, C., Schofield, C.L., Munson, R. and Holsapple, J., 1995. The role of dissolved organic carbon in the chemistry and bioavailability of mercury in remote Adirondack lakes. Water Air and Soil Pollution, 80: 499-508.

EPA, 1995. Method 1631: Mercury in water by oxidation, purge and trap, and cold vapor atomic fluorescence spectrometry. US EPA 821-R-95-027, US EPA, Washington, DC.

EPA, 1996a. United states environmental protection agency methods and guidance for analysis of water. Cd-rom compilation of analytical methods, US EPA, Rockville, MD.

EPA, 1996b. Method 9215: Potentiometric determination of sulfide in aqueous samples and distillates with ion-selective electrode, US EPA.

Evans, R.D., 1994. Empirical evidence of the importance of sediment resuspension in lakes. Hydrobiologia, 284: 5-12.

Fisher, N.S., Teyssie, J.-L., Fowler, S.W. and Wang, W. X., 1996. Accumulation and retention of metals in mussels from food and water: A comparison under field and laboratory conditions. Environmental Science & Technology, 30(11): 3232-3242.

Fisher, N.S., Stupakoff, I., Sañudo-Wilhelmy, S., Wang, W.X., Teyssié, J.L., Fowler, S.W. and Crusius, J., 2000. Trace metals in marine copepods: A field test of a bioaccumulation model coupled to laboratory uptake kinetics data. Marine Ecology-Progress Series, 194: 211-218.

Fitzgerald, W.F. and Clarkson, T.W., 1991. Mercury and monomethylmercury - present and future concerns. Environmental Health Perspectives, 96: 159-166.

Froneman, P.W., 2000. Feeding studies on selected zooplankton in a temperate estuary, South Africa. Estuarine and Coastal Marine Science, 51: 543-552.

Gagnon, C., Pelletier, E., Mucci, A. and Fitzgerald, W.F., 1996. Diagenetic behavior of methylmercury in organic-rich coastal sediments. Limnology and Oceanography, 41(3): 428-434.
Gagnon, C., Pelletier, E. and Mucci, A., 1997. Behaviour of anthropogentic mercury in coastal marine sediments. Marine Chemistry, 59: 159-176.
Gagnon, C. and Fisher, N.S., 1997. The bioavailability of sediment-bound Cd, Co, and Ag to the mussel *Mytilus edulis*. Canadian Journal of Fisheries and Aquatic Sciences, 54(1): 147-156.
Gilmour, C.C., Henry, E.A, 1991. Mercury methylation in aquatic systems affected by acid deposition. Environmetal Pollution, 71: 131-169.
Gilmour, C.C., Riedel, G.S., Ederington, M.C., Bell, J.T., Benoit, J.M., Gill, G.A. and Stordal, M.C., 1998. Methylmercury concentrations and production rates across a trophic gradient in the Northern Everglades. Biogeochemistry, 40(2-3): 327-345.
Gill, G.A., Bloom, N.S., Cappellino, S., Driscoll, C.T., Dobbs, C., McShea, L., Mason, R. and Rudd, J.W.M., 1999. Sediment-water fluxes of mercury in Lavaca bay, Texas. Environmental Science & Technology, 33(5): 663-669.
Gobeil, C. and Cossa, D., 1993. Mercury in sediments and sediment pore-water in the Laurentian Trough. Canadian Journal of Fisheries and Aquatic Sciences, 50(8): 1794-1800.
Gorsky, G., Dallot, S., Sardou, J., Fenaux, R., Carrie, C. and Palazzoli, I., 1988. C and N composition of some Northwestern Mediterranean zooplankton and micronekton species. Journal of Experimental Marine Biology and Ecology, 124(2): 133-144.
Griffin, S.L., Herzfeld, M., Hamilton, D.P., 2001. Modelling the impact of zooplankton grazing on phytoplankton biomaass during a dinoflagellate bloom in the Swan River Estuary, Western Australia. Ecological Engineering, 16: 373-394.
Grizzle, R.E., Bricelj, V.M. and Shumway, S.E., 2001. Physiological ecology of *Mercenaria mercenaria*. In: J.N. Kraeuter and M. Castagna (Editors), Biology of the hard clam. Elsevier Health Sciences.
Halvorsen, E., Pedersen, O.P., Slagstad, D., Tande, K.S., Fileman, E.S., Batten, S.D., 2001. Microzooplankton and mesozooplankton in an upwelling filament off galicia: Modelling and sensitivity analysis of the linkage and their impact on the carbon dynamics. Progress in Oceanography, 51: 499-513.
Hansen, D.J., Berry, W.J., Mahony, J.D., Boothman, W.S., Di Toro, D.M., Robson, D.L., Ankley, G.T., Ma, D., Yan, Q. and Pesch, C.E., 1996. Predicting the toxicity of metal-contaminated field sediments using interstitial concentration of metals and acid-volatile sulfide normalizations. Environmental Toxicology and Chemistry, 15(12): 2080-2094.
Hammerschmidt, C.R. and Fitzgerald, W.F., 2004. Geochemical controls on the production and distribution of merthylmercury in near-shore marine sediments. Environmental Science & Technology, 38(5): 1487-1495.
Hammerschmidt, C.R., Fitzgerald, W.F., Lamborg, C.H., Balcom, P.H., Visscher, P.T., 2004. Biogeochemistry of methylmercury in sediments of long island sound. Marine Chemistry, 90(1-4): 31-52.

Harding, L.W.J., Mallonee, M.E., Perry, E.S., 2002. Toward a predictive understanding of primary productivity in a temperate, partially stratified estuary. Estuarine and Coastal Marine Science, 55(437-463).
Harte, M.E., 2001. Systematics and taxonomy. In: J.N. Kraeuter and M. Castagna (Editors), Biology of the hard clams. Elsevier Health Sciences.
Heyes, A., Miller, C., Mason, R.P., 2004. Mercury and methylmercury in hudson river sediment: Impact of tidal resuspension on partitioning and methylation. Marine Chemistry, 90(1-4): 75-89.
Hintelmann, H. and Wilken, R.D., 1995. Levels of total mercury and methylmercury compounds in sediments of the polluted Elbe River: Influence of seasonally and spatially varying environmental factors. The Science for the Total Environment, 166: 1-10.
Hintelmann, H., Keppel-Jones, K. and Evans, R.D., 2000. Constants of mercury methylation and demethylation rates in sediments and comparison of tracer and ambient mercury availability. Environmental Toxicology and Chemistry, 19(9): 2204-2211.
Hintelmann, H., Harris, R., 2004. Application of multiple stable mercury isotopes to determine the adsorption and desorption dynamics of hg (ii) and mehg to sediments. Marine Chemistry, 90(1-4): 165-173.
Hoetzel, G. and Croome, R., 1994. Long-term phytoplankton monitoring of the Darling River at Burtunday, New South Wales: Incidence and significance of cyanobacterial blooms. Aust. J. Mar. Freshwater Res., 45: 747-759.
Horvat, M., Bloom, N.S. and Liang, L., 1993. Comparison of distillation with other current isolation methods for the determination of methyl mercury-compounds in low-level environmental-samples .1. Sediments. Analytica Chimica Acta, 281(1): 135-152.
Huerta-Diaz, M.A. and Morse, J.W., 1990. A quantitative method for determination of trace-metal concentrations in sedimentary pyrite. Marine Chemistry, 29(2-3): 119-144.
Hurley, J.P., Cowell, S.E., Shafer, M.M. and Hughes, P.E., 1998. Partitioning and transport of total and methyl mercury in the lower Fox River, Wisconsin. Environmental Science & Technology, 32(10): 1424-1432.
Jackson, T.A., 1988. Accumulation of mercury by plankton and benthic invertebrates in riverin lakes of Northern Manitoba (Canada): Importance of regionally and seasonally varying environmental factors. Canadian Journal of Fisheries and Aquatic Sciences, 45: 1744-1757.
Jay, J.A., Morel, F.M.M. and Hemond, H.F., 2000. Mercury speciation in the presence of polysulfides. Environmental Science & Technology, 34(11): 2196-2200.
Jerling, H.L. and Wooldridge, T.H., 1995. Feeding of two mysid species on plankton in a temperate estuary. Journal of Experimental Marine Biology and Ecology, 188: 243-259.
Jorgensen, S.E., 1994. Fundamentals of ecological modelling. Elsevier, Amsterdam, The Netherlands.

Kainz, M. and Lucotte, M., 2002. Can flooded organic matter from sediments predict mercury concentration in zooplankton of a perturbed lake ? The Science for the Total Environment, 293: 151-161.
Kawaguchi, T., Porter, D., Bushek, D. and Jones, B., 1999. Mercury in the American oyster *Crassostrea virginica* in South Carolina, USA, and public health concerns. Marine Pollution Bulletin, 38(4): 324-327.
Keith, L.H., 1991. Compilation of EPA's sampling and analytical methods. Lewis Publishers, Boca Raton.
Kibirige, I. and Perissinotto, R., 2003. The zooplankton community of the Mpenjati Estuary, a South Africa temporarily open/closed system. Estuarine, Coastal and Shelf Science, 58(4): 727-741.
Kiorbe, T., Mohlenberg, F., Riisgard, H.U., 1985. *In situ* feeding rates of planktonic copepods: A comparison of four methods. Journal of Experimental Marine Biology and Ecology, 88: 67-81.
Kim, E., Mason, R.P., Porter, E.T. and Soulen, H.L., 2004. The effect of resuspension on the fate of total mercury and methyl mercury in a shallow estuarine ecosystem: A mesocosm study. Marine Chemistry, 86: 121-137.
Kirk, J.T.O., 1985. Effects of suspensoids (turbidity) on penetration of solar radiation in aquatic ecosystems. Hydrobiologia, 125: 195-208.
Korthals, E.T. and Winfrey, M.R., 1987. Seasonal and spatial variations in mercury methylation and demethylation in an oligotrophic lake. Applied and Environmental Microbiology, 53(10): 2397-2404.
Lacerda, L.D. and Gonçalves, G.O., 2001. Mercury distribution and speciation in waters of the coastal lagoons of Rio de Janeiro, Se Brazil. Marine Chemistry, 76: 47-58.
Laima, M.J.C., Matthiesen, H., Lund-Hansen, L.C. and Christiansen, C., 1998. Resuspension studies in cylindrical microcosms: Effects of stirring velocity on the dynamics of redox sensitive elements in coastal sediments. Biogeochemistry, 43: 293-309.
LaSalle, M.W. and de la Cruz, A.A., 1985. Species profiles: Life histories and environmental requirements of coastal fishes and invertebrates (Gulf of Mexico): Common *rangia*. Biological Report 82 (11.32), United States Fish and Wildlife Service.
Latima, M.J.C., Davis, W.R. and Keith, D.J., 1999. Mobilization of PAHs and PCBs from in-place contaminated marine sediments during simulated resuspension events. Estuarine, Coastal and Shelf Science, 49: 577-595.
Lawrence, A.L., McAloon, K.M., Mason, R.P. and Mayer, L.M., 1999. Intestinal solubilization of particle-associated organic and inorganic mercury as a measure of bioavailability to benthic invertebrates. Environmental Science & Technology, 33(11): 1871-1876.
Lawrence A.L., M.R.P., 2001. Factors controlling the bioaccumulation of mercury and methylmercury by the estuarine amphipod *Leptocheirus plumulosus*. Environmental Pollution, 111(2): 217-231.
Lawson, N.M., Mason, R.P. and Laporte, J.M., 2001. The fate and transport of mercury, methylmercury, and other trace metals in Chesapeake Bay tributaries. Water Research, 35(2): 501-515.

Lewis, M.A., Weber, D.E., Stanley, R.S. and Moore, J.C., 2001. Dredging impact on an urbanized Florida bayou: Effects on benthos and algal-periphyton. Environmental Pollution, 115: 161-171.

Lin, S., Huang, K.-M. and Chen, S.-K., 2002. Sulfate reduction and iron sulfide mineral formation in the Southern East China Sea continental slope sediment. Deep-Sea Research Part I, 49: 1837-1852.

Lindqvist, O., Johansson, K., Aastrup, M., Andersson, A., Bringmark, L., Hovsenius, G., Hakanson, L., Iverfeldt, A., Meili, M. and Timm, B., 1991. Mercury in the Swedish environment - recent research on causes, consequences and corrective methods. Water Air and Soil Pollution, 55(1-2): 131-157.

Luoma, S.N., Johns, C., Fisher, N.S., Steinberg, N.A., Oremland, R.S. and Reinfelder, J.R., 1992. Determination of selenium bioavailability to a benthic bivalve from particulate and solute pathways. Environmental Science & Technology, 26(3): 485-491.

Lu, F.C., 1996. Basic toxicology: Fundamentals, target organs, and risk assessment. Taylor & Francis, 3rd Edition, Washington DC.

Marvin-Dipasquale, M.C. and Oremland, R.S., 1998. Bacterial methylmercury degradation in Florida Everglades peat sediment. Environmental Science & Technology, 32(17): 2556-2563.

Marvin-Dipasquale, M., Agee, J., McGowan, C., Oremland, R.S., Thomas, M., Krabbenhoft, D. and Gilmour, C.C., 2000. Methyl-mercury degradation pathways: A comparison among three mercury-impacted ecosystems. Environmental Science & Technology, 34(23): 4908-4916.

Mason, R.P., Fitzgerald, W.F., Hurley, J., Hanson, A.K., Donaghay, P.L. and Sieburth, J.M., 1993. Mercury biogeochemical cycling in a stratified estuary. Limnology and Oceanography, 38(6): 1227-1241.

Mason, R.P., Fitzgerald, W.F. and Morel, F.M.M., 1994. The biogeochemical cycling of elemental mercury - anthropogenic influences. Geochimica et Cosmochimica Acta, 58(15): 3191-3198.

Mason, R.P., Reinfelder, J.R., Morel, F.M.M., 1996. Uptake, toxicity, aand trophic transfer of mercury in a coastal diatom. Environmental Science & Technology, 30: 1835-1845.

Mason, R.P. and Sullivan, K.A., 1997. Mercury in Lake Michigan. Environmental Science & Technology, 31(3): 942-947.

Mason, R.P. and Sullivan, K.A., 1998. Mercury and methylmercury transport through an urban watershed. Water Research, 32: 321-330.

Mason, R., Bloom, N., Cappellino, S., Gill, G., Benoit, J. and Dobbs, C., 1998. Investigation of porewater sampling methods for mercury and methylmercury. Environmental Science & Technology, 32(24): 4031-4040.

Mason, R.P. and Lawrence, A.L., 1999. Concentration, distribution, and bioavailability of mercury and methylmercury in sediments of Baltimore Harbor and Chesapeake Bay, Maryland, USA. Environmental Toxicology and Chemistry, 18(11): 2438-2447.

Mason, R.P., Lawson, N.M., Lawrence, A.L., Leaner, J.J., Lee, J.G. and Sheu, G.R., 1999. Mercury in the Chesapeake Bay. Marine Chemistry, 65(1-2): 77-96.

Mason, R.P., Kim, E. and Cornwell, J.C., 2004. Metal accumulation in Baltimore Harbor: Current and past inputs. Applied Geochemistry, 19(11): 1655-1889.
Mason, R.P., Kim, E., Cornwell, J., and Heyes, D., 2004. The influence of sediment redox status on the flux of mercury, methylmercury and other constituents from estuarine sediment. Marine Chemistry, in review.
Matilainen, T. and Verta, M., 1995. Mercury methylation and demethylation waters. Canadian Journal of Fisheries and Aquatic Sciences, 52(8): 1597-1608.
McConnell, M.A. and Harrel, R.C., 1995. The estuarine clam *Rangia-cuneata* (gray) as a biomonitor of heavy-metals under laboratory and field conditions. Amercian Malacological Bulletin, 11(2): 191-201.
Miller, C., Heyes, A. and Mason, R.P., 2002. The role of tidal resuspension mercury dynamics at the sediment-water interface in the lower Hudson River, ASLO Summer Meeting, Victoria, BC, Canada.
Miller, C. and Mason, R.P., 2004. The influence of dissolved organic matter on the interaction of inorganic and methylmercury with hydrou ferric oxide. Environmental Science & Technology, in review.
Monson, B.A. and Brezonik, P.L., 1998. Seasonal patterns of mercury species in water and plankton from softwater lakes in northeastern Minnesota. Biogeochemistry, 40(2-3): 147-162.
Morrison, H.A., Gobas, F.A., Lazar, R., Whittle, D.M. and Haffner, G.D., 1997. Development and verification of a benthic/pelagic food web bioaccumulation model for PCB congers in Western Lake Erie. Environmental Science & Technology, 31(11): 3267-3273.
Morton, B., 1969. Studies on the biology of *Dreissena polymorpha* Pall II. Correlation of the rhythms of adductor activity, feeding, digestion and excretion. Proc. Malac. Soc. Lond., 38: 401-414.
Newell, R.I.E., 2004. Ecosystem influences of natural and cultivated populations of suspension-feeding bivalve molluscs: A review. Journal of Shellfish Research, 23(1): 51-61.
Ni, I.H., Wang, W.X. and Tam, Y.K., 2000. Transfer of Cd, Cr, and Zn from zooplankton prey to mudskipper *Periophthalmus cantonensis* and glassy *Ambassis urotaenia* fishes. Marine Ecology-Progress Series, 194: 203-210.
Nyffeler, U.P., Li, Y.-H. and Santschi, P.H., 1984. A kinetic approach to describe trace-element distribution between particles and solution in natural aquatic systems. Geochimica et Cosmochimica Acta, 48: 1513-1522.
Oenema, O., Steneker, R. and Reynders, J., 1988. The soil environment of the intertidal area in the westerschelde. Hydrological Bulletin, 22: 21-30.
Oremland, R.S., Culbertson, C.W. and Winfrey, M.R., 1991. Methylmercury decomposition in sediments and bacterial cultures - involvement of methanogens and sulfate reducers in oxidative demethylation. Applied and Environmental Microbiology, 57(1): 130-137.
Oremland, R.S., Miller, L.G., Dowdle, P., Connell, T. and Barkay, T., 1995. Methylmercury oxidative-degradation potentials in contaminated and pristine sediments of the Carson River, Nevada. Applied and Environmental Microbiology, 1(7): 2745-2753.

Padilla, D.K., Adolph, S.C., Cottingham, K.L., Schneider, D.W., 1996. Predicting the consequences of dreissenid musels on a pelagic food web. Ecological Modeling, 85: 129-144.

Pak, K.R. and Bartha, R., 1998. Mercury methylation and demethylation in anoxic lake sediments and by strictly anaerobic bacteria. Applied and Environmental Microbiology, 64(3): 1013-1017.

Paquette, K. and Helz, G., 1995. Solubility of cinnabar (red hgs) and implications for mercury speciation in sulfidic waters. Water Air and Soil Pollution, 80(1-4): 1053-1056.

Park, J. and Curtis, L.R, 1997. Mercury distribution in sediments and bioaccumulation by fish in two Oregon Reservoirs: Point-source and nonpoint-source impacted systems. Archives of Environmental Contamination and Toxicology, 33: 423-429.

Park, J.-C., Aizaki, M., Fukushima, T. and Otsuki, A., 1997. Production of labile and refractory dissolved organic carbon by zooplankton excretion: An experimental study using large outdoor continuous flow-through ponds. Canadian Journal of Fisheries and Aquatic Sciences, 54: 434-443.

Parks, J.W., Lutz, A. and Sutton, J.A., 1989. Water column methylmercury in the Wabigoon/English River-Lake system: Factors controlling concentrations, speciation, and net production. Canadian Journal of Fisheries and Aquatic Sciences, 46: 2184-2202.

Paterson, M.J., Rudd, J.W.M. and Louis, V.S., 1998. Increases in total and methylmercury in zooplankton following flooding of a Peatland Reservoir. Environmental Science & Technology, 32: 3868-3874.

Petersen, W., Willer, E. and Willamowski, C., 1997. Remobilization of trace elements from polluted anoxic sediments after resuspension in oxic water. Water Air and Soil Pollution, 99: 515-522.

Pickhardt, R.C., Folt, C.L., Chen, C.Y., Klaue, B., Blum, J.D., 2002. Algal blooms reduce the uptake of toxic methylmercury in freshwater food webs. Proceedings of the National Academy of Science of the United States of America, 99(7): 4419-4423.

Plourde, Y., Lucotte, M. and Pichet, P., 1997. Contribution of suspended particulate matter and zooplankton to MeHg contamination of the food chain in midnorthern Quebec (Canada) reservoirs. Canadian Journal of Fisheries and Aquatic Sciences, 54: 821-831.

Porter, E.T., 1999. Physical and biological scaling of benthic-pelagic coupling in experimental ecosystem studies. PhD dissertation Thesis, University of Maryland, College Park.

Porter, E.T., Sanford, L.P., Gust, G. and Porter, F.S., 2004a. Combined water-column mixing and benthic boundary-layer flow in mesocosms: Key for realistic benthic-pelagic coupling studies. Marine Ecology-Progress Series, 271: 43-60.

Porter, E.T., Cornwell, J.C. and Sanford, L.P., 2004b. Effect of oysters (*Crassostrea virginica*) and bottom shear velocity on benthic-pelagic coupling and estuarine water quality. Marine Ecology-Progress Series, 271: 61-75.

Ravichandran, M., 2004. Interactions between mercury and dissolved organic matter - a review. Chemosphere, 55(3): 319-331.

Regnell, O., Ewald, G. and Lord, E., 1997. Factors controlling temporal variation in methyl mercury levels in sediment and water in a seasonally stratified lake. Limnology and Oceanography, 42(8): 1784-1795.

Riisgård, H.U., 1998. Filter feeding and plankton dynamics in a Danish Fjord: A review of the importance of flow, mixing and density-driven circulation. Journal of Environmental Management, 53: 195-207.

Riisgård, H.U., Kittner, C. and Seerup, D.F., 2003. Regulation of opening state and filtratioin rate in filter-feeding bivalves (C*ardium edule, Mytilus eduliis, Mya arenaria*) in response to low algal concentration. Journal of Experimental Marine Biology and Ecology, 284: 105-127.

Roditi, H.A., Fisher, N.S. and Sanudo-Wilhelmy, S.A., 2000. Field testing a metal bioaccumulataion model for zebra mussels. Environmental Science & Technology, 34(13): 2817-2825.

Roman, M.R., Holliday, D.V., Sanford, L.P., 2001. Temperal and spatial patterns of zooplankton in the Chesapeake Bay turbidity maximum. Marine Ecology-Progress Series, 213: 215-227.

Roper, J.M., Cherry, D.S., Simmers, J.W. and Tatem, H.E., 1996. Bioaccumulation of toxicants in the zebra mussels, *Dreissena polymorpha*, at the times beach confined disposal facility, Buffalo, New York. Environmental Pollution, 94(2): 117-129.

Ryan, P.A., 1991. An environmental effect of sediment on New Zealand streams: A review. New Zeal. J. Mar. Freshwat. Res., 25: 207-221.

Sager, D.R., 2002. Long-term variation in mercury concentrations in estuarine organisms with changes in release into Lavaca Bay, Texas. Marine Pollution Bulletin, 44(8): 807-815.

Sanford, L.P., Panageotou, W. and Halka, J.P., 1991. Tidal resuspension of sediments in northern Chesapeake Bay. Marine Geology, 97: 87-103.

Sanford, L.P. and Halka, J.P., 1993. Assessing the paradigm of mutually exclusive erosion and deposition of mud, with examples from upper Chesapeake Bay. Marine Geology, 114(1-2): 37-57.

Schallenberg, M. and Burns, C.W., 2004. Effects of sediment resuspension on phytoplankton production: Teasing apart the influences of light, nutrients and algal entrainment. Freshwater Biology, 49(2): 143-159.

Schoellhamer, D.H., 1996. Anthropogenic sediment resuspension mechanisms in a shallow microtidal estuary. Estuarine, Coastal, and Shelf Science, 43: 533-548.

Schnoor, J.L., 1996. Environmental modeling. Wiley-Interscience; 1st edition.

Sellers, P., Kelly, C.A., Rudd, J.W.M. and MacHutchon, A.R., 1996. Photodegradation of methylmercury in lakes. Nature, 38(6576): 694-697.

Simas, T.C., Ribeiro, A.P. and Ferreira, J.G., 2001. Shrimp - a dynamic model of heavy-metal uptake in aquatic macrofauna. Environmental Toxicology and Chemistry, 20(11): 2649-2656.

Simpson, L.S., Apte, S.C., and Batley, G.E., 1998. Effect of short-term resuspension events on trace metal speciation in polluted anoxic sediments. Environmental Science & Technology, 32(5): 620-625.

Siokou-Frangou, I., Bianchi, M., Christaki, U., Christou, E., Giannakourou, A., Gotsis, O., Ignatiades, L., Pagou, K., Pitta, P., Psarra, S., Souvermezoglou, E., Van Wambeke, F. and Zervakis, V., 2002. Carbon flow in the planktonic food web along a gradient of oligotrophy in aegean sea (mediterranean sea). Journal of Marine Systems, 33: 335-353.

Skyring, G.W., 1987. Sulfate reduction in coastal ecosystems. Geomicrobiology Journal, 5(3-4): 295-374.

Sloth, N.P., Riemann, B., Nielsen, L.P., and Blackburn, T.H., 1996. Resilience of pelagic and benthic microbial communities to sediment resuspension in a coastal ecosystem, Knebel, Vig, Denmark. Estuarine, Coastal, and Shelf Science, 42: 405-415.

Stanley, J.G., 1985. Species profiles: Life histories and environmental requirements of coastal fishes and invertebrates (mid-Atlantic) -- hard clam. U.S. Fish Wildl. Serv. Biol. Rep. 82(11.41), U.S. Army Corps of Engineers, TR EL-82(11.41).

Stordal, M.C., Santschi, P.H. and Gill, G.A., 1996. Colloidal pumping: Evidence for the coagulation process using natural colloids tagged with Hg-203. Environmental Science & Technology, 30(11): 3335-3340.

Sunderland, E.M., Gobas, F.A.P.C., Heyes, A., Branfireun, B.A., Bayer, A.K., Cranston, R.E., Parsons, M.B., 2004. Speciation and bioavailability of mercury in well-mixed estuarine sediments. Marine Chemistry, 90(1-4): 91-105.

Thomann, R.V., Mahony, J.D. and Mueller, R., 1995. Steady-state model of biota sediment accumulation factor for metals in two marine bivalves. Environmental Toxicology and Chemistry, 14(11): 1989-1998.

Tremblay, A., Lucotte, M. and Schetagne, R., 1998. Total mercury and methylmercury accumulation in zooplankton of hydroelectric reservoirs in northern Quebec (Canada). The Science for the Total Environment, 213: 307-315.

Tsui, M.T.K. and Wang, W.X., 2004. Uptake and elimination routes of inorganic mercury and methylmercury in *Daphnia magna*. Environmental Science & Technology, 38: 808-816.

Turner, E.J. and Miller, D.C., 1991. Behavior and growth of *Mercenaria mercenaria* during simulated storm events. Marine Biology, 111: 55-64.

van den Berg, G.A., Gustav Loch, J.P., Van Der Heudt, L.M. and Zwolsman, J.J.G., 1998. Vertical distribution of acid-volatile sulfide and simultaneously extracted metals in a recent sedimentation area of the river Meuse in the Netherlands. Environmental Toxicology and Chemistry, 17(4): 758-763.

van Griethuysen, C., Gillissen, F. and Koelmans, A.A., 2002. Measuring acid volatile sulphide in floodplain lake sediments: Effect of reaction time, sample size and aeration. Chemosphere, 47: 395-400.

Verity, P.G., 2000. Grazing experiments and model simulations of the role of zooplankton in *phaeocystis* food webs. Journal of Sea Research, 43: 317-343.

Viroux, L., 2000. Dynamique du metazooplancton en milieu fluvial. PhD Thesis, University of Namur, Namur, Belgium.

Wainright, S.C., 1987. Stimulation of heterotrophic microplankton production by resuspended marine sediments. Science, 238: 1710-1712.
Wainright, S.C., 1990. Sediment-to-water fluxes of particulate material and microbes by resuspension and their contribution to the planktonic food web. Marine Ecology-Progress Series, 62: 271-281.
Wainright, S.C., Hopkinson, C.S. Jr, 1997. Effects of sediment resuspension on organic matter processing in coastal environments: A simulataaion model. Journal of Marine Systems, 11: 353-368.
Walz, N., 1978. The energy balance of the freshwater mussel *Dreissena polymorpha* pallas in laboratory experiments and in lake constance. I. Pattern of activity, feeding and assimilation efficiency. Arch. Hydrobiol. (Suppl.), 55: 83-105.
Wang, W., Driscoll, C.T, 1995. Patterns of total mercury concentrations in Onondaga lake, New York. Environmental Science & Technology, 29(9): 2261-2266.
Wang, W.X., Stupakoff, I., Gagnon, C. and Fisher, N.S., 1998. Bioavailability of inorganic and methylmercury to a marine deposit feeding polychaete. Environmental Science & Technology, 32(17): 2564-2571.
Watras, C.J. and Bloom, N.S., 1992. Mercury and methylmercury in individual zooplankton - implications for bioaccumulation. Limnology and Oceanography, 37(6): 1313-1318.
Watras, C.J., Morrison, K.A., Bloom, N.S, 1995. Mercury in remote rocky mountain lakes of Glacier National Park, Montana, in comparison with other temperate North American regions. Canadian Journal of Fisheries and Aquatic Sciences, 52: 1220-1228.
Weber, J.H., 1993. Review of possible paths for abiotic methylation of mercury(II) in the aquatic environment. Chemosphere, 26(11): 2063-2077.
White, J.R., Roman, M.R., 1992. Seasonal study of grazing by metazoan zooplankton in the mesohaline Chesapeake Bay. Marine Ecology-Progress Series, 86: 251-261.
Winfrey, M.R. and Rudd, J.W.M., 1990. Environmental factors affecting the formatiion of methylmercury in low ph lakes. Environmental Toxicology and Chemistry, 9(7): 853-869.
Winkels, H.J., Blom, G., Korrnenberg, S.B., Lijklema, L., 1998. Dilution of riverin heavy metal input concentrations by suspension of sediments and algal growth in the Ijsselmeer. Water Research, 32(10): 2931-2940.
Young, B.L., Padilla, D.K., Schneider, D.W., Hewett, S.W., 1996. The importance of size-frequency relationships for predicting ecological impact of zebra mussel populations. Hydrobiologia, 332: 151-158.